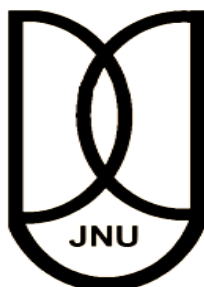


**SOLUTE GEOCHEMISTRY, ARSENIC  
MOBILIZATION AND THEIR EFFECT ON  
HUMAN HEALTH IN GHAZIPUR AND  
GORAKHPUR DISTRICTS, UTTAR  
PRADESH, INDIA**

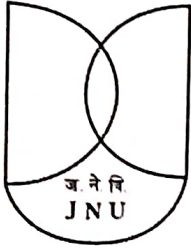
*Dissertation submitted to the Jawaharlal Nehru University in  
partial fulfilment for the award of the degree of*

**DOCTORATE OF PHILOSOPHY**

**SHAILESH KUMAR YADAV**



SCHOOL OF ENVIRONMENTAL SCIENCES  
JAWAHARLAL NEHRU UNIVERSITY  
NEW DELHI – 110067  
INDIA  
2021



जवाहरलाल नेहरु विश्वविद्यालय  
**Jawaharlal Nehru University**  
 SCHOOL OF ENVIRONMENTAL SCIENCES  
 NEW DELHI - 110 067, INDIA

**CERTIFICATE**

This is to certify that the research work embodied in this thesis entitled "Solute Geochemistry, Arsenic Mobilization and their effect on Human Health in Ghazipur and Gorakhpur districts, Uttar Pradesh, India" has been carried in the School of Environmental Sciences, Jawaharlal Nehru University, New Delhi in partial fulfilment for the award of Doctorate of Philosophy. This work is original and has not been submitted in part or full for any other degree or diploma in any university.

*Shailesh Kumar Yadav*

Shailesh Kumar Yadav  
 (Candidate)


*U.C. Kulshrestha*  
 31/8/21

Prof. U.C. Kulshrestha  
 (Dean, S.E.S.)

 डीन/एस.ई.एस./जे.एन.यू.  
 Dean/SES/JNU  
 नई दिल्ली-110067  
 New Delhi-110067

*AL. Ramanathan*  
 31/8/21

Prof. AL. Ramanathan  
 (Supervisor)

 AL. Ramanathan  
 Professor  
 School of Environmental Sciences  
 Jawaharlal Nehru University  
 New Delhi - 110067, India

---

## Abstract

The Indo-Gangetic plain is one of the ideal regions for agricultural practices. Over-exploitation, unmanaged use of groundwater resources, and geogenic and anthropogenic pollutions threaten the aquifer system of Gangetic plain. Arsenic pollution in groundwater and sediment of Gangetic plain is a growing problem due to its toxicity and widespread distribution. Hence, understanding the arsenic sources and mobilization in groundwater, soil and sediment and their toxicity to human health is the prime aim of this study. The study area is geomorphologically differentiated into older alluvium (OA) and younger alluvium (YA). It was observed that younger alluvium is associated with an elevated As concentration in groundwater and sediment both in the study area. The hydrogeochemical facies (Piper diagram) shows that  $\text{CaHCO}_3$  water type is dominated in the study area. In addition, a thermodynamically stable Eh-pH diagram was plotted to understand the As and Fe species in the groundwater. A mineralogy study has been done to identify the As source and mobilization through the available minerals. The hydrogeochemical evolution has been carried out to understand the dominant processes governing the major ion chemistry. A geochemical model (PHREEQC) was used to identify the saturation indices (SI) in groundwater. It shows that groundwater is supersaturated with fibrous goethite, hematite, kaolinite, and illite minerals, which tend to precipitate from groundwater. The bivariate plots between As and other physicochemical parameters show that reductive dissolution of Fe oxyhydroxide is the prime mechanism for As mobilization in younger alluvium, while in older alluvium, reductive dissolution and other processes are involved in As mobilization. Objective two aim to understand the distribution and fractional of As in groundwater and sediment. The results show that As(III) is dominated in younger alluvium while As(V) is dominated in older alluvium in the study area. The vertical distribution plot of As with depth shows shallow aquifers (20-35 mbgl) are more prone to As contamination than the deeper aquifers. A three-step sequential extraction method was used to identify fractionated bind with the different forms. The results show residual fraction is the dominated fractionated followed by reducible, acid-soluble and oxidizable fractions. A sediment tool color chart was used to understand the association of total As with sediment color, but a significant association was missing. The presence of the secondary mineral-like siderite act as a potential sink for arsenic and partial dissolution of fibrous goethite ( $\text{FeOOH}$ ) liberates As into the groundwater. In the present study, stable isotopes tracer ( $\delta^2\text{H}$  and  $\delta^{18}\text{O}$ ) was used to understand

---

the groundwater recharge and organic carbon dynamics. The results show OA and YA groundwater recharged from local meteoric water, which undergoes little evaporation. While the river water is getting recharged from meteoric water in both the study area. The enrichment of  $\delta^{13}\text{C}_{\text{TIC}}$  in YA groundwater shows that carbonate dissolution is dominated over silicate weathering. The  $\delta^{13}\text{C}_{\text{TIC}}$  vs.  $p\text{CO}_2$  indicating silicate and carbonate weathering was the major source of DIC in the groundwater of both the study area. Finally, As exposure was calculated for adults and children from different exposure pathways in groundwater. A person correlation plot is plotted for the sediment core to identify the source of As and TMs in sediment. The result shows that fine silt and clay act as reservoir pools for As and TMs. The geochemical interpretation like geoaccumulation index ( $I_{\text{geo}}$ ), enrichment factor (EF) and degree of contamination (DC) was calculated and it shows sediments are unpolluted in the study area.

**Keywords:** As mobilization; Central Gangetic plain; Stable isotopes; Dissolved organic carbon; As exposure.

---

## Acknowledgments

I owe my deepest gratitude to my supervisor, Prof. AL Ramanathan, School of Environmental Sciences (SES), JNU, for his affectionate guidance, incessant inspiration and constructive criticism at all the stages of this work. His intellectual brilliance, overwhelming experience and enthusiasm had been the path of light to the objectives of this study. I am highly indebted for the encouragement infused in me by him to do research.

I would like to express my most profound appreciation to my doctoral research committee members, prof. N. J Raju SES, Dr. S. Sreelesh, for his valuable suggestion and help in deciding my Ph.D. title and objectives.

I am grateful to Prof. Umesh Kulshrestha, Dean of School of Environmental Sciences, JNU, former deans Prof AL Ramanathan and Prof S. Mukherjee for their multidirectional support and academic suggestions whenever possible needed. I am also thankful to CIF Staffs, Dr. P.D. Gaikwad, Mr. Ramesh Bhardwaj, Mrs. Rashmi Sinha, Mr. Nitin Gedam, Mr. A.S Rawat, Mr. Rajinder Kumar and those who help me to access the Centre's Instrument Facility (CIF) to complete my research work.

I would also extend my gratitude to Dr. Meenakshi and Dr. Deeksha, IUAC (Inter-University Accelerator Centre), New Delhi, for providing me the XRD and XRF facility during my Ph.D. I am also thankful to NIH, Roorkee, for providing me the isotopes analysis facility and results.

I heartfelt thanks to my younger brothers (Ritesh and Prince), who helped me during the field sampling.

I expressed my special regards to my lab mates Dr. Shayam Ranjan, Dr. Hemant Singh, Dr. Arbind Patel, Dr. Thupsthan Angchuk, Dr. Naveen Kumar, Dr. Namrata Priya and Dr. Om Kumar, Arindan, Soheb, Karuna, Sarvagya, Monica, Kalyan, Anshula, Som, Chetan, Himanshu, Deepika and Stuti and those who, directly or indirectly, helped me during my Ph.D. submission. I am also thankful to Late. Bheem Bhaiya (our lab attendant), who help me in my sediment processing and analysis. I would also like to thank Dada and Murli.

How can I forget to thank my lab seniors Dr. Rajesh Ranjan, Dr. Gurmeet Singh, Dr. Alok Kumar, Dr. Musarrat Parveen, Dr. Swati Sappal, Dr. Manoj Kumar, Dr. Virendra Bahadur Singh, Dr.K. K, and all those whose name is missed here.

---

*I would also like to give special thanks to all my College, MSc, M.Phill /Ph.D., Hostel friends who gave me strength and motivation during my Ph.D. work,*

*Words alone cannot suffice my indebtedness to my parents, brothers and sisters for their unconditional love and numerous sacrifices. Their support and motivation were the fuel for me, without which I would not have reached this stage of academic destination.*

*Shailesh Kumar Yadav*

---

## Contents

Certificate	i
Abstract	ii
Acknowledgements	iv
Contents	vi
List of Tables	x
List of Figures	xii
Abbreviations	xvi
<b>1. Introduction</b>	<b>1</b>
<b>1.1</b> Sources and occurrences of arsenic in the environment	2
<b>1.2</b> Global scenario of As contamination (an overview)	3
<b>1.3</b> Arsenic contamination in India	4
<b>1.4</b> Arsenic contamination in groundwater, soil and sediment	7
<b>1.5</b> Arsenic mobilization	8
a. Pyrite dissolution	8
b. Reductive dissolution of iron oxyhydroxide	9
c. Alkali desorption	9
d. Geothermal	10
<b>1.6</b> Arsenic speciation and its role in mobilization	10
<b>1.7</b> Application of stable isotopes in As contamination	11
<b>1.8</b> Arsenic and trace metal exposure and health effect	12
<b>1.9</b> Arsenic contamination in Central Gangetic Basin	13
<b>1.10</b> Relevance of the study	14
<b>1.11</b> Research hypothesis and objectives	15
<b>2. Study Area</b>	<b>18</b>
<b>3 Identification of arsenic provenance and fate by examining the geochemical/hydrochemical processes and geomorphological variations</b>	
<b>3.1. Introduction</b>	21
<b>3.2 Materials and Methods</b>	22

---

3.2.1.	Background of the study area	22
3.2.2.	Remote sensing and geology/geomorphic classification	23
3.2.3.	Study area geomorphology	23
3.2.4.	Sampling and analysis	27
3.2.5.	Sediment preparation and digestion	28
3.2.6.	Instrumentation	28
3.2.7.	Quality control and quality assurance	29
3.2.8.	Hydrogeochemical and statistical modelling	30
3.2.9.	Data analysis	30
<b>3.3.</b>	<b>Results and discussion</b>	30
3.3.1.	Major ion chemistry of water samples	30
3.3.2.	Geochemistry of subsurface sediment	35
3.3.3.	Arsenic speciation and other trace metal in groundwater	43
3.3.4.	Mineralogy of the sediment	47
3.3.5.	Hydrogeochemical evolution of groundwater and river water	48
3.3.6.	Geochemical speciation modelling in solution	57
3.3.7.	As fate and mobilization in groundwater and surface water	59
<b>3.4.</b>	<b>Conclusion</b>	66
<b>4</b>	<b>Distribution and fractionation of As in groundwater, soil and sediment</b>	
<b>4.1.</b>	<b>Introduction</b>	69
<b>4.2</b>	<b>Materials and Methods</b>	71
4.2.1.	Study Area	71
4.2.2.	Sampling and analysis	75
4.2.2.1.	Groundwater	75
4.2.2.2.	Subsurface sediment	75
4.2.3.	Chemical and reagents	75
4.2.4.	Sediment processing and digestion methodology	76
4.2.5.	Apparatus and analysis	77
4.2.6.	X-Ray diffraction (XRD) analysis	77
4.2.7.	Quality assurance and quality control	77
<b>4.3.</b>	<b>Results and discussion</b>	78
4.3.1.	Inorganic arsenic in groundwater	78
4.3.2.	Spatial distribution of As(III) in groundwater	80
4.3.3.	Principle component analysis in groundwater	82
4.3.4.	Arsenic species in subsurface sediments	85
4.3.4.1.	Vertical distribution of As in subsurface sediment	85
a.	Study area 1 (Gorakhpur)	87
b.	Study area 2 (Ghazipur)	92
4.3.4.2.	Multivariate analysis for subsurface sediment	95

---



---

4.3.4.3.	Mineralogy of the subsurface sediment	97
<b>4.4.</b>	<b>Conclusions</b>	100
<b>4.5.</b>	<b>Supplementary material</b>	102
<b>5</b>	<b>Understand the groundwater dynamics, recharge/discharge and DOC behavior using stable isotopes in relation to arsenic mobilization</b>	
5.1	Introduction	105
5.2	Material and methods	107
5.2.1.	Study area	107
5.2.2.	Sample collection and analysis	107
5.2.3.	Isotopic analysis	109
5.3.	Results and discussion	110
5.3.1.	Solute chemistry and isotope signature	110
5.3.2.	Stable isotope signature of water samples	117
5.3.3.	Sources of groundwater DIC, $p\text{CO}_2$ and $\delta^{13}\text{C}$	125
5.3.4.	Interrelationship among stable isotopes and physicochemical parameters	127
5.4.	Conclusions	129
5.5.	Supplementary material	131
<b>6</b>	<b>Identification of source and health risk of arsenic and other trace metals to the human population</b>	
6.1	Introduction	138
6.2	Material and methods	139
6.2.1.	Study area description, sample collection and preparation	139
6.2.2.	Chemical and reagents	139
6.2.3.	Sediment digestion procedure	139
6.2.4.	Instrumentation	139
6.2.5.	Quality control and quality assurance	140
6.2.6.	Statistical analysis	140
6.2.7.	Pollution evaluation indices and chemical toxicity	141
6.2.7.1.	Degree of contamination	141
6.2.7.2.	Chemical toxicity	141
a.	Ingestion pathway	142
b.	Dermal contact pathway	144
6.2.8.	Assessment of the heavy metals in sediment	145
6.2.8.1.	Geoaccumulation index	145
6.2.8.2.	Enrichment factor	146
6.2.8.3.	Contamination factor	147
6.3.	Results and discussion	148

---

---

6.3.1.	Descriptive analysis of As and trace metals in groundwater	148
6.3.2.	Health risk assessment due to As and trace metals exposure	148
6.3.3.	Descriptive analysis of As and trace metals in sediment	150
6.3.4.	Statistical analysis (Pearson's correlation matrix)	152
6.3.5.	Sediment quality assessment	157
6.3.5.1.	Geoaccumulation Index	157
6.3.5.2.	Enrichment factor	159
6.3.5.3.	Contamination factor	161
<b>6.4.</b>	<b>Conclusions</b>	<b>163</b>
<b>7</b>	<b>Conclusions and future research</b>	<b>164</b>
<b>7.1.</b>	<b>Summary and conclusions</b>	<b>164</b>
<b>7.2.</b>	<b>Outlook for future research</b>	<b>168</b>
	References	169
	Curriculum vitae	195

---

## List of Table

Table 3.1: Summarized statistical results of major and trace metals in the groundwater of younger and older alluvium and river water in study area 1 (Gorakhpur) (ND = Not detected)	33
Table 3.2: Summarized statistical results of major and trace metals in the groundwater of younger and older alluvium and river water in study area 1 (Ghazipur) (ND = Not detected)	34
Table 3.3: Statistical summary of sediment geochemistry (older and younger alluvium) of the study area 1 (Gorakhpur)	36
Table 3.4: Statistical summary of sediment geochemistry (older and younger alluvium) of the study area 2 (Ghazipur)	40
Table 3.5: Mineralogy of the selected sediment core from both the study area	48
Table 4.1: As species in the groundwater of older and younger alluvium with depth, pH and ORP in different geomorphological setups of both the study areas (Gorakhpur) and (Ghazipur).	79
Table 4.2: Variation of principal component (PC) unit with different parameters in the groundwater of different geomorphic setups of the study areas.	83
Table 4.3: Statistical summary of As and soil texture in the sediment core of study area 1 (Gorakhpur)	86
Table 4.4: Statistical summary of As and soil texture in the sediment core of study area 2 (Ghazipur) a. Jagadishpur and b. Firozpur	91
Table 4.5: PCA loading for the physicochemical parameter, soil texture and arsenic species in sediment cores	102
Table 5.1: Physiochemical and isotopic composition of groundwater (Gorakhpur)	111
Table 5.2: Physiochemical and isotopic composition of groundwater (Ghazipur)	114
Table 5.3: Groundwater data collected in Gorakhpur district. (Note: depth expressed in meter, HCO <sub>3</sub> , Ca and DOC in mg/L and isotopic signature expressed in (‰)).	131
Table 5.4: Groundwater data collected in Ghazipur district. (Note: depth expressed in meter, HCO <sub>3</sub> , Ca and DOC in mg/L and isotopic signature expressed in (‰)).	134
Table 6.1: Elements with their corresponding wavelength and method detection limit	140
Table 6.2: Input parameter and abbreviation for risk calculation	143

---

Table 6.3: Heavy metal and reference doses for the calculation of non-carcinogenic exposure to human health	145
Table 6.4: Statistical summary of As and trace metal, degree of contamination and hazards index in groundwater study areas.	148
Table 6.5: Statistical summary of the sediment core in the study area 1 (Gorakhpur)	151
Table 6.6: Statistical summary of the sediment core in the study area 2 (Ghazipur)	152

---

## List of Figures

<i>Figure 1.1: World map illustrating the Arsenic-affected countries with the intensity shown by the red circles (Adapted from: Shaji et al., 2021).</i> .....	4
<i>Figure 1.2: Arsenic contamination scenario in states and Union Territories of India. Twenty states and four Union territories are affected till now (Adapted from: Shaji et al., 2021).</i> .....	6
<i>Figure 1.3: Arsenic-affected states and union territories superimposed on geology map of India. The alluvial aquifer is more affected in the diagram compared to the hard rock terrane (Adapted from: Shaji et al., 2021, CGWB, 17-18).</i> .....	7
<i>Figure 2.1: Showing the Geology of the Gangetic basin and surrounding areas. Cubic areas on the map are our study areas, Gorakhpur and Ghazipur. River Rapti is flowing through the Gorakhpur and river Ganga flowing through the Ghazipur districts. (Adapted from: Heroy et al., 2003).</i> ...	20
<i>Figure 3.1: Map of the study area, (a). India with state boundary and study area marked as a square, (b). Landsat images are prepared from FCC (false-color composite) band combinations (5, 4 and 3) to distinguish the image in different geomorphic features available in the study area, (c). Study area map with different geomorphic features (older alluvium, younger alluvium, point bars, forest and river etc. with As concentration</i> .....	6
<i>Figure 3.2: Map of the study area, (a). India with state boundary and study area marked as a square, (b). Landsat images are prepared from FCC (false-color composite) band combinations (5, 4 and 3) to distinguish the image in different geomorphic features available in the study area, (c). Study area map with different geomorphic features (older alluvium, younger alluvium, point bars, forest and river etc. with As concentration</i> .....	7
<i>Figure 3.3: Depth-wise variation of elements in the sediment cores of older and younger alluvium</i> .....	19
<i>Figure 3.4: Litholog illustrating the various lithofacies and depth-wise distribution of As in sediment cores (Study area 1, Gorakhpur)</i> .....	20
<i>Figure 3.5: Depth-wise variation of elements in the sediment cores of older and younger alluvium.</i> .....	22
<i>Figure 3.6: Litholog illustrating the various lithofacies and depth-wise distribution of As in sediment cores (Study area 2, Ghazipur)</i> .....	23
<i>Figure 3.7: Eh-pH diagram showing the thermodynamically stable area in groundwater (a) arsenic and (b) iron species in the study area 1 (Gorakhpur)</i> .....	26
<i>Figure 3.8: Eh-pH diagram showing the thermodynamically stable area in groundwater (a) arsenic and (b) iron species in the study area 1 (Ghazipur)</i> .....	27
<i>Figure 3.9: Piper plot showing groundwater evolution in study area 1 (Gorakhpur), a. Cumulative piper plot for all the samples b. Piper plot for groundwater of YA, c. Piper plot for groundwater of OA and, d. Piper plot for river water samples</i> .....	30

<i>Figure 3.10: Piper plot showing groundwater evolution in study area 1 (Ghazipur), a. Cumulative piper plot for all the samples b. Piper plot for groundwater of YA, c. Piper plot for groundwater of OA and, d. Piper plot for river water samples.....</i>	<i>31</i>
<i>Figure 3.11: Bivariate scatter diagrams tracing the hydrogeochemistry of the groundwater and river water. Possible weathering in OA, YA and river water (a-f). Evaporation and mineral mediated enrichment in Ya, OA and river water (g-l). Anthropogenic influences in YA, OA and river water (m-r) in study area 1 (Gorakhpur).....</i>	<i>34</i>
<i>Figure 3.12: Bivariate scatter plot tracing the major hydrogeochemical processes in the groundwater and river water of study area 1 (Gorakhpur).....</i>	<i>35</i>
<i>Figure 3.13: Bivariate scatter diagrams tracing the hydrogeochemistry of the groundwater and river water. Possible weathering in OA, YA and river water (a-f). Evaporation and mineral mediated enrichment in Ya, OA and river water (g-l). Anthropogenic influences in YA, OA and river water (m-r) in study area 2 (Ghazipur).....</i>	<i>37</i>
<i>Figure 3.14: Bivariate scatter plot tracing the major hydrogeochemical processes in the groundwater and river water of study area 2 (Ghazipur) .....</i>	<i>38</i>
<i>Figure 3.15: Saturation indices of various minerals obtained from modeling (PHREEQC)in YA, OA and river water of the study area 1 (Gorakhpur).....</i>	<i>40</i>
<i>Figure 3.16: Saturation indices of various minerals obtained from modeling (PHREEQC)in YA, OA and river water of the study area 1 (Ghazipur).....</i>	<i>40</i>
<i>Figure 3.17: Scattered plot of As with physicochemical parameters in YA, OA and river water of study area 1 (Gorakhpur) .....</i>	<i>42</i>
<i>Figure 3.18: Scattered plot of As with Al, Fe and Mn; a. older alluvium, b. younger alluvium, in study area 1 (Gorakhpur) .....</i>	<i>43</i>
<i>Figure 3.19: Scattered plot of As with physicochemical parameters in YA, OA and river water in study area 2 (Ghazipur).....</i>	<i>44</i>
<i>Figure 3.20: Scattered plot of As with Al, Fe and Mn for; a. older alluvium, b. younger alluvium (study area 2, Ghazipur).....</i>	<i>46</i>
<i>Figure 4.1: Map of the study area, (a). India with state boundary, (b). Landsat images are prepared from FCC (false-color composite) band combinations (5, 4 and 3), (c). Study area map with different geomorphic features (older alluvium, younger alluvium, point bars, forest and river etc. The map shows sample location in groundwater and sediment core.....</i>	<i>72</i>
<i>Figure 4.2: Map of the study area, (a). India with state boundary, (b). Landsat images are prepared from FCC (false-color composite) band combinations (5, 4 and 3), (c). Study area map with different geomorphic features (older alluvium, younger alluvium, point bars, forest and river etc. The map shows sample location in groundwater and sediment core.....</i>	<i>74</i>
<i>Figure 4.3: Flow chart of three-step sequential extraction method.....</i>	<i>76</i>
<i>Figure 4.4: pe-pH diagram of the study area, a. Gorakhpur b. Ghazipur .....</i>	<i>80</i>

<i>Figure 4.5: A generalized Geomorphological (older and younger alluvium) map of the study area 1 (Gorakhpur). It also depicts elevated As concentration and distribution based on geomorphology and depth.....</i>	<i>81</i>
<i>Figure 4.6: A generalized Geomorphological (older and younger alluvium) map of the study area 1 (Ghazipur). It also depicts elevated As concentration and distribution based on geomorphology and depth.....</i>	<i>81</i>
<i>Figure 4.7: Four-color of sand with the corresponding risk of As in groundwater as well as redox conditions (Adapted from: Hossain et al., 2014. ....</i>	<i>85</i>
<i>Figure 4.8: a. Litholog of the sediment core, b. photographic view of the fresh sediment of field, c. vertical distribution of As species in the sore sediment (Khorabar) .....</i>	<i>88</i>
<i>Figure 4.9: a. Litholog of the sediment core, b. photographic view of the fresh sediment of field, c. vertical distribution of As species in the sore sediment (Farsiya).....</i>	<i>90</i>
<i>Figure 4.10: a. Litholog of the sediment core, b. photographic view of the fresh sediment of field, c. vertical distribution of As species in the sore sediment (Jagadishpur) .....</i>	<i>93</i>
<i>Figure 4.11: a. Litholog of the sediment core, b. photographic view of the fresh sediment of field, c. vertical distribution of As species in the sore sediment (Jagadishpur) .....</i>	<i>94</i>
<i>Figure 4.12: 3D Component plot in rotates space, a. Khorabar, b. Farshiya .....</i>	<i>95</i>
<i>Figure 4.13: 3D Component plot in rotates space, a. Jagadishpur, b. Firozpur .....</i>	<i>96</i>
<i>Figure 4.14: The mineralogical composition of the core sediment (XRD analysis results), Khorabar (a. at surface sediment, b. at 12.19 mbgl and c. at 30.48 mbgl) and Farshiya (a'. at surface sediment, b'. at 15.4 mbgl and c'. 21.34 mbgl). (A high-resolution image was attached in the supplementary material) .....</i>	<i>98</i>
<i>Figure 4.15: The mineralogical composition of the core sediment (XRD analysis results), Jagadishpur (a. at surface sediment, b. at 15.0 mbgl and c. at 33.12 mbgl) and Firozpur (a'. at surface sediment, b'. at 18.29 mbgl and c'. 30.28 mbgl) (A high-resolution image was attached in annexure) .....</i>	<i>99</i>
<i>Figure 4.16: The mineralogical composition of the core sediment; a. Khorabar and a'. Farshiya .....</i>	<i>103</i>
<i>Figure 4.17: The mineralogical composition of the core sediment; a. Jagadishpur and a'. Firozpur .....</i>	<i>104</i>
<i>Figure 5.1: Box and Whisker plot of the selected parameters in different geomorphic setups (Gorakhpur).....</i>	<i>112</i>
<i>Figure 5.2: Box and Whisker plot of the selected parameters in different geomorphic setups in study area 2 (Ghazipur).....</i>	<i>115</i>
<i>Figure 5.3: Bivariate plot of stable <math>\delta^{18}O</math> and <math>\delta^2H</math>, the Global Meteoric Waterline (GMWL) of Craig (1961) and Local Meteoric water line (LMWL) Patna (Kumar et al., 2010) in study area 1 (Gorakhpur).....</i>	<i>118</i>

<i>Figure 5.4: Vertical variation (depth-wise) of isotopic species in Gorakhpur district .....</i>	<i>120</i>
<i>Figure 5.5: The evaporation plot between d-excess and <math>\delta^{18}O</math> .....</i>	<i>121</i>
<i>Figure 5.6: Bivariate plot of stable <math>\delta^{18}O</math> and <math>\delta^2H</math> for Ghazipur, the Global Meteoric Waterline (GMWL) of Craig (1961) and Local Meteoric water line (LMWL) Patna (Kumar et al., 2010) .....</i>	<i>122</i>
<i>Figure 5.7: Vertical variation of isotopic species in the study area (Ghazipur).....</i>	<i>123</i>
<i>Figure 5.8: The evaporation plot between d-excess and <math>\delta^{18}O</math> .....</i>	<i>124</i>
<i>Figure 5.9: Variation between <math>\delta^{13}CTIC</math> and <math>pCO_2</math>. Boxes show <math>\delta^{13}CTIC</math> and <math>pCO_2</math> for DIC derived from various potentials discussed above. The dotted line (atm.) expressed atmospheric <math>CO_2</math> around 410 ppm. The Arrow line shows the expected processes and changes in the Gorakhpur district. Figure adapted from (Telmer &amp; Veizer, 1999; Li et al., 2019).....</i>	<i>125</i>
<i>Figure 5.10: Variation between <math>\delta^{13}CTIC</math> and <math>pCO_2</math>. Boxes show <math>\delta^{13}CTIC</math> and <math>pCO_2</math> for DIC derived from various potentials discussed above. The dotted line (atm.) expressed atmospheric <math>CO_2</math> around 410 ppm. The Arrow line shows the expected processes and changes in the Ghazipur district. Figure adapted from (Telmer &amp; Veizer, 1999; Li et al., 2019).....</i>	<i>126</i>
<i>Figure 5.11: Bivariate plots of (a) <math>\delta^{13}CTIC</math> vs. ORP, (b) <math>\delta^{13}CTIC</math> vs. DOC, (c) <math>\delta^{13}CTIC</math> vs. TIC, (d) <math>\delta^{13}CTIC</math> vs. <math>HCO_3</math> in study area 1 (Gorakhpur).....</i>	<i>127</i>
<i>Figure 5.12: Bivariate plots of (a) <math>\delta^{13}CTIC</math> vs. ORP, (b) <math>\delta^{13}CTIC</math> vs. DOC, (c) <math>\delta^{13}CTIC</math> vs. Ca, (d) <math>\delta^{13}CTIC</math> vs. <math>HCO_3</math>, study area 2 (Ghazipur).....</i>	<i>128</i>
<i>Figure 6.1: Pearson's correlation matrix (at <math>p=0.05</math>) for sediment core one at Khorabar, Gorakhpur.....</i>	<i>153</i>
<i>Figure 6.2: Pearson's correlation matrix (at <math>p=0.05</math>) for sediment core two at Farshiya, Gorakhpur.....</i>	<i>154</i>
<i>Figure 6.3: Pearson's correlation matrix (at <math>p=0.05</math>) for sediment core one at Jagadishpur, Ghazipur .....</i>	<i>155</i>
<i>Figure 6.4: Pearson's correlation matrix (at <math>p=0.05</math>) for sediment core one at Firozpur, Ghazipur .....</i>	<i>156</i>
<i>Figure 6.5: Geoaccumulation index (Igeo) plot for sediment core at, a. Khorabar b. Farshiya.....</i>	<i>157</i>
<i>Figure 6.6: Geoaccumulation index (Igeo) plot for sediment core at, a. Jagadishpur b. Firozpur .....</i>	<i>158</i>
<i>Figure 6.7: Enrichment factor (EF) plot for sediment core at, a. Khorabar b. Farshiya .....</i>	<i>160</i>
<i>Figure 6.8: Enrichment factor (EF) plot for sediment core at, a. Jagadishpur b. Firozpur .....</i>	<i>161</i>
<i>Figure 6.9: Contamination factor (CF) plot for sediment core at, a. Khorabar b. Farshiya ....</i>	<i>161</i>
<i>Figure 6.10: Contamination factor (CF) plot for sediment core at, a. Jagadishpur b. Firozpur .....</i>	<i>162</i>



---

## Abbreviation

As (III)	= Arsenite
As (V)	= Arsenate
As (t)	= Arsenic (total)
BGS	= British Geological Survey
BIS	= Bureau of Indian Standard
CGP	= Central Gangetic Plain
DMA	= Di-methylarsinic Acid
DPHE	= Department of Public Health Engineering, Dhaka
MDL	= Method Detection Limit
MMA	= Mono-methylarsonic Acid
OA	= Older Alluvium
ORP	= Oxidation Reduction Potential
PHED	= Public Health Engineering Department
TMs	= Trace Metals
USEPA	= U.S. Environmental Protection Agency
WHO	= World Health Organization
PCA	= Principal Component Analysis
LLNL	= Lawrence Livermore National Laboratory
ICDD	= International Centre for Diffraction Data
SRM	= Standard Reference Material
NIST	= National Institute of Standards and Technology
RSD	= Relative Standard Deviation
FCC	= False Color Composite
UTM	= Universal Transverse Mercator
WGS	= World Geodetic System
USGS	= United States Geological Survey
XRF	= X-ray Fluorescence
XRD	= X-ray Diffraction
DOC	= Dissolved Organic Carbon
NRDWP	= National Rural Drinking Water Programme
MoJS	= Ministry of Jal Shakti

# Chapter 1

## Introduction

### 1. Introduction

- 1.1 Sources and occurrences of arsenic in the environment
- 1.2 Global scenario of As contamination (an overview)
- 1.3 Arsenic contamination in India
- 1.4 Arsenic contamination in groundwater, soil and sediment
- 1.5 Arsenic mobilization
  - a. Pyrite dissolution
  - b. Reductive dissolution of iron oxyhydroxide
  - c. Alkali desorption
  - d. Geothermal
- 1.6 Arsenic speciation and its role in mobilization
- 1.7 Application of stable isotopes in As contamination
- 1.8 Arsenic and trace metal exposure and health effect
- 1.9 Arsenic contamination in Central Gangetic Basin
- 1.10 Relevance of the study
- 1.11 Research hypothesis and objectives

## 1. Introduction

Water is not only a vital component for human survival, but it also serves as the foundation for the long-term viability of our global ecology. In humans, around 60% of our body's weight is built up by the water. More than 90% of body weight in some organisms resulted from water (Popkin et al., 2010). On Earth, only 2.8% of the total water, contributed by surface (river, lake, glacier, etc.) and groundwater, is considered fresh (Meissner & Mampane, 2009; Gupta & Sarma, 2016). Groundwater is their primary water source for millions of people worldwide, from shallow drilled wells or deeper tube wells (Carrard et al., 2019). India covers only ~3% of the entire world's land area, with ~23% of the total global population (Mukherjee et al., 2015; Sharma et al., 2018; FAO, 2021). Increasing population and development of the economy increase the human water demand. Water is a valuable resource that can never be replaced. Many countries and regions are currently experiencing varying degrees of water scarcity (Rijsberman, 2006; Garg & Hassan, 2007; Boretti et al., 2019). Toxic substance contamination of public drinking water systems causes a severe problem on a global scale (Page, 1981). Groundwater pollution is assumed to be less vulnerable than surface water (Konikow & Kendy, 2005; Sasakova et al., 2018). The requirement of groundwater daily increases to enhancement industrialization, urbanization and agricultural sectors etc., development. The unmanaged withdrawal of water from an aquifer causes groundwater depletion. Groundwater depletion is a severe problem in Middle and South-East Asia, North America, North China, North Africa, Australia, and isolated regions around the globe (Konikow & Kendy, 2005). Other natural events like climate change and scorching summer also contributed to groundwater depletion and frequently causes drought severity (Udmale et al., 2016).

In India, the primary source of groundwater recharge is rainfall, but uncertainty regarding rainfall time and place and undeveloped rainwater management cause floods. However, India is one of the most drought-prone nations in the world. Drought affects almost two-thirds of the country, and the per capita water supply diminishes as the population grows (Udmale et al., 2016). According to World Resources Institute (WRI), India falls in the extremely high baseline water-stressed region in National Water Stress Ranking. Groundwater is one of the crucial water resources for Indian people, and about 85 percent of the population relying on it. The physical and chemical properties of groundwater in an area are mainly altered by geological and anthropogenic

input (Srinivasamoorthy et al., 2014). Many researched revealed groundwater contamination occurs due to agricultural and industrial wastewater discharge (Stefanakis et al., 2015; Herath et al., 2016; Venkatesan & Subramani, 2018; Sharma et al., 2020; Nath et al., 2021). The groundwater quality also deteriorated by the influence of geogenic sources such as As (arsenic), F (fluoride), trace metals, radioactive pollutions etc., (Shah, 2015; Verma et al., 2015; Mukherjee, 2018; Yadav et al., 2020; Chattopadhyay et al., 2020).

## 1.1 Sources and occurrences of arsenic in the environment

As (arsenic) is a p-block element with an atomic number of 33 and molecular weight 74.9 g/mol. In the outer shell, As having five electrons that belong to the nitrogen group row and 20<sup>th</sup> most prevalent naturally occurring element in Earth's crust. As(-III), As(0), As(III), and As(V) are the most common oxidation states of As. In natural groundwater, inorganic arsenic is found in the form of arsenite (AsIII) and arsenate (AsV). Arsenite is predominantly present in reducing water, while arsenate is dominant in oxidizing water. Organic species of As are mostly detected at an ultra-trace level in groundwater. Three major organic species of As such as mono-methylarsonic acid (MMA), di-methylarsinic acid (DMA), and arsenobetain has been reported in aquatic animal (Schramel et al., 2002; Gault et al., 2003; Khairul et al., 2017). The toxicity of inorganic As is much higher than the organic forms of As, and both are harmful to human health. In the case of inorganic arsenic species, As(III) is more poisonous and mobile than As(V).

As is a metalloid and naturally available in numerous minerals. Arsenic is also found in allotropes (solid form) with yellow, grey and black colors. Arsenic present in more than 200 minerals species, mainly sulfide and iron-containing minerals, reported high As concentration (Bissen & Frimmel, 2003; Shankar et al., 2014). The most common mineral of As is arsenopyrite, made up of iron, sulfur and As and generally present in an anoxic environment. Other minerals like realgar, orpiment and enargite also contain As on a small scale (Acharyya et al., 1999). The nature of the minerals and their texture also significantly influences the concentration of the As in sediment, ranging from 3 to 10 mg/kg (Brammer & Ravenscroft, 2009). Large quantities of Fe oxide, hydrous metal oxides or pyrites have exceptionally high amounts of As in sediments than other oxides. The depth-wise As concentration in the sediment increases with reducing sedimental condition (Roychowdhury, 2010; Robinson et al., 2016; ). Arsenic in the soil or sediment can

easily dissolve in the groundwater and become the source of river water contamination and seawater (Kim et al., 2015; Chatterjee et al., 2017). Geothermal water, such as the hot springs at Hot Creek, Nevada, may also be a source of direct arsenic mixing into the aquatic environment (Wilkie & Hering, 1998). Adsorption of arsenic to mineral surfaces (Fe oxide, hydrous oxide of metals and fine sediment with organic matter) serves as a significant sink. The minerals assemblages are presumed to be the essential source for As mobilization in the groundwater of India and Bangladesh basin. The reductive dissolution of weathered alluvial sediment coated with Fe(III) oxides is the well-accepted hypothesis of As mobilization in the groundwater (Nickson et al., 1998; Acharyya et al., 1999; Acharyya & Shah, 2007; Ghosh et al., 2010; Barringer & Reilly, 2013; Verma et al., 2015; Kumar et al., 2018; Mukherjee, 2018; Yadav et al., 2020).

## 1.2 Global scenario of As contamination (an overview)

Groundwater As contamination can be geogenic or anthropogenic and spread improperly throughout the groundwater system (e.g., hydraulic fracturing). As a result, its contamination can affect a significant number of individuals (Bagchi, 2007; Murcott, 2012). As first discovered in a well in Argentina in 1917 and has since been found in shallow aquifers in over seventy nations, with India being the most prominent (Mukherjee et al., 2006). Groundwater pollution caused by As has been documented in many places around the globe, including the United States, China, Africa, Europe, and South Asian countries (Nickson et al., 1998; Schreiber et al., 2000; Chen & Ma, 2001; Mandal, 2002; Smith et al., 2003; Appleyard et al., 2006; Mukherjee et al., 2006; Zavala et al., 2008; Sappa et al., 2014; Shankar et al., 2014; Wu et al., 2014; Mahanta et al., 2015; Herath et al., 2016; Mayer & Goldman, 2016; Chatterjee et al., 2017; DeVore et al., 2019; Yadav et al., 2020; Rahman et al., 2021) (Figure 1.1).

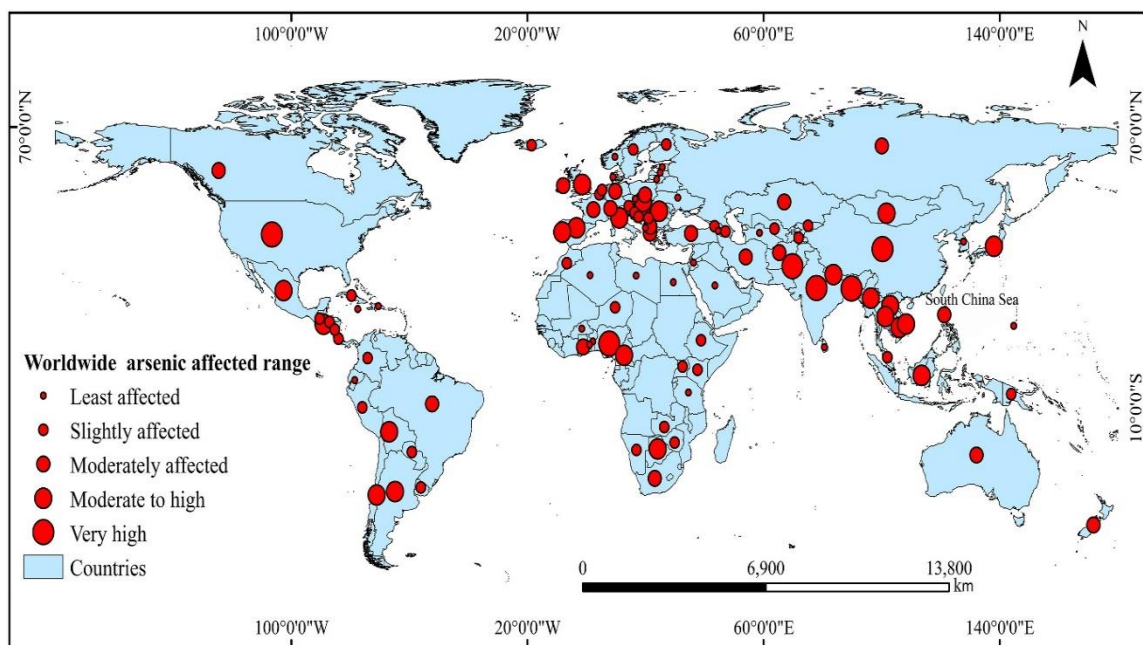


Figure 1.1: World map illustrating the Arsenic-affected countries with the intensity shown by the red circles (Adapted from: [Shaji et al., 2021](#)).

In Asia, the river delta aquifers from India, Bangladesh and Vietnam are reported As contamination regularly ([Berg et al., 2001](#); [Smedley, 2005](#); [Van Geen et al., 2006](#); [Winkel et al., 2011](#)). The As finding in Latin America is relatively newer, and new studies from various sections of the continent are being identified every day ([Budschuh et al., 2012](#)). For the African continent, significantly fewer studies have been reported. Around the globe, India (particularly West Bengal) and Bangladesh are highly vulnerable ([PHED, 1993](#); [BGS and DPHE, 2001](#)), and hundreds of millions of individuals are at risk of developing As-related diseases ([Smith et al., 2000](#); [Mandal 2002](#); [Smedley, 2005](#); [Martinez et al., 2011](#); [Chakraborty et al., 2018](#)).

### 1.3 Arsenic contamination in India

In India, [Datta & Kaul \(1976\)](#) reported the first case of As toxicity from drinking water in Chandigarh in early 1976, followed by several reports of As-induced skin lesions in Kolkata, the capital of West Bengal state, has been reported in 1984 ([Garat et al., 1984](#)). Since then, several states bordering the upper, middle, and lower Gangetic and Brahmaputra plains have been infected with chronic As illnesses ([Sarin & Krishnaswami, 1984](#); [Chakraborti et al., 2003](#); [Ghosh et al., 2007](#); [Shah, 2008](#); [Chauhan et al., 2009](#); [Bhardwaj et al., 2010](#); [Chakraborty et al., 2015](#); [Saha &](#)

Sahu, 2016; Chakraborti et al., 2017; Kumar et al., 2018; Singh et al., 2020; Yadav et al., 2020). The NRDWP (National Rural Drinking Water Programme), a subdivision of the Ministry of Jal Shakti (MoJS) has published a recent report on As contamination and an estimated number of people's lives at risk. According to the NRDWP report, more than ten million people are at immediate threat by drinking As contaminated water in West Bengal, Assam, Bihar, Uttar Pradesh, Haryana, Punjab and Jharkhand. Several workers conducted substantial research on groundwater As contamination in India, particularly in the Ganga basin (Chakraborti et al., 2018; Shaji et al., 2021; references therein).

The Ganga and Brahmaputra river basin is one of the wealthiest groundwater provinces of the country (Singh, 2006). The majority of the extraction occurs in Northern and Northwestern India throughout the Indo-Gangetic basin, resulting in considerable drawdown and water table fall in several areas (Shaji et al., 2021). According to Shaji et al. (2021), around 20 Indian states and four union territories are highly As contaminated (Figure 1.2).

In India, two types of terrane identified with high As contamination in the groundwater; a. alluvial terrane and b. hard rock terrane. Approximately 90% As contamination was centered in the alluvial aquifer, only 10% was associated with hard rock terrane (Figure 1.3). As is mainly limited to gold-mining sites from Karnataka, while in Chattisgarh, As associated with the acid volcanic linked with the Kotri lineament.

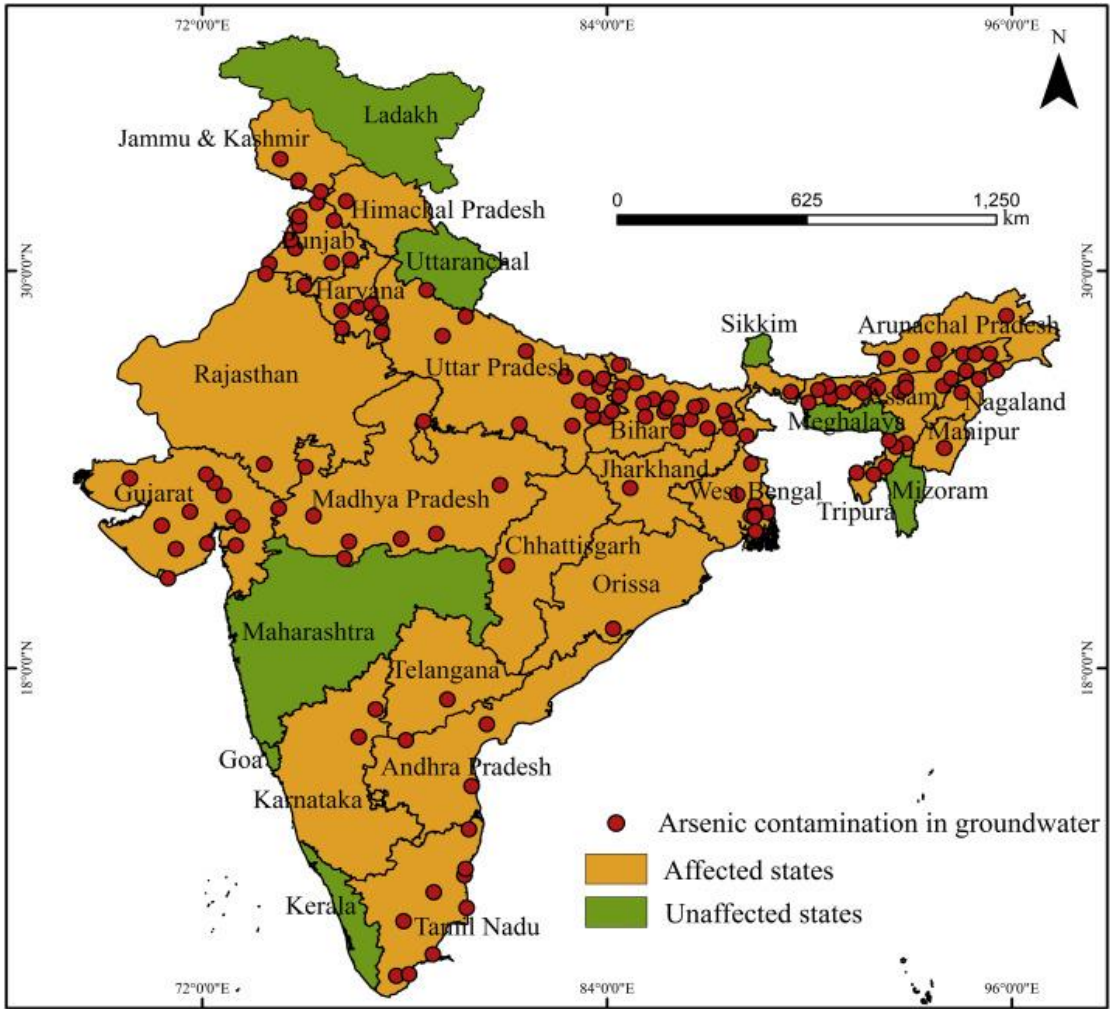


Figure 1.2: Arsenic contamination scenario in states and Union Territories of India. Twenty states and four Union territories are affected till now (Adapted from: [Shaji et al., 2021](#)).



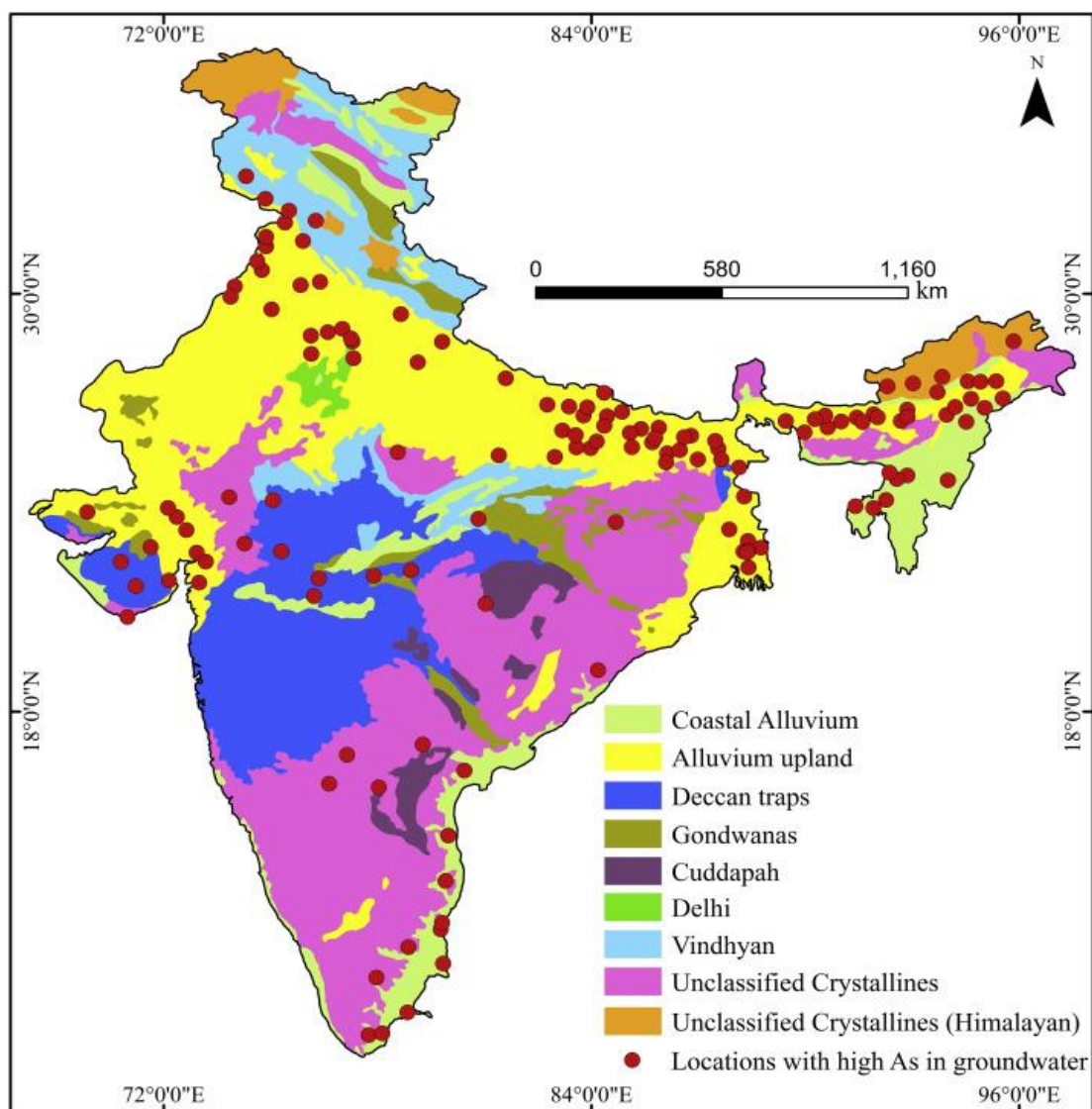


Figure 1.3: Arsenic-affected states and union territories superimposed on geology map of India. The alluvial aquifer is more affected in the diagram compared to the hard rock terrane (Adapted from: *Shaji et al., 2021, CGWB, 17-18*).

#### 1.4 Arsenic contamination in groundwater, soil and sediment

Arsenic enters the food chain via irrigation water, soil-plant systems once prevalent in the environment (*Shankar et al., 2014*). The direct consumption of As-contaminated groundwater has proven disastrous in several parts of India and worldwide (*Shankar et al., 2014; Srivastava, 2020*). As contamination of agricultural soil has become a growing concern, arsenic passes from soil to various trophic levels of the ecosystem and humans, particularly through plant uptake animal

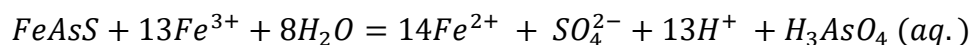
consumption (Kumar et al., 2016b). The maximum permissible limit for As in agricultural soil is 20 mg/kg prescribed by U.S. Environmental Protection Agency (Rahaman et al., 2013). According to research, As distribution in the sediment is significantly influenced by metal oxides and organic matters. The size of the soil texture also influences the adsorption and desorption of As in the soil. Usually, the As concentration in clays and peats is ten times higher than in the sandy sediment. Clays sediment or peat contains a maximum of 100 mg/kg As, while sand sediment contains a maximum of 10 mg/kg As (Nickson et al., 1998; Chakraborty et al., 2015). The concentration of the solid phase of As is usually high in the irrigated soil. However, this could be due to arsenic input through groundwater irrigation and sorption of the soil (Harvey et al., 2005).

## 1.5 Arsenic mobilization

Four major processes predominantly control arsenic transportation and mobilization in the groundwater; Pyrite oxidation, competitive ion exchange, reductive dissolution of iron oxyhydroxide and reduction and reoxidation (Srivastava, 2020).

### a. Pyrite dissolution

Pyrite dissolution is also known as sulfide oxidation. Several authors have suggested that pyrite oxidation is thought to play a crucial role in mobilization in the alluvial aquifer of India and Bangladesh (Chakraborty et al., 2015). In this process, sulfide minerals such as pyrite or arsenopyrite are oxidized in oxygen near the water table. The water should be sulfide-rich and acidic but not necessary to contain a high Fe concentration (Kumar et al., 2018). In pristine condition, As and S was dominant species and existed in multivalent oxidation state. Fe oxyhydroxides constituted the main Fe surface species after reaction with air-saturated distilled water. At the same time, As(V), As(III), and As(I) also exist in the aqueous environment and As(I) is the dominant surface species (Blowes et al., 2014). The equation for the As-bearing pyrite minerals dissolution can be expressed as follows:

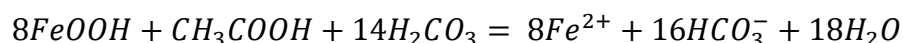


The shallow water well with over-exploitation of groundwater is more prone to pyrite oxidation than deeper wells. Sulphide oxidation and As mobilization was reported from

Washington state USA, Nova scotia, Ghana, France and central Asia (Ravenscroft et al., 2005, 2009).

### b. Reductive dissolution of iron oxyhydroxide

The desorption of As from iron oxyhydroxide in reducing conditions is the most widely recognized theory for India and Bangladesh. According to this theory, As is mobilized by the dissolution of metal oxides and Fe hydroxides (Shah, 2015; Verma et al., 2015; Kumar et al., 2018; Yadav et al., 2020). Most As-contaminated water worldwide has been discovered to have an extremely low redox potential, which is a sign of reduced circumstances. According to this theory, As has been adsorbed on clay surface coated with iron oxyhydroxide in alluvial and deltaic regions (Yadav et al., 2020). The bacterial decomposition of organic matter breaks down the metal oxides and iron oxyhydroxide minerals and releases As in the aqueous solution. A group of bacteria known as *Geobacter*, involved in the decomposition of organic matter and metals oxides and reduced Fe(III) into Fe(II) and helped to release the As(V) in the aqueous environment (Smedley & Kinniburgh, 2002; Acharyya & Shah, 2007; Shah, 2015). Bicarbonate is also significantly involved in As mobilization in the aqueous environment, while  $\text{NO}_3^-$  and  $\text{SO}_4^{2-}$  are most probably absent (Kumar et al., 2018). The processes of organic matter decomposition in the presence of bacteria and reductive dissolution of iron is represented by the following equation;



South Asian provenances such as India, Bangladesh, China, and Vietnam face the As contamination in the groundwater and As mobilization is mainly governed by dissolution processes.

### c. Alkali desorption

Alkali desorption is the second most common process of As mobilization. In this process, As is mobilized in the presence of higher pH ( $\leq 8$ ) and high dissolved  $\text{O}_2$ ,  $\text{NO}_3^-$ , and  $\text{SO}_4^{2-}$  and low concentration of Fe and Mn with evolving water known as "alkali-oxic" (Ghosh et al., 2010). Research has been identified that maximum adsorption of As(V) occurred at pH 5 and As(III) was occurred at pH 8-9. The sorption/desorption of arsenic in the groundwater is dependent on the pH

and competitive ions (Luo et al., 2019). The basin-Range provinces of the USA and Pampean plain of Argentina are the best example of this process.

#### d. Geothermal

In the deep geothermal reservoir, As present in pyrite and arsenopyrite minerals. Naturally occurred As in the geothermal reservoir has been detected in many countries including Alaska, Central America, western USA, Northern Chile, Japan, Taiwan, Iceland, Indonesia, France and Philippines etc., (Bundschuh & Maity, 2015). The As concentration in the geothermal water is very high and temperature-dependent. As is predominantly present as neutral  $\text{H}_3\text{As(III)O}_3$  (arsenous acid) in geothermal reservoirs, while in the deeper part of the geothermal system, it is present in thioarsenites under sulfidic conditions (Bundschuh & Maity, 2015). The upper surface of the earth system, which is close to the atmospheric oxygen, causes an oxidizing environment where As(V) is the dominant species, but it is a slow process. A few meters up from the spring outflow, As(III) is the dominant species in the geothermal spring, but it was swiftly oxidized by microbial catalysis and converted to As(V) (Connon et al., 2008).

### 1.6 Arsenic speciation and its role in mobilization

Arsenic enters the environment through hydro-geochemical processes and anthropogenic inputs (Smedley & Kinniburgh, 2002). Arsenic is a multivalent element and is involved in various biogeochemical activities. As causes severe toxicity effect on human health at a low level of exposure and categories as class I carcinogen (Wang et al., 2016; Kumar & Ramanathan, 2018). Arsenic is most commonly found in the form of inorganic As species such as  $\text{AsH}_3$ , As(III) and As(V). The organic form of As is rare, and it is present in the form of methyl and dimethyl compound. The inorganic As species are more toxic than organic As species, while inorganic As(III) is more toxic and mobile than inorganic As(V) (Dixit & Hering, 2003; Gault et al., 2003). The behavior of As is distinctly different from the other oxyanions forming metalloids, and the pH of the groundwater significantly influences its mobilization (Smedley & Kinniburgh, 2002). As the pH rises, arsenate becomes more mobile (Kumar et al., 2016). The bioavailability of As in sediment, its mobilization, toxicity, retention time, chemical behavior and potential risk to human health in the environment are all influenced by the form in which As is available in the groundwater

(Kumar et al., 2016). In oxygenated or well-drained soil, arsenate is the dominant species, while in reducing conditions, generated by degradation of organic matter and regularly flooded areas associated with elevated arsenite (Acharyya et al., 1999). The availability of total As in groundwater and sediment are insufficient to calculate the environmental exposure scenario (Kumar et al., 2016). So, arsenic speciation is a robust tool for determining the environmental impact and risk to human health.

In soil or sediment, the geochemistry of As was widely controlled by metal (Fe and Mn) oxides and aluminosilicate minerals through adsorption and desorption processes (Chen et al., 2019). The arsenic availability in soil is also dependent on the amount of the sorbing compound, pH and redox potential of the soil. Arsenic mobility in the sediment is very low. It has been shown that solubility of As increased with high salinity, extreme pH and high P concentration, and high resuspension events.

### 1.7 Application of stable isotopes in As contamination

The application of stable isotopes ( $\delta^{18}\text{O}$  and  $\delta^2\text{H}$ ) is an important tool for understanding the aquifer recharge/discharge and subsurface hydrological processes on a regional scale (Saha et al., 2011; Mukherjee et al., 2012; Parda et al., 2016; Thilagavathi et al., 2016; Das & Pal, 2020). Since the early 1990s, naturally occurring environmental isotopes in natural water investigations have grown in popularity (Bishop, 1990). The use of stable isotopes in groundwater research is critical for determining the source, age, and kind of water. Stable isotopes are also used to study various hydrological processes in nature, including precipitation source, groundwater recharge, river and lake source identification, hydrograph separation, surface water groundwater interaction, evaporation and evapotranspiration etc., (Rai et al., 2014). The changes in the behavior of isotopic composition in water along the flow channel reveal information about the water's history, including mixing, mineralization, and recharge/discharge (Kumar et al., 2016; Joshi et al., 2018).

It is well known that water on the Earth's surface was primarily derived from precipitation and evaporation. At a particular site, meteoric activities alter the isotopic signature of precipitation. This characteristic acts as a natural tracer for locating groundwater recharge sources (Gupta & Deshpande, 2003; Rai et al., 2014). Hence, understanding the variation in precipitation and

evaporation in an area, a stable isotopic signature tool has been used widely. Various research has been conducted to understand the origin of precipitation and evaporation processes in groundwater its role on groundwater recharge using stable isotopes ( $\delta^{18}\text{O}$  and  $\delta^2\text{H}$ ) in The Gangetic basin (Sengupta et al., 2008; Kumar et al., 2010; Saha et al., 2011; Mukherjee et al., 2012; Singh et al., 2013; Rai et al., 2014; Kumar et al., 2016; Joshi et al., 2018).

Dissolve organic carbon (DOC) plays various significant roles in groundwater. It is one of the primary carbon and energy sources for heterotrophic microbial communities to thrive and is responsible for reducing conditions in the middle Gangetic basin (Cooper et al., 2016). And it is well known that reducing conditions are significantly involved in carbon cycling and metal transportation, including As mobilization in groundwater. The ratio of  $\delta^{13}\text{C}$  to  $^{12}\text{C}$  is 1 percent in the natural water. The alteration in this ratio can be related to the environmental history of carbon, which aids in tracing the DOC source in the natural water (Kumar et al., 2016).

## 1.8 Arsenic and trace metal exposure and health effect

Due to its extraordinarily high toxicity, arsenic has been considered one of the most severe hazards to living organisms for ages. Thus, it is referred to as the “king of poisons” (Nriagu et al., 2007). Millions of people around the globe are infected with As. It entered into human lives through food, water and air (Shankar et al., 2014; Chakraborti et al., 2017). It was estimated that around 99% absorption of As occurs through ingestion of food and drinking, while dermal absorption of As is negligible except occupational accidental (Saha et al., 1999). Consumption of arsenic cause acute and chronic dysfunction of the organs and several types of cancers. As existed in both inorganic and organic form, and inorganic As is more mobile and toxic than organic arsenic (Smedley & Kinniburgh, 2002; Shankar et al., 2014). Arsenite is 20-50 times severely harmful than arsenate and obstructs the methylation mechanism by degenerating the neurons in the human body (Intarasunanont et al., 2012). Long-term exposure to As contaminated water causes chronic poisoning such as skin cancer, liver disorder, renal failure, etc. Men are more susceptible to As poisoning than the female (Mazumder, 2008).

The distribution of As and trace metals in sediment and water can determine the extent of the metals poisoning caused by geogenic and anthropogenic inputs. Estimating the possible human

health risk associated with As exposure through contaminated water has become a widely used approach in recent years (Saha et al., 2011; Saha et al., 2017). A standard approach has been used to calculate human risk assessment, prescribed by US Environmental Protection Agency (USEPA, 1989). Human risk assessment was assigned for a single representative value for each potentially harmful metal, resulting in a single risk output value (Saha et al., 2017; Zhang et al., 2019).

Globally, there is no effective cure for arsenicosis, mitigation techniques and long-term water development are the only hope for avoiding diseases associated with the As threat. Another best strategy to treat your conditions by eliminating yourself from As exposure. Furthermore, finding a maximum value of As in water and food is difficult due to the lack of a dose-response relationship for determining the carcinogenicity of As. The maximum acceptable limit for As in potable water is 10 ppb prescribed by WHO (2011) and BIS (Bureau of Indian standard, 2012).

### 1.9 Arsenic contamination in Central Gangetic Basin

Previously it was assumed that As contamination was limited to the shallow aquifer of Bhagirathi and Hooghly rivers in West Bengal. But several research studies have confirmed the elevated As concentration in the groundwater of the upper and middle Gangetic basin in Uttar Pradesh, Bihar and adjoining areas such as Haryana, Punjab and Jharkhand (Mandal, 2002; Acharyya & Shah, 2007; Shah, 2008; Shankar et al., 2014; Verma et al., 2015; Mahanta et al., 2015; Kumar et al., 2016; Shaji et al., 2021). In India, a large geological domain is affected by As contamination, mainly derived from natural geogenic settings. The anthropogenic inputs include mining, industrial and thermal water activity also contribute As on a localized scale (Acharyya & Shah, 2007). The geology of the Central Gangetic plain is made up of Holocene and Pleistocene deposits. Holocene deposits are again divided into older and younger alluvium. The younger alluvium mainly consists of freshly deposited silt and clay and is highly rich in organic matter, enhancing As mobilization in the study area. (Singh, 2006; Saha, 2009). The As contamination was limited to shallow depth (0 to 40 mbgl) in the central Gangetic plain, also known as the hot spots region. The elevated As concentration is significantly associated with fine silty clay lenses with micaceous grey enriched with organic matter (Saha et al., 2010; Saha & Sahu, 2016). As concentration significantly changed between the tube well on a short distance due to groundwater recharge/discharge and river influences (Kumar et al., 2018). The central Gangetic plain has well

distinct geology and geomorphology setup compared to the lower Gangetic plain. River geomorphology such as river meandering, avulsion, river bed and levees etc., significantly influence the As mobilization in the central Gangetic plain. Due to these uneven changes in a short location, the concentration of As is highly variable.

### 1.10 Relevance of the study

Several studies on As pollution in groundwater, soil, and sediment in the middle and lower Gangetic plains have been conducted (Ahamed et al., 2006; Ali et al., 2012; Srivastava & Sharma, 2013; Kumar et al., 2014; Saha & Sahu, 2016; Kumar et al., 2018). Only a few researchers have attempted to comprehend the role of geochemical processes, the behavior of the subsurface chemistry in different geomorphic setups in two different study areas, and their role on As distribution and quantification in groundwater, soil and sediment in the central Gangetic plain. To identify the groundwater and subsurface sediment interaction, geochemical processes and their role on As mobilization in the central Gangetic plain.

Stable isotopes ( $\delta^{18}\text{O}$  and  $\delta^2\text{H}$ ) applications were used to understand the groundwater recharge and discharge, source, history and age of the groundwater, and the interlinkage between groundwater and surface water. Several studies have been conducted thoroughly to apply stable isotopic signature tools to identify the origin and interaction of aquifer and surface water in the lower Gangetic plain (Saha et al., 2011; Thilagavathi et al., 2016; Das & Pal, 2020). However, very limited research has been documented from the central Gangetic plain (Mukherjee et al., 2012; Kumar et al., 2019). Thus, an attempt has been made to identify the groundwater recharge/discharge processes and their interaction with the surface and stagnant water, and how the recharge or discharge influences the As mobilization, etc., using the stable isotopes application. Also, examine the groundwater recharge source regarding meteoric circulation/ rainfall and understand the inter-relationship between the shallow aquifer and the deeper aquifer. Test the hypothesis of organic carbon deposits, sources and their role in As mobilization in the study area.

According to the published research, it is well accepted and hypothesized that As desorption occurs from the metal oxyhydroxide triggered by bacterial reduction of organic matter in the Gangetic plain (Kumar et al., 2018; Yadav et al., 2020). Previous studies based on the



estimation of total As in groundwater and soil and sediment, and only a few studies focused on the As speciation in groundwater, soil and sediment in the middle Gangetic plain (Chandrasekharam et al., 2007; Kumar et al., 2016). Thus, an attempt was made to fill the gaps and understand the different behavior of inorganic As species in the groundwater. Sequential digestion of sediment samples has been carried out to recognize the association of As with the solid phases in the environmental media based on the chemical activity in the aquifer system. Mineralogical studies have been carried out to identify the minerals assemblage with As and its mobilization processes in the aquifer system. Finally, a sediment tool application (Hossain et al., 2014) was used to distinguish the sediment based on the four colors in the central Gangetic plain.

Arsenic and trace metals (TMs) contamination in groundwater is causing skin diseases and different kinds of cancers in human beings. Two common As exposure pathways, ingestion and absorption, have been identified for acute and chronic As effects on living beings. So, it is needed to understand the As and TMs assessment in drinking water. Calculate the cancer risk and hazard index due to ingestion of As contaminated water through ingestion and absorption. Understanding the spatiotemporal distribution of As and TMs in the sediment core help to determine their sources and behavior in the aquifer environment. The elemental composition of sediment profiles in the research area is currently unknown. Hence, calculating the degree of contamination, geo accumulation index and enrichment factor etc. will be helpful to determine the pollution sources and their level.

### 1.11 Research hypothesis and objectives

The current study has been conducted to understand the hydrogeochemical characterization of groundwater and subsurface sediment from two geomorphic units, older and younger alluvium, in two study areas. This study is focused on groundwater chemistry and subsurface sediment geochemistry, their interdependency. Identify the groundwater recharge/discharge processes and delineate the source with the help of stable isotopes ( $\delta^{18}\text{O}$  and  $\delta^2\text{H}$ ) and DOC. This study also aims to enhance the knowledge of the role of inorganic As speciation in groundwater, soil and sediment. And also, an attempt has been made to identify the possible contamination source of As and TMs in groundwater and sediment. So to fulfill these gaps, a comprehensive study has been carried out with the following objective and their respective research questions or hypothesis.

**The following hypothesis was tested in this thesis;**

1. Do geomorphological, lithological /geochemical variations are responsible for the variable concentration of arsenic in the study area?
2. Are mineralogy plays an important role in the mobilization of arsenic and enrichment in As-contaminated water, sediment, soil?
3. Is rivers or stagnant water bodies and DOC play any direct/ indirect role in groundwater dynamics and arsenic mobilization?
4. Evaluate the potential risk of heavy metals and their exposure related to the human population.

**Objectives:**

- 1. Identification of arsenic provenance and fate by examining the geochemical/hydrochemical processes and geomorphological variations.**

Questions;

- i. What is the role of weathering on solute chemistry and dynamics of major ions and arsenic?
- ii. How is the Geomorphology of an area significantly influenced the As concentration in groundwater, soil and sediment? Is there any particular geochemical processes between groundwater and subsurface sediment in As librations?

- 2. Distribution and fractionation of arsenic in groundwater, soil, sediment.**

Questions;

How are As(III) and As(V) species variable in groundwater? What are the role of geochemical sediment fractions and assessing the potential mobilization of As in the sediment (coarse and fine particles) in the study area? What is the role of mineralogy in As distribution and mobilization?

- 3. Understand the groundwater dynamics, recharge/discharge and DOC behavior using stable isotopes in relation to arsenic mobilization.**

Questions;

Are river channels involved in the recharging of the specific aquifer in the study areas? What are the major source of DOC and  $p\text{CO}_2$  in the study area, and how do help in As mobilization?

**4. Identification of degree of contamination and potential health risk of arsenic and trace metals to the human population.**

Questions;

Identify the degree of contamination and level of cancer risk of As and TMs in groundwater and sediment. What are the probable source of TMs in groundwater and sediment?

## **Chapter 2**

### **Study area**

#### **2. Study area**

---

## 2. Study Area:

Both the study areas, Gorakhpur (study area 1) and Ghazipur (study area 2), are the eastern district of Uttar Pradesh and part of the central Gangetic basin (CGB). These areas are densely populated because of highly fertile soils, favorable climate, numerous river drainage systems and flat terrain. In this current study, two study areas were identified by the preliminary survey. Study area 1 is a part of the Gorakhpur district, which lies between  $83^{\circ} 20'$  to  $83^{\circ} 27'$  E and  $26^{\circ}43'$  to  $26^{\circ}50'$  N. Two major river (Rapti and Rohini) drainage system has been reported from the Gorakhpur district. Another river Ghaghara is flowing through the south-western boundary of the Gorakhpur district, but the current study was focused on a small part of the district. The entire drainage system of the district is finally discharged into the Ghaghara river. Small lake and water bodies like Ramgarh lake Nandaur Tal, Amir Tal, Taraina Tal and Bheuri Tal were reported. Gorakhpur district comes under the Tarai region of the Himalayan foothills. The sedimentation load of the Rapti and Rihini is very high during the flood. A periodic has been reported due to the low-lying area in Gorakhpur city. As a result, the Rapti River is also known as Gorakhpur's Sorrow (Singh et al., 2015).

Study area 2 is a part of the Ghazipur district and located between  $83^{\circ}04'$  to  $83^{\circ} 58'$  E and  $25^{\circ}19'$  to  $25^{\circ}54'$  N. The entire district is formed by the alluvium deposition transported from Himalaya and Craton peninsular with the holy river “Ganga” (Singh et al., 2007; Kumar et al., 2018). The deposition of alluvial sediment of the Ganga and its tributaries remains in excess throughout the sedimentation rate, resulting in the exposure of the Pleistocene to easy and steady fresh groundwater (Shah, 2015; Singh, 2004; Saha & Sahu, 2016).

In CGB, a very shallow water table has been reported due to enough groundwater recharge from monsoon precipitation (Saha & Sahu, 2016). The cultivation and cropping activities are dependent on monsoonal rainfall during summer, but during winter, agricultural activities are dependent on groundwater to meet irrigational and other requirements (Saha et al., 2011; Kumar et al., 2018). The economy of both the study area is based on agricultural practices.

Several authors have been suggested that As is evenly distributed in the groundwater and sediment, and its mobilization is highly dependent on redox condition and pH of the groundwater,

geology and geomorphology of that location (Saha & Shukla, 2013). Previous studies have been explained the geology and geomorphology of the central Gangetic. The geographical features such as active flood plain ( $T_0$ ), river valley terrace ( $T_1$ ) and upland interfluvial surface ( $T_2$ ) can be easily distinguished as a topographical mapping scale of the Quaternary accumulation basin (Ahamed et al., 2006; Acharyya & Shah, 2007; Saha & Shukla, 2013; Kumar et al., 2018). A significant surface feature has been identified in the CGB, showing a successive sediment deposition of Holocene over the Pleistocene epoch deposited by river Ganga (Shah, 2008, 2014).

The quaternary alluvium is made up of older and younger alluvium. Older alluvium is well oxidized, radish brown in color, and mainly consists of sand silt and clay with ample kankar, calcareous and pisolitic Fe nodules (Kumar et al., 2018). Older alluvium is also known as Bhangar. However, younger alluvium consists of greyish-yellow to brown fine sediment particles (silt and clay dominated) with a highly reducing environment. Younger alluvium is reported along with the stream courses, levees, swamps and flood plains. At some locations, the younger alluvium sequence can be distinguished as older and present-day flood plain, representing the past and present oscillation limits of Ganga and its tributaries. The newest sediments in the Ganga basin are less compact, with a high carbonaceous content; they appear grey or black and form a porous and water-bearing layer (Lourma, 2010).

The Holocene aquifer system of the central Gangetic plain is confined or semiconfined and used for water extraction. Generally, a two-tier aquifer system has been reported in and around the study area; a. shallow aquifer up to the depth of 120-140 mbgl and b. deeper aquifer system 220-240 mbgl. In central Gangetic, most hand pumps were installed in shallow depth (20-60 mbgl) only, and shallow aquifers are more prone to As and TMs contamination (Saha & Shukla, 2013; Kumar et al., 2018).

Three climatic conditions have been experienced; a. hot season (March to July), b. rainy season (June to September) and c. winter season (October to September). The average annual rainfall is 1060 mm, with the south-western monsoon accounting for 88 percent. Pre-monsoon rainfall is contributed by local convective storms (5% of yearly rainfall), while winter rainfall accounts for the remaining 7%. The economy of this area is mainly based on agricultural practices,

which are dependent on monsoonal rainfall. But winter crops are dependent on groundwater that fill the gap between soil moisture availability and crop water requirement.

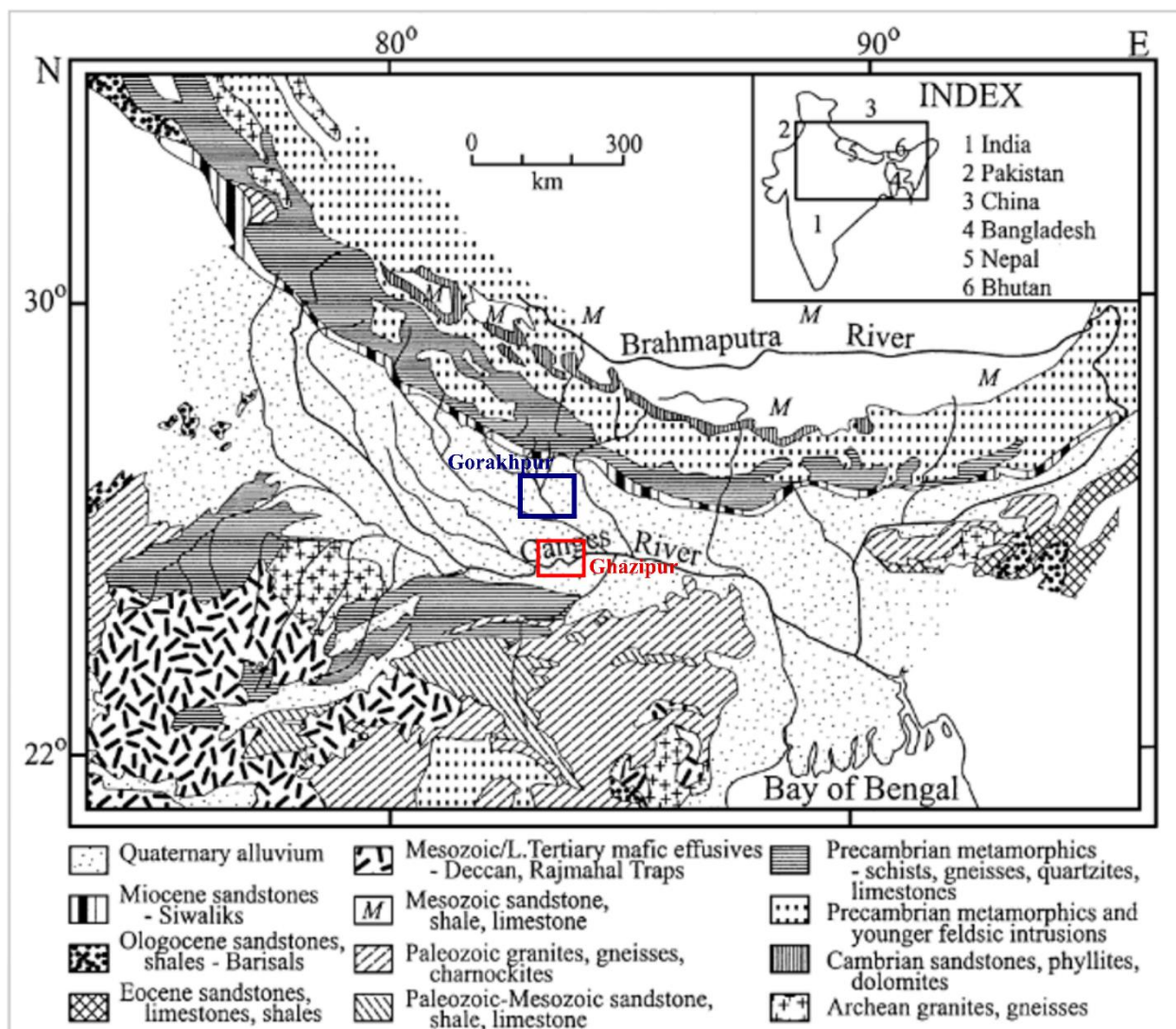


Figure 2.1: Showing the Geology of the Gangetic basin and surrounding areas. Cubic areas on the map are our study areas, Gorakhpur and Ghazipur. River Rapti is flowing through the Gorakhpur and river Ganga flowing through the Ghazipur districts. (Adapted from Heroy et al., 2003).

The details of the study area with sampling location and lithology have been separately given in each objective (Chapter 3-6).

## Chapter 3

# Identification of arsenic provenance and fate by examining the geochemical/hydrochemical processes and geomorphological variations

- 3 Identification of arsenic provenance and fate by examining the geochemical/hydrochemical processes and geomorphological variations**
  - 3.1 Introduction**
  - 3.2 Materials and Methods**
    - 3.2.1 Background of the study area
    - 3.2.2 Remote sensing and geology/geomorphic classification
    - 3.2.3 Study area geomorphology
    - 3.2.4 Sampling and analysis
    - 3.2.5 Sediment preparation and digestion
    - 3.2.6 Instrumentation
    - 3.2.7 Quality control and quality assurance
    - 3.2.8 Hydrogeochemical and statistical modelling
    - 3.2.9 Data analysis
  - 3.3 Results and discussion**
    - 3.3.1 Major ion chemistry of water samples
    - 3.3.2 Geochemistry of subsurface sediment
    - 3.3.3 Arsenic speciation and other trace metal in groundwater
    - 3.3.4 Mineralogy of the sediment
    - 3.3.5 Hydrogeochemical evolution of groundwater and river water
    - 3.3.6 Geochemical speciation modelling in solution
    - 3.3.7 As fate and mobilization in groundwater and surface water
  - 3.4 Conclusion**



## Abstract

Groundwater and sediment cores of four boreholes (to a depth of 35 mbgl) from two geomorphological units (OA and YA) of Gorakhpur and Ghazipur districts of eastern Uttar Pradesh, India, were collected to analyze the As content and geochemical processes. The As concentration in Gorakhpur district's groundwater ranged from ND to 0.24 mg/L in older alluvium (OA), ND to 0.26 mg/L in younger alluvium (YA) and ND to 0.05 mg/L in river water. However, As concentration in sediment cores ranged from 5.03 mg/kg to 19.19 mg/kg in Khorabar (OA) and 3.6 mg/kg to 23.96 mg/kg in Farshiya (YA). In the borehole of older alluvium, As decreased with depth, while in the younger alluvium, high As concentration was reported at a depth of 15 mbgl. As concentration in Ghazipur's groundwater ranged from ND to 0.125 mg/L in OA, ND to 0.621 mg/L in YA and ND to 0.03 mg/L in river water. The As in sediment cores ranged from 1.40 mg/kg to 26.31 mg/kg in Jagadishpur (OA) and 2.6 mg/kg to 31.52 mg/kg in Firozpur (YA). In both the sediment cores, As decreased with the depth while a sharp peak of elevated As concentration was observed in YA at 27.4 mbgl. Groundwater of both the study area was dominated by  $\text{CaHCO}_3$  type. In addition, to better understand the arsenic and iron speciation in groundwater, a pH–Eh diagram was generated using the Geochemist's Workbench (GWB) software. An X-ray mineralogy study of sediment samples was done to understand the availability of minerals for As liberation in the groundwater. Hydrogeochemical investigation suggested that weathering was the important process that governed the major ion chemistry, followed by evaporation enrichment and anthropogenic inputs. In study area 1, the bivariate plots indicated As liberated in OA groundwater by the dissolution of iron oxyhydroxide and  $\text{Cl}$  and  $\text{SO}_4$  oxidation while in YA groundwater reductive dissolution of iron oxyhydroxide and microbial degradation of DOC was a major process of As mobilization. In study area 2, As is liberated in the groundwater by the dissolution of Fe and Mn oxyhydroxide; although, in YA groundwater, reductive dissolution of Fe and Mn oxyhydroxide and competitive  $\text{PO}_4$  were significantly controlled As mobilization processes.

**Keywords:** Older alluvium; Younger alluvium; Reductive dissolution; As mobilization; Sediment

### 3.1 Introduction

Elevated geogenic As (arsenic) contamination of groundwater is reported notably in South and South-East Asian countries. It causes an alarming menace to human health and threatens the availability of safe drinking water in an affected area (Biswas et al., 2012; Mukherjee et al., 2015; Kumar et al., 2016). The upraised arsenic concentration in the drinking water than the WHO prescribed limit ( $10 \mu\text{g/L}$ ) was documented in more than 20 countries globally (Mukherjee et al., 2008; Verma et al., 2015). High levels of arsenic-contaminated groundwater aquifers are mainly associated with fluvial and Fluvio deltaic regions (Shankar et al., 2014; Kumar et al., 2016). The Bengal basin and Bangladesh are formed by the sedimentary deposition of the Ganga-Brahmaputra-Meghna mega fans delta. Recently these delta's are considered the most seriously arsenic-affected region globally (Mukherjee et al., 2009; Burgess et al., 2010; Bonsor et al., 2017; Kumar et al., 2018). Freshly deposited mega fans are highly enriched with nutrients provide favorable conditions for the microbe. The metabolism of nutrients in sediment stimulates microbial activities and creates a reducing environment (Brevik et al., 2020). The local conditions such as geology, geomorphology and hydrogeochemistry of groundwater significantly influence the As occurrences and mobility in the aquifer system (Nickson et al., 1998; Biswas et al., 2012b; Kumar et al., 2016).

As is widely distributed in rock and weathered soil. According to the published research, the river originating from Himalayan mountain and Tibetan plateaus is susceptible to arsenic pollution due to high arsenic-containing weathered sediment load (Chakraborti et al., 2004, 2018). The weathered sediments of the Gangetic basin are derived from sulfide deposition and allowing the arsenic into the groundwater (Nickson et al., 1998). However, south of the Ganga river, arsenopyrite mineral permits moderate arsenic contamination in the copper belt of Bihar and Chhattisgarh (Acharyya et al., 1999). Presently, it is hypothesized that quaternary alluvium from the upper and central Gangetic basin having characteristic properties that favor the holding and releasing mechanism of arsenic in the groundwater (Chakraborty et al., 2015).

The Gangetic Basin is one of the greatest quaternary alluvial-deposited terrains in Asia. A large population lives on a limited alluvial track area (Shah, 2014a), mainly occupied by Uttar Pradesh, Bihar, and West Bengal. The alluvial sediment deposited by Ganga-Brahmaputra-

Meghana makes this region highly fertile for agriculture and provides favorable conditions for developing large cities and villages (Islam, 2016). In recent decades, groundwater has been over-exploited for household and irrigational purposes (Mukherjee et al., 2012; Bhanja et al., 2017). The overexploitation of groundwater causes water table declination and quality deterioration. The weathered alluvial sediment differentiates between the deposits of Holocene and Pleistocene and seems correspondingly to be grey and brown. It was speculated that elevated groundwater arsenic concentrations were recorded high in shallow Holocene aquifers' gray and dark gray sediments (Nickson et al., 1998; Acharyya et al., 1999; Mukherjee & Fryar, 2008; Saha & Sahu, 2016).

The first case of arsenic poisoning due to prolonged As intake has been reported in West Bengal and Bangladesh. Several scientific and social reports on groundwater arsenic poisoning have been published from the upper Gangetic plain (Mukherjee et al., 2009). More than twenty-one states are reported to have high As contaminated groundwater (Jadhav, 2017). At present, more than 70 million people in the middle Gangetic plain (MGP) are affected by the increasingly elevated arsenic concentration in groundwater (Jadhav, 2017).

In the CGB, several surveys and scientific research on elevated arsenic contamination in groundwater have been well established (Ahamed et al., 2006; Saha, 2009; Janardhana Raju, 2012; Mukherjee et al., 2012a; Singh & Pandey, 2014; Kumar et al., 2014). There is still a significant lack of documentation about the occurrence and mobilization of arsenic in central Gangetic basins. The CGB is consists of heterogeneous topography with an irregular upland surface, plain area, and low laying natural bodies (Shah, 2015). The objective aims to investigate the chemistry of groundwater and river water and the role of the subsurface geochemical processes in arsenic mobilization. The heterogeneous topography is responsible for distinctive geomorphic and geological terrains in the study area (Mukherjee et al., 2012).

## 3.2 Materials and methods

### 3.2.1 Background of the study area

The study area is a part of CGB (Central Gangetic Basin) and covered 2610 km<sup>2</sup>. The study area is divided into two distinctive districts (Gorakhpur and Ghazipur) based on the river flows through the region. Study area 1 (Gorakhpur) is located along the banks of river Rapti, originating

from the Dhaulagiri Himalayas region in Nepal. A small tributary, Rohini flows from the city's western side and integrates with the river Rapti. Further 60 km beyond the Gorakhpur city, river Rapti falls confluence with the river Ghaghara (Shah, 2015). The Rapti River also is known as ‘Gorakhpur’s Sorrow’ due to its recurrent flood in the monsoon season.

Study area 2 (Ghazipur) is unearthed on the bank of river Ganga. The holy Ganga originated from the Gangotri glacier, Himalaya. The study areas extend from the Gangetic plain to the Tarai zone of the Himalayan foothills. It consists of weathered alluvial sediment commonly transported from the Himalayas foothills and Peninsular Craton (Ahamed et al., 2006; Kumar et al., 2018). The sediment accumulation of the river Ganga and its leading tributaries always remain surplus over the sedimentation rate resulting in quickly and continuous fresh groundwater accessible during the Pleistocene (Singh, 2004; Saha & Sahu, 2016).

### 3.2.2 Remote sensing and geology/geomorphic classification

The geology/geomorphic identification of the study area was recognized by using remote sensing & GIS. The satellite image was acquired from Landsat 8, Operational Land Imager (LOI) sensor on 07<sup>th</sup> September 2017 from USGS scientific agency, USA (Earthexplorer, <https://earthexplorer.usgs.gov>) based on digital image processing. The Landsat picture pixel has a resolution of 30 m in a multispectral band refined to a resolution of 15 m panchromatic band. The Landsat images were used to construct the false color composite (FCC). The geomorphological changes of the study area were identified with three-band combinations 5,4 and 3 (Near-infrared, red and green) of FCC. The Landsat satellite images were already orthorectified and georeferenced to UTM 45 (Universal Transverse Mercator) projection with Datum-WGS 84 (World Geodetic System). The geomorphic feature of the landforms was differentiated by remote sensing & GIS and confirmed by field visit surveys. The available feature was also compared with the reported scientific publications in this area (Singh & Pandey, 2014; Saha & Sahu, 2016; Kumar et al., 2018).

### 3.2.3 Study area geomorphology

The Central Gangetic plain is one of the most dynamic and active fluvial depositional basins in the world. It is significantly influenced by climate-driven sediment, soil water regime, and extra and intravaginal tectonics (Sinha et al., 2005; Singh & Pandey, 2014). The study areas

are classified into different geomorphological units: younger alluvium, older alluvium, active flood plains, channels deposition, river water bodies, paleochannels, and active river channels (Figure 3.1&3.2).

CGB constitutes recent unconsolidated sediment, including stream, flood channels referred to as quaternary alluvium, and classified into older and younger alluvium. The older alluvium consists of sand silt and clay, reported during Late Pleistocene to the Early Holocene. The younger alluvial is predominantly argillaceous and consists of silty clay or sandy clay (Acharyya & Shah, 2004). Sometimes, underlain clay lenses are reported and forming a shallow aquifer system. The width of the younger alluvium is very narrow; it mostly covers the area bordering the Rivers. The younger alluvial and active flood plains are generally uniformly flooded every year, so the sediment's moisture holding capacity is high (Guo et al., 2017). They give high spectral resolution in their satellite images. The younger and older alluvium also differentiates based on the soil color (Hossain et al., 2014). The older alluvium is yellowish; however, the younger alluvium is grey and represents the reductive subsurface condition due to high microbial activities (Chakraborty et al., 2015). Conversely, older alluvial plain is mainly upland, having less moisture content and therefore low spectral resolution observed compared to younger alluvium, giving blurred image appearances in satellite images.

The present is mainly focused on the As sources and As mobilization governing factor in the study area. Water sampling was carried out during October 2017 (post-monsoon) and February 2018 (premonsoon). However, sediment coring was done in February 2018. In both the study areas, it was observed that there were no any significant factors involved in As mobilization during pre and post-monsoon. However, the geomorphology of the study area played an important role in As occurrence and mobilization. Therefore, our study was focused on available geomorphology and its role in As mobilization.

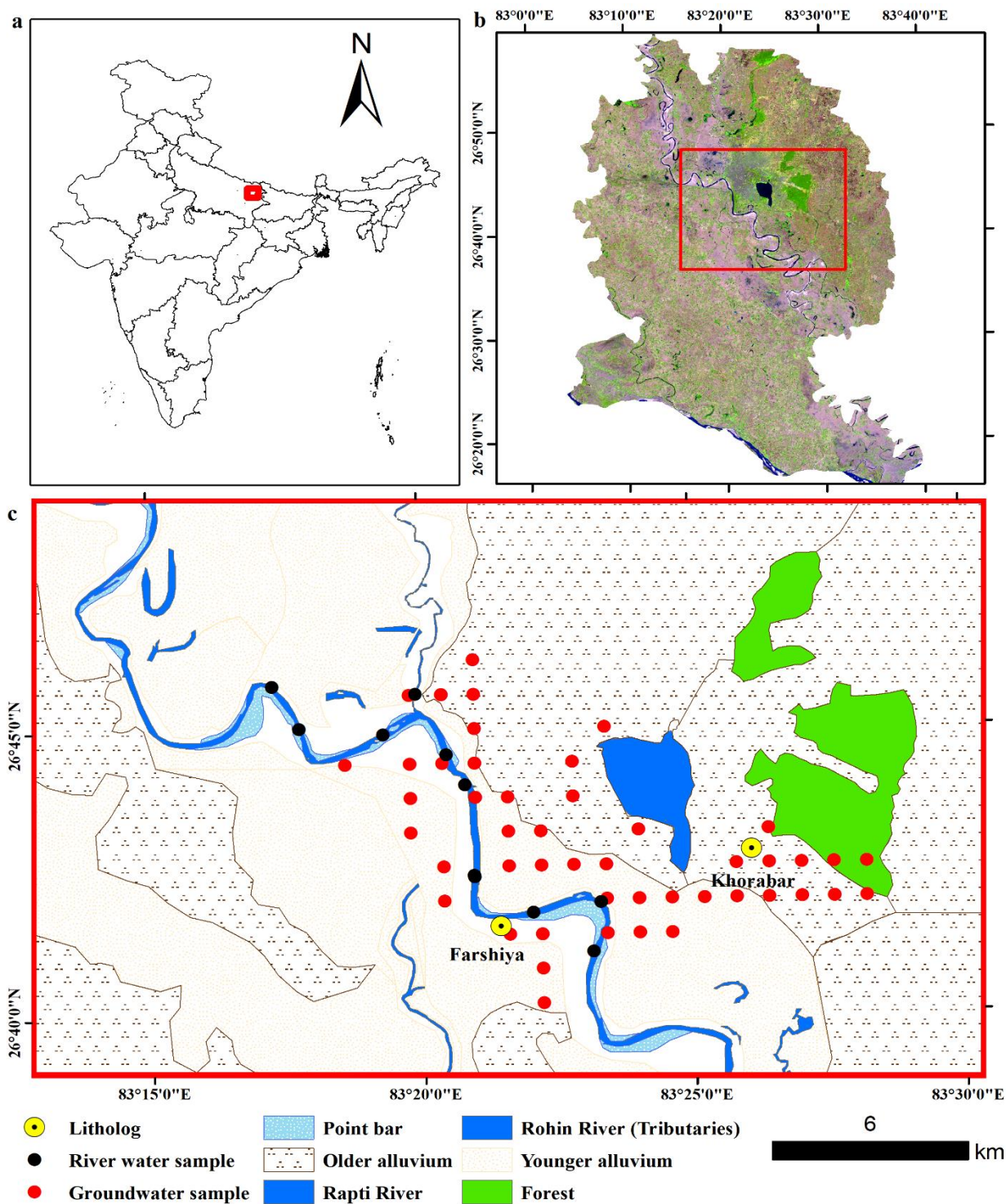


Figure 3.1: Map of the study area, (a). India with state boundary and study area marked as a square, (b). Landsat images are prepared from FCC (false-color composite) band combinations (5, 4 and 3) to distinguish the image in different geomorphic features available in the study area, (c). Study area map with different geomorphic features (older alluvium, younger alluvium, point bars, forest and river etc.) with As concentration.

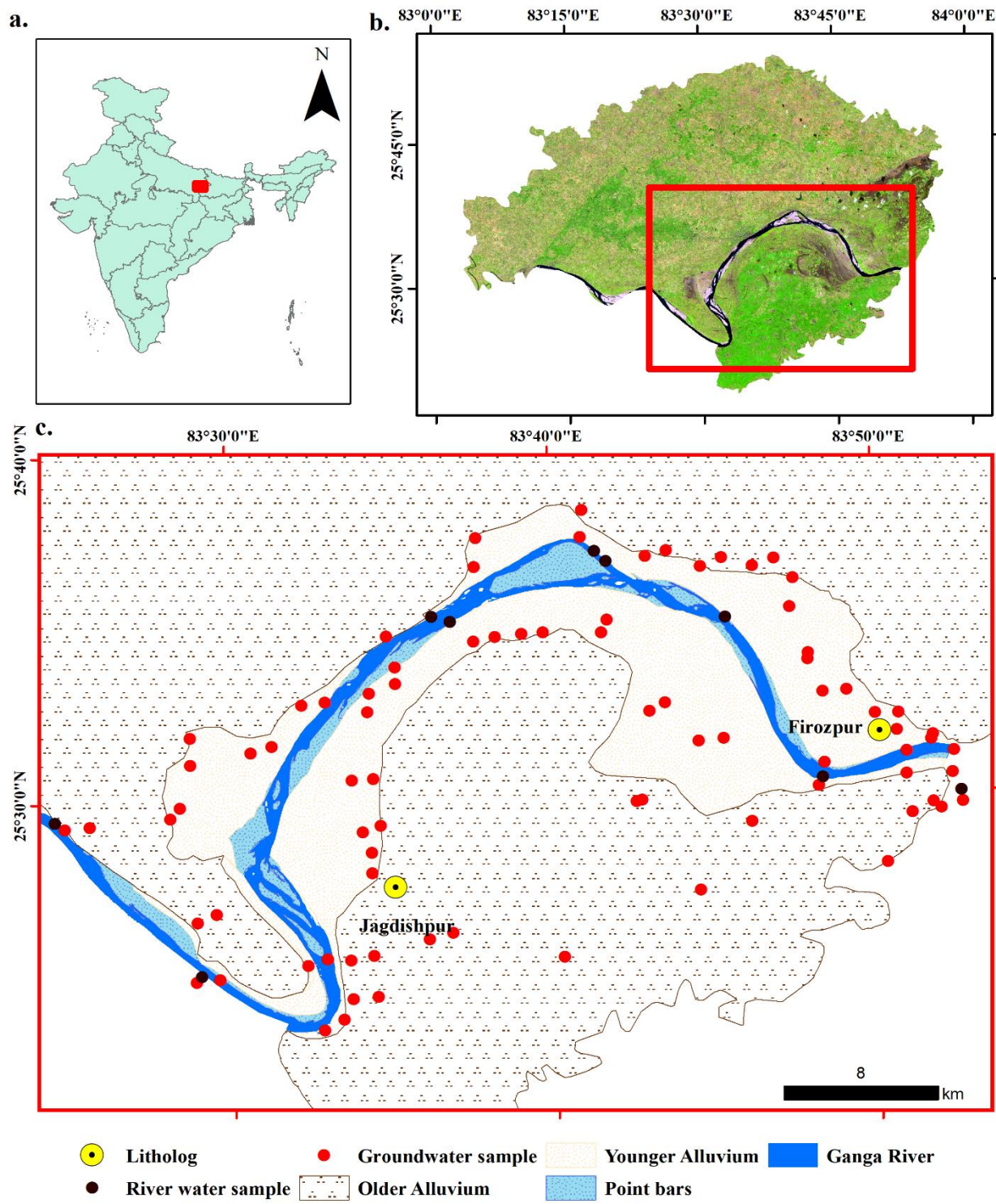


Figure 3.2: Map of the study area, (a). India with state boundary and study area marked as a square, (b). Landsat images are prepared from FCC (false-color composite) band combinations (5, 4 and 3) to distinguish the image in different geomorphic features available in the study area, (c). Study area map with different geomorphic features (older alluvium, younger alluvium, point bars, forest and river etc.) with As concentration

### 3.2.4 Sampling and analysis

A total of 70 groundwater and 13 river water samples from Gorakhpur and 84 groundwater and 13 river water samples from Ghazipur district were collected during August 2017 and February 2018. Two areas have been chosen for the study because both are located on different Riverbank and having different geomorphological features. The groundwater samples of both the districts were further classified into older and younger alluvium. In Ghazipur, out of 84 groundwater samples, 26 were collected from the older alluvium region and 58 from the younger alluvium region. The river water samples were collected from the Ganga. Similarly, In Gorakhpur, out of 70 groundwater samples, 28 were collected from the older alluvium region, 42 from the younger alluvium region and 12 from the Rapti river and its tributary Rohin river, one from the Ramgarh lake. The groundwater samples were collected from both the side of the Riverbanks in the study area, either from the government-installed India Mark II hand pump or privately installed tube well.

Groundwater samples were collected after purging water 5-10 minutes from the tube well to remove the standing water in the well's casing. Purging was conducted to stabilize the physical parameters such as pH, electrical conductivity (EC), temperature, and oxidation-reduction potential (ORP). A portable HORIBA (U-50 series) multiparameter was used to measure the water quality parameters such as pH, EC, TDS, and ORP in situ. The accuracy of the multiparameter for the measurement of the parameters like pH, EC, TDS and ORP were  $\pm 0.1$ ,  $\pm 1\%$  full scale,  $\pm 5$  mg/L and  $\pm 15$  mV, respectively. In the field, the multiparameter were fitted with the cell flow to minimize the contact of the atmospheric oxygen. The groundwater/river water samples for total arsenic and trace metals were collected in 50 ml in a pre-washed polypropylene bottle. Each sample was filtered in a hand-operated vacuum pump through a  $0.45 \mu\text{m}$  Axiva membrane filter followed by the addition of 3.4 drops of 5M nitric acid ( $\text{HNO}_3$ ) to preserved the sample. A replicate (second set) of each sample was collected in a 100 ml pre-washed polypropylene bottle without adding any preservatives for major cation and anions. All the samples were transferred in a transportable icebox in situ to minimize the chemical alteration. Further, all the samples were transferred to the laboratory's refrigerator at  $4^\circ\text{C}$  until analysis.



Core (subsurface) sediment was collected from both districts. Based on the geomorphological feature (younger and older alluvial region), two locations have been chosen for the coring in each study area (Singh & Pandey, 2014; Kumar et al., 2018). A common and localized hand flapper drilling method was applied for coring. A total of four cores were collected to a depth of 110 feet (33.53 m) below ground level at Khorabar and Farshiya (Gorakhpur) and Jagadishpur and Firozpur (Ghazipur). Sediment samples were collected at a regular interval around 10 feet (3.05 m) from these above cores and taken into account if any anomalies were perceived during the regular sediment interval. The collected sediment samples were packed in a zip lock bag. Finally, samples were brought to the lab air-dried for 24 hours, then oven-dried at 50 °C for 72 hours and stored in a dark place until the analysis start.

### 3.2.5 Sediment preparation and digestion

The soil or sediment sample was digested using a method developed by Shapiro (1975). Approx. 0.10 gm sediment samples were accurately weighed and transferred to the Teflon vessels, and 2 ml of aqua regia (HNO<sub>3</sub> and HCl ratio 3:1) and 5 ml hydrofluoric acid (HF) were added. The vessels were kept open for 30 min allowed to predigestion. Next, put the cap and seal the Teflon vessels appropriately and placed in an oven heated for 1 hr at 100 °C and allowed to cool down at room temperature. Now, a complete digested sediment sample was obtained, which was visually clear and transparent.

A separate boric acid solution was prepared by adding 5.6 g boric acid and 2 ml of distilled water. The prepared boric acid solution was transferred to the vessel and make the final volume 100 ml by adding distilled water. Next, the solution was mixed with the digested samples in a polypropylene bottle. Samples were kept overnight to allow the borosilicate precipitate formation and settling down. The gelatinous precipitate was separated from the solution using a 0.45 µm membrane filter and keep the extract at 4 °C for elemental analysis.

### 3.2.6 Instrumentation

Analysis of major cations and trace metals were done on inductively coupled plasma optical emission spectrometry (ICP-OES 5110, Agilent Technologies, USA). A standard reference material (SRM-1643d) provided with the instrument was used to calibrate the instrument. The

instrument was standardized against the standard with best fitted linear regression ( $r^2=0.9998$ ) for As. The method detection limit (MDL) for As at 188.98 nm wavelength was  $0.5\mu\text{g/L}$ . MDL is three times higher than the instrument detection limit (DL). Anions were analyzed on an ion chromatograph (Metrohm-930 Compact IC). The instrument was calibrated with IC standards provided by the Metrohm itself. Percent RSD and percent recovery were within  $\pm 5\%$ . A laser particle size analyzer analyzed the percent distribution of soil texture in the sediment (Microtrac, S3500 coupled with Microtrac SDC unit). The dried sediment was treated with  $\text{H}_2\text{O}_2$  to remove organic carbon, boiled with 10% HCl to remove inorganic carbon and added tetrasodium pyrophosphate as a dispersive agent (Konert & Vandenberghe, 1997). Treated samples were dried and analyzed. The dissolved organic carbon (DOC) was analyzed on Shimadzu TOC 5000 (Kyoto, Japan, detection limit  $0.5\text{ mg/l}$  and precision  $\pm 10\%$ ). The samples were treated with dilute HCl to pH  $\sim 3$  to purge the DOC from the samples.

Mineralogical analysis has been done on X-ray powder diffractometer, Malvern Empyrean, PANalytical (UK) model. The instrument was worked on  $< 1\ \mu\text{Sv/h}$  radiation level and over an angular range of 5 to 85 ( $2\theta$ ) with 0.02 degree steps 2s count time on unoriented side-packed powder mounts. The peak identification was made with the PANalytical Xpert High score software with ICDD (International Centre for Diffraction Data) database to identify the minerals in the aquifer sediment using calculated powder pattern and Rietveld full pattern fitting options (Gates-Rector & Blanton, 2019).

An X-ray fluorescence spectrometer analyzed the trace metal concentration in core sediment (WD-XRF, Axios Max, PANalytical, UK). In this technique, simultaneously, we can analyze multi elements. The instrument's resolution was Mn-K $\alpha$  based with 35eV and detection range, 0.1 ppm (Lower limit of detection) to 100%. For the analysis, the pellet was prepared on a Kameo pellet pressed machine. Around 8 grams of sediment samples were appropriately mixed with polyvinyl alcohol (binding agent) and applied pressure of 40 tons to prepared the pellet.

### 3.2.7 Quality control and quality assurance

All the equipment and utensils used in the laboratory were “A” grade and made up of borosilicate or polypropylene. Required utensils and vessels wash properly and shock in 5 M

HNO<sub>3</sub> (overnight) before being used. The reagent and compound used in the analysis were analytical grades. A standard reference material (SRM), NIST-8704, also known as Buffalo river sediment (n=4) was used to verify the As results in sediment. The standard certified value for As is 17 mg/kg and the observed was detected 16.72±0.08 mg/kg. The recovery of the As was obtained 98.32%. JA-2 and GSP-2 standard reference material in XRF analysis was used parallel to check the instrument's accuracy. The percent error for all the elements were <10% except for Co(+24%) in JA-2 and CaO (+19.7%) and Cr (+21.4%) in GSP-2.

### 3.2.8 Hydrogeochemical and statistical modelling

Saturation Indices were calculated to understand the subsurface minerals solubility of the selected elements in the groundwater. The mineral phases speciation modeling was calculated with PHREEQC, USGS software (Parkhurst, 1995). A Geochemist workbench software (community version, 15.0) was used to identify the As species in the aqueous environment. LLNL thermo database (thermo.dat) was used in the software. The study area map was prepared in ArcMap (version 9.3). All the statistical analysis was carried out in SPSS (version 21).

### 3.2.9 Data analysis

A principal component analysis (PCA) was carried out to understand the relationship among the groundwater samples. It is a statistical procedure to reduce the dimension of a large dataset with more interpretation without losing the information. The hydrogeochemical grouping was constructed based on the distribution of major cations, anions, heavy metals (Fe, Mn, and Zn).

## 3.3 Results and discussion

### 3.3.1 Major ion chemistry of water samples

In study area 1 (Gorakhpur), pH was reported neutral to little alkaline in nature (Table 3.1). The means value of pH was 6.86 in the groundwater of younger alluvium (YA), followed by older alluvium (OA) (7.00). The mean pH value in the river water (RW) was slightly alkaline (7.28) in nature. The pH of the river water was highly variable and depended on monsoon, local geomorphology, upland and lowland terrace, and man-made contaminants (Hamid et al., 2020). The potential electrode (*pe*) was observed more reducing in the groundwater of YA (-0.94 volts) in contrast to OA (-0.39 volts) and river water (1.09 volts). The highest mean concentration of

$\text{Ca}^{2+}$  was detected in the groundwater of YA (82.83 mg/L), followed by OA (50.23 mg/L) and river water (50.12 mg/L). The concentration of  $\text{Ca}^{2+}$  and  $\text{Mg}^{2+}$  was almost similar in the groundwater of Older and younger alluvium. Among anions,  $\text{HCO}_3^-$  was the dominant, followed by  $\text{Cl}^-$ ,  $\text{NO}_3^-$  and  $\text{SO}_4^{2-}$ , respectively. The mean concentration of  $\text{HCO}_3^-$  was reported high in the groundwater of YA (461 mg/L) followed by OA (421 mg/L) and river water (205 mg/L), respectively. A similar trend of the concentration of anions was reported in OA, YA and river water except for  $\text{PO}_4^{3-}$  and  $\text{SO}_4^{2-}$ . The mean concentration of  $\text{PO}_4^{3-}$  and  $\text{SO}_4^{2-}$  were observed higher in river water rather than groundwater, indicate anthropogenic activities significantly influence the concentration of phosphate and sulphate in surface water.

In study area 2 (Ghazipur), the pH was neutral to alkaline in nature (Table 3.2). The standard deviation of pH in the river water was higher than OA and YA might be due to anthropogenic influences. The potential electrode (*pe*) was reported more negative (reducing in nature) in the groundwater of YA (-1.02 volts) compared to OA (-0.57 volts) and river water (1.31 volts). Negative redox potential cause a reducing environment in the aquifer system (Naudet et al., 2004). Among all the cations,  $\text{Ca}^{2+}$  was dominant in the groundwater of all the geomorphic setups. The mean concentration of  $\text{Ca}^{2+}$  was reported higher in the groundwater of OA (107 mg/L) followed by YA (87 mg/L) and river water (49 mg/L), respectively. Bicarbonate was the dominant anion in the study area. The mean concentration of  $\text{HCO}_3^-$  was reported high in the groundwater of OA (774 mg/L) followed by YA (610 mg/L) and river water (286 mg/L), respectively. The mean concentration of  $\text{SO}_4^{2-}$  was higher in the river water than groundwater of both the geomorphic setup, indicating anthropogenic activities such as sewage discharge, agricultural runoff and industrial waste might be there and elevate  $\text{SO}_4^{2-}$  in river water.

The mean concentration of dissolved organic carbon (DOC) was observed slightly higher in the groundwater of YA (0.88 mg/L) followed by OA (0.81 mg/L) in study area 1 (Gorakhpur). A similar trend was also observed in study area 2 (Ghazipur); the concentration of DOC in the groundwater of YA (0.85 mg/L) was slightly higher than the OA (0.80 mg/L). However, the mean concentration of DOC in the river water was almost similar (0.13 mg/L) in both the study area. The dissolved organic carbon in the groundwater stimulates microbial activity, which might involve in As mobilization (Anawar et al., 2003; Shah, 2008).

In Gorakhpur, the mean concentration of silica was observed moderately higher in the groundwater of YA (35.3 mg/L) compared to the groundwater of OA (32.5 mg/L) and river water (32.3 mg/L), respectively. A similar kind of trend was also reported in study area 2 (Ghazipur); the concentration of silica in the groundwater of YA (33.4 mg/L) was a bit higher than the groundwater of OA (29.8 mg/L) and river water (23.4 mg/L), respectively. The high concentration of silica in groundwater indicating might be silicate weathering is dominant in the study area. The silica concentration in groundwater is dependent on residence time. Prolonged interaction with silicate minerals raises silica concentration in groundwater (Khan et al., 2015). As a result, deeper aquifers are rich in silica content compared to shallow aquifers. The degree of water-rock interaction is controlled by permeability, lithology, and groundwater residence time (Hem, 1959; Marchand, 2001).

In study area 1 (Gorakhpur), the concentration of Fe was reported slightly higher in the groundwater of YA (1.45 mg/L) compared to the groundwater of OA (1.33 mg/L) and river water (0.24 mg/L). A similar trend was also observed from study area 2 (Ghazipur). The mean concentration of Fe in the groundwater of YA was reported (2.33 mg/L) higher than the mean concentration of Fe in the groundwater of OA (1.50 mg/L) and river water (0.25 mg/L). The high Fe concentration in the groundwater of YA might be due to the dissolution of Fe-bearing minerals in a reducing environment (Chakraborti et al., 2003).

The mean concentration of Mn was reported somewhat more remarkable in the groundwater of YA (0.48 mg/L) followed by the groundwater of OA (0.39 mg/L) and river water (0.17 mg/L) in the study area 1 (Gorakhpur). A Similar trend was also observed in study area 2 (Ghazipur); the mean concentration of Mn was found 3.56 mg/L in the groundwater of YA followed by groundwater of OA (1.50 mg/L) and river water (0.25 mg/L). The source of Mn in the groundwater of YA might be mineral dissolution in reducing conditions (Chakraborti et al., 2003).

Table 3.1: Summarized statistical results of major and trace metals in the groundwater of younger and older alluvium and river water in study area I (Gorakhpur) (ND = Not detected)

Parameter	Younger Alluvium (n=42)				Older Alluvium (n=24)				River Water (n=13)			
	Median	Range	Mean	St. Dev	Median	Range	Mean	St. Dev	Median	Range	Mean	St. Dev
Depth (m)	30.78	15.24 - 45.7	30.7	7.15	30.48	21.3 - 45.7	30.8	4.4	-	-	-	-
pH	6.82	6.19 - 7.39	6.85	0.38	7.11	6.15 - 7.48	7.00	0.32	7.27	7.21 - 7.38	7.28	0.05
pe	-1.10	-3.06 - 2.72	-0.94	1.71	-0.28	-3.04 - 2.8	-0.39	1.34	1.03	0.6 - 1.5	1.09	0.27
ORP (mV)	-65.5	-180 - 162	-55.9	93.01	-16.50	-179 - 167	-22.92	72.84	59	34 - 86	62.54	14.82
TDS (mg/L)	907	383 - 1800	879.5	288.4	691	300 - 2270	826.9	476.6	620	460 - 693	588.77	69.8
EC ( $\mu$ S/cm)	1420	590 - 2680	1357.7	425.8	1070	538 - 3540	1288.8	697.3	960	705 - 1018	903.69	103.8
HCO <sub>3</sub> (mg/L)	477.5	129.92 - 972.2	461.1	179.8	364.9	98.7 - 1237.9	421.3	275.7	212.1	118.5 - 278.9	205	43.51
F (mg/L)	0.58	0.03 - 2.61	0.83	0.71	0.71	0.21 - 2.12	0.77	0.48	0.49	ND - 1.03	0.48	0.33
Cl (mg/L)	53.18	1.52 - 144.7	49.3	31.61	53.18	8.97 - 252.5	63.13	48.62	114.6	49 - 175	121.14	39.83
NO <sub>3</sub> (mg/L)	22.91	ND - 170.24	33.72	37.08	11.88	2.58 - 86.41	19.49	20.22	12.3	0.45 - 27.54	12.42	7.77
PO <sub>4</sub> (mg/L)	0.00	ND - 0.97	0.05	0.19	0.00	ND - 0.1	0.01	0.02	1.71	ND - 54.32	5.54	14.11
SO <sub>4</sub> (mg/L)	4.7	ND - 161.6	17.61	33.28	9.08	ND - 128.7	21.01	31.54	23	ND - 42	22.62	10.27
Na (mg/L)	44.12	5.46 - 142.2	49.48	26.27	30.88	6.3 - 131.43	35.19	25.10	29.6	16.8 - 40.8	28.48	7.11
K (mg/L)	4.5	0.75 - 69.75	9.09	12.34	2.50	1 - 13	3.08	2.39	11.4	0.6 - 17.4	10.98	4.67
Ca (mg/L)	90.83	20.9 - 191.8	82.84	33.67	48.40	12.69 - 129	50.23	26.94	51.57	30.7 - 71.1	50.12	11.01
Mg (mg/L)	70.27	13.8 - 181.7	72.69	31.95	42.79	9.8 - 141.2	45.74	28.47	44.49	27.1 - 64.3	45.32	10.33
DOC (mg/L)	0.51	0.01 - 3.19	0.88	0.87	0.57	0.02 - 3.26	0.81	0.79	0.12	0.09 - 0.18	0.13	0.03
Si (mg/L)	36.30	23.5 - 46.7	35.29	5.83	31.60	24.28 - 46.52	32.53	5.26	35.45	13.59 - 42.6	32.26	8.76
Al (mg/L)	0.18	0.02 - 0.27	0.18	0.05	0.17	0.08 - 0.231	0.16	0.04	0.23	0.1 - 0.47	0.25	0.11
Fe (mg/L)	0.26	ND - 17.34	1.45	3.30	0.22	0.017 - 21.2	1.33	4.19	0.15	0.04 - 0.59	0.24	0.18
Cr (mg/L)	0.00	ND - 0.03	0.01	0.01	0.00	ND - 0.07	0.00	0.01	0.00	ND - 0.02	0.01	0.00
Cu (mg/L)	0.01	ND - 0.04	0.01	0.01	0.00	ND - 0.03	0.01	0.01	0.02	ND - 0.05	0.02	0.01
Mn (mg/L)	0.23	ND - 3.28	0.48	0.66	0.16	ND - 3.9	0.39	0.76	0.16	ND - 0.31	0.17	0.08
Pb (mg/L)	0.02	ND - 0.07	0.02	0.02	0.01	ND - 0.08	0.02	0.02	0.01	ND - 0.03	0.01	0.01
Zn (mg/L)	0.80	0.02 - 36.7	2.95	6.17	0.63	0.04 - 24.6	2.97	5.88	0.06	0.01 - 0.26	0.09	0.07
As (mg/L)	0.03	ND - 0.26	0.05	0.06	0.00	ND - 0.24	0.03	0.06	0.02	ND - 0.05	0.01	0.01

Table 3.2: Summarized statistical results of major and trace metals in the groundwater of younger and older alluvium and river water in study area I (Ghazipur) (ND = Not detected)

	Younger Alluvium (n=58)				Older Alluvium (n=26)				River Water (n=13)			
	Median	Range	Mean	St. Dev	Median	Range	Mean	St. Dev	Median	Range	Mean	St. Dev
Depth (m)	36.6	24.5 - 54.86	35.58	8.27	36.58	18.3 - 54.8	37.3	8.9	-	-	-	-
pH	7.1	6.36 - 7.67	7.06	0.31	7.11	6.31 - 7.46	7.00	0.33	7.18	6.2 - 7.54	7.09	0.40
pe	-1.1	-3.23 - 1.98	-1.02	1.32	-0.54	-2.14 - 0.78	-0.57	0.86	1.35	0.56 - 1.77	1.31	0.32
ORP (mV)	-65	-192 - 118	-60.5	78.60	-32	-128 - 46	-33.96	50.9	78	32 - 102	75.6	17.2
TDS (mg/L)	985	306 - 3480	1136	615.62	1321	231 - 3940	1407.9	959.2	543	480 - 690	545.54	47.67
EC ( $\mu$ S/cm)	1555	471 - 5520	1833.4	1055.8	2043.5	356 - 6260	2299.1	1611.8	900	809 - 1197	923.2	88.57
HCO <sub>3</sub> (mg/L)	517.2	98.52 - 2066	609.7	369.2	745.4	90.9 - 2173.4	774.22	550.04	285	236 - 334	286.2	27.48
F (mg/L)	0.56	ND - 3.13	0.74	0.63	0.94	ND - 2.37	0.98	0.60	0.15	ND - 1.02	0.33	0.37
Cl (mg/L)	80.9	28.6 - 296.9	90.77	47.88	84.95	21.45 - 244.3	99.31	61.51	26.23	18.5 - 48	29.52	7.65
NO <sub>3</sub> (mg/L)	8.57	ND - 59.6	15.27	14.18	18.54	ND - 176.3	29.07	36.70	0.76	0.18 - 4.56	1.35	1.34
PO <sub>4</sub> (mg/L)	0.00	ND - 68.7	6.10	14.70	0.01	ND - 45.82	6.66	11.88	0.32	ND - 3.19	1.06	1.11
SO <sub>4</sub> (mg/L)	6.71	ND - 82.11	14.25	19.28	7.26	ND - 97.09	19.43	26.34	23.00	9 - 42	23.60	9.60
Na (mg/L)	59.27	6.68 - 244.1	67.28	40.67	83.81	5.36 - 217.4	80.51	57.28	23.33	10.67 - 41.33	23.74	8.43
K (mg/L)	3.67	ND - 63.3	7.16	9.27	3.77	1.3 - 59.3	8.75	12.97	13.67	9 - 20.3	14.53	3.79
Ca (mg/L)	76.2	20.9 - 251.7	86.59	46.63	105.84	18.87 - 295.3	106.93	67.95	48.00	35.27 - 58.08	48.82	6.76
Mg (mg/L)	64.7	14.3 - 201.1	74.28	37.13	82.81	16.1 - 198.8	90.79	53.91	35.33	19.37 - 48.87	36.07	7.02
DOC (mg/L)	0.52	0.01 - 3.19	0.85	0.92	0.55	0.03 - 2.95	0.80	0.66	0.13	0.1 - 0.19	0.13	0.02
Si (mg/L)	31.02	24.6 - 52.6	33.39	6.89	29.50	13.45 - 47.8	29.85	8.76	23.50	10.26 - 37.58	23.37	6.96
Al (mg/L)	0.21	0.11 - 0.64	0.23	0.10	0.25	0.11 - 0.64	0.28	0.12	0.29	0.13 - 0.52	0.29	0.10
Fe (mg/L)	1.07	ND - 13.81	2.33	3.23	0.46	ND - 19.5	1.50	3.70	0.21	0.09 - 0.46	0.25	0.10
Cr (mg/L)	0.00	ND - 0.02	0.00	0.01	0.01	ND - 0.02	0.01	0.01	0.04	0.01 - 0.08	0.03	0.02
Cu (mg/L)	0.01	ND - 0.08	0.01	0.02	0.01	ND - 0.08	0.02	0.02	0.04	0.01 - 0.08	0.04	0.02
Mn (mg/L)	2.76	0.03 - 20.62	3.56	3.63	0.90	0.04 - 9	1.41	1.79	0.31	0.13 - 0.49	0.31	0.11
Pb (mg/L)	0.01	ND - 0.12	0.02	0.03	0.04	ND - 0.17	0.03	0.04	0.15	0.05 - 0.29	0.15	0.06
Zn (mg/L)	0.96	0.02 - 8.48	1.57	1.82	1.10	0.02 - 12.23	1.69	2.35	0.13	0.05 - 0.26	0.15	0.06
As (mg/L)	0.03	ND - 0.62	0.06	0.04	0.00	ND - 0.12	0.03	0.02	0.00	ND - 0.03	0.01	0.01

As concentration in groundwater varies from location to location, influence by regional geology. In Gorakhpur, the mean concentration of As was reported high in the groundwater of YA (0.05 mg/L) followed by the groundwater of OA (0.03 mg/L) and river water (0.01 mg/L), respectively (Table 3.1). Similar results were also observed in Ghazipur. The mean concentration of As in the groundwater of YA (0.06 mg/L) was moderately higher than the groundwater of OA (0.03 mg/L) and river water (0.01 mg/L), respectively (Table 3.2). The high As in the groundwater of YA indicating unoxidized conditions with rich organic matter might be responsible for elevated arsenic.

A few studies have reported elevated arsenic concentration in small river streams (Gobra) in Murshidabad and river Jalangi in upper Ichamati of West Bengal (Stüben et al., 2003). These studies have suggested that rivers get recharged from groundwater (effluent nature), which enhanced As concentration in river water of Gobra and Ichamati. Our study found that rivers Ganga and Rapti contained extremely low arsenic concentrations, indicating no recharge from groundwater.

The concentration of trace metals such as aluminum, chromium, and copper was slightly higher in the river water than in groundwater in both the study area might be due to unwanted man-made pollutants (Sankhla et al., 2018).

### 3.3.2 Geochemistry of subsurface sediment

Subsurface sediment cores were collected from older and younger alluvium regions of both the study area.

In study area 1 (Gorakhpur), the aluminum (Al) concentration was almost constant throughout the entire core sediments except for a few depths (Figure 3.3). Aluminum is considered a conservative element in the upper continental crust (Ho et al., 2012). The presence of aluminum in core sediments might be due to the mineral-like albite, muscovite and aluminosilicate. The mean value of Al-oxide in older and younger alluvium core sediments was observed 9.91% and 11.21%, respectively.



Table 3.3: Statistical summary of sediment geochemistry (older and younger alluvium) of the study area I (Gorakhpur)

	OA (n=12)			YA (n=13)		
	Mean	Median	Range	Mean	Median	Range
Depth (m)	16.64	16.00	0 - 33.53	17.47	18.29	0 - 33.53
As (ppm)	11.50	11.57	5.03 - 19.19	11.42	10.04	3.6 - 23.96
SiO <sub>2</sub> (%)	71.90	72.54	59.55 - 86.91	69.57	68.35	58.87 - 81.35
Al <sub>2</sub> O <sub>3</sub> (%)	9.97	9.57	5.98 - 16.09	11.21	10.86	9.06 - 14.54
TiO <sub>2</sub> (%)	0.33	0.28	0.19 - 0.77	0.54	0.51	0.38 - 0.73
Fe <sub>2</sub> O <sub>3</sub> (%)	2.87	2.66	1.58 - 5.03	3.30	2.96	2.45 - 4.87
MnO (%)	0.04	0.03	0.006 - 0.13	0.04	0.04	0.03 - 0.05
MgO (%)	0.97	0.90	0.47 - 1.58	1.66	1.61	1.29 - 2.56
CaO (%)	1.84	1.09	0.03 - 5.19	5.68	5.45	1.41 - 9.03
Na <sub>2</sub> O (%)	1.60	1.55	1.09 - 2.12	1.10	1.14	0.68 - 1.53
K <sub>2</sub> O (%)	1.99	1.84	1.45 - 2.9	2.36	2.26	1.85 - 3.02
P <sub>2</sub> O <sub>5</sub> (%)	0.13	0.10	0.07 - 0.43	0.13	0.13	0.08 - 0.17
Co (ppm)	1.36	0.00	ND - 12.3	2.31	1.27	ND - 9.66
Cr (ppm)	251.70	204.35	73.74 - 728.9	309.28	239.60	73.3 - 858.01
Zr (ppm)	188.35	142.62	70.8 - 500.8	451.58	347.17	139.4 - 958.9
Ni (ppm)	19.47	17.43	8.94 - 42.17	21.83	21.12	15.4 - 32.6

The mean concentration of Fe<sub>2</sub>O<sub>3</sub> in older and younger alluvium was observed 2.87% and 3.30%, respectively. Fe shows a zigzag pattern throughout the sediment core below the depth (Figure 3). In the sediment core of older alluvium, the highest concentration of Fe<sub>2</sub>O<sub>3</sub> (5.03%) was observed near the depth of 3.0 mbgl; however, in the sediment core of younger alluvium, two sharp peaks of Fe-oxide were observed at the depth of 15.0 mbgl and 33.0 mbgl with a Fe concentration of 4.35% and 4.87% respectively. The high Fe concentration at these depths might be due to the presence of the iron minerals like hematite, magnetite and goethite (Mukherjee et al., 2012; Saha & Shukla 2013; Kumar et al., 2018). The mean concentration of MnO was almost comparable throughout the sediment core below the depth except for the surface sediment sample in the older alluvium. The mean concentration of MnO was reported 0.4% in both older and younger alluvium sediment cores.

The mean concentration of As in the older and younger alluvium sediment core was reported 11.5 and 11.42 mg/kg, respectively (Figure 3.3). It was clear from the figure that As did not show any distinct trend throughout the core below the depth. As concentration in the sediment core of older alluvium (at Khorabar) was elevated in the upper section of core sediment and shown

a good correlation with elevated Fe and Mn. A comparative litholog was illustrated with As concentration in sediment cores (Figure 3.4). The litholog indicated high As was associated with light yellow color and silty clay. The upper section of the sediment core was oxidized in older alluvium due to low water table 4.37 mbgl (Rampur piezometer well, CGWB, 2018) indicating, Fe gets precipitated from water and might be adsorbed As on Fe-oxides and elevate As in the sediment core. In the sediment core of younger alluvium (at Farshiya), an elevated As concentration was reported at a depth of 15 mbgl (Figure 3.3). A similar trend was observed in Al, Fe, Mg, Ni and Cr below the sediment core depth. They were associated with the dark grey fine silty clay (Figure 3.4), indicating As might be adsorbed on metal (Fe and Al) oxides and clay minerals.

The property of soil texture and percentage plays an important role in binding As with sediment (Reza et al., 2010; Hossain et al., 2014). Several studies have reported that aluminosilicate clay minerals tend to adsorb remarkable amounts of arsenate over arsenite (McLean, 1992; Doušová et al., 2006).

The mean concentration of CaO in the sediment core of OA was reported 1.84% and 5.68% in the sediment core of YA. In comparison, the mean concentration of MgO was observed 0.97% in the sediment core of OA and 1.66% in the sediment core YA. The concentration of Ca and Mg increased in the sediment core below the depth (Figure 3.3), indicating sedimentary deposited silicate and carbonate minerals might be responsible for the enrichment of Ca and Mg in the study area. The concentration of Na<sub>2</sub>O was almost constant with the depth in both the litholog of OA and YA (Figure 3.3). The mean concentration of Na<sub>2</sub>O was slightly higher in the sediment core of OA (1.60%) compared to YA (1.10%), suggesting that Na-containing minerals such as feldspar and halite might be responsible for Na enrichment in the study area. Evaporation also significantly influenced the Na concentration in sediment (Zhou et al., 2020). The mean concentration of K<sub>2</sub>O was observed 1.99% in the sediment of OA and 2.36% in the sediment core of YA. The vertical distribution of K<sub>2</sub>O followed a similar trend to Al<sub>2</sub>O<sub>3</sub>, indicating, both may be coming from similar sources like K-feldspar and aluminosilicate in the study area. The mean concentration of P<sub>2</sub>O<sub>5</sub> was observed 0.13% in the sediment core of OA and YA (Table 3.3). The common phosphate minerals such as apatite and hydroxyapatite might be responsible for elevated phosphate in sediment cores.

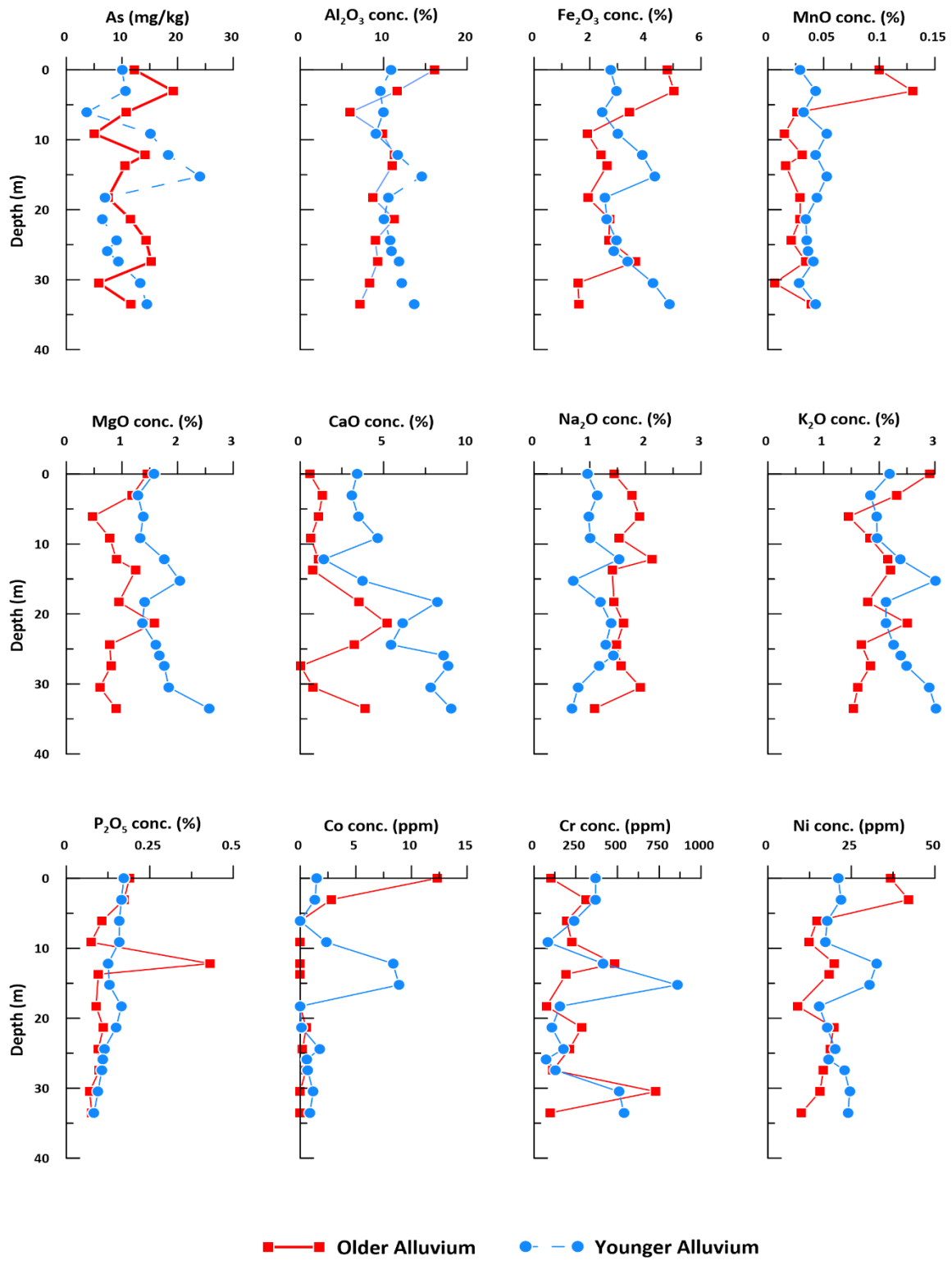


Figure 3.3: Depth-wise variation of elements in the sediment cores of older and younger alluvium

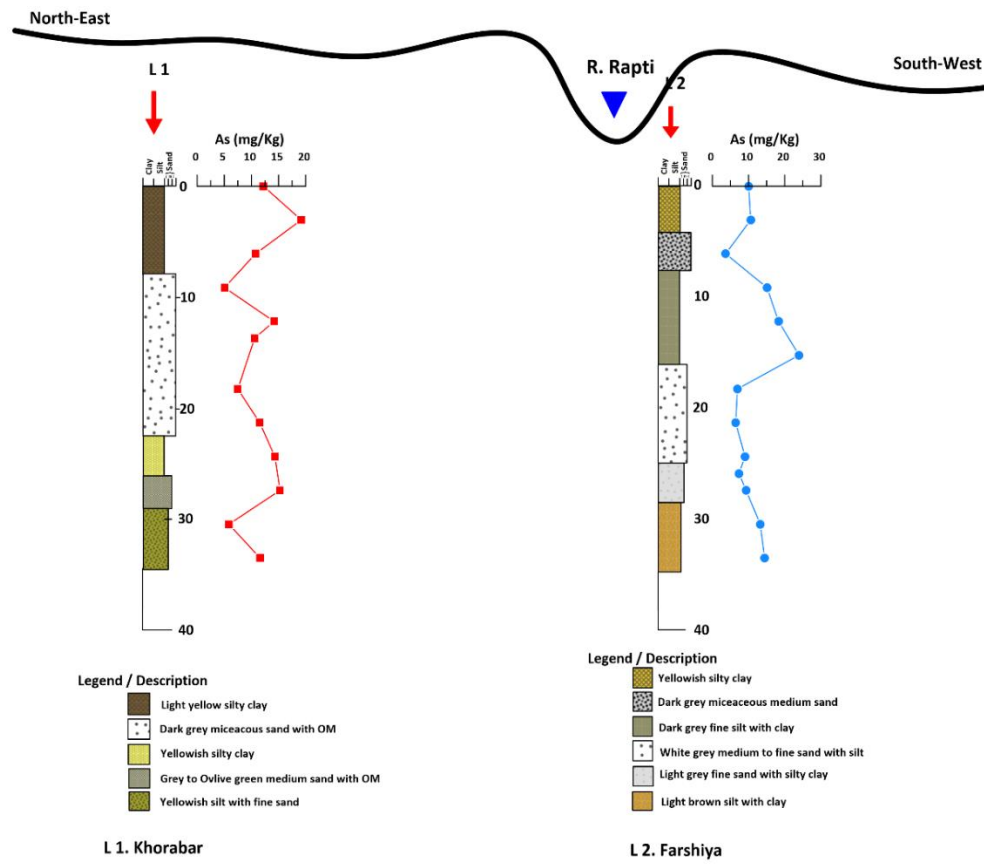


Figure 3.4: Litholog illustrating the various lithofacies and depth-wise distribution of As in sediment cores (Study area 1, Gorakhpur)

The mean concentration of Co was observed slightly higher in the sediment core (Table 3.3) of YA (2.31 ppm) compared to OA (1.36 ppm). A positive correlation of Co with Fe<sub>2</sub>O<sub>3</sub> and Al<sub>2</sub>O<sub>3</sub> indicates that minerals of the Al and Fe such as mica and magnetite might be responsible for Co in the study area (Nikova et al., 2016). Similarity Ni also positively correlated with Al<sub>2</sub>O<sub>3</sub>, Fe<sub>2</sub>O<sub>3</sub>, and MnO (Figure 3.3), suggesting the availability of accessory minerals such as mica, pyroxene, magnetite etc., were associated with the contribution of Ni to the sediment. The mean value of Cr in the sediment core of OA and YA was observed 251.7 ppm and 309.3 ppm, respectively (Table 3.3). From figure 3.3, it was cleared that there was not any significant trend observed between the Cr concentration and depth. A sharp peak was observed at 15.0 mbgl (Figure 3.3). It showed a constructive interference with other elements like Al<sub>2</sub>O<sub>3</sub>, Fe<sub>2</sub>O<sub>3</sub>, Ni, Co, P<sub>2</sub>O<sub>5</sub>, etc. These elements in the sediment core might come from accessory minerals like mica, pyroxene etc.

In study area 2 (Ghazipur), the mean concentration of  $\text{Al}_2\text{O}_3$  in the sediment core of OA and YA was observed 10.80% and 12.68%, respectively. The concentration of  $\text{Al}_2\text{O}_3$  was almost constant throughout the depth in the core sediments (Figure 3.5). A sharp peak of high aluminum was observed in the sediment core of YA at a depth of 25 mbgl indicates minerals like albite, muscovite and aluminosilicate might be there (Kumar et al., 2018b). The depth-wise distribution of  $\text{Fe}_2\text{O}_3$  shown a similar pattern to  $\text{Al}_2\text{O}_3$  in study area 2. The mean  $\text{Fe}_2\text{O}_3$  concentration was observed higher in the sediment core of YA (4.32%) than OA (3.20%). The concentration of Fe was decreasing with the depth in both the geomorphic setups (Figure 3.5). A sharp peak of high Fe concentration was found at 25 mbgl in the core sediment of YA, indicating minerals of the Fe, goethite, magnetite and hematite might be there for Fe enrichment.

Table 3.4: Statistical summary of sediment geochemistry (older and younger alluvium) of the study area 2 (Ghazipur)

	OA (n=14)			YA (n=13)		
	Mean	Median	Range	Mean	Median	Range
Depth (m)	16.76	16.76	0 - 33.53	15.73	15.24	0 - 33.53
As (ppm)	11.08	10.89	1.40 - 26.31	14.26	13.31	2.6 - 31.52
$\text{SiO}_2$ (%)	70.49	72.61	47.49 - 85.73	65.70	64.36	53.79 - 83.45
$\text{Al}_2\text{O}_3$ (%)	10.80	10.74	6.79 - 15.09	12.68	11.46	9.46 - 17.79
$\text{TiO}_2$ (%)	0.48	0.41	0.29 - 0.85	0.79	0.80	0.53 - 1.06
$\text{Fe}_2\text{O}_3$ (%)	3.20	2.99	2.03 - 5.46	4.32	3.89	2.43 - 7.62
MnO (%)	0.04	0.04	0.01 - 0.07	0.05	0.05	0.03 - 0.08
MgO (%)	1.46	1.41	0.96 - 2.32	1.79	1.75	1.24 - 2.53
CaO (%)	2.07	1.63	1.05 - 6.06	2.90	3.35	0.65 - 4.42
$\text{Na}_2\text{O}$ (%)	1.41	1.40	0.85 - 1.86	1.12	1.08	0.43 - 1.94
$\text{K}_2\text{O}$ (%)	2.10	2.14	1.77 - 2.43	2.20	2.20	1.62 - 2.85
$\text{P}_2\text{O}_5$ (%)	0.14	0.11	0.08 - 0.39	0.16	0.15	0.12 - 0.2
Co (ppm)	3.92	2.53	0 - 16.21	7.97	5.67	0 - 25.9
Cr (ppm)	578.49	434.8	64.6 - 1494.1	542.15	287.48	118.6 - 1145.9
Zr (ppm)	271.41	259.21	125.5 - 446.5	432.17	349.77	250.5 - 835.6
Ni (ppm)	23.53	20.97	12.2 - 49.5	34.34	28.26	14.5 - 59.5

The mean concentration of MnO in the sediment core of OA was observed slightly low (0.04%) compared to YA (0.05%). In the depth-wise distribution plot, MnO was not shown any distinct trend with the depth in both the geomorphic setups (Figure 3.5).

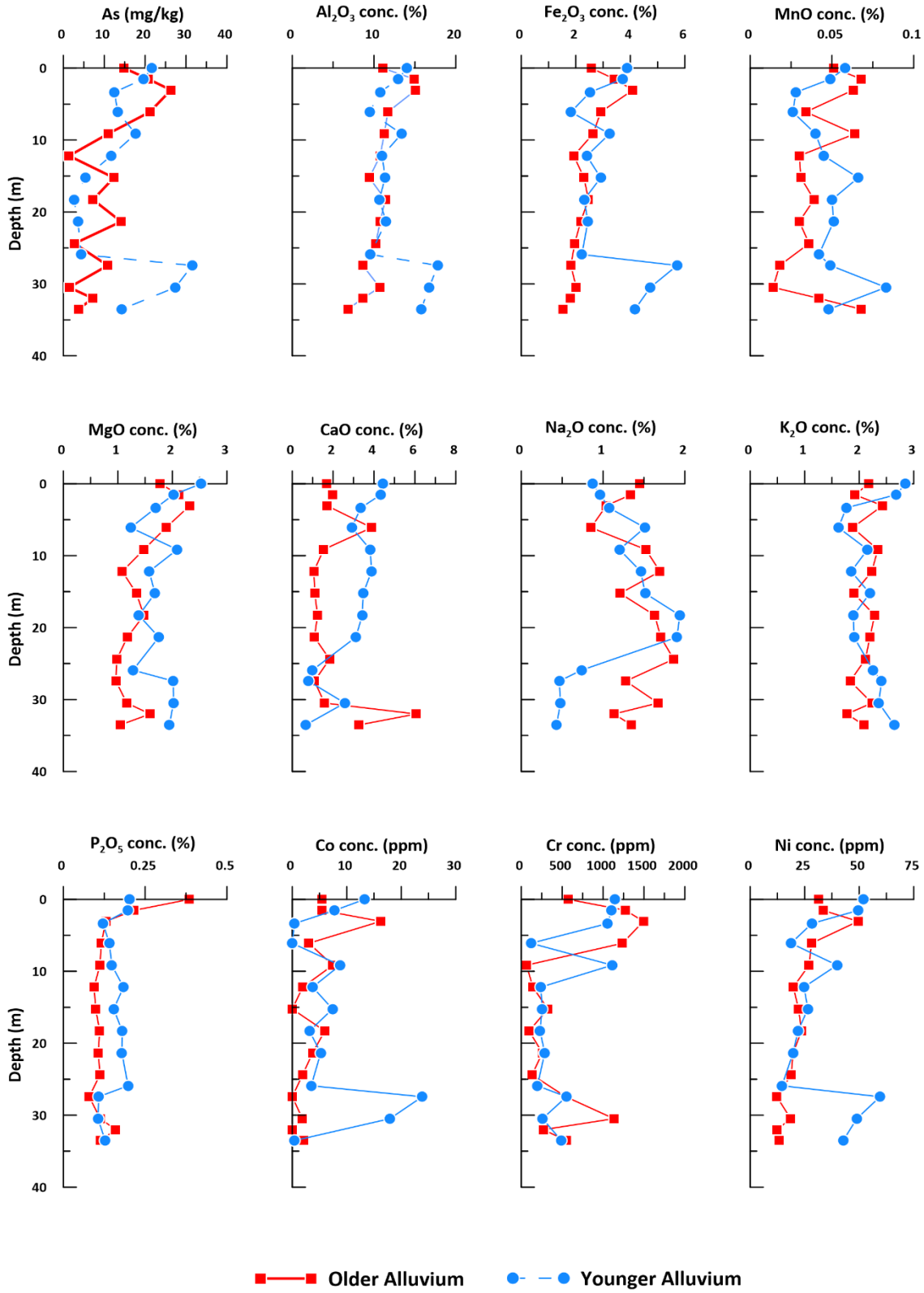


Figure 3.5: Depth-wise variation of elements in the sediment cores of older and younger alluvium.

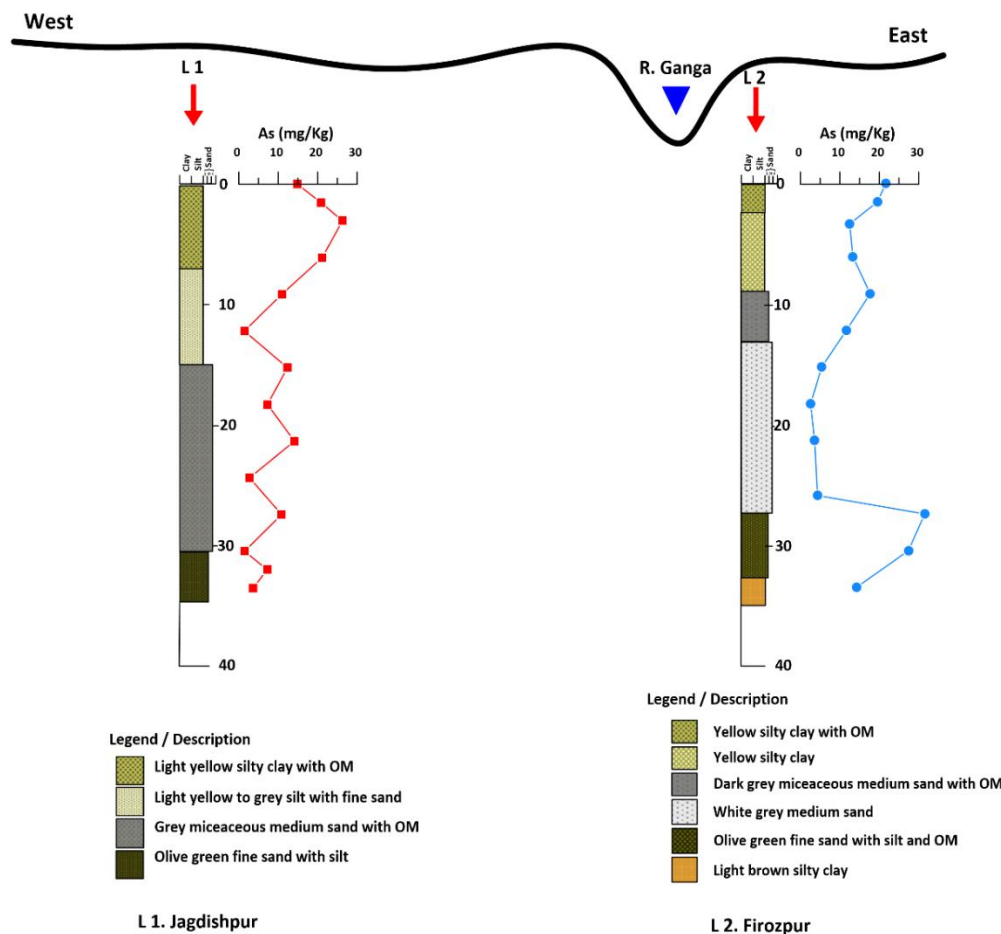


Figure 3.6: Litholog illustrating the various lithofacies and depth-wise distribution of As in sediment cores (Study area 2, Ghazipur)

The mean concentration of As was observed higher in the sediment of YA (14.3 mg/kg) compared to OA (11.1 mg/kg) (Table 3.4). In OA, a significantly elevated As concentration was observed in the upper section of the sediment core at Jagdishpur. A similar trend was also observed in Al, Fe and Mn throughout the depth. The litholog indicated a higher concentration of As was associated with light yellow silty clay (Figure 3.6). In the study area, the water table was fluctuated 5.4 to 4.76 mbgl during premonsoon and post-monsoon, and it was recorded from the nearest piezometer well station at Ghazipur Sadar (CGWB, 2018). The oxidizing condition in the upper section of the sediment core facilitated oxidation and precipitation of Fe and Mn, which might be responsible for As adsorption and elevate As in the upper section of the sediment core. The sediment core of YA (at Firozpur), a depth-wise distribution of As, Fe, Al, Mg, Co, Cr and Ni

showed a similar trend, indicating some secondary Fe and Al minerals that adsorbed and elevated As in sediment core (Figure 3.6).

Depth-wise distribution plot of major ion oxides shown the concentration of CaO, MgO and K<sub>2</sub>O was almost constant throughout the cores below the depth (Figure 3.5). An elevated Ca and Mg concentration in older alluvium indicates minerals like mica, calcite and dolomite etc., might be at those depths. In the Na<sub>2</sub>O plot, the Na concentration increased up to 25 mg/l and below that, it decreased, indicated Na containing minerals like feldspar and plagioclase might be enhanced Na in the sediment core. Evaporation also significantly influenced the Na concentration in sediment (Zhou et al., 2020).

The mean concentration of P<sub>2</sub>O<sub>5</sub> in the sediment of OA and YA was reported 0.14 and 0.16%, respectively. The phosphate concentration in the surface sediment core was observed very high and below the depth, was decreasing. The trend of the phosphate was independent with other metals indicating anthropogenic influences might be there. However, in YA, it was almost the same throughout the core below the depth, indicating some common minerals such as apatite and hydroxyapatite might be responsible for phosphate in YA sediment.

The average concentration of Co, Ni and Cr were reported 3.92 ppm, 23.5 ppm and 578.5 ppm respectively in older alluvium, whereas 7.97 ppm, 34.3 ppm and 542.2 ppm respectively in younger alluvium (Table 3.4). The concentration of Co and Ni was observed higher in younger alluvium, although Cr was reported higher in older alluvium. The vertical distribution plots of Co, Ni and Cr, were almost shown similar trends like Fe<sub>2</sub>O<sub>3</sub> and Al<sub>2</sub>O<sub>3</sub> and MnO suggested, accessory minerals such as mica, pyroxene, magnetite etc., were associated with the availability of these elements in sediment core (Nikova et al., 2016).

### 3.3.3 Arsenic speciation and other trace elements in groundwater

As speciation and its oxidation state are highly dependent on the redox condition and pH of the aquifer system (Villa-lojo et al., 1997; Stollenwerk, 2003). Generally, the redox processes are associated with the adsorption/desorption mechanism of elemental species to the mineral surfaces. Several previous studies have been exemplified that As species are strongly sorbed in the oxide and hydroxide minerals of Fe and Mn (Sappa et al., 2014; Yadav et al., 2020). During field



sampling, we have measured oxidation-reduction potential (Eh), which was used to calculate the  $pe$ , to identify the As species present in the groundwater using the following expression:

$$pe = \frac{F * Eh}{2.303 RT}$$

Where F is the Faraday constant ( $F = 96490 \text{ kJ ve-eq}$ ), T is the temperature in K and R is a constant ( $R = 8.314 \text{ J/mol.K}$ )

In study area 1 (Gorakhpur), the calculated  $pe$  value for the groundwaters of OA was varied between a narrow range -3.04 to 2.8 with the mean of -0.39, which indicates anoxic to post-oxic condition (Figure 3.7). The range of the calculated  $pe$  value for groundwater in YA varied -3.06 to 2.72, with the mean of -0.94 indicating the aquifer system existed in highly anoxic to post oxic conditions. From the Eh-pH plot (Figure 3.7a), it was observed that approximately 83% of OA groundwater samples fall in  $\text{As(OH)}_3$  domain, and the remaining 17% OA groundwater samples fall in the  $\text{HAsO}_4^{2-}$  domain. In contrast, approximately 88% YA groundwater fall in  $\text{As(OH)}_3$  domain, and the remaining 12% YA groundwater fall in the  $\text{HAsO}_4^{2-}$  indicating As (III) was the dominant species in the groundwater. The Eh-pH diagram for Fe (Figure 3.7b) indicates ~79% OA groundwater samples and 76% YA groundwater samples fall into the Iron oxy(hydr)oxide ( $\text{FeOOH}$ ) field. The remaining 21% groundwater samples of the younger alluvium region and 24% groundwater samples from the older alluvium were falling in the  $\text{Fe}^{2+}$  domain, indicating that Fe (oxyhydr)oxide was significantly involved in As mobilization.

In study area 2 (Ghazipur), the calculated  $pe$  value for OA and YA groundwater were ranged from -2.14 to 0.78 and -3.23 to 1.98, respectively. The mean  $pe$  value for the groundwater of OA and YA was -0.57 and -1.02, respectively. From the plot (Figure 3.8a), it was cleared that a broad spectrum of redox potential was reported in younger alluvium compared to older alluvium and justify the anoxic condition in groundwater. And it was observed that ~88.5% of OA groundwater samples ~91.4% of the YA groundwater samples fall in  $\text{As(OH)}_3$  domain, and the remaining 11.5% of OA groundwater and 8.6% of the YA groundwater samples fall in  $\text{HAsO}_4^{2-}$ . The Eh-pH diagram for Fe (Figure 3.8b) indicates around 81% OA groundwater samples and 69% YA groundwater samples fall into the Iron oxyhydroxide ( $\text{FeOOH}$ ) domain. And the remaining 19%

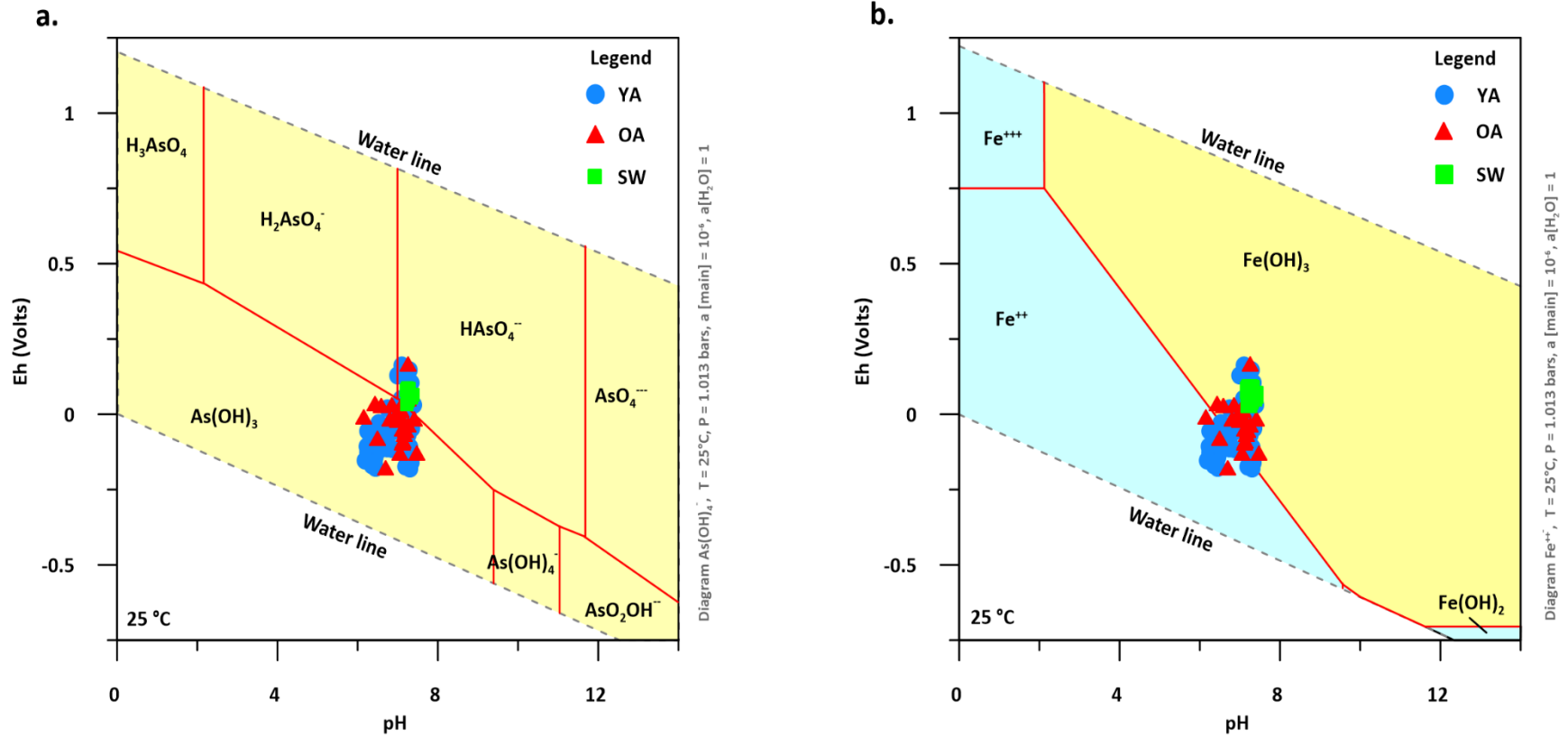


Figure 3.7: Eh-pH diagram showing the thermodynamically stable area in groundwater (a) arsenic and (b) iron species in the study area 1 (Gorakhpur)

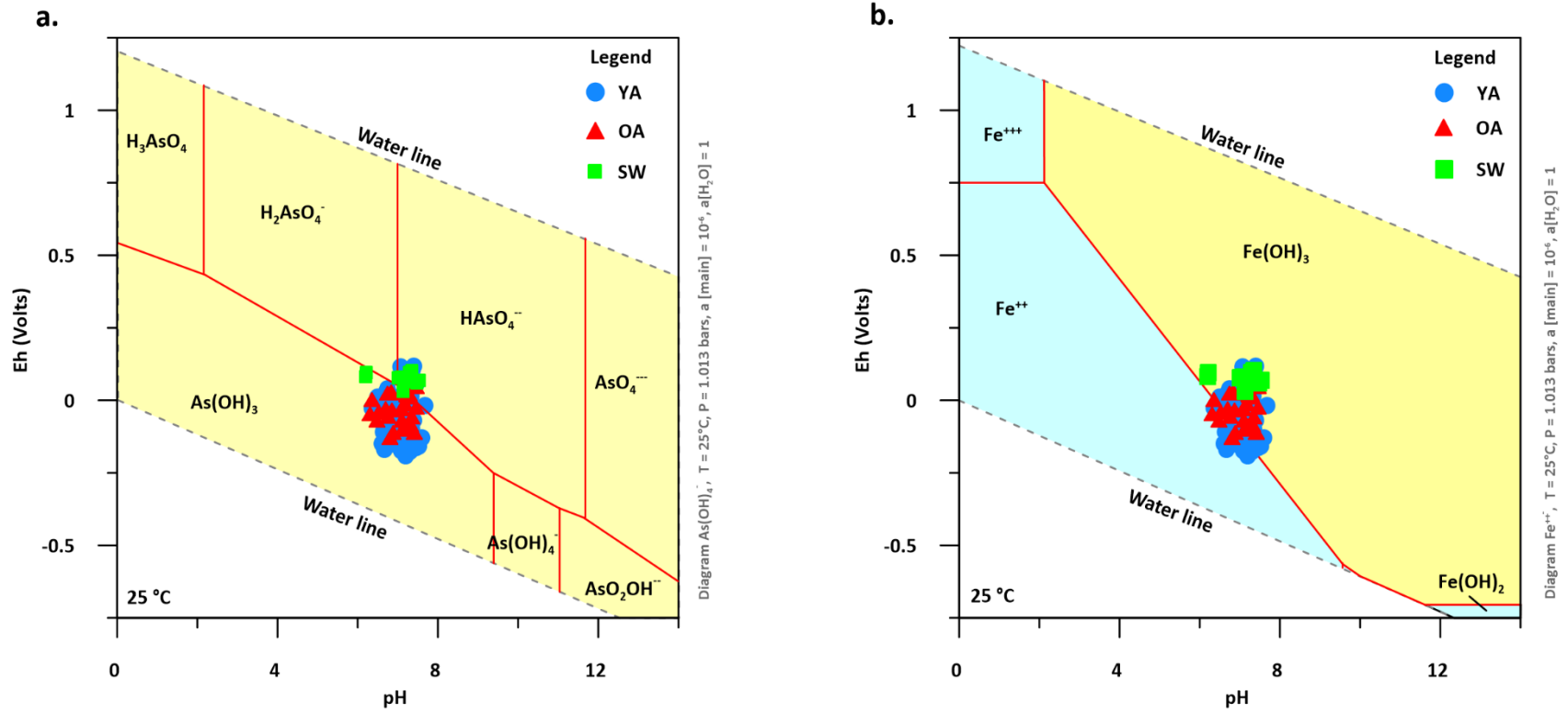


Figure 3.8: Eh- pH diagram showing the thermodynamically stable area in groundwater (a) arsenic and (b) iron species in the study area 1 (Ghazipur)

OA groundwater and 31% YA groundwater samples fall in the  $\text{Fe}^{2+}$  domain, indicating that Fe oxy(hydr)oxide was significantly involved in As mobilization.

The river water samples from both the study area were highly oxidized in nature. The mean  $pe$  value of the river water was observed at 1.09 and 1.31 in Gorakhpur and Ghazipur districts. The Eh-pH diagram for As (Figure 3.7&3.8) shown that all the river water samples were fell in the  $\text{HAsO}_4^{2-}$  field except one sample in study area 2 (Ghazipur). In the Eh-pH diagram for Fe, all the river water samples fell in  $\text{Fe}(\text{OH})_3$  field., indicating  $\text{Fe}^{3+}$  was dominated species in the river water.

### 3.3.4 Mineralogy of the sediment

Mineralogical study of any terrain plays a significant role in understanding the mineral composition, secondary mineral assemblages, and physical properties. The minerals available in the Indo-Gangetic plain were derived from the Himalayas by weathering and deposition of the Indo-Gangetic River system (Sidhu & Gilkes, 1977; Heroy et al., 2003). The X-ray diffraction (XRD) of the sediments gives a sharp reflection of the available minerals in the study area (Table 3.5). Common minerals such as quartz, muscovite, albite, orthoclase, mica, and illite were observed in all the sediment cores. The XRD peaks of calcium were only reported in the deeper section of the sediment cores.

The iron minerals like goethite, hematite, magnetite and siderite were reported in the sediment cores, but their occurrences were not consistent below the verticle depth (Figure 4.11&12, Chapter 4). Siderite is a carbonate-containing Fe mineral. In the groundwater, samples were saturated with siderite, goethite and hematite minerals. Guo et al., (2009) reported that  $\text{SI}_{\text{siderite}}$  and concentration of As in groundwater are inversely proportional to each other. Siderite worked as a sink and adsorbed dissolve As in the alluvial region, and it was suggested that mobilization of As was partially hindered by siderite precipitation (Guo et al., 2014; Shah, 2014; Kumar et al., 2018). Shah (2014) reported the minerals like quartz, muscovite, chlorite, feldspar, kaolinite, amphiboles and goethite were available in the sediment of the Gangetic plain. Pyrite is one of the common minerals for arsenic, but it was not reported in the study area. Shah (2008) also found similar results from Uttar Pradesh and Bihar. Our study found almost the same mineral

composition reported in previously published research articles around the study area (Shah, 2014; Verma et al., 2015b; Kumar et al., 2018b).

Table 3.5: Mineralogy of the selected sediment core from both the study area

Gorakhpur		Ghazipur	
Older Alluvium	Younger alluvium	Older Alluvium	Younger Alluvium
Quartz	Quartz	Quartz	Quartz
Albite	Albite	Muscovite	Muscovite
Muscovite	Muscovite	Orthoclase	Orthoclase
Illite	Illite	Albite	Albite
Anorthite	Anorthite	Anorthite	Anorthite
Mica	Mica	Mica	Mica
Chlorite	Chlorite	Chlorite	Chlorite
Orthoclase	Orthoclase	Illite	Calcite
Calcite	Calcite	Calcite	K feldspar
Hematite	Hematite	Kaolinite	Kaolinite
Magnetite	Magnetite	Hematite	Hematite
Goethite	Goethite	Goethite	Magnetite
–	Siderite	–	Goethite
–	–	–	Siderite

\*minerals like hematite, magnetite, goethite, and siderite were detected in a minor amount.

### 3.3.5 Hydrogeochemical evolution of groundwater and river water

Geochemical reaction and the intermixing of the different aquifer systems influence hydrogeochemistry of groundwater. The composition of the rock type and water component plays an essential role in the evolution of groundwater. The Piper diagram is an interpretation tool used to identify the type of water in the study area (Piper, 1944). A piper plot has been used to classify the water type in study area 1, based on different geomorphological units (Figure 3.9a). In the YA region, out of 42 groundwater samples, 38 (approx. 90%) showed Ca-Mg-HCO<sub>3</sub> type of water, one (approx. 2%) was NaCl type, and 3 (approx. 7%) were Ca-MgCl type of water represented (Figure 3.9c). Similarly, out of 24 groundwater samples in the OA region, 22 (~95%) showed CaMg-HCO<sub>3</sub> type of water, and the remaining 2 (~5%) Ca-Cl type of water was observed. The groundwater showing alkaline earth metal with weak acid was dominated in study area 1. However, river water shown alkaline earth metals with a strong acid (chloride and sulfate) were dominated (approx. 69%) water type followed by Ca-MgHCO<sub>3</sub> type of water in study area 1. The piper plot revealed that CaHCO<sub>3</sub> dominated water significantly elevates As concentration in the groundwater of OA

and YA. However, a few groundwater samples from YA shown elevated As in the mixed type of water, indicating chloride and sulphate oxidation might be involved in As mobilization. In the case of river water samples, As was associated with chloride-dominated water type.

a.

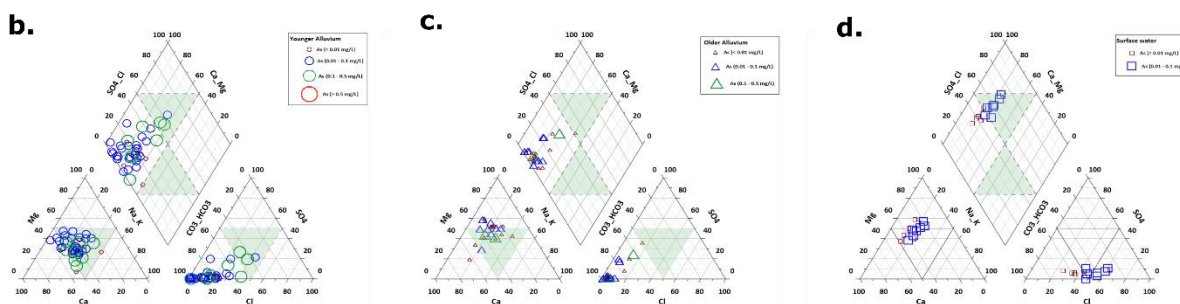
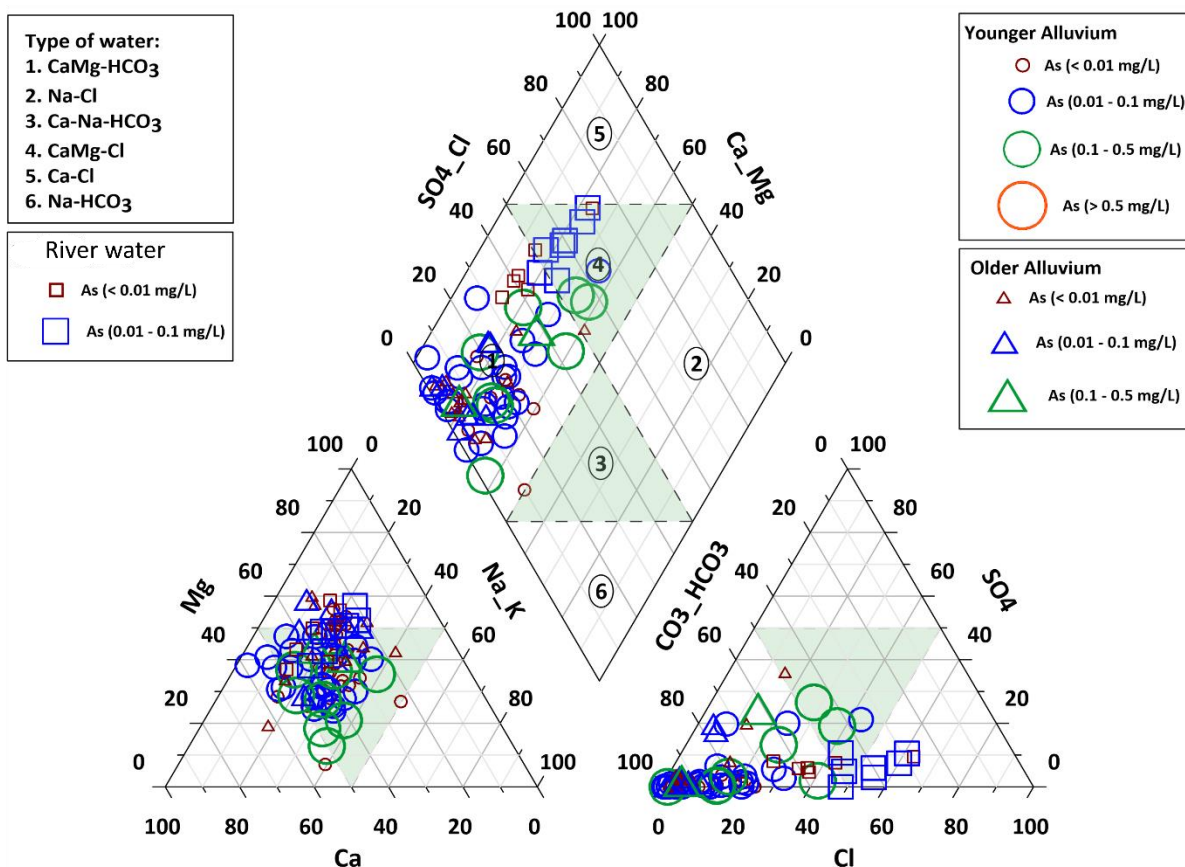


Figure 3.9: Piper plot showing groundwater evolution in study area 1 (Gorakhpur), a. Cumulative piper plot for all the samples b. Piper plot for groundwater of YA, c. Piper plot for groundwater of OA and, d. Piper plot for river water samples.

In study area 2 (Ghazipur), the piper plot revealed that alkaline earth metals and bicarbonate were dominant ions, and the major water type is Ca-MgHCO<sub>3</sub> (Figure 3.10a).

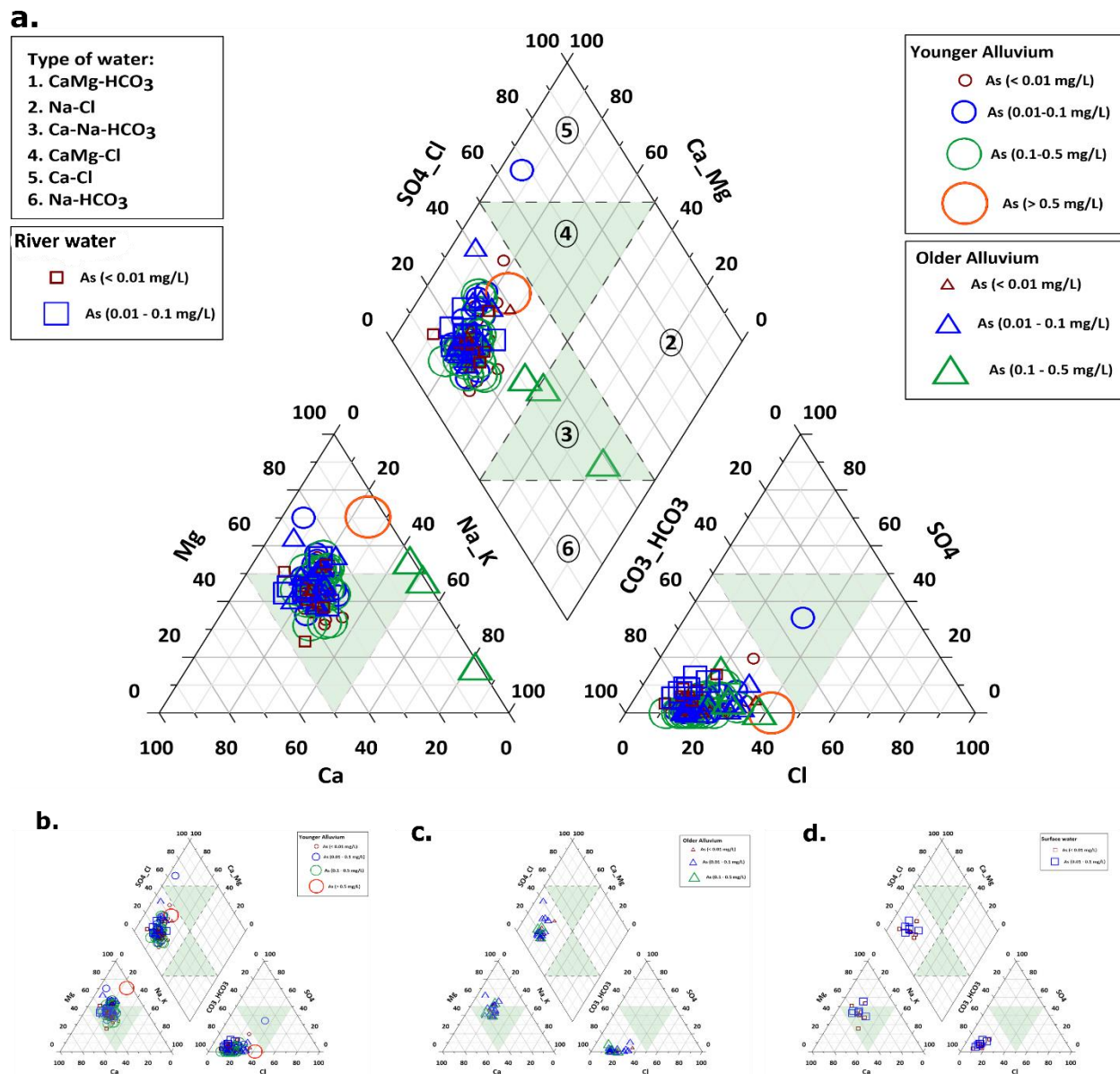


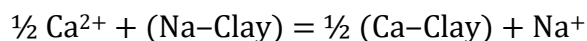
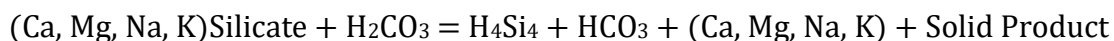
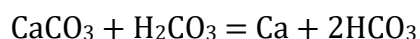
Figure 3.10: Piper plot showing groundwater evolution in study area 1 (Ghazipur), a. Cumulative piper plot for all the samples b. Piper plot for groundwater of YA, c. Piper plot for groundwater of OA and, d. Piper plot for river water samples.

We have plotted three piper plots for OA, YA, and river water on different geomorphological units available in the study area (Figure 3.10). In YA groundwater, out of 58 samples, 57 (approx. 98%) were Ca-Mg-HCO<sub>3</sub>, and one sample was CaCl type of water (Figure 3.10b). The OA groundwater and river water samples were shown Ca-MgHCO<sub>3</sub> type of

hydrogeochemical facies in the study area (Figure 10b&c). Previous studies documented that high bicarbonate ion in downstream or Central Gangetic plain plays an essential role in hydrogeochemical evolution and trace metal mobilization (Kumar et al., 2010; Mukherjee et al., 2012; Kumar et al., 2018). This study revealed the same results. It was observed that the Ca-HCO<sub>3</sub> type of water showed a high As concentration in groundwater and river water.

### Hydrogeochemical evolution:

The hydrogeochemical evolution of groundwater is mainly determined by the chemistry of the recharge water, rock water interaction and groundwater residence time within the aquifer matrix. Carbonate dissolution, silicate weathering, and evaporate dissolution are the three major governing processes that influenced groundwater chemistry and, through these processes, solutes enter into the aquifer system (Verma et al., 2015; Kumar et al., 2018). Solutes of the groundwater are mainly derived from the weathered rock and are dependable on rock water interaction and rate of weathering (Yadav et al., 2020). Weathering of carbonate rock is ~12 times faster than silicate weathering; hence the concentration of solutes in the groundwater is significantly dependent on the leachability of the lithophytes and residence time (Meybeck, 1987; Verma et al., 2015a; Yadav et al., 2020). A simple weathering reaction for minerals viz. carbonate dissolution, silicate weathering and ions exchange are given below (Mackenzie & Garrels, 1971; Meybeck, 1987; Sarin et al., 1989; Kumar et al., 2018).



The composition of groundwater is significantly influenced by the mixing of groundwater recharge and rock water interaction. Bivariate scattered plots were plotted between the several parameters to understand the major processes governing hydrogeochemical evolution and anthropogenic activity (Figure 3.11a-r). The scatter plot between total cations (Tz<sup>+</sup>) vs. Ca<sup>2+</sup> + Mg<sup>2+</sup> and total cations (Tz<sup>+</sup>) vs. Na<sup>+</sup> + K<sup>+</sup> (Figure 3.11a-f) indicates, silicate weathering was dominated over carbonate dissolution and CaHCO<sub>3</sub> water type in all the geomorphic setups. Most



of the groundwater samples of YA were fell between 2:1 and 1:1 lines (Figure 3.11a), while groundwater of OA and river water samples were fallen close to the 1:1 line (Figure 3.11b and c). The positive correlation of  $\text{Na}^+$  with TDS and EC confirmed the dominance of silicate weathering over carbonate weathering. The presence of minerals like albite and feldspar (Table 5) in the study area also supported silicate weathering. Studies published from the Central Gangetic plain also found the same mineralogy and results (Kumar et al., 2018; Singh et al., 2020). The plots between Na/Cl with EC (Figure 3.11g-i) showed that the excess of Na/Cl was increased in OA groundwater, indicating that silicate weathering was dominated. However, few samples showed a constant ratio of Na/Cl with the increased EC, indicating evaporation also significantly involved in the hydrogeochemical processes. The plots between  $\text{Na}^+$  and  $\text{Cl}^-$  (Figure 3.11j-l) showed that most of the groundwater sample fell 1:1 line, indicating halite dissolution. The Na/Cl ratio was greater than 1, indicating silicate weathering (Lakshmanan et al., 2003). In our study area, around 58% of the YA groundwater sample showed Na/Cl ratio greater than 1, indicating silicate weathering. Few groundwater samples from OA and YA and river water samples showed significant  $\text{Cl}^-$  enrichment. They fell below the 1:1 line, indicating dissolved Na might be removed by cation exchange processes or maybe anthropogenic inputs like septic tank effluents, industrial waste and inorganic fertilizers enhanced Cl in groundwater and river water (Kaur et al., 2019; Singh et al., 2020). From the plots  $\text{K}^+$  vs.  $\text{NO}_3^-$  (Figure 3.11m-o), most of the YA groundwater samples fell below the 1:1 line, indicating sewage discharge and domestic waste might be responsible. A few YA groundwater and all the river water samples were falling along the 1:1 line, indicating inorganic fertilizers inputs might be the possible source for  $\text{K}^+$  and  $\text{NO}_3^-$  in groundwater and river water. In OA groundwater, the concentration of  $\text{NO}_3^-$  exceeded over  $\text{K}^+$ , indicating sewage discharge might be responsible for enriched  $\text{NO}_3^-$  in the groundwater. In the scatter plots  $\text{Cl}^-$  vs.  $\text{NO}_3^-$  (Figure 3.11p-r), the correlation was missing. The concentration of  $\text{Cl}^-$  was higher in all the geomorphic setups compare to  $\text{NO}_3^-$  indicates interferences like bleaching powder and industrial waste, septic tank effluents might be responsible. The scatter plot between the molar ratio of Ca/Mg vs. sample number was plotted (Figure 3.12 a-c), and the majority of the groundwater samples fell between the molar ratio 1 and 2. If the ratio is close to 1, indicate dolomite weathering, while a ratio close to 2 indicates calcite weathering.

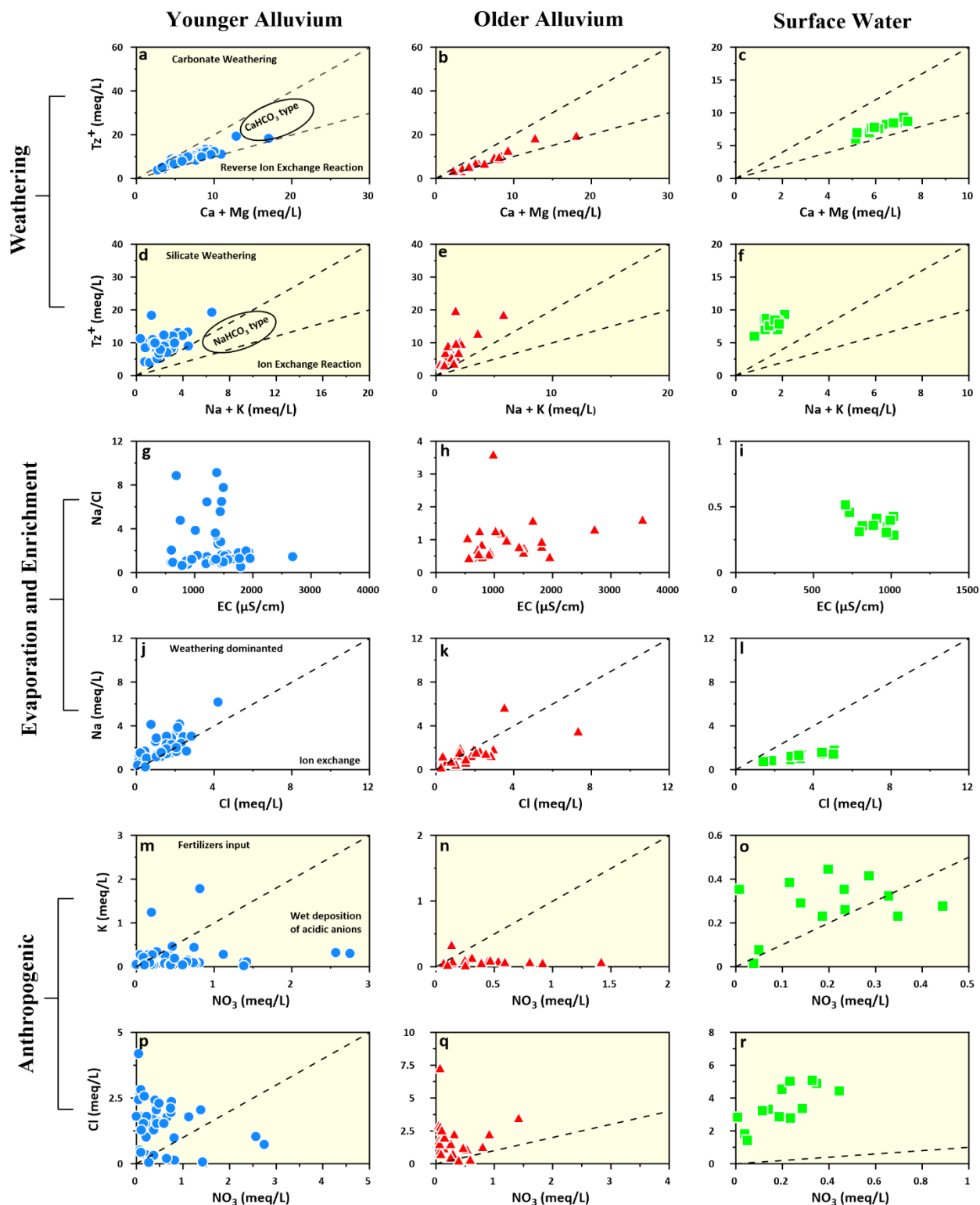


Figure 3.11: Bivariate scatter diagrams tracing the hydrogeochemistry of the groundwater and river water. Possible weathering in OA, YA and river water (a-f). Evaporation and mineral mediated enrichment in Ya, OA and river water (g-l). Anthropogenic influences in YA, OA and river water (m-r) in study area 1 (Gorakhpur).

In YA groundwater, most of the samples fall between the molar ratio of 1 and 2, indicating calcite dissolution; however, OA groundwater and river water samples represented molar ratio  $\leq 1$ , indicating dolomite dissolution. The plot between  $\text{Ca}^{2+} + \text{Mg}^{2+}$  vs.  $\text{HCO}_3^- + \text{SO}_4^{2-}$  (Figure 3.12d-f) also supported the carbonate dissolution in the study area (Singh et al., 2020). The plot between  $\text{Ca}^{2+} + \text{Mg}^{2+}$  vs.  $\text{Cl}^-$  (Figure 3.12g-i), was not showing any significant correlation between alkaline earth metals and chloride in OA and YA groundwater. The high ratios of  $\text{Ca}^{2+} + \text{Mg}^{2+} / \text{HCO}_3^-$  cannot be attributable to  $\text{HCO}_3^-$  depletion because  $\text{HCO}_3^-$  does not produce carbonic acid in an alkaline environment. However, in river water,  $\text{Cl}^-$  positively correlated with alkaline earth metals indicate Ca and Mg might be added to the aquifer at the same increased salinity rate (Sakizadeh et al., 2016).

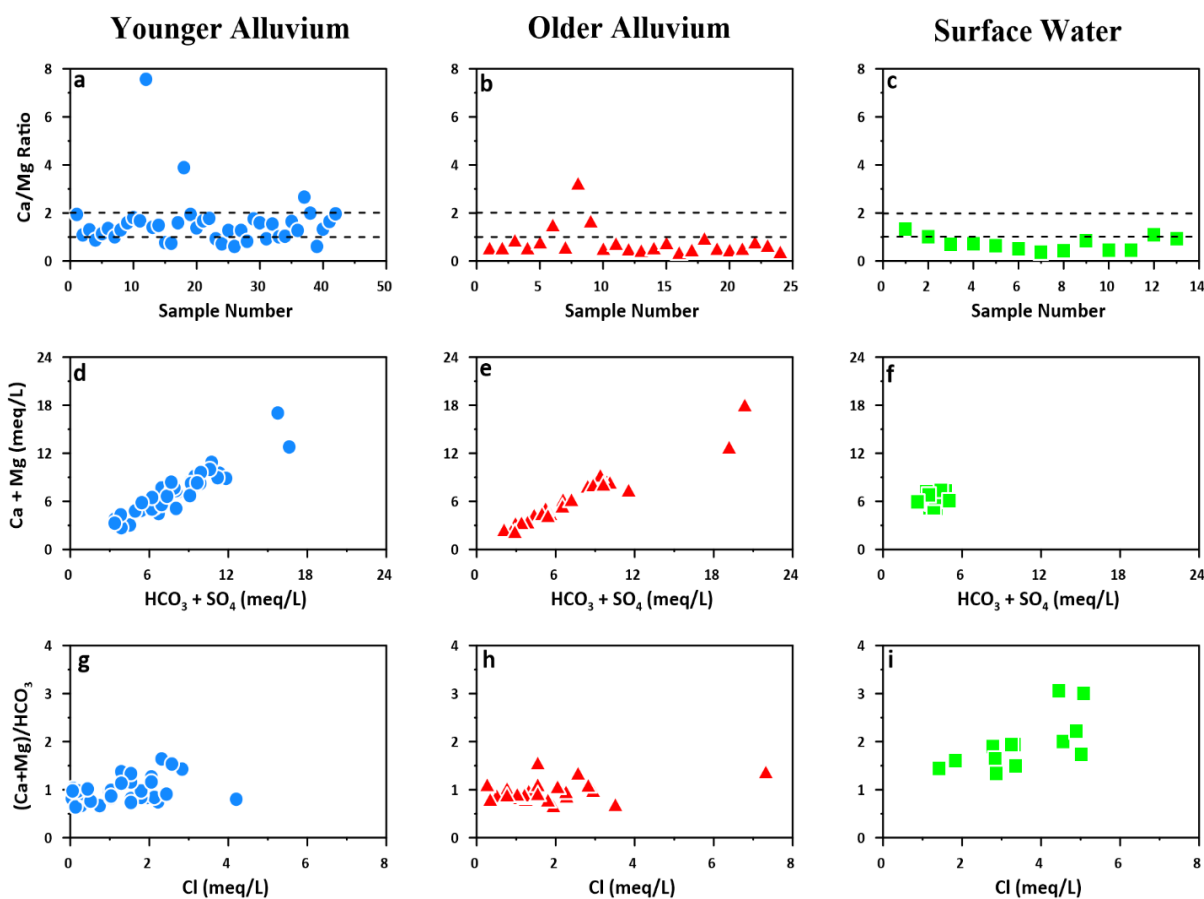


Figure 3.12: Bivariate scatter plot tracing the major hydrogeochemical processes in the groundwater and river water of study area 1 (Gorakhpur)

In study area 2 (Ghazipur), the scatter plots between  $\text{Tz}^+$  vs.  $\text{Ca}^{2+} + \text{Mg}^{2+}$  (Figure 3.13a-c) showed all the groundwater samples from OA and YA regions and river water samples fell

between 1:2 line, indicate alkaline earth metals were the dominant cation in the study area. The plots  $Tz^+$  vs.  $Na^+ + K^+$  (Figure 3.13d-f) showed all the OA and YA groundwater samples fallen above the 1:1 line, indicated silicate weathering and carbonate dissolution were dominated over ion exchange processes. Plots showed that the groundwater was of  $CaHCO_3$  type in both the geomorphic setups.  $Na^+$  showed a positive correlation with TDS and EC, while  $K^+$  showed a negative correlation with EC and TDS, indicating silicate weathering was dominated over carbonate dissolution, and the processes like Na-feldspar and albite (Table 3.5) dissolution might be involved (Kumar et al., 2018; Singh et al., 2020). In the study area, Na positively correlated with  $HCO_3^-$  indicates exchange of the ions could be possible with  $CaMg-HCO_3$  type of water. The plots between  $Na/Cl$  with EC (Figure 3.13g-i) showed that the ratio of  $Na/Cl$  was not constant with the increased EC, indicating weathering was the dominant process over the evaporation. In the groundwater of YA, a few samples showed a constant  $Na/Cl$  ratio with EC, indicated evaporation processes were significantly involved in the hydrogeochemical evolution of those samples. The plot between  $Na^+$  vs.  $Cl^-$  (Figure 3.13j-l) also supported the surplus concentration of  $Na^+$  in groundwater from silicate weathering, while samples close to the 1:1 line indicate halite dissolution. A very few groundwater samples (from OA and YA) showed  $Cl^-$  enrichment, indicating dissolved Na might be removed by cation exchange processes or anthropogenic inputs of  $Cl^-$  ions such as septic tank effluents and inorganic fertilizers (Kaur et al., 2019; A. Singh et al., 2020). The chemistry of groundwater is also significantly influenced by anthropogenic activities like fertilizers, industrial sewage, domestic waste, etc. (Kumar et al., 2007; Yadav et al., 2020). The plots between  $K^+$  vs.  $NO_3^-$  (Figure 3.13m-o) show that the 35% groundwater sample and all the river water samples fell close or above the 1:1 line, indicating fertilizers could be the possible source for  $K^+$  and  $NO_3^-$  in those water samples. From the same plots, it was clearly shown that around 65% of groundwater samples (from both geomorphic setups) fell below 1:1 line indicate domestic waste and wet deposition of acid might be elevated  $NO_3^-$  concentration in groundwater. The plots between  $Cl^-$  vs.  $NO_3^-$  (Figure 3.14p-r) indicate that  $Cl^-$  concentrations exceeded  $NO_3^-$  in groundwater and river water, specify the influence of anthropogenic activities such as bleaching powder and industrial waste, septic tank effluents might be responsible for elevated  $Cl^-$  in groundwater and river water.

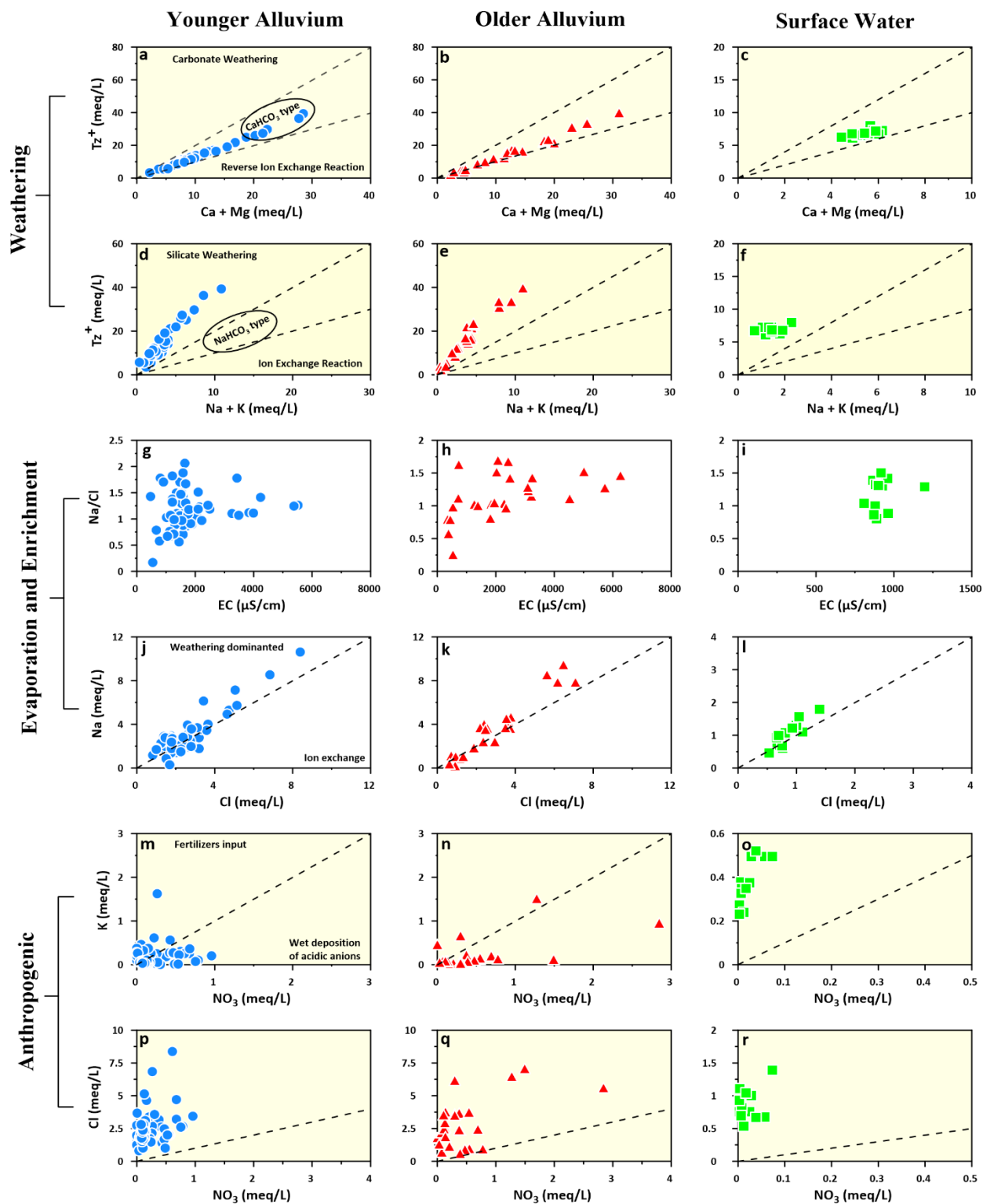


Figure 3.13: Bivariate scatter diagrams tracing the hydrogeochemistry of the groundwater and river water. Possible weathering in OA, YA and river water (a-f). Evaporation and mineral mediated enrichment in Ya, OA and river water (g-l). Anthropogenic influences in YA, OA and river water (m-r) in study area 2 (Ghazipur)

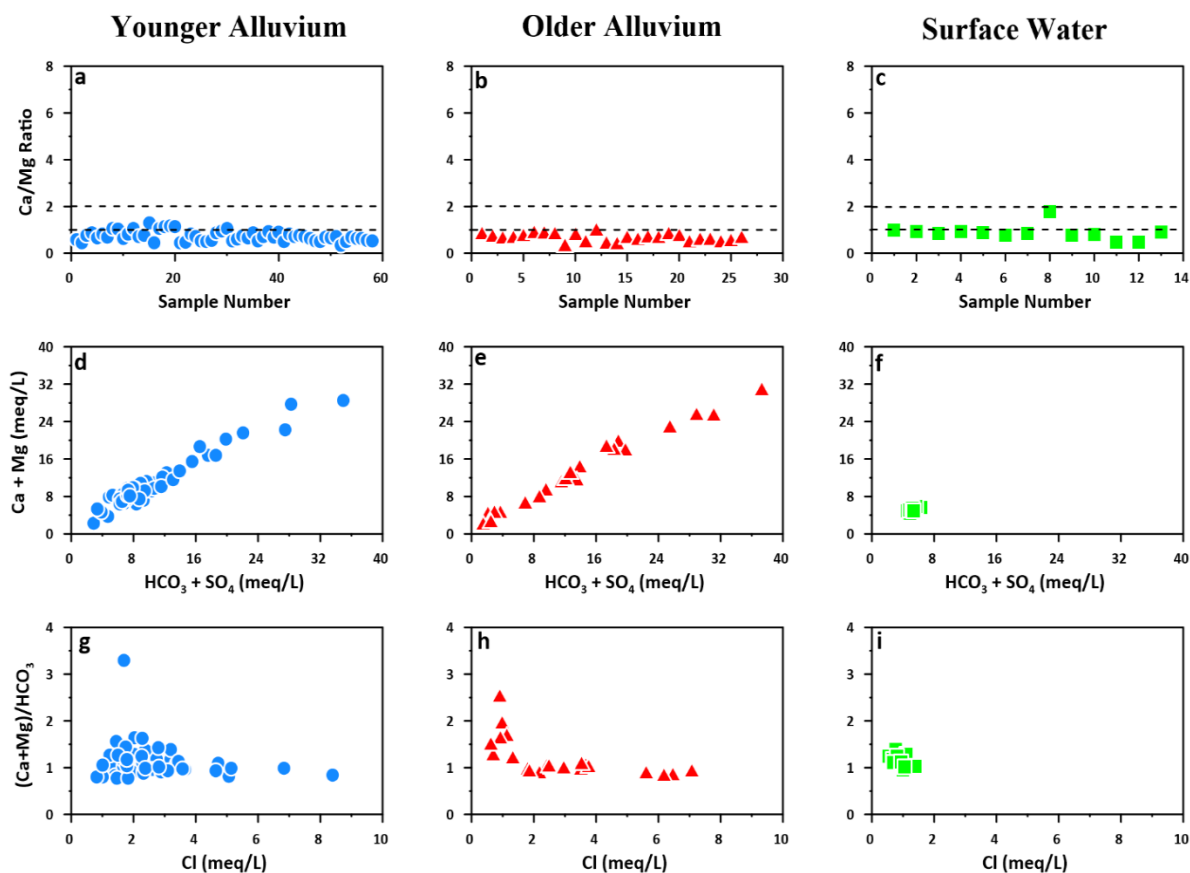


Figure 3.14: Bivariate scatter plot tracing the major hydrogeochemical processes in the groundwater and river water of study area 2 (Ghazipur)

The plots between molar ratio  $\text{Ca}^{2+}/\text{Mg}^{2+}$  vs. sample number were plotted (Figure 3.14 a-c). The molar ratio of  $\text{Ca}^{2+}/\text{Mg}^{2+}$  was fallen between 0-1, indicate dolomite weathering in the groundwater of older and younger alluvium. The plot between  $\text{Ca}^{2+} + \text{Mg}^{2+}$  vs.  $\text{HCO}_3^- + \text{SO}_4^{2-}$  (Figure 3.14d-f) supports the carbonate dissolution in the study area (Singh et al., 2020). From the plots between  $\text{Ca}^{2+} + \text{Mg}^{2+}/\text{HCO}_3^-$  vs.  $\text{Cl}^-$  (Figure 3.14g-i), it was observed That the ratio of  $\text{Ca}^{2+} + \text{Mg}^{2+}/\text{HCO}_3^-$  was constant with increasing salinity, indicating that  $\text{Ca}^{2+}$  and  $\text{Mg}^{2+}$  were added to the aquifer at the same rate as salinity increased (Sakizadeh et al., 2016).

### 3.3.6 Geochemical speciation modelling in solution

Saturation index (SI) is a method of determining the degree of equilibrium between the aqueous and solid (minerals) phases. It refers to the tendency of the minerals to remain dissolved or precipitate once they enter the aquifer. The saturation indices of water samples were calculated using WATEQ4F software (Ball & Nordstrom, 1991). Saturation indices were determined by the

log of ionic activity to the minerals solubility product (Chidambaram et al., 2011; Yadav et al., 2020). A positive SI value represents supersaturation that refers to the tendency of the minerals being precipitated from the groundwater. At the same time, a negative SI represents undersaturation, which refers to a mineral's tendency to dissolve into the groundwater. If the saturation indices value 0 or with the range of  $\pm 0.5$  for a given mineral represent apparent equilibrium with the groundwater (Srinivasamoorthy et al., 2014). The SI was calculated for all water samples to identify the essential minerals assemblages, and the results were plotted in figure (3.15). Some essential minerals such as anhydrite, hydroxyapatite, pyrolusite, and manganite are undersaturated and remain dissolved once they contact groundwater. Calcite, dolomite and gibbsite are slightly saturated indicated carbonate minerals-rich deposition in the alluvial plain. Iron and manganese-bearing minerals such as hematite, goethite, and siderite are supersaturated in all geomorphic setups, referring to the mineral being precipitated. The precipitated minerals of Fe and Mn provide a suitable solid surface for As adsorption. It is well accepted; arsenic successfully adsorbed into Fe and Mn oxides surface (McArthur et al., 2010; Kumar et al., 2018). Although, redox-sensitive species such as pH are also significantly involved in As sorption and desorption on iron-oxyhydroxide. The adsorption of As(V) into goethite, hematite, magnetite and other zero-valent iron (ZVI) is a function of pH, and maximum adsorption was found at pH 2 to 8. When pH raised above 11, the adsorption rate decreased (Mamindy-Pajany et al., 2011; Yang et al., 2017; Kumar et al., 2018). Some studies also found that As(III) adsorption into the hematite and goethite minerals is higher at pH 6-8 (Dixit & Hering, 2003; Yang et al., 2017). In study area 1 (Gorakhpur), the groundwater pH varies between 6.1 to 7.5, and groundwater was slightly saturated for dolomite and gibbsite. However, in study area 2 (Ghazipur), groundwater was slightly saturated for calcite, dolomite, chlorite, and gibbsite, indicating that carbonate minerals dissolution was dominated in study area 2 compared to study area 1. However, In both the study areas, groundwater was supersaturated with respect to some common minerals like; gibbsite, illite, mica, kaolinite, and orthoclase, indicating solubility of alumino-silicate minerals in groundwater. Minerals of Fe such as hematite, goethite and siderite were supersaturated in both the study area. So, they were precipitated in the aquifer system and might provide an adsorption surface for As in the aquifer system.

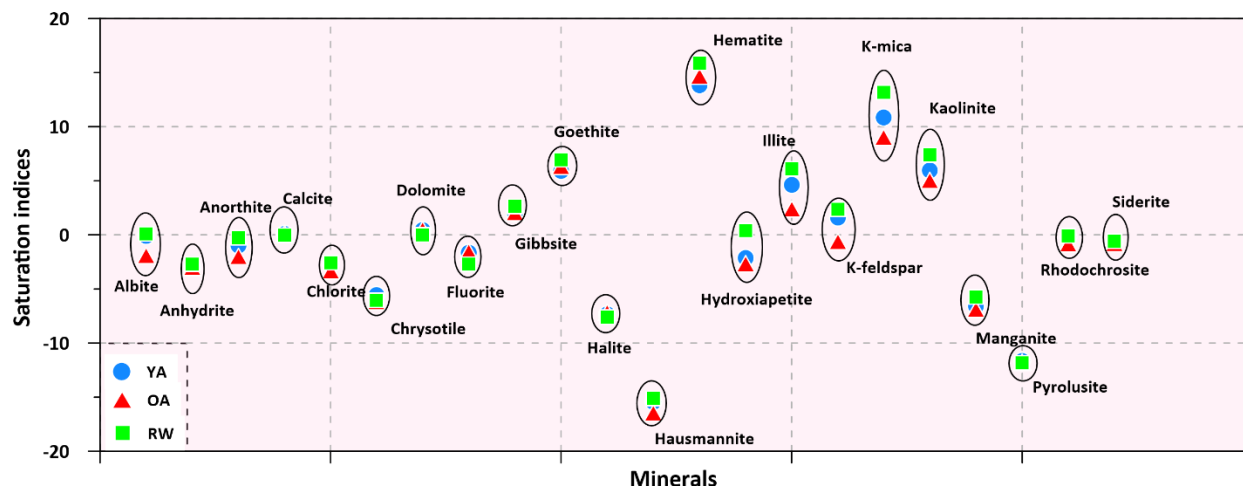


Figure 3.15: Saturation indices of various minerals obtained from modeling (PHREEQC) in YA, OA and river water of the study area 1 (Gorakhpur)

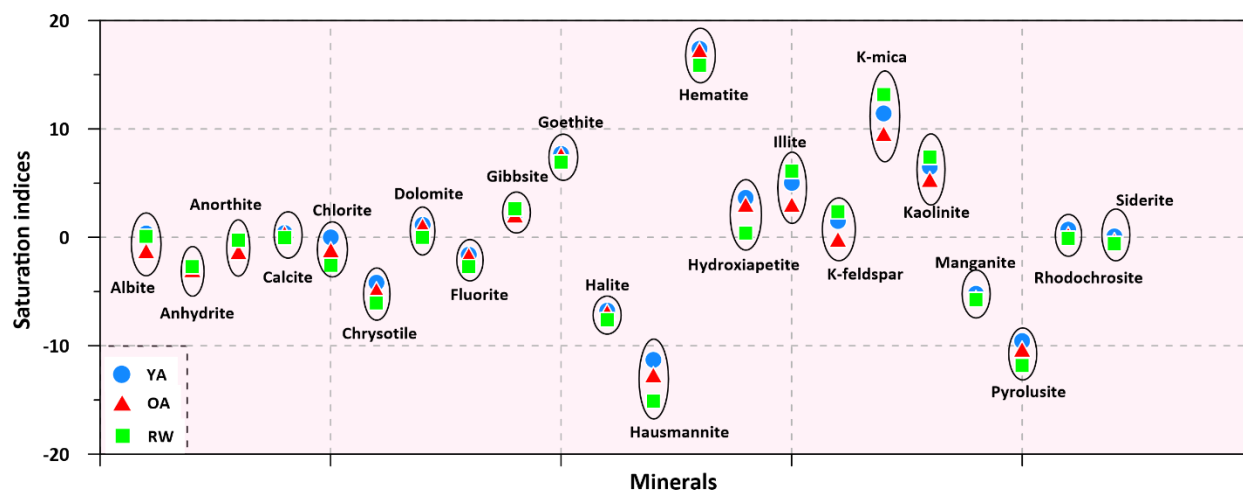


Figure 3.16: Saturation indices of various minerals obtained from modeling (PHREEQC) in YA, OA and river water of the study area 1 (Ghazipur)

### 3.3.7 As fate and mobilization in groundwater and surface water

The bivariate plots of As with physicochemical parameters were plotted in the study area (Figure 3.17a). From the plot As vs. depth, it was clear that maximum As concentration was observed in shallow depth (15.0 to 35.0 mbgl) in both OA and YA groundwater and gradually decreases with depth. Although in the present study was limited to the maximum 45.0 mbgl. Deeper wells were less prone to be arsenic contamination because As was predicated on being adsorbed into various sedimentary deposited secondary minerals and as well as arsenopyrite (Kumar et al., 2006; Ghosh et al., 2007). The bivariate plots of As vs. different redox-sensitive



species suggested, more than one reaction pathway was involved in As mobilization. The maximum As concentration was observed near neutral to slightly alkaline pH and with increasing pH i.e. 7.3, the As concentration was decreased in OA and YA groundwater (Figure 3.17b). River water samples were scattered near to the pH 7.2 to 7.4. It was observed that As concentration decreased with increasing the pH i.e. 7.3. An increased pH reduces the As adsorption capacity into the metal oxyhydroxide because of a higher net negative charge which repels negatively charged As oxyanions (Kim et al., 2012; Kumar et al., 2017).

As vs. ORP, bivariate plot indicates an insignificant correlation in OA and YA groundwater and river water (Figure 3.17c). The figure shows that a highly reducing groundwater had an elevated As concentration, indicating microbial degradation of organic matter that was responsible for the subsurface reducing condition. A very few YA groundwater samples were fell in an oxidizing environment, indicating some other processes also controlling As mobilization processes.

The bivariate correlation plot of As vs.  $\text{HCO}_3$ ,  $\text{PO}_4$  and Si are not showing any significant relationship in OA and YA groundwater of the study area. However, it is considered that bicarbonate enhances As leaching in the groundwater (Anawar et al., 2004). Similarly, phosphate behaves as a competitive surface completion ions in oxic and anoxic under both the conditions (Maier et al., 2019) and enhanced As concentration in an aqueous medium. The OA and YA groundwater was not showing any significant correlation with  $\text{PO}_4$ , while river water was moderately correlated, indicating  $\text{PO}_4$  is also involved in As mobilization processes.

Correlation of As with DOC ( $r^2=0.55$  and  $r^2=0.62$  in OA and YA groundwater, respectively) indicates microbial degradation of organic matter in the sediment. Degradation of sewage waste also triggers As mobilization in groundwater (Islam et al., 2004; Mahanta et al., 2015). In river water, a weak correlation existed between As and DOC.

The scattered plot of As vs. Fe in OA and YA groundwater and river water were plotted in figure (3.17h). A good correlation ( $r^2=0.73$  and  $r^2=0.7$ ) reported in OA and YA groundwater indicates Fe plays a significant role in As mobilization in OA and YA groundwater. In the saturation indices plot (Figure 3.15), it was observed that siderite was undersaturated in both OA and YA groundwater so, Fe remains dissolved in the groundwater. A good correlation between As

and Fe explaining the same in groundwater. Previous studies also documented that reductive dissolution of Fe oxyhydroxides is the key mechanism for As mobilization in the central Gangetic plain (Bhattacharya et al., 1997; Nickson et al., 1998).

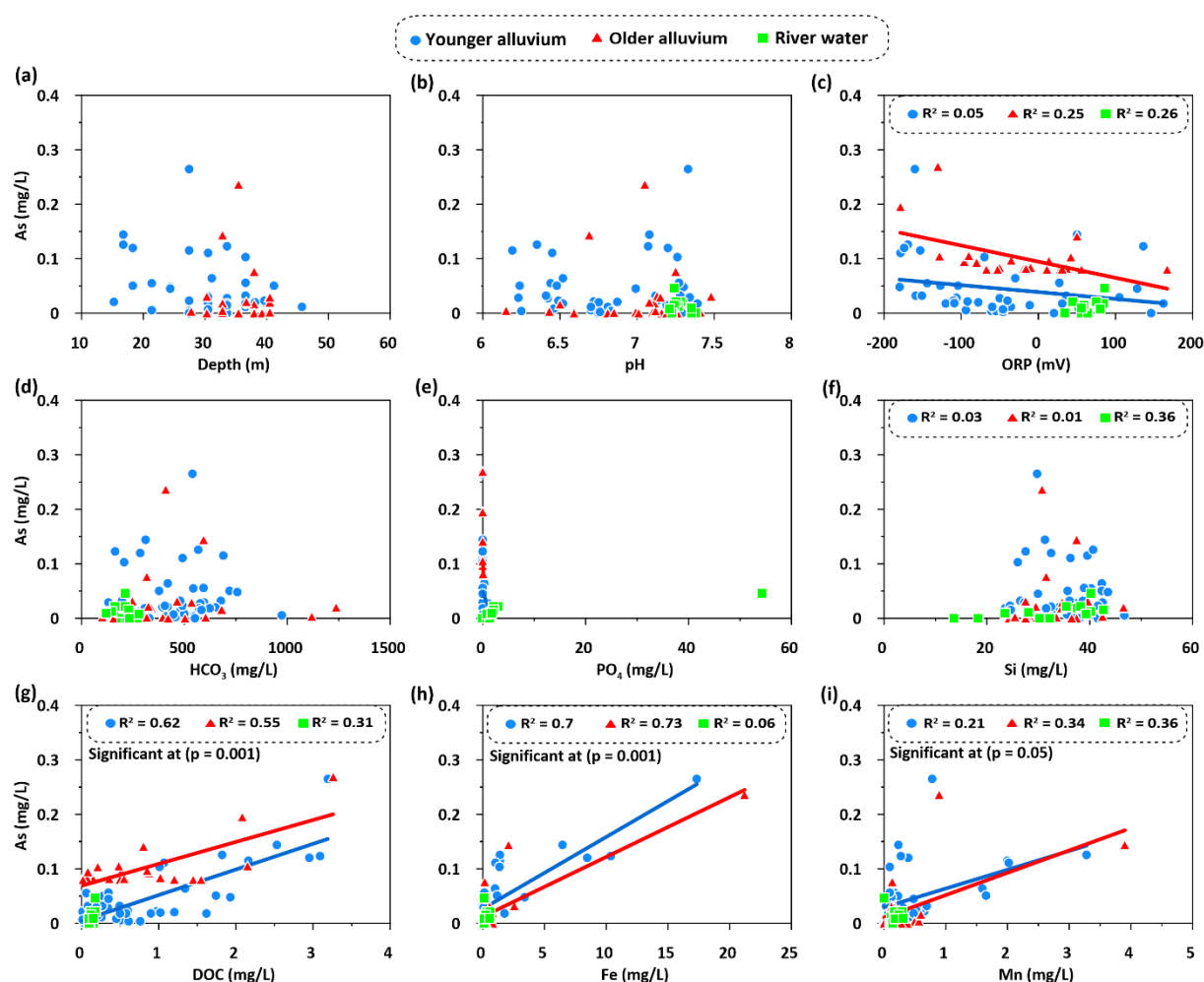


Figure 3.17: Scattered plot of As with physicochemical parameters in YA, OA and river water of study area I (Gorakhpur)

The scattered plot of As vs. Mn was weakly correlated in OA and YA groundwater and river water samples indicate Mn was not significantly involved in As mobilization in study area one. A few studies have been documented that Mn oxide or hydroxide adsorption/desorption sometimes does not play a significant role in As mobilization in the central Gangetic plain (von Brömssen et al., 2007; Hassan et al., 2007; Mukherjee et al., 2008).

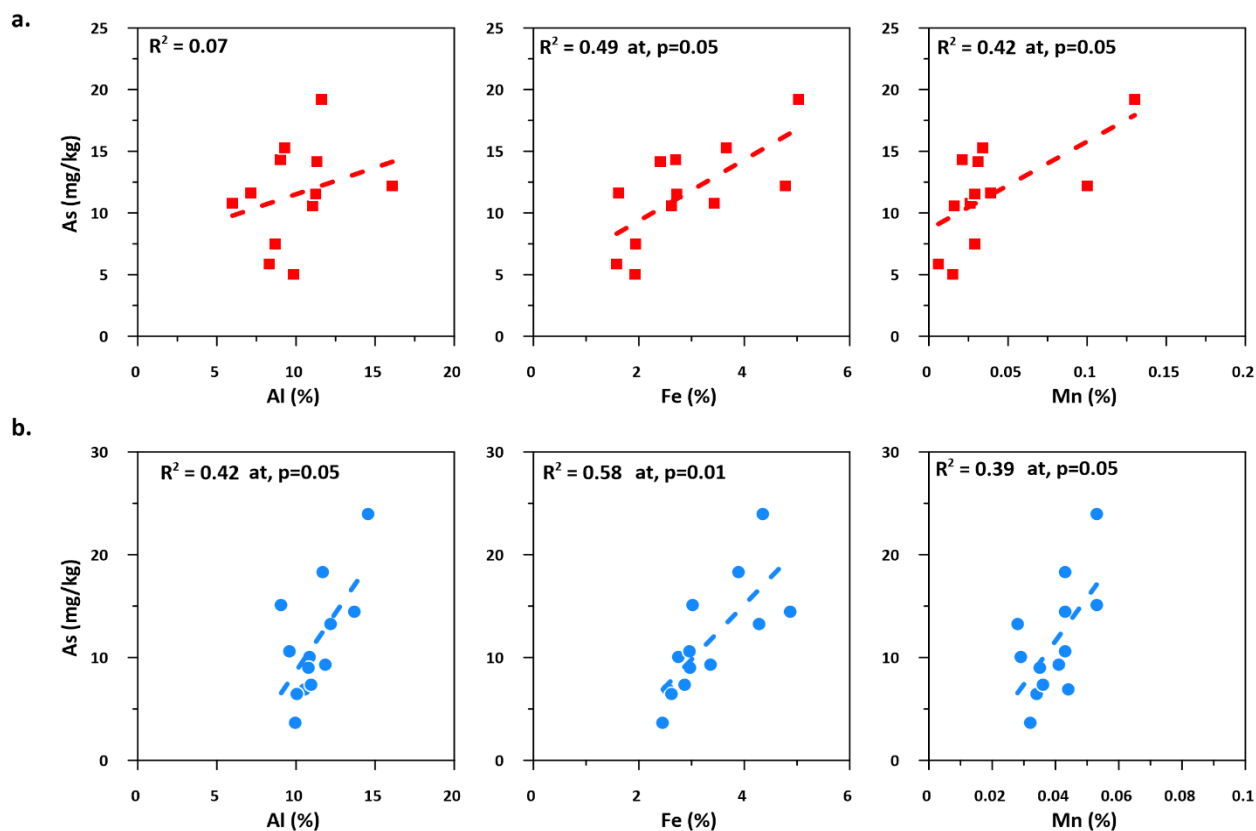


Figure 3.18: Scattered plot of As with Al, Fe and Mn; a. older alluvium, b. younger alluvium, in study area 1 (Gorakhpur)

Scattered plots were plotted between As Al, Fe and Mn in subsurface sediment of OA and YA (Figure 3.18). The scattered OA sediment plots (Figure 3.18a) shown As was weakly correlated with Al ( $r^2=0.07$ ), whereas a moderate correlation was observed with Fe ( $r^2=0.49$ ) and Mn ( $r^2=0.42$ ), indicates iron minerals such as goethite, hematite, and siderite tend to adsorb or desorb As on their solid phases. Mineralogical studies of the OA sediment core (Table 3.5) supported this hypothesis. Minerals of Mn, such as rhodochrosite ( $\text{MnCO}_3$ ), generally controlled Mn in groundwater and are sometimes involved as a minor constituent of siderite. However, in younger alluvium sediment (Figure 3.18b), As was moderately correlated with Al ( $r^2=0.42$ ) and Fe ( $r^2=0.58$ ) while weakly correlated with Mn ( $r^2=0.39$ ), indicates iron minerals goethite and siderite act and a source and a sink for As mobilization. Mineralogical studies also support the availability of these iron minerals in the YA sediment core (Table 3.5). A positive correlation of As with Al, suggested a significant role of Al oxides in As adsorption due to comparable charges and radius like Fe(III). Aluminum minerals such as amorphous  $\text{Al}(\text{OH})_3$ , gibbsite, clay minerals,

and other phyllosilicates are expected to act as As sinks (Stollenwerk, 2003; Jeong et al., 2007; Herath et al., 2016).

In study area 2 (Ghazipur), the scattered plots of As with different physicochemical parameters were plotted in figure 3.19. The As vs. depth plot showed that the shallow aquifers (20 to 40 mbgl) in OA and YA groundwater are more As contaminated, and concentration gradually decreased toward the deeper aquifers.

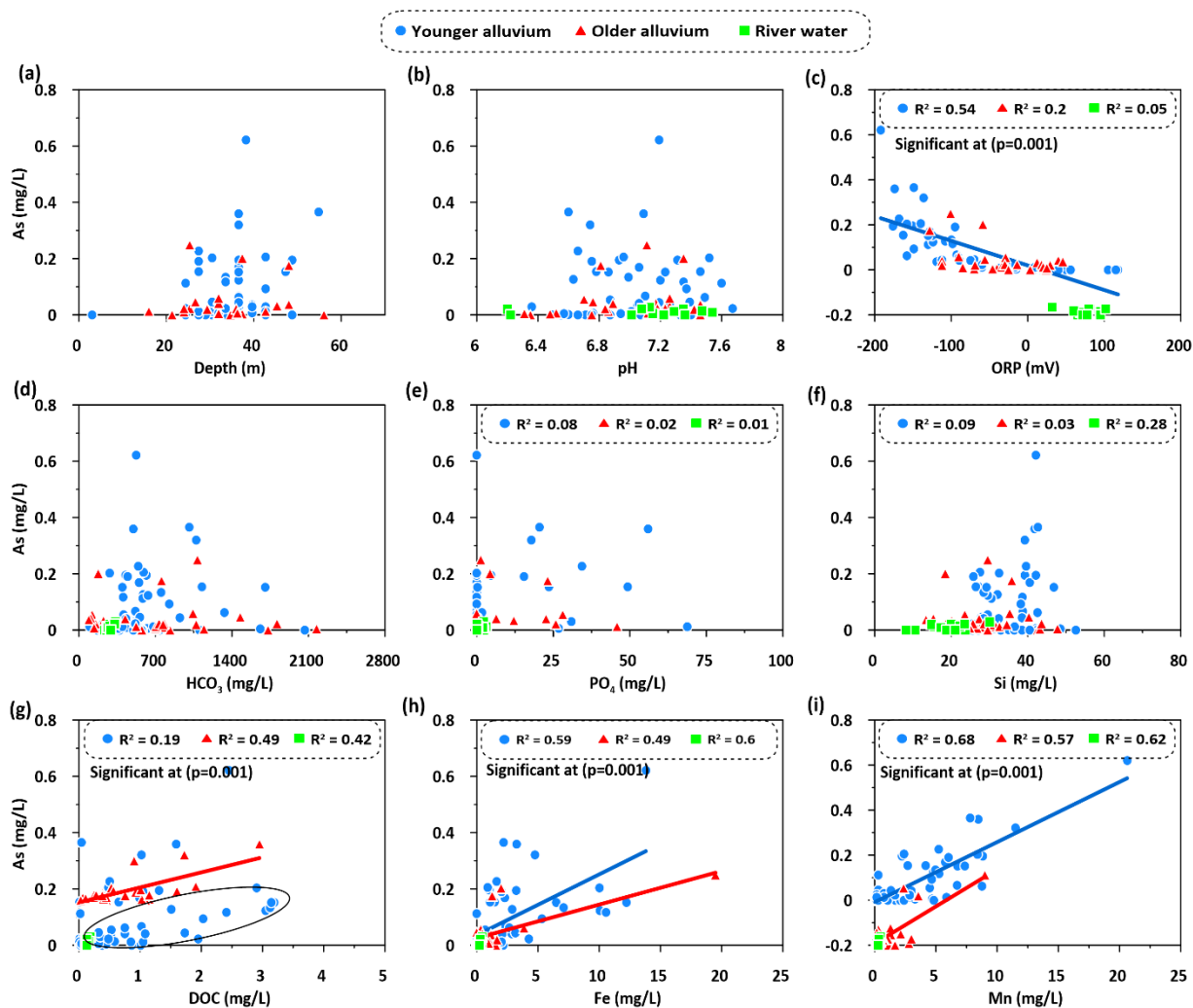


Figure 3.19: Scattered plot of As with physicochemical parameters in YA, OA and river water in study area 2 (Ghazipur)

Deeper aquifers are confined aquifers and hardly get contaminated by geogenic or anthropogenic pollutants due to the thick sandy layer between (60-80 m) of the tier-one and tier-

two aquifer (Saha 2010). Secondly, it was predicted that As getting adsorbed on secondary minerals of iron and clay (Kumar et al., 2006).

The bivariate correlation plots of As with pH were not displayed any significant correlation (Figure 3.19b) in OA and YA groundwater. Similarly, like study area 1, the maximum As concentration was observed at neutral to slightly alkaline pH. Highest As concentration was reported at pH=7.2 in both OA and YA groundwater and above that As decreases. Previous studies suggested that high alkalinity in groundwater promotes As mobilization, yet pH plays a significant role in the alkalinity changes (Kumar et al., 2017; DeVore et al., 2019). A scattered plot of As vs.  $\text{HCO}_3$  was plotted for OA and YA groundwater and river water samples (Figure 3.19d). The lack of correlation between As and  $\text{HCO}_3$  indicates multiple sources and sink for  $\text{HCO}_3$  like silicate weathering and influence of precipitation in groundwater and DOC dissolution. Carbonate mineral dissolution releases Ca, Mg and  $\text{HCO}_3$ , and the molar ratio of  $\text{HCO}_3$  to Ca and Mg indicate the source of origin of  $\text{HCO}_3$  (Mahanta et al., 2015). The redox potential of groundwater plays a significant role in the mobilization processes of As (Smedley & Kinniburgh, 2002; Kumar et al., 2010). The scattered plot of As with ORP in the groundwater in younger alluvium showed As concentration was elevated with the more reducing environment. However, the correlation was not significant in OA groundwater and river water (Figure 3.19c).

The scattered plot of As with  $\text{PO}_4$  shown a weak correlation in YA and OA groundwater; however, a group of groundwater samples from OA and YA showed an inverse correlation indicating  $\text{PO}_4$  enhanced As in groundwater. However, in the case of river water, there was no significant correlation observed between As and  $\text{PO}_4$ . In the scattered plot (Figure 3.19f) of As vs. Si, there was not any remarkable correlation was observed in groundwater and river water.

The scattered plot of As with DOC in OA and YA groundwater and river water was plotted in figure (3.19g). A lack of correlation was observed between As and DOC in the YA groundwater. However, a group of YA groundwater was shown a good correlation with DOC. In OA groundwater, a moderate correlation was observed between As and DOC. The mobilization of As in the aquifer is facilitated by the degradation of organic matter in the underlying sediments. Elevated concentration of  $\text{PO}_4$  is also an indicator of microbial degradation (Bhattacharya et al., 2002a,b).

The scattered plot between As with Fe and Mn in OA and YA groundwater and river water has shown a good correlation (at  $p=0.001$  significant level), indicating Fe and Mn play a significant role in As mobilization in the aqueous medium. The SI indicates iron minerals like goethite and hematite were supersaturated (Figure 3.16) in the groundwater, while siderite, a secondary mineral of iron and carbonate, was in equilibrium with the aqueous and solid phases, indicating the reductive dissolution of Fe and Mn already reached its maximum in the groundwater, and with the dissolution of Fe and Mn oxyhydroxide, As was mobilized in the groundwater.

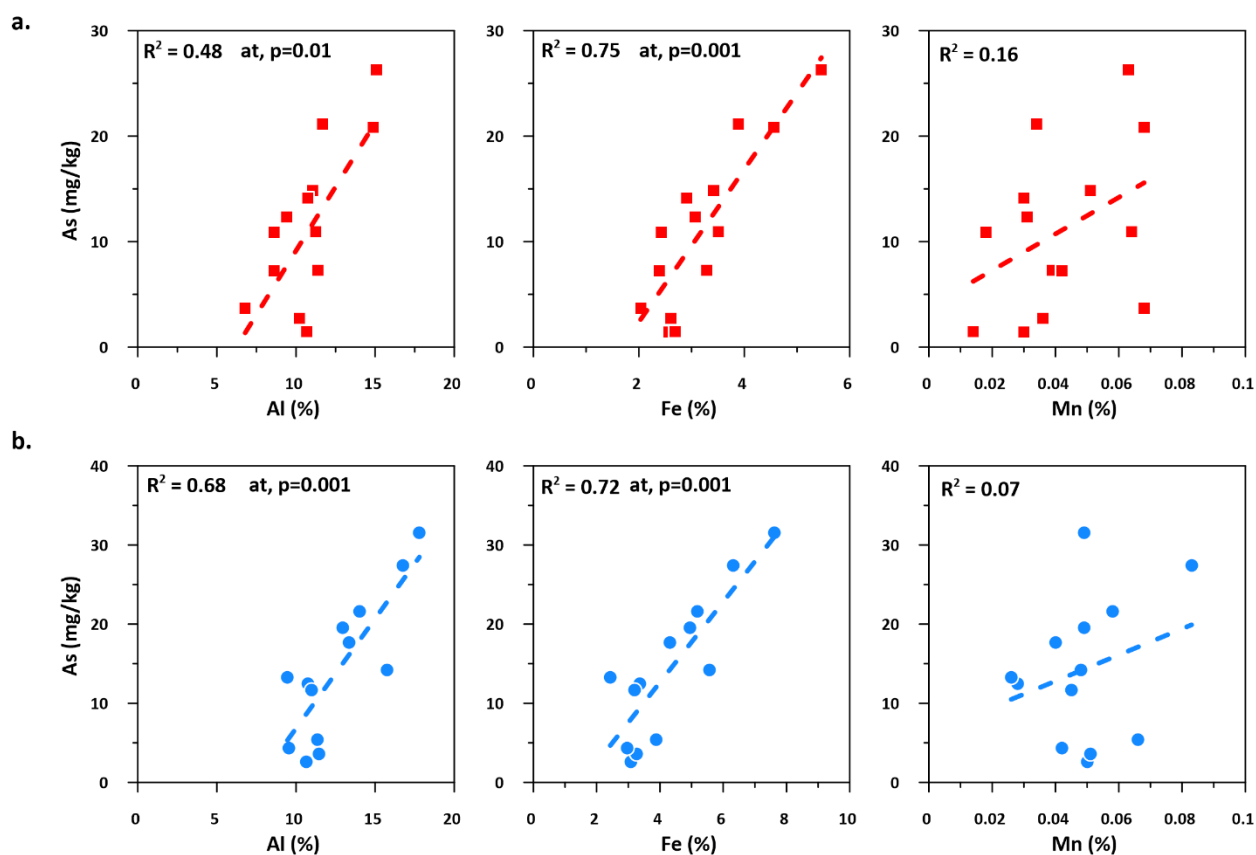


Figure 3.20: Scattered plot of As with Al, Fe and Mn for; a. older alluvium, b. younger alluvium (study area 2, Ghazipur)

Published research from central Gangetic plain had well documented that reductive dissolution likely to be mediated by metal oxide reducing bacteria is the most accepted mechanism for arsenic mobilization in the CGB and Bangal delta, validated by numerous literature (Bhattacharya et al., 1997; Acharyya & Shah, 2007; Chauhan et al., 2009; Saha, Sarangam, et al., 2010; Singh et al., 2010).

In order to understand the association of As with Al, Fe and Mn in the sediment core of OA and YA, a scattered correlation plot was drawn (Figure 3.20a&b). The OA sediment plots showed that As was weakly correlated with Mn ( $r^2=0.16$ ), while a significant correlation was observed with Al ( $r^2=0.48$ ) and Fe ( $r^2=0.75$ ). Similar results were also observed in the YA sediment core. As poorly correlated with Mn (0.07) while strongly correlated with Al ( $r^2=0.68$ ) and Fe ( $r^2=0.72$ ). A good correlation of As with Al and Fe indicates minerals of Fe such as hematite, magnetite, goethite and siderite, and minerals of Al such as amorphous  $\text{Al}(\text{OH})_3$ , clay minerals, gibbsite and other phyllosilicates are likely to act as a sink for As in sediment. A positive correlation of As with Al, suggested a significant role of Al oxides in As adsorption due to comparable charges and radius like Fe(III). Several published research reported a similar mechanism for As mobilization in the central Gangetic plain. As adsorbed into the hydrated Fe-Al hydroxide coated fine-grained sediments. The organic matter-rich argillaceous sediments (grey to black color) are preferentially trapped more As in the weathered alluvium sediment of the Ganga river channel and floodplain (Nickson et al., 1998; Shah, 2014).

### 3.4 Conclusions

This study investigates the two geomorphological features (older and younger alluvium) in two selected areas (Gorakhpur and Ghazipur), and a comparative study was attempted. As concentration was observed higher in the groundwater of YA in both the study area. As in sediment cores in Gorakhpur was almost comparable in both older (11.5 mg/kg) and YA (11.45 mg/kg). However, As in the sediment cores of Ghazipur were observed to be high in YA (14.5 mg/kg) compared to older alluvium (11.08 mg/kg). The piper plot indicates all the groundwater from OA was of  $\text{CaHCO}_3$  type, while 91% of the groundwater from YA was of  $\text{CaHCO}_3$  type and the remaining 9% groundwater from YA and the river water samples were alkaline earth metals with strong acid (Cl and  $\text{SO}_4$ ) type indicates As mobilization processes significantly enhanced by Cl and  $\text{SO}_4$ . However, in study area 2 (Ghazipur), all the samples (Groundwater and river water) were of  $\text{CaHCO}_3$  type, and the alkaline nature of groundwater supports As mobilization in Ghazipur.

Aquifer showed anoxic to post-oxic condition OA and YA region of both the study area. The Eh-pH diagram indicated 83% groundwater from OA and 88% groundwater from YA were falling in  $\text{As}(\text{OH})_3$  field and the remaining 17% groundwater from OA and 12% groundwater from

YA were falling in  $\text{HAsO}_4^{2-}$  field in the study area 1 (Gorakhpur). In study area 2 (Ghazipur), the Eh-pH diagram indicated 88% groundwater from OA and 91% groundwater from the YA was falling in  $\text{As}(\text{OH})_3$  field, and the remaining 12% groundwater from OA and 9% groundwater from YA were falling in  $\text{HAsO}_4^{2-}$  field. The pe-pH plot for Fe indicated that 79% OA groundwater and 76% YA groundwater fell in  $\text{Fe}(\text{OOH})$  region, and the remaining 21% and 24% fell in  $\text{Fe}^{2+}$  field in the study area 1. In comparison, 81% OA groundwater and 69% YA groundwater fell in the  $\text{Fe}(\text{OOH})$  region. The remaining 19% and 31% groundwater from OA and YA, respectively, were fell in the  $\text{Fe}^{2+}$  field in study area 2 (Ghazipur). In the case of river water, all the water samples were fell in  $\text{As}(\text{OH})_3$  and  $\text{Fe}(\text{OOH})$  regions in both the study area.

In study area 1, the hydrogeochemical processes indicate silicate and carbonate weathering were dominant over ion exchange and reverse ion exchange processes. YA groundwater shows dominant calcite dissolution processes in carbonate weathering, while OA groundwater and river samples show dominant dolomite dissolution. The source of nitrate in the YA groundwater is sewage and domestic waste, while a few YA groundwater samples show nitrate fertilizers contribution. However, in OA groundwater and river water samples, nitrate coming from sewage discharge and domestic waste. In study area 2 (Ghazipur), the hydrogeochemical processes indicate silicate and carbonate weathering dominated over ion exchange processes. Carbonate weathering was mainly governed by dolomite dissolution in all the samples (Groundwater and river water). Na vs. Cl plot indicates Na was contributed to the groundwater from silicate weathering and halite dissolution. K and  $\text{NO}_3$  plot indicates sewage discharge and fertilizer inputs enhanced nitrate in OA and YA groundwater, while in river water, nitrate contributed mainly from fertilizers.

Saturation indices showed that groundwater was in equilibrium with common minerals such as albite, anorthite, calcite, dolomite and feldspar in both the study area, while groundwater was supersaturated to the minerals like goethite, hematite, kaolinite, mica and illite, indicated dissolved minerals get precipitated and provide a solid phase for As adsorption in both the study area. Siderite, a secondary mineral of iron and carbonate, was in equilibrium with the groundwater and acted as a sink for As in the central Gangetic plain.



In study area 1, the scattered plots of As with physicochemical parameters in groundwater and sediment suggested shallow aquifer is heavily contaminated with As and the depth of 35 mbgl As concentration is decreased in OA and YA groundwater. A neutral to slightly alkaline pH elevated the As in OA and YA groundwater. A high DOC in OA and YA groundwater indicates degradation of organic matter during microbial metabolism. A favorable reducing environment was generated and allowed As to be released more easily into the groundwater.

In the groundwater of older alluvium, the As mobilization processes were governed by the dissolution of Fe oxyhydroxide in a reducing environment generated by microbial degradation of DOC and involvement of Cl and SO<sub>4</sub> also elevated As mobilization processes. However, in YA groundwater, reductive dissolution of Fe oxyhydroxide supported by microbial degradation of DOC are the primary processes of As mobilization. In the sediment core, minerals of Al and Fe were responsible for the adsorption of As in solid phases.

In study area 2, shallow aquifers (20-40 mbgl) are more As contaminated. In the OA groundwater, As mobilization processes are controlled by the dissolution of Fe and Mn oxyhydroxide. However, in YA groundwater, several factors are involved in As mobilization. The reductive dissolution of oxyhydroxide mediated by microbial degradation was the primary mechanism of As mobilization. A group of YA groundwater also showing that As release into the groundwater due to competitive adsorption of PO<sub>4</sub> on solid phases. In the sediment core, As shows, a good correlation with Fe and Al, which suggests hematite, magnetite, goethite and siderite, and Al minerals such as gibbsite, clay minerals, amorphous Al(OH)<sub>3</sub> and other aluminosilicates are expected to act as a potential sink for As in sediment.

## Chapter 4

# Distribution and fractionation of arsenic in groundwater, soil and sediment

### 4 Distribution and fractionation of As in groundwater, soil and sediment

#### 4.1. Introduction

#### 4.2 Materials and Methods

4.2.1. Study Area

4.2.2. Sampling and analysis

4.2.2.1. Groundwater

4.2.2.2. Subsurface sediment

4.2.3. Chemical and reagents

4.2.4. Sediment processing and digestion methodology

4.2.5. Apparatus and analysis

4.2.6. X-Ray diffraction (XRD) analysis

4.2.7. Quality assurance and quality control

#### 4.3. Results and discussion

4.3.1. Inorganic arsenic in groundwater

4.3.2. Spatial distribution of As(III) in groundwater

4.3.3. Principle component analysis in groundwater

4.3.4. Arsenic species in subsurface sediments

4.3.4.1. Vertical distribution of As in subsurface sediment

a. Study area 1 (Gorakhpur)

b. Study area 2 (Ghazipur)

4.3.4.2. Multivariate analysis for subsurface sediment

4.3.4.3. Mineralogy of the subsurface sediment

#### 4.4. Conclusions

#### 4.5. Supplementary material

## Abstract

Estimating total and inorganic arsenic species (As<sup>III</sup> and As<sup>V</sup>) in groundwater and mineral bound fractions of As species in sediment using the three-step sequential extraction method is the primary objective of the study area. As speciation in groundwater was done with the help of As speciation cartridge. Groundwater samples were collected from two geomorphological units (older alluvium and younger alluvium). It was observed that As(III) was dominated in younger alluvium (YA), while As(V) was dominated in older alluvium (OA). Arsenite (As<sup>III</sup>) concentration was reported higher in the shallow aquifer (30-35 mbgl). A statistical approach (PCA) was applied to understand the relationship of As species with different physicochemical parameters and As mobilization in the study area. The sequential extraction results of the sediment core indicating that the residual fraction was dominated, followed by a reducible, oxidizable, and acid-soluble fraction. Acid soluble fraction is highly mobile in the groundwater. A four-color sediment tool was used to understand the association of total As with sediment color, but a significant association was missing. The sediment core's mineralogy indicates the existence of iron minerals such as goethite, hematite, magnetite and siderite in both the study areas. Presence of the secondary mineral-like siderite act as a potential sink. Partial dissolution of fibrous goethite (FeOOH) releases the As in the groundwater.

**Keywords:** Arsenic speciation; Sediment color tool; As mobilization, As sequential extraction; Central Gangetic plain.

## 4.1. Introduction

Groundwater occurs in the subsurface zone of the Earth, and it is a prime source of drinking throughout the world. Safe drinking water is a basic human right and an essential constituent of a successful health care policy (Mukherjee et al., 2021). Arsenic is a metalloid and exists in the environment and our biological system in various compounds, but in groundwater, it mainly exists in the form of As-oxyanions (Smedley & Kinniburgh 2002, Baig et al., 2009; Shankar et al., 2014). The inorganic As having two common oxidation states: As(III) and As(V). The mobility and toxicity of As(III) are much higher than As(V). Globally more than hundreds of countries have been affected by naturally occurring As poison in groundwater worldwide. Arsenic in any environment, the mobilization process may occur due to various natural processes, such as weathering reactions, volcanic emissions and biological activities, and anthropogenic sources like coal combustion, metal smelting, As-based pesticides, wood preservative, and mining activities (Mandal, 2002; Ghosh et al., 2009). Generally, the geogenic occurrence of arsenic in sediment is up to 1.5 to 2 ppm, and through dissolution or desorption processes, As get into the pore or surface water (Alam & Sattar, 2000; Javed et al., 2013). Plant absorption, methylation, and erosion are the main features of As depletion into the soil. As a result, As it rapidly accumulates in the natural weather, fine alluvial sediment and serves as a sink (Harvey et al., 2005; Hossain et al., 2014; Kumar et al., 2016). Besides, the mobilization of As is also influenced by the physicochemical and solid-liquid phase interactions between As and sediment. Many research articles published elevated As pollution in groundwater and soils from Gangetic plain (Ghosh et al., 2007; Chauhan et al., 2009; Singh & Choudhary, 2010; Kumar et al., 2010; Shah, 2014; Kumar et al., 2016; Singh et al., 2020; Yadav et al., 2020) and Bangladesh (Hasan et al., 2008; Ahsan et al., 2009; Jamil & Feng, 2017; Islam et al., 2018; Islam et al., 2019; Haque et al., 2020; Mihajlov et al., 2020). Seasonal variation also influences the microbiological activities and the availability of As in sediment (Brammer & Ravenscroft, 2009). Furthermore, research and study are needed to understand the factor that impacts As mobilization in sediment under subsurface environmental conditions.

The mobility of As in sediment and its transport to water bodies are influence by its distribution and chemical interaction with different solid constituents. Solid-phase interaction

between As and soil particles is critical for As mobilization (Sadiq, 1997; Javed et al., 2013). Arsenic can get adsorbed on the surfaces of many different metal oxides, especially aluminum (Al), iron (Fe), and manganese (Mn) (Smith et al., 1998). Under the oxic environment, the bioavailability of metal oxides is restricted by their extremely low solubility, which causes metal (oxy-hydr)oxide minerals to precipitate and then become stable. These redox reactive mineral phases are well-known for their ability to adsorb As and a wide range of inorganic and organic contaminants (Cornell & Schwertmann, 2003; Sherman & Randall, 2003; Bjorn & Roychoudhury, 2015; Hao et al., 2018). Minerals of clay and calcite also act as a sink for As and provide an adsorption surface (Manning & Goldberg, 1997; Roman-Ross et al., 2006). The other naturally occurring As-bearing sulfide ores and aluminosilicates can release As into the environment. Sometimes, secondary minerals which are thermodynamically stable can also trigger the release of As into the aquifer system (Sadiq, 1997).

To understand the mobility, bioavailability, retention time, and potential risk of As, it is essential to determine the chemical behavior of arsenic associated with different phases of sediments (Baig et al., 2009). In well-drained or oxygenated soil, As(V) is dominated species, while organic matter-rich area or regularly flooded soil is an encounter with the reducing condition and dominated by As(III) (Wuana & Okieimen, 2011; Wu et al., 2017). The inorganic forms of As are more toxic than the organic forms. While in the case of inorganic forms, As(III) is ten times more toxic, soluble, and mobile as compared to As(V) (Mandal & Suzuki, 2002; Jang et al., 2016). Since the bioavailability and toxicity of As are dependent on its chemical nature, surrounding subsurface environmental scenario, amount of sorbing compound, pH, and the redox potential (Mandal & Suzuki, 2002; Zheng et al., 2003).

The analysis of bioavailable or labile As fractionation is the prime isolation process for explaining As availability in the sediments through geochemical and anthropogenic input (Wenzel et al., 2001). Sequential extraction methods are most widely used to evaluate the relative availability of arsenic and trace metals in sediment (Lombi et al., 2000; Keon et al., 2001; Mihaljevič et al., 2003; Rodriguez et al., 2003; Tlustoš et al., 2005; Baig et al., 2009). The mineralogical evidence plays a remarkable role in the identification of As sources and mobilization in groundwater. As is more likely to be co-precipitated or scavenged by metal (Fe and Mn) oxides in the liquid-solid phase interaction (Acharyya et al., 1999).

For the last 3-4 decades, groundwater As contamination is one of the severe problems identified in the Gangetic plain (Shah 2008, Kumar et al., 2014, Chauhan et al., 2009; Chakraborti et al., 2016). According to the published research, reductive dissolution of metal oxyhydroxide are a well-accepted and significant hypothesis for the chemical association of As mobilization in the central Gangetic plain (Kumar et al., 2018; Yadav et al., 2020). Rivers originating in the Himalayas carry As-rich sediments to downstream basins and deltaic regions, where they are deposited (Lupker et al., 2012). The recent depositional feature is also known as quaternary alluvial deposition, and it is two types; (a) older alluvium (Bhangar), which was corresponding to the middle Pleistocene, and newer alluvium (Khadar), which was corresponding to the late Holocene (Sinha et al., 2005; Tandon et al., 2008). Previous studies mainly focused on the total As speciation. A very few studies focused solely on As speciation in the groundwater and sediment (Chandrasekharam et al., 2007; Kumar et al., 2016). The objective aims to quantify the As speciation in groundwater and sediment, examine the role of minerals assemblage and their role in As source and mobilization, and finally, use a four-color code application for the sediment in the Gangetic plain.

## 4.2. Material and methods

### 4.2.1. Study area

The study area covered two districts (Gorakhpur and Ghazipur) of eastern Uttar Pradesh. Study area 1 (Gorakhpur) lies between 26.25° to 27.1° N and 83.10° to 83.75° E. The district is located on the Rapti riverbank of Nepal. Rapti is one of the supreme tributaries of the river Ganga. Gorakhpur is densely populated because of the easy availability of water resources for domestic and agricultural activity, highly fertile soil, and gentle slope landscape (Singh et al., 2009; Bhardwaj & Singh, 2011). River bending, monsoonal rain, and sedimentation load are the primary threats to this district's constant flood (Singh et al., 2015).

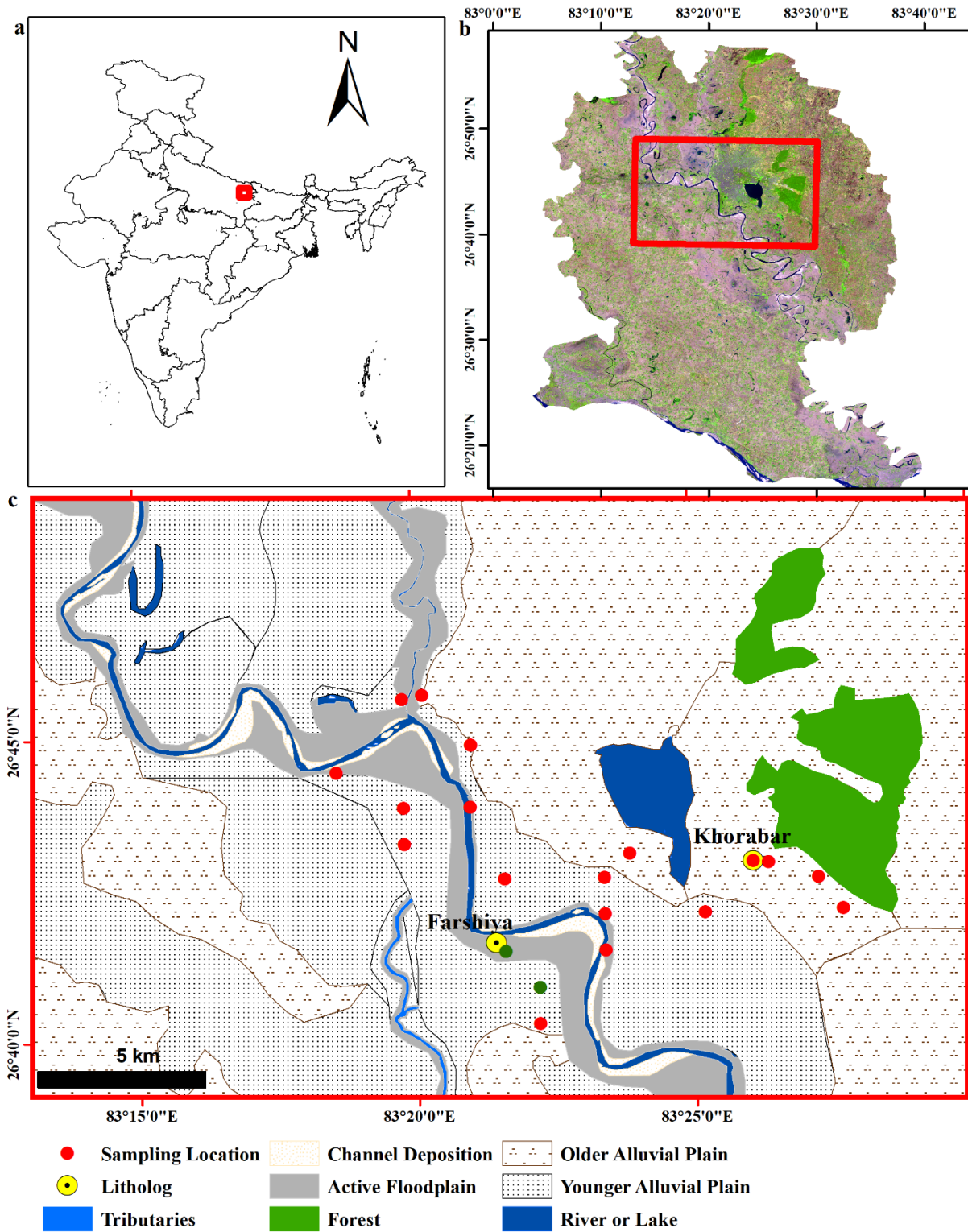


Figure 4.1: Map of the study area, (a). India with state boundary, (b). Landsat images are prepared from FCC (false-color composite) band combinations (5, 4 and 3), (c). Study area map with different geomorphic features (older alluvium, younger alluvium, point bars, forest and river etc). The map shows sample location in groundwater and sediment core

Sand bars, flood plain, alluvial plain, and meander scar are the prime geomorphological units that have been identified in the study area (CGWB, 2013). The study area is a part of the quaternary alluvium, mainly formed by Ghaghara and Rapti river systems deposits (Singh et al., 2015). The quaternary alluvial deposits are divided into older alluvium and younger alluvium (Figure 4.1).

The older is also known as “Bangar” or high land soil due to denudation; however, the younger alluvium is known as “Kachhar” or the marginal track of Ghaghara and Rapti river system (Bhardwaj & Singh, 2011; Shah, 2014; Saha & Sahu, 2016). The study area has identified a three-tier aquifer system (40-50mbgl, 80-100mbgl and 180-195mbgl) (CGWB, 2013). The district has a sub-humid to a humid climate, and it is somehow influenced by north and terai swamps. The maximum rainfall (>87%) has been taken place from June to September, and excess water is accessible for deep percolation into the groundwater system.

Study area 2 (Ghazipur) lies between 25.07° to 25.97° N and 83.32° to 83.9° E. The district has a gentle undulation with various streams running through it. Topography is mainly influenced by the rivers flowing through the district, such as Ganga, Karmanasa, and Gomti. The seasons have been identified in the study area; the hot season (March to June) and monsoon (July to October), and the cold season (November to February). Around 70-75% of rainfall has occurred in the monsoon season. The average maximum temperature (Above 38°C) has been recorded in May and the average minimum (<15°C) in January.

The differences in the geomorphic features like elevation, nature of the sediments, the pattern of soil deposition, and spatial distribution in the Gangetic plain imply that they are deeply influenced by climate-driven sediment, water regime, and sedimentation load (Shah, 2014). The study area is a part of the central Gangetic plain where two geomorphic units have been identified based on the axial division of river Ganga; a) North Ganga plain (NGP) and South Ganga plain (SGP) (Saha & Sahu, 2016). The entire study area is made of quaternary alluvial deposits, and it is further divided into two categories; older and younger alluvium (Figure 4.2). Older alluvium forms upland surfaces and occupied the major part of the study area. They are recognized by yellow-brown colored sediment. Younger alluvium constituted the low-lying flood plains and was incorporated by grey to black argillaceous deposits (Kumar et al., 1996; Shah, 2014).



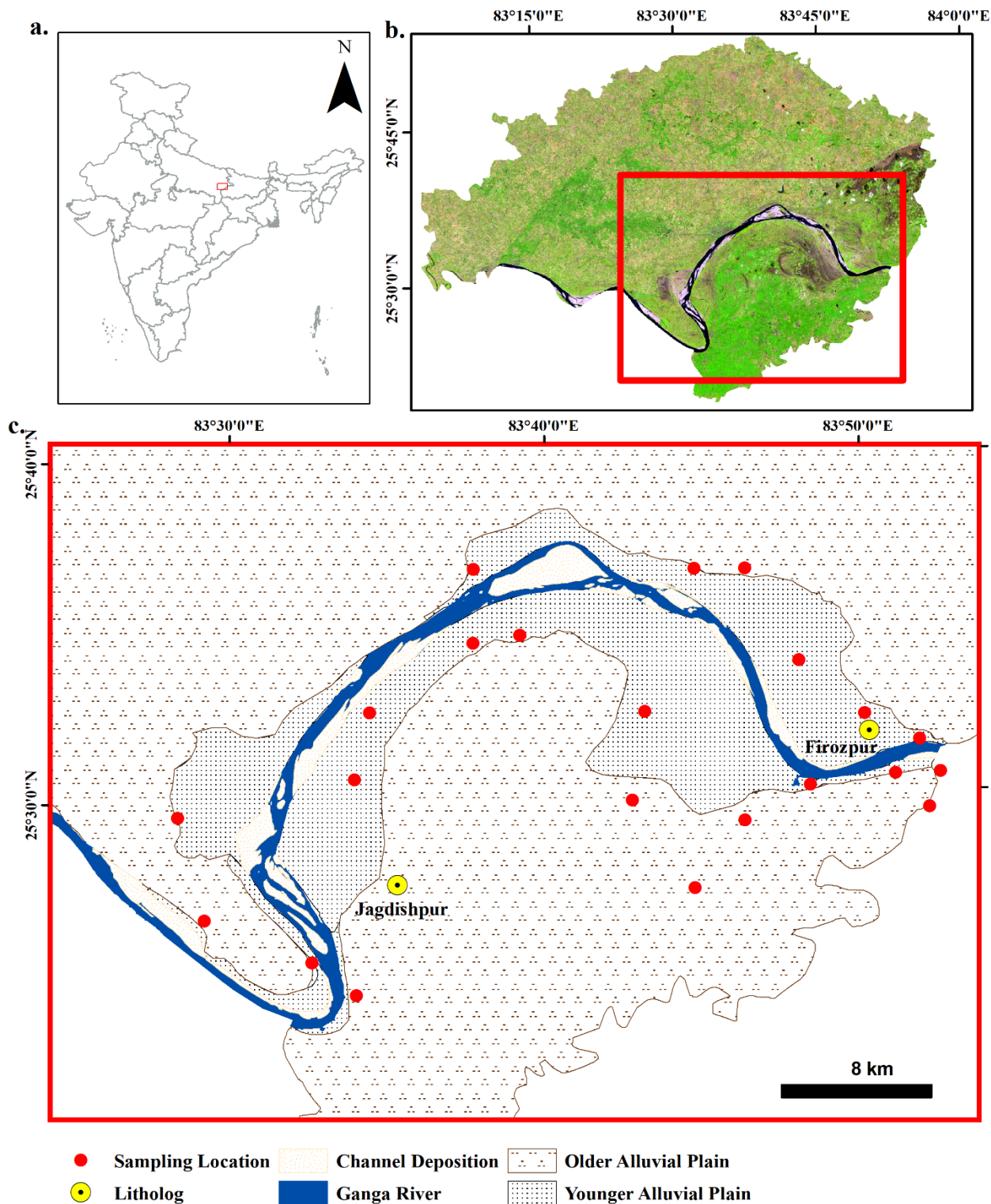


Figure 4.2: Map of the study area, (a). India with state boundary, (b). Landsat images are prepared from FCC (false-color composite) band combinations (5, 4 and 3), (c). Study area map with different geomorphic features (older alluvium, younger alluvium, point bars, forest and river etc). The map shows sample location in groundwater and sediment core

## 4.2.2. Sampling and analysis

### 4.2.2.1. Groundwater

A total (42) groundwater samples were collected from both the study areas by following the standard procedure and methods of APHA (2005) from the hand pump and bore well during August 2017 and February 2018. Two representative groundwater samples were collected in polypropylene bottles from each location. One was for total As (acidified) estimation, and another was for As(III). Arsenate and arsenite were separated by using a disposable cartridge (Metal Soft Center, PA, USA). Groundwater samples were passed through the cartridge to absorb all As(V) and allow only As(III). Filtered water samples were kept at 4°C to avoid chemical alteration.

### 4.2.2.2. Subsurface sediment

Two subsurface sediment cores, especially one from older alluvium and another from younger alluvium deposits, were considered to collect subsurface sediment cores from both the study areas (Singh & Pandey, 2014; Kumar et al., 2018). So, a total of four cores were collected from both districts (study area). A common and localized hand flapper drilling method was used in the field to collect the sediment cores. The depth of each core was around 33.5 mbgl. The sediment samples were taken at a regular 10 feet (3.048 m) interval from each selected core. We have also considered any anomalies that come across the sediment core. The collected sediment samples were sealed in a zip bag and transferred to the laboratory. Samples were kept for air-dries and then transferred to an oven for 72 hours at 50 °C.

### 4.2.3. Chemical and reagents

The analytical grade chemicals were used in the analysis and purchased either from Merck (Darmstadt, Germany) or Sigma-Aldrich (Milwaukee, WI, USA). They were employed without any further purification. Milli-Q water (MilliporeSigma Direct-Q5) with a resistivity of 18.2 MΩ/cm was used to make all solutions and reagents. All the standards were prepared from their stock solution and kept in darkness at 4 °C until the analysis started. Those standards which are freshly required for the analysis were prepared on the same day.

#### 4.2.4. Sediment processing and digestion methodology

Sediment samples were digested using a method developed by Shapiro (1975). Detailed methodology for sediment processing and digestion has been given in Chapter 3, Section 3.2.5). A three-step sequential extraction method (modified BCR) was used to identify the arsenic species in sediment (Rauret et al., 1999). Step one, account for the acid-soluble exchangeable or carbonate-bound fraction by applying the acid. Step two represents a reducible fraction of the metal. In this step, hydroxyl ammonium hydrochloride was used to reduce metal-bound oxyhydroxide of Fe/Mn. Finally, step three represents an oxidizable fraction. In this step, hydrogen peroxide and ammonium acetate oxidized the organic matter and sulphide bound fraction. Further, we recovered the residue fraction from step three, digested with aqua regia. Detailed methodology is given in the below chart:

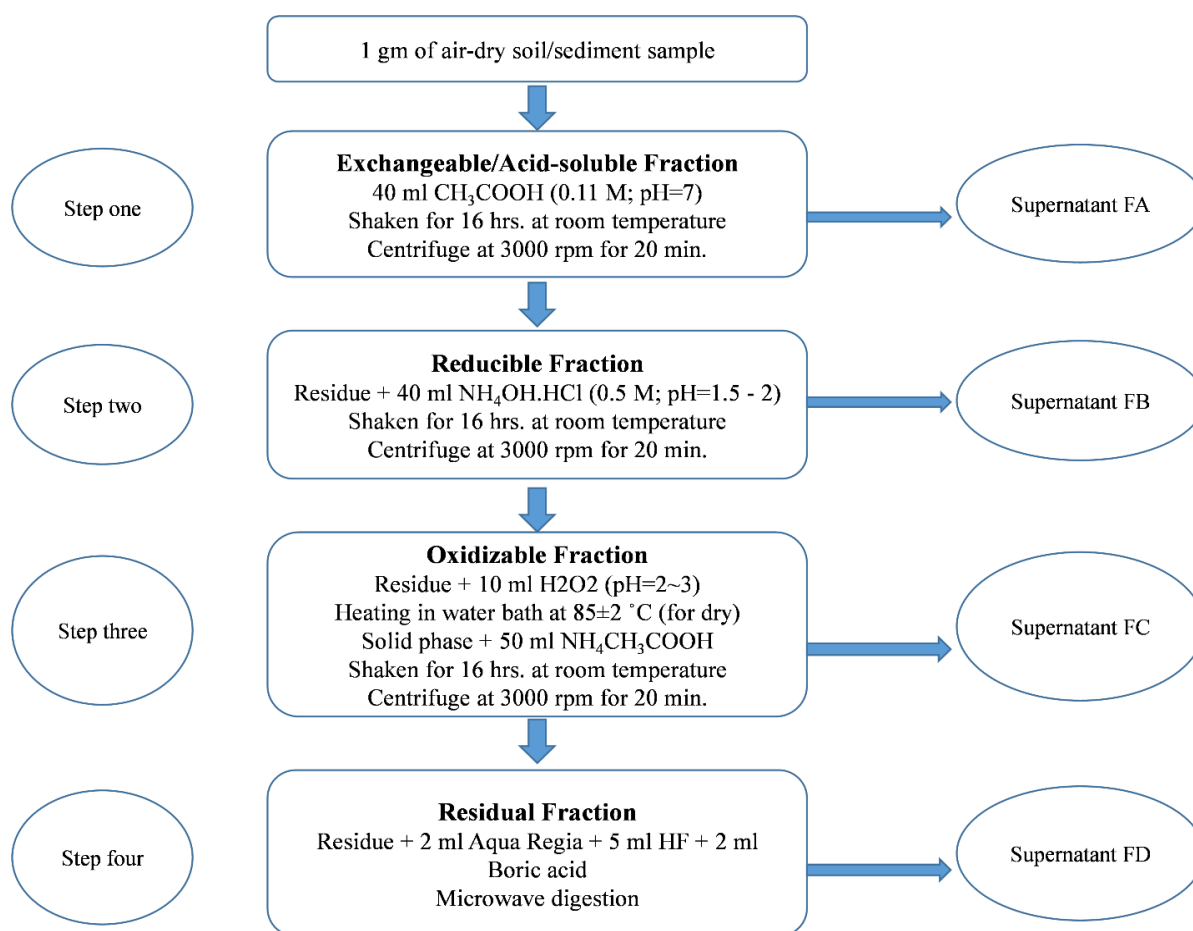


Figure 4.3: Flow chart of three-step sequential extraction method

#### 4.2.5. Apparatus and analysis

All the apparatus used in the laboratory were a grade and made up of borosilicate glass or polypropylene. Teflon vessels were soaked in 4 M HNO<sub>3</sub> (overnight) before being used. All the acids and compounds used in the digestion procedure and analyses were analytical grade. A standard reference material (SRM), NIST-8704, also known as Buffalo river sediments (n= 4), was used to verify the As results in the sediment. The reference standard certified value for As was 17 mg/kg, and the observed was detected 16.72±0.08 mg/kg. The recovery of the As was obtained 98.32%.

#### 4.2.6. X-Ray diffraction (XRD) analysis

The mineralogy of the sediment samples was determined by the standard method of the X-ray powder diffractometer (XRD). A Malvern Empyrean, PANalytical (UK) model was used to analyze the mineral composition of soil or sediment. It worked on the radiation level less than 1 µSv/h and was determined with the Mo source (60 kV, 50 mA) over an angular range of 5 to 85 (2θ) with 0.02-degree steps 2s count time on unoriented side-packed powder mounts. The maximum angular reproducibility of the instrument was <0.0002 degrees. The peaks of the minerals were identified by PANalytical Xpert High score software with ICDD (International Centre for Diffraction Data) database to identify the minerals in the aquifer sediment using calculated powder pattern and Rietveld full pattern fitting options (Gates-Rector & Blanton, 2019).

#### 4.2.7. Quality assurance and quality control

A standard reference material (SRM), 8704 (Buffalo river sediments), was selected from the National Institute of Standards and Technology (NIST), USA. NIST-8704 was used to verify the results of As in the sediment. The standard certified value for arsenic was 17 mg/kg, and the observed was detected 16.72±0.08 mg/kg (average of 4 observed values). The recovery of the As was obtained 98.32%, which was under the 10% error. In each batch of sediment and soil samples, several (10% of the total number of samples) duplicate samples were used to check precision by analytical splits.

### 4.3. Result and discussion

#### 4.3.1. Inorganic arsenic in groundwater

The results of the inorganic arsenic with other physicochemical parameters in the groundwater were shown in [table 4.1](#). The average concentration of total arsenic (As) in study areas 1 and 2 were reported 0.04 mg/l and 0.15 mg/L, respectively. The pH of the groundwater varies from 6.15 to 7.11 in study area 1 (Gorakhpur); however, it varies from 6.35 to 7.46 in study area 2 (Ghazipur). The average reduction potential of both the study areas was negative, indicating a reducing groundwater condition. In study area 1, ~78% (out of 20 samples) of groundwater was unsafe for drinking purposes. WHO (2004) prescribes the maximum 10 ppb limit for As in drinking water. Similarly, in study area 2, ~81% (out of 22 samples) of groundwater was unsuitable for drinking purposes. Yet during the As (III) sampling, we mainly considered those hand pumps which were having red platforms. In our study, the average As concentration in the groundwater was comparable with other reported studies. The average As concentration in Bhojpur, Bihar, reported the 89 µg/L and 123 µg/L, respectively by [Saha \(2009\)](#) and [Saha et al. \(2011\)](#). The average As concentration in Samastipur, Bihar has been reported 20 µg/L ([Kumar et al., 2016](#)). Other studies from Ballia reported elevated As concentration in groundwater with an average of 331 µg/L ([Srivastava & Sharma, 2013](#)).

In study area one (Gorakhpur), the As(III) concentration in the OA groundwater was ranged from ND to 0.06 mg/L with an average of 0.01 mg/L, while As(V) ranged from ND to 0.05 mg/L with an average of 0.01 mg/L ([Table 4.1](#)). However, in YA groundwater, arsenite (As III) ranged from ND to 0.09 with an average of 0.02 mg/l, while As(V) ranged from ND to 0.05 with an average of 0.01 mg/L. The average concentration of As(III) was higher in younger alluvium than the older alluvium might be due to reducing subsurface environmental conditions. As(III) was plotted along with the older and younger alluvium in [Figure 4.5](#).

In study area two (Ghazipur), As(III) was ranged ND - 0.02 mg/L (average 0.004 mg/L), while As(V) ranged ND - 0.19 mg/L (average of 0.06 mg/L) in the groundwater of OA indicating, oxidizing older alluvium might be responsible for low As (III) in OA groundwater. However, arsenite was observed higher than the As(V) in the groundwater of YA. The average As(III) concentration was reported 0.11 mg/L (range, ND – 0.25 mg/L), and As(V) was reported 0.08

mg/L (range ND – 0.44 mg/L). The high As(III) concentration in the groundwater of YA, indicating a reducing condition, might be involved in elevated As(III) concentration.

*Table 4.1: As species in the groundwater of older and younger alluvium with depth, pH and ORP in different geomorphological setups of both the study areas (Gorakhpur) and (Ghazipur).*

Study area 1 (Gorakhpur)									
	Unit	Older alluvium (OA)				Younger alluvium (YA)			
		Min.	Max.	Average	St. dev	Min.	Max.	Average	St. dev
Depth (m)	<i>m</i>	27.44	33.54	30.05	2.54	15.24	45.73	30.75	6.54
pH		6.15	7.11	6.71	0.31	6.15	7.11	6.57	0.27
ORP (mV)	<i>mV</i>	-179.00	28.00	-52.71	65.03	-179.00	28.00	-84.65	60.70
<i>pe</i>		-3.01	0.47	-0.89	1.10	-3.03	0.47	-1.43	1.02
As(total)	<i>mg/L</i>	ND	0.14	0.02	0.05	ND	0.14	0.04	0.05
As (III)	<i>mg/L</i>	ND	0.06	0.01	0.02	ND	0.09	0.02	0.03
As(V)	<i>mg/L</i>	ND	0.05	0.01	0.02	ND	0.05	0.01	0.01
As(III)/As(V)		ND	0.00	0.00	0.00	ND	0.01	0.00	0.00
Study area 2 (Ghazipur)									
Depth	<i>m</i>	27.43	48.77	38.07	6.16	24.86	48.77	33.27	6.61
pH		6.35	7.35	6.96	0.32	6.36	7.46	6.83	0.27
ORP	<i>mV</i>	-128.00	40.00	-53.57	56.45	-192.00	28.00	-111.40	62.05
<i>pe</i>		-2.14	0.67	-0.90	0.95	-3.23	0.47	-1.87	1.04
As(total)	<i>mg/L</i>	ND	0.20	0.07	0.08	ND	0.62	0.19	0.16
As (III)	<i>mg/L</i>	ND	0.02	0.00	0.01	ND	0.25	0.11	0.08
As(V)	<i>mg/L</i>	ND	0.19	0.06	0.07	ND	0.44	0.08	0.13
As(III)/As(V)		ND	0.14	0.03	0.05	ND	18.73	4.76	5.84

\*Note: Min.= Minimum, Max. = Maximum, St.dev = Standard deviation, ND = Not detected

A pe-pH diagram was plotted to identify the As species in groundwater (Figure 4.4). The figure shows that all the groundwater samples fall in As(OH)<sub>3</sub> domain, indicating As(III) was a dominant species in the groundwater.

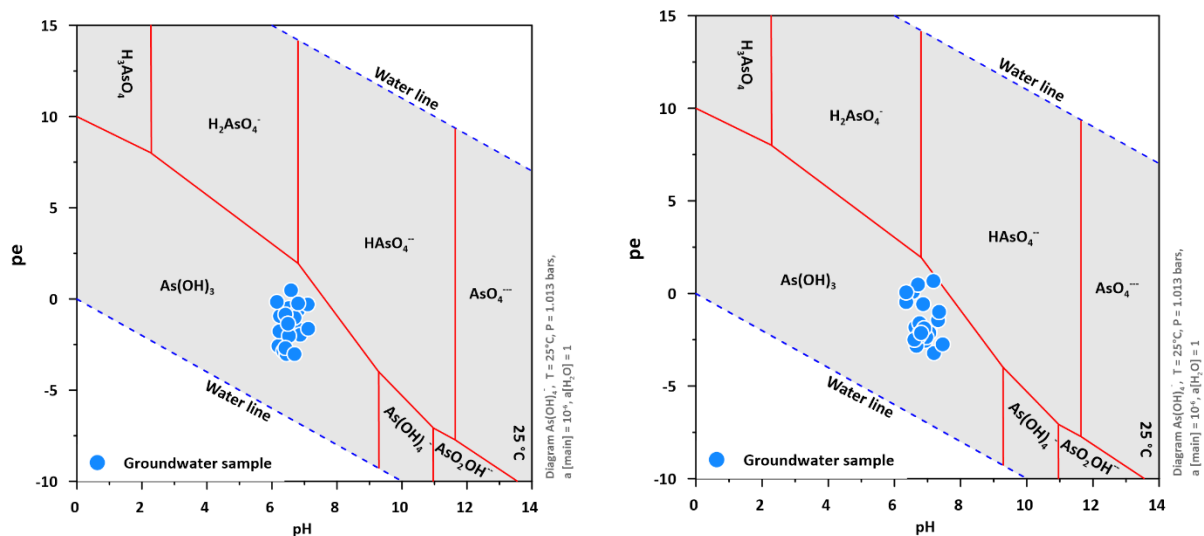


Figure 4.4: *pe-pH diagram of the study area, a. Gorakhpur b. Ghazipur*

The reduction potential of the groundwater supported this result. The average oxidation-reduction potential was observed (-84) mV in study area 1 while (-93) mV in study area 2. The regional geology and pH influenced As availability in the groundwater (Kumar et al., 2016). Arsenite was also reported to be the predominant As species in groundwater of the central Gangetic plain and West Bengal (Kumar et al., 2014; Kumar et al., 2016, Saha & Shukla, 2013).

#### 4.3.2. Spatial distribution of As (III) in groundwater

Similar to West Bengal and Bangladesh, As is heterogeneously distributed in the sediment and water. The younger alluvium, also known as the Ganga river corridor, is high As polluted compared to the older alluvium. Mukherjee et al. (2007) has been reported that geology and geomorphology significantly influence the As distribution in the shallow aquifers. In both the study areas, As(III) was plotted along with the geomorphology and groundwater depth (Figure 4.5 and 4.6). The As(III) concentration was reported significantly higher in younger alluvium. However, it was comparatively very less or not detected in older alluvium in both the study area. In the central Gangetic plain, it is well documented that younger alluvium is nutrient-rich with active microbial degradation, which generates a reducing environment in the subsurface soil (Srivastava & Sharma, 2013) and triggers As and metal mobilization. A similar mechanism is observed in our study areas.

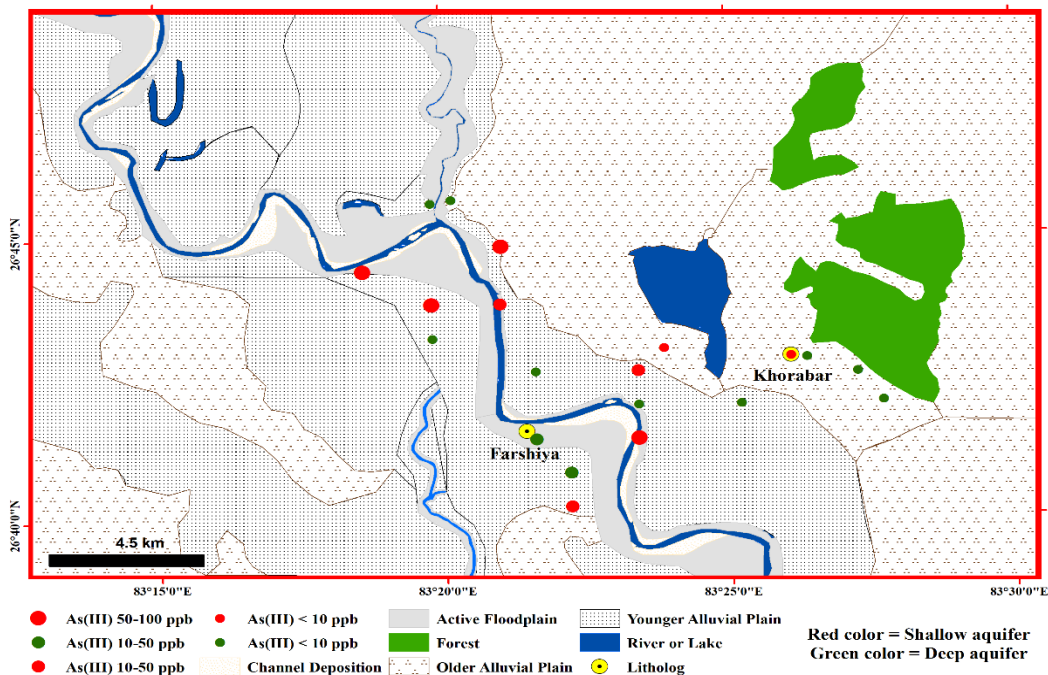


Figure 4.5: A generalized Geomorphological (older and younger alluvium) map of the study area 1 (Gorakhpur). It also depicts elevated As concentration and distribution based on geomorphology and depth.

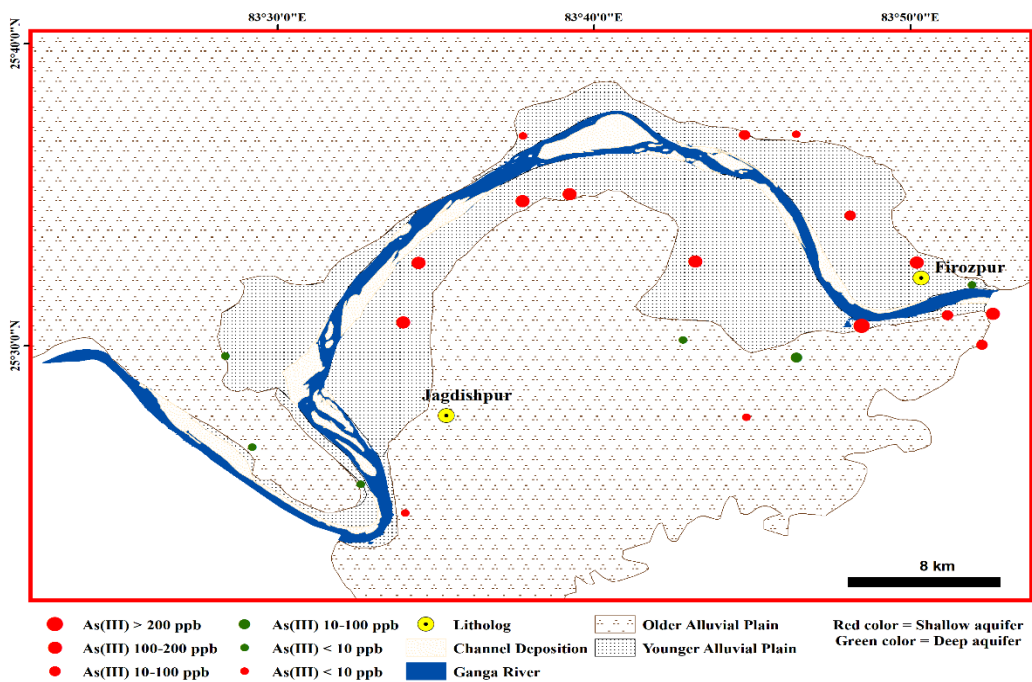


Figure 4.6: A generalized Geomorphological (older and younger alluvium) map of the study area 1 (Ghazipur). It also depicts elevated As concentration and distribution based on geomorphology and depth.



As contamination was significantly influenced by the depth, it was hypothesized that shallow aquifers are more prone to As contamination (Saha et al., 2011). As (III) also plotted with the depth (red color shallow aquifer, green color deeper aquifer) (Figure 4.5 and 4.6). The figure shows that shallow aquifers (20-35 mbgl) were promoted As contamination while the depth above 35 mbgl, the As concentration decreases in the groundwater.

#### 4.3.3. Principle component analysis in groundwater

The PCA was carried out to understand the relationship of As species with the physicochemical parameters in both the study area (Table 4.2). In Gorakhpur, groundwater of older alluvium, the PCA generated three significant components and inferred 86.35% of total sample data variance. PC1 explained 55.62% of the total variance with the positive loading of Fe, Mn, As(t), As(III) and As(V), and moderate loading of DOC, HCO<sub>3</sub> and NO<sub>3</sub> while negative loading of ORP indicating As(t) and As(V) mobilization might be controlled by several processes such as dissolution of Fe and Mn oxyhydroxides, alkaline nature of groundwater and oxidizing environment in the presence of NO<sub>3</sub> may also enhance As(V) liberation in the groundwater. As(III) was reported in one sample out of seven samples. So based on one sample, we cannot decipher any significant conclusion for As(III) mobilization in OA. (Kumar et al., 2016; Yadav et al., 2020). However, in the groundwater of younger alluvium, the PCA has shown three major components, explaining 79.77% of the total data variance. PC1 explained 39.13% of the total variance with the strong positive loading of As species with Fe, Mn and DOC and negative loading of ORP, indicating liberation of As species in the aquifer environment by reductive dissolution of Fe oxyhydroxide in the presence of dissolved organic carbon. In PC2, arsenite negatively correlated with the ORP, indicating reducing conditions promoting arsenite in the groundwater. PC3 explained 14.95% of the total variance with a positive loading of depth. This component is independent of any other parameter. PC4 explained 11.34% of the total variance with the positive loading of As(V), ORP and PO<sub>4</sub>, indicating that PO<sub>4</sub> acts as a competitive surface complexation ion in an oxidizing environment and adsorbed into the solid surface and elevate As concentration into the aqueous medium.

Table 4.2: Variation of principal component (PC) unit with different parameters in the groundwater of different geomorphic setups of the study areas.

	Gorakhpur								Ghazipur							
	Older Alluvium (n=7)			Younger alluvium (n=13)					Older Alluvium (n=8)				Younger alluvium (n=14)			
	1	2	3	1	2	3	4	1	2	3	4	1	2	3	4	
Depth	-.324	.112	.807	-.286	.042	.863	-.027	.232	.912	.091	-.052	.403	.140	.897	.030	
pH	.120	-.913	-.012	-.334	-.866	.047	-.032	.168	.172	-.012	.899	.009	-.931	-.275	-.003	
ORP	-.688	.117	.217	-.736	-.262	.290	.477	-.568	.089	-.319	-.653	-.616	.127	-.138	.621	
HCO <sub>3</sub>	.587	.060	.792	.402	.814	.247	.171	.165	.517	.688	-.023	-.104	.947	-.075	-.057	
NO <sub>3</sub>	.546	.113	-.511	.280	-.734	.341	-.156	-.175	.831	.056	.245	.120	.834	-.161	.484	
PO <sub>4</sub>	-.153	-.738	-.069	-.166	.134	.124	.870	-.106	-.034	.853	.100	-.281	-.045	.872	-.243	
DOC	.626	.707	-.016	.922	.217	.090	-.100	.761	-.208	-.496	-.044	.812	.091	-.122	-.046	
Fe	.970	.165	.107	.973	.018	-.132	-.051	.922	.077	-.241	.128	.926	.261	-.225	.017	
Mn	.982	.135	-.049	.904	.095	-.343	.071	.969	.092	-.014	.118	.834	.016	.165	-.489	
As(t)	.973	.144	-.159	.890	.201	-.368	.007	.924	.091	.104	.238	.867	-.380	.251	-.056	
As(III)	.980	.120	-.149	.887	.152	-.374	-.101	.897	.154	.069	.256	.869	-.341	.266	-.131	
As(V)	.964	.138	-.184	.541	.299	-.295	.619	.679	-.399	.306	-.045	.620	-.580	-.033	.525	
Total	6.708	2.020	1.640	5.135	2.249	1.794	1.366	4.962	2.078	1.728	1.464	4.468	3.171	1.920	1.683	
% of Variance	55.897	16.833	13.666	42.794	18.738	14.953	11.385	41.349	17.317	14.397	12.198	37.237	26.421	16.003	14.024	
Cumulative %	55.897	72.731	86.397	42.794	61.532	76.486	87.871	41.349	58.666	73.063	85.261	37.237	63.658	79.661	93.686	

In study area 2, OA groundwater is represented by four major principle components (PCs), explained 85.26% of the total data set variance. PC1 explained 41.35% of the total variance with the positive loading of Fe, Mn As(t) and As(III) while a moderate positive loading of DOC, As(V) and negative loading of ORP indicating reductive desorption of Fe and Mn oxyhydroxide in the presence of microbial degradation of organic matter, might be responsible for elevated As into the groundwater. It is a well-accepted hypothesis of As mobilization in the central Gangetic plain (Saha 2010; Mukherjee et al., 2009; Kumar et al., 2018). PC2 explained 17.32% of the total variance with a positive loading of depth and nitrate, indicating leaching of the nitrate from sewage and fertilizers might be enhanced nitrate in groundwater. PC3 explained 14.39% of the total variance with a positive loading of  $\text{PO}_4$  and  $\text{HCO}_3$ , indicating phosphate might be coming significantly from the geogenic origin. PC4 explained 12.19% of the total variance with the positive loading of pH and negative loading of ORP, indicating that on increasing the pH, oxidation-reduction potential decreases. Studies has been reported that the oxidation-reduction potential and pH are inversely proportional to each other, if oxidant type and concentration retain constant for a solution (James et al., 2004).

Groundwater of younger alluvium, The PCA analysis generated four principal components and inferred about 93.69% of the total data set variance. PC1 explained 37.23% of the total variance with positive loading of DOC, Fe Mn As(t) As(III) and negative loading of ORP, indicating the reductive dissolution of metal oxyhydroxides, which was triggered by microbial degradation of organic matter, and responsible for As(III) mobilization (Yadav et al., 2020). PC2 deciphered 26.42% of the total data variance with a positive loading of  $\text{HCO}_3$  and  $\text{NO}_3$  while negative loading of pH and As(V), indicating As(V) mobilized in an oxidizing environment triggered by the breakdown of ammonium ion into the nitrate in an oxic environment (Mahanta et al., 2015). PC3 explained 16% of the total variance with the positive loading of  $\text{PO}_4$  and depth, indicating leaching of fertilizers or phosphate minerals dissolution might be the possible source of  $\text{PO}_4$  in the deeper aquifer. PC3 explained 14% of the total variance with the positive loading of ORP and As(V), indicating arsenate liberated in the groundwater in the oxidizing conditions.

In both the study areas, reductive dissolution of Fe and Mn oxyhydroxide was the primary mechanism for As(III) mobilization, while As(V) was released in an oxidizing environment. Besides, other factors also contributed to the As(III) and As(V) mobilization processes.

#### 4.3.4. Arsenic species in subsurface sediments

##### 4.3.3.1. Vertical distribution of As in subsurface sediment

A four-color sediment tool was used to identify the sediment through straight and appropriate sediment color comparisons at each depth. Hossain et al. (2014) modified the Munsell Color Chart into a four-color tool based on a relative analysis of 2240 sediment samples. This sediment color tool chart was assigned four colors; black, white, off-white, and red sand (Figure 4.7). The figure has shown that black color sediments have a high affinity toward As contamination while the red color sediments are comparatively safe from arsenic pollution.

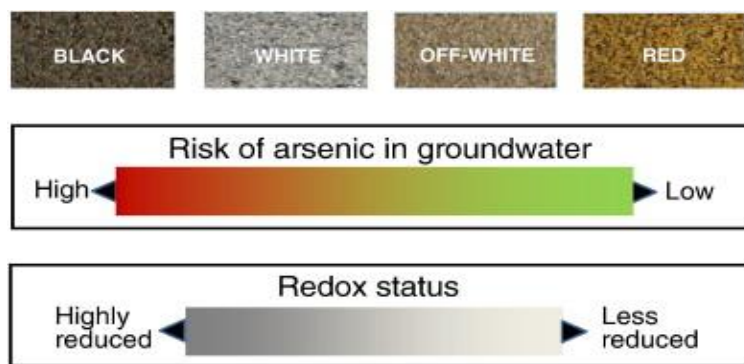


Figure 4.7: Four-color of sand with the corresponding risk of As in groundwater as well as redox conditions (Adapted from: Hossain et al., 2014).

The above chart also explained how the redox potential is associated with the As contamination in groundwater. Highly reduce conditions in groundwater were supported by the high risk of As contamination in groundwater. In contrast, the less reduced condition was accountable for safe or less risk of As contamination in groundwater.

Table 4.3: Statistical summary of As and soil texture in the sediment core of study area 1 (Gorakhpur)

<b>a. Sediment core 1 (Khorabar).</b> Unit = concentration of arsenic was expressed in mg/kg. (As recovery 98.32%, Detail mentioned in section 4.2.7)											
Sr. No.	Depth (m)	pH	As (acid-soluble)	As (reducible)	As (oxidisable)	As (residual)	As (total)	Sand %	Silt %	Clay %	OM %
1	0.00	8.18	0.12	3.11	0.82	8.16	12.21	42.17	50.92	6.91	0.20
2	3.05	8.36	0.67	5.28	1.53	11.71	19.19	42.06	49.84	8.10	0.04
3	6.10	8.22	0.25	3.98	0.23	6.31	10.77	41.56	52.21	6.23	0.45
4	9.14	8.14	0.09	1.07	0.41	3.46	5.03	45.35	51.37	3.28	0.76
5	12.19	8.29	0.57	3.82	0.48	9.29	14.16	67.58	30.73	1.69	0.14
6	15.72	8.23	0.66	2.59	0.65	6.68	10.59	69.20	29.22	1.58	0.17
7	18.29	8.09	0.17	1.97	0.52	4.83	7.49	72.67	25.37	1.96	0.10
8	21.34	8.25	0.91	2.53	1.24	6.86	11.54	63.66	40.28	6.06	0.50
9	24.38	8.29	0.64	3.88	1.48	8.33	14.32	47.64	43.71	8.65	0.57
10	27.43	8.34	0.42	5.29	1.29	8.27	15.27	39.33	54.45	6.22	0.17
11	30.48	8.13	0.06	1.47	0.25	4.07	5.85	43.38	42.59	14.03	0.44
12	33.53	8.21	0.21	4.99	0.48	5.92	11.60	36.84	53.60	9.56	0.20
<b>Mean</b>	16.80	8.23	0.40	3.33	0.78	6.99	11.50	50.95	43.69	6.19	0.31
<b>Min.</b>	0.00	8.09	0.06	1.07	0.23	3.46	5.03	36.84	25.37	1.58	0.04
<b>Max.</b>	33.53	8.36	0.91	5.29	1.53	11.71	19.19	72.67	54.45	14.03	0.76
<b>b. Sediment core 2 (Farshiya)</b>											
1	0.00	8.12	0.42	3.23	1.04	5.35	10.04	24.07	66.61	9.32	1.11
2	3.05	8.01	0.40	2.66	1.06	6.48	10.60	24.49	56.93	8.58	0.50
3	6.10	8.24	0.12	0.65	0.26	2.63	3.65	70.19	27.26	2.55	0.27
4	9.14	8.19	0.39	3.10	1.26	10.34	15.10	28.26	61.28	10.46	1.22
5	12.19	8.23	0.18	4.59	1.44	12.10	18.31	22.55	65.90	11.55	0.47
6	15.24	7.92	1.28	8.05	2.10	12.53	23.96	15.56	71.62	12.82	0.67
7	18.29	8.25	0.16	1.28	0.56	4.92	6.92	57.14	42.41	1.45	0.34
8	21.34	8.21	0.12	1.55	0.39	4.39	6.45	58.83	38.09	3.08	0.24
9	24.38	8.37	0.28	1.91	0.62	6.21	9.02	57.71	38.17	4.12	0.47
10	25.91	8.24	0.10	2.09	0.52	4.64	7.35	62.26	35.73	2.01	0.25
11	27.43	8.12	0.22	2.04	0.53	6.54	9.33	42.07	49.66	8.27	0.57
12	30.48	8.12	0.41	4.13	0.83	7.87	13.24	30.75	62.20	7.05	0.21
13	33.53	7.99	0.42	4.20	1.14	8.69	14.45	38.32	54.97	6.71	0.13
<b>Mean</b>	17.47	8.15	0.35	3.04	0.90	7.13	11.42	40.94	51.60	6.77	0.63
<b>Min.</b>	0.00	7.92	0.10	0.65	0.26	2.63	3.65	15.56	27.26	1.45	0.24
<b>Max.</b>	33.53	8.37	1.28	8.05	2.10	12.53	23.96	70.19	71.62	12.82	1.22

#### a. Study area 1 (Gorakhpur):

A litholog was prepared for all the sediment cores in the study area (Figure 4.8). The depth-wise distribution of As fractionated species and sediment texture were summarized in table 4.2. The first (older alluvium) sediment core was drilled at Khorabar, a small town of the Gorakhpur district. The second core (younger alluvium) was drilled at Farshiya village. Farshiya gets submerged every year during the flood in the Rapti River. A photograph was also taken for each fresh sediment sample during the drilling, along with the lithologs. The lithologs of the study area were classified based on the soil texture. The sediment core was having five lithofacies at Khorabar while six lithofacies at Farshiya village. The upper section of both the sediment cores in study area 1 mainly consisted of silty clay. The upper layer of the sediment core at Khorabar having around 40% sand and 60 % silt and clay, while at Farshiya, 24% sand and 76% silt and clay were reported.

A photographic color of the sediment was light yellowish to brown, while in the sediment color tool, it came under off-white color. The average As concentration at Khorabar was reported 11.50 mg/kg (minimum 5.03 mg/kg at 9.1 mbgl, maximum 19.19 mg/kg at 3.05 mbgl) and at Farshiya, it was 11.42 mg/kg (min. 3.12 mg/kg at 6.10 mbgl and max 23.96 mg/kg at 15.24 mbgl). The higher concentration of As at Khorabar was reported at shallow depth sediment. The water table in the study area was very shallow. It fluctuated between 3 to 5 mbgl during pre and post-monsoon of 2017-18 (Jal Jeevan Mission, Uttar Pradesh, Ministry of Jal Shakti, 2017-18). Fluctuation of the water table at this shallow depth may be responsible for changes in the redox condition of the study area and significantly influences the adsorption of As to the sediment (Shankar et al., 2014; Xiao et al., 2018). Clay minerals act as adsorbents by providing the oxides-like surface for metal adsorption (Smedley & Kinniburgh, 2002).

The average percent of sand varied from 50.95% at Khorabar (min. 37.84% at 33.5 mbgl and max. 72.56% at 18.3 mbgl) and 40.9% at Farshiya (min. 15.56% at 15.24 mbgl and max. 70.19% at 7.10 mbgl). The texture analysis suggested that sand was the dominant grain observed in the overall lengths in the sediment cores. The total extracted As from the fractionation process was less than the total digested As in all the sediment cores. The average As residual fraction in the sediment core was observed to be 62% at Khorabar and 64% at Farshiya.

A high percentage of the residual fraction in core sediments indicated metal incorporated with crystal structure which was quickly not breakable with the application of weak acids (Zimmerman & Weindorf, 2010). The pH of the study area was slightly alkaline and varied, with an average of 8.23 at Khorabar and 8.15 at Farshiya. pH also plays a significant role in the adsorption and desorption of arsenic on metal oxides (Singh, 2006; Charlet et al., 2007).

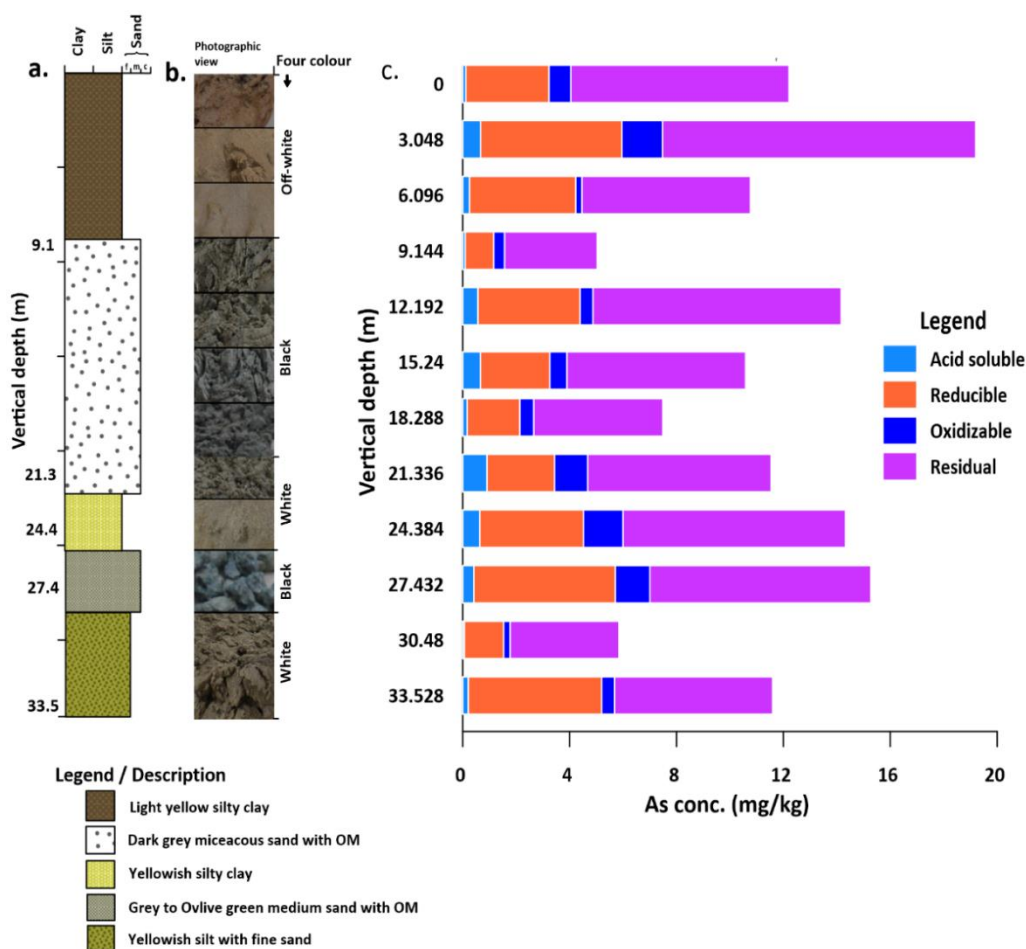


Figure 4.8: a. Litholog of the sediment core, b. photographic view of the fresh sediment of field, c. vertical distribution of As species in the sore sediment (Khorabar)

In the sediment core of Khorabar, the high As concentration was found in yellow silty clay of upper section (0-3 mbgl) depicted to off-white color on sediment color tool chart. An elevated level of As contamination was also found at a depth of 27.4 mbgl in grey to olive-green sand with silt which was depicted as black in sediment tool color. A shallow water table (3-5 mbgl) in the

study area might be responsible for the oxidizing environment and As gets precipitated on solid surfaces (silt and clay). Hence, the shallow aquifer of older alluvium is less As contaminated. While at a depth of 27.4 mbgl, the upper aquifer tier system (30-50 mbgl) was observed. The elevated As in this depth might be associated with the available minerals. Groundwater results also revealed that 20-35 mbgl aquifer systems were inflated As contaminated. Redox-induced minerals of Fe and Mn get dissolved in the aquifer system and release As in the groundwater. The presence of arsenic in sediment core and groundwater might be regulated by the reduction potential of groundwater and redox-dependent physical parameters and mineral saturation indices.

In the sediment core of Farshiya, a different trend was observed. The concentration of As was found higher at 15.24 mbgl in dark grey fine silty clay, depicted to black color (Figure 4.9). The concentration of As in the Gangetic basin has been dependent on sediment color and soil texture. Fine-grain sediments had a high affinity toward As adsorption compares to coarser sediment (Hasan et al., 2009). The presence of the organic matter in subsurface sediment also elevated As concentration in the groundwater through metal oxides desorption. The average percentage of organic matter was reported at 0.31% at Khorabar and 0.63% at Farshiya (Table 4.1). In Khorabar, organic matter was not showing any trend with the depth because this was collected from a densely populated town. In sediment core 2 (Farshiya), the highest percentage of organic matter was found in the upper surface of the core sediments. It was located in the agricultural field and flooded every year during the Rapti river flood. So agricultural practices and nutrient metabolism by microbial activity might be the primary source for organic matter in the soil (Harvey et al., 2005). Due to high microbial activity in the upper section of the sediment core, a reducing environment was generated that triggered the reductive dissolution of metal oxyhydroxide and releasing As in the groundwater.

The sequential extraction results were plotted alongside the litholog (Figure 4.8c). The parallel plot shows the soluble/available fraction and residual fractions of As in the core sediments. A significant amount of As was bound with the residual fraction, followed by reducible, oxidizable, and acid-soluble fractions. The acid-soluble fraction is interconnected with carbonate-bound form. The reducible fraction was accounted for the reduction of Fe and Mn bound oxides and was the second dominant fraction after the residual fraction. In the last step of sequential extraction, sulphide and organic matter were oxidized by using the oxidizing acids. In Khorabar,



the residual fraction accounted for 62% of the total extraction, while the reducible fraction accounted for 28% of the total extraction. The oxidizable fraction accounted for 6% of the total extraction, and the acid-soluble fraction accounted for 3% of the total extraction.

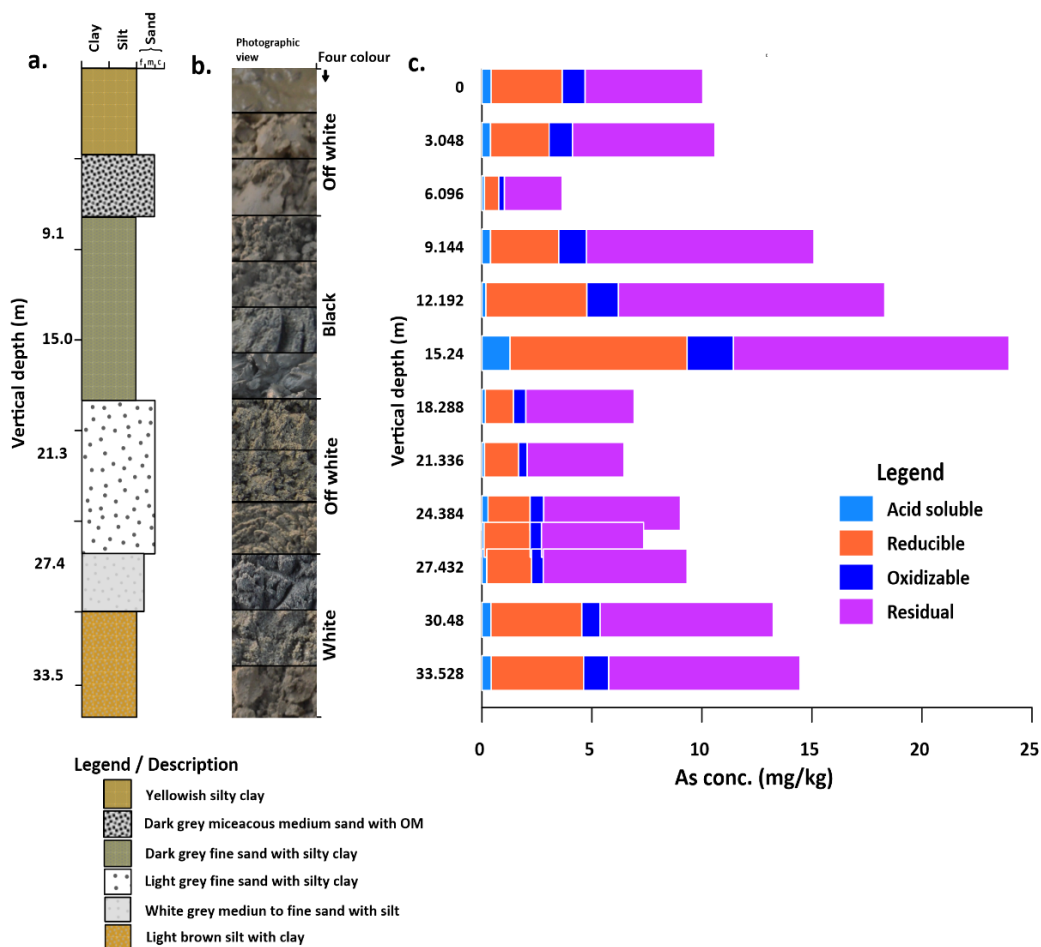


Figure 4.9: a. Litholog of the sediment core, b. photographic view of the fresh sediment of field, c. vertical distribution of As species in the sore sediment (Farsiya)

However, for the core sediments of Farshiya the residual fraction accounted for 65% of the total extraction. The second most dominant fraction was the reducible fraction accounted for 25% of the total extraction. The oxidizing fraction was the third dominant fraction followed by the reducible fraction and accounted for 7% of the total extraction. The last factor was the acid-soluble fraction, which accounted for 3% of the total extraction.

Table 4.4: Statistical summary of As and soil texture in the sediment core of study area 2 (Ghazipur)a. Jagadishpur and b. Firozpur

<b>a. Sediment core 3 (Jagadishpur).</b> #Unit = Concentration of As were expressed in mg/kg. (As recovery = 98.32%, )											
Sr. No.	Depth (m)	pH	As (acid-soluble)	As (reducible)	As (oxidisable)	As (residual)	As (total)	Sand %	Silt %	Clay %	OM %
1	0.00	8.14	0.40	3.97	1.10	9.39	14.85	10.35	81.61	8.04	1.96
2	1.52	8.31	0.55	6.03	1.98	12.27	20.83	31.10	64.26	5.64	0.81
3	3.05	8.34	1.10	9.01	2.27	13.93	26.31	28.66	62.12	9.22	0.67
4	6.10	8.21	0.73	7.30	2.02	11.10	21.15	31.42	62.22	6.36	0.35
5	9.14	8.07	0.39	3.17	0.80	6.55	10.91	66.17	32.16	1.67	0.24
6	12.19	8.01	0.01	0.30	0.12	0.97	1.40	76.32	22.47	1.21	0.05
7	15.24	8.22	0.49	4.08	0.91	6.87	12.35	59.41	40.67	2.08	0.11
8	18.29	8.18	0.16	2.36	0.53	4.22	7.27	56.42	40.33	6.25	0.17
9	21.34	8.29	0.41	5.07	1.48	7.15	14.12	59.40	39.20	1.40	0.17
10	24.38	8.00	0.14	0.26	0.20	2.12	2.73	71.45	17.01	1.54	0.06
11	27.43	8.23	0.24	3.58	1.01	6.04	10.87	58.85	33.91	7.24	0.23
12	30.48	8.12	0.02	0.31	0.09	1.04	1.45	63.67	29.39	6.94	0.09
13	32.00	8.05	0.14	2.28	0.41	4.38	7.21	41.99	51.50	6.51	0.14
14	33.53	8.08	0.07	1.52	0.20	1.89	3.68	40.87	51.77	8.36	0.07
<b>Mean</b>	16.76	8.16	0.35	3.52	0.94	6.28	11.08	49.72	44.90	5.18	0.36
<b>Min.</b>	0.00	8.00	0.01	0.26	0.09	0.97	1.40	10.35	17.01	1.21	0.05
<b>Max.</b>	33.53	8.34	1.10	9.01	2.27	13.93	26.31	76.32	81.61	9.22	1.96
<b>b. Sediment core 4 (Firozpur)</b>											
1	0.00	8.06	0.97	6.09	1.22	13.36	21.64	7.62	81.81	10.57	1.23
2	1.52	8.06	0.82	5.38	1.52	11.84	19.56	9.87	79.40	10.73	0.80
3	3.35	8.10	0.58	3.16	0.28	8.48	12.50	33.95	60.30	5.75	0.77
4	6.10	8.26	0.59	3.53	1.17	8.02	13.31	32.64	61.32	6.04	0.74
5	9.14	8.21	0.72	5.19	1.49	10.30	17.70	25.24	68.63	6.13	0.57
6	12.19	8.19	0.45	2.60	0.19	8.43	11.67	43.77	52.68	3.55	0.20
7	15.24	8.26	0.25	0.77	0.42	3.94	5.38	88.69	11.31	0.00	0.34
8	18.29	8.22	0.20	0.22	0.23	1.94	2.59	97.18	2.82	0.00	0.17
9	21.34	8.34	0.22	0.47	0.35	2.55	3.59	82.93	16.03	1.04	0.20
10	25.91	8.31	0.25	0.53	0.31	3.23	4.32	80.97	18.19	0.84	0.11
11	27.43	7.97	1.59	8.41	3.59	17.93	31.52	14.60	78.17	7.23	0.94
12	30.48	8.13	1.29	6.72	2.39	17.02	27.42	24.42	68.71	6.87	0.31
13	33.53	8.35	0.58	4.33	1.01	8.32	14.24	48.34	48.92	2.74	0.15
<b>Mean</b>	15.73	8.19	0.65	3.65	1.09	8.87	14.26	45.40	49.87	4.73	0.50
<b>Min.</b>	0.00	7.97	0.20	0.22	0.19	1.94	2.59	7.62	2.82	0.00	0.11
<b>Max.</b>	33.53	8.35	1.59	8.41	3.59	17.93	31.52	97.18	81.81	10.73	1.23

## b. Study area 2 (Ghazipur):

The summary of the As fractionated species with sediment texture and organic matter was given in [Table 4.3](#). The average pH of the core sediment at Jagadishpur was almost comparable to the average pH at Firozpur. A notable change in pH can significantly affect metal adsorption on sediment, and above pH=6, the metal's solubility was reduced ([Jain & Ram, 1997](#)). The litholog was prepared for sediment cores at Jagadishpur and Firozpur ([Figure 4.10a and 4.11a](#)). Along with the litholog, a photographic picture of the fresh sediments was illustrated. Based on the soil texture, the litholog at Jagadishpur and Firozpur were divided into four and six lithofacies, respectively. Based on the sediment color tool, photographs of Jagadishpur were deciphered into black and off-white color, while photographs of Firozpur were deciphered into black, off-white, and red color. In the study area, the role of the pH was not significant due to its alkaline nature. The average concentration of total arsenic was reported 11.08 mg/kg at Jagadishpur (min. 1.4 mg/kg at 12.19 mbgl and max. 26.31 mg/kg at 3.05 mbgl) and 14.26 mg/kg at Firozpur (min. 1.92 mg/kg at 18.29 mbgl and max. 31.52 mg/kg at 27.43 mbgl). A Significant variation was observed in the sand and silt percentage throughout the core sediment at both locations.

The upper section of both the cores was mainly incorporated with silt and clay. In Jagadishpur, the maximum concentration of As was observed at 3.05 mbgl associated with light yellow silty clay with organic matter and depicted as black in sediment tool color. The water table at Ghazipur city was reported 5.5 to 6.5 mbgl during pre and post-monsoon 2017-18 ([Jal Jeevan Mission, Uttar Pradesh, Ministry of Jal Shakti, 2017-18](#)). Above the water table, an oxidizing environment was made possible by exchanging oxygen with the atmosphere. In the oxidizing environment, the bioavailability of the metal oxides is limited due to extremely low solubility, which causes metal oxide minerals to precipitate ([Bjorn & Roychoudhury, 2015; Hao et al., 2018](#)). Hence, dissolved groundwater As gets adsorbed into the precipitated metal oxyhydroxide or clay minerals, and an elevated As concentration was reported in the upper section of the sediment core. At 21.35 mbgl, the high As concentration was associated with grey micaceous medium sand with organic matter and depicted as black in the sediment color tool. Minerals of clay and calcite act as a metal sink by providing adsorption surfaces ([Manning & Goldberg, 1997; Roman-Ross et al., 2006](#)).

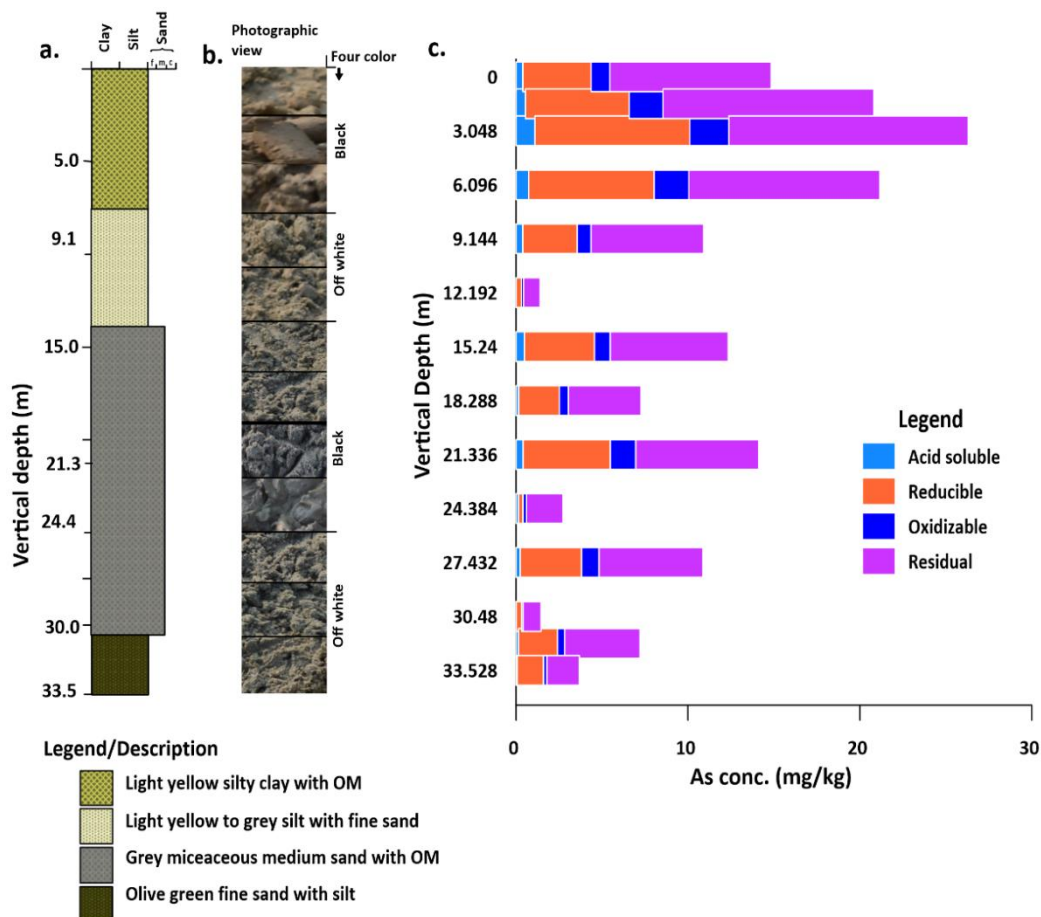


Figure 4.10: a. Litholog of the sediment core, b. photographic view of the fresh sediment of field, c. vertical distribution of As species in the sore sediment (Jagadishpur)

In the core sediment of Firozpur, the high As concentration was reported in olive green fine sand and silt section (27.43 mbgl) depicted to black color. The yellow silty clay of the upper section (0-2 mbgl) also had a high As concentration. In the sediment tool color, this section was depicted as black. The sediment core at Firozpur was collected from the agricultural field near the Ganga river and repeatedly inundated. During the flood, the river deposited fresh and nutrient-rich sediment in the study area (Kumar et al., 2016). The degradation of the nutrient-rich sediment by bacterial metabolism produced a reducing subsurface environmental condition and supporting the metal and As mobilization and leaching. Secondly, metal oxide gets precipitated in the oxidizing environment during the dry season because of the lower down the water table. Hence, metal and As concentrations were reported higher in the upper section during the dry season. At 27 to 33 mbgl, an elevated As concentration was observed in olive green fine sand with silt (Figure 4.11c) with organic matter. The reducing environment of the aquifer system causes Fe and Mn

oxyhydroxide dissolution and triggers the As mobilization from sediment to the groundwater. So, minerals of iron and manganese behave as a secondary source and sink for As in the sediment.

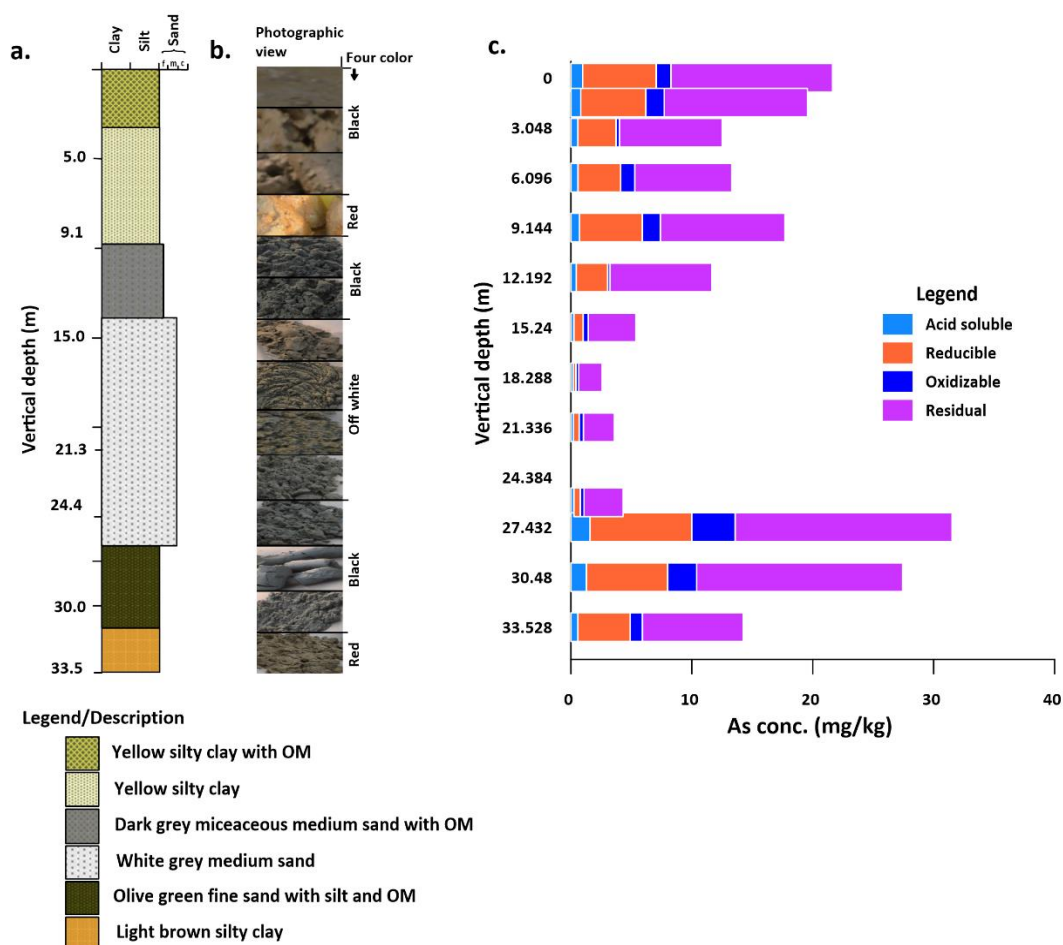


Figure 4.11: a. Litholog of the sediment core, b. photographic view of the fresh sediment of field, c. vertical distribution of As species in the sore sediment (Jagadishpur)

A parallel plot was prepared for the As fractionated species at Jagadishpur and Firozpur (Figure 4.10c and 4.11c). A significant amount of As was bound with residual fraction. In Jagadishpur, the residual fraction accounted for 60% of the total extraction, followed by the reducible fraction (29% of the total extraction), an oxidizable fraction (8% of the total extraction), and an acid-soluble fraction (3% of the total extraction), respectively. However, in Firozpur, the residual fraction accounted for 66% of the total extraction. The reducible fraction accounted for 22% of the total extraction. The oxidizable fraction accounted for 7% of the total extraction, and acid-soluble fraction accounted for 5% of the total extraction.

#### 4.3.3.2. Multivariate analysis for subsurface sediments

The principal component analysis is a technique applied to large data set to reduce dimensionality with improved interpretation without losing the information. In the study area, PCA was used to identify the geochemical processes occurring in the region. In the PC analysis, only those factors were considered for data interpretation, whose eigenvalue  $>1$ . Four factors (PCs) were considered for the core one at Khorabar, while all three cores had only two factors. A scatter plot (3D or 2D graphic of PCA) was plotted for all the sediment core ([Supplementary Table 1&2](#)).

At Khorabar, factor 1 was accountable for 38% of the total variance with the positive loading of pH and As fractionated species (acid-soluble, reducible, oxidizable, and residual fractions); however, moderately correlated with clay and silt indicating As adsorbed on silt and clay ([Figure 4.12](#)). Factor 2, accountable for 25.75% of the total variance. It was negatively correlated with silt and clay while independent of other species of the data set. Factor 3 and 4 are accountable for 14% and 12% of the total variance, respectively. Factor 3 was positively loaded with organic matter, while factor 4 was positively loaded with depth. Both are independently available in their respective factors, so they were not considered in the interpretation (PCA table were attached in annexure files).

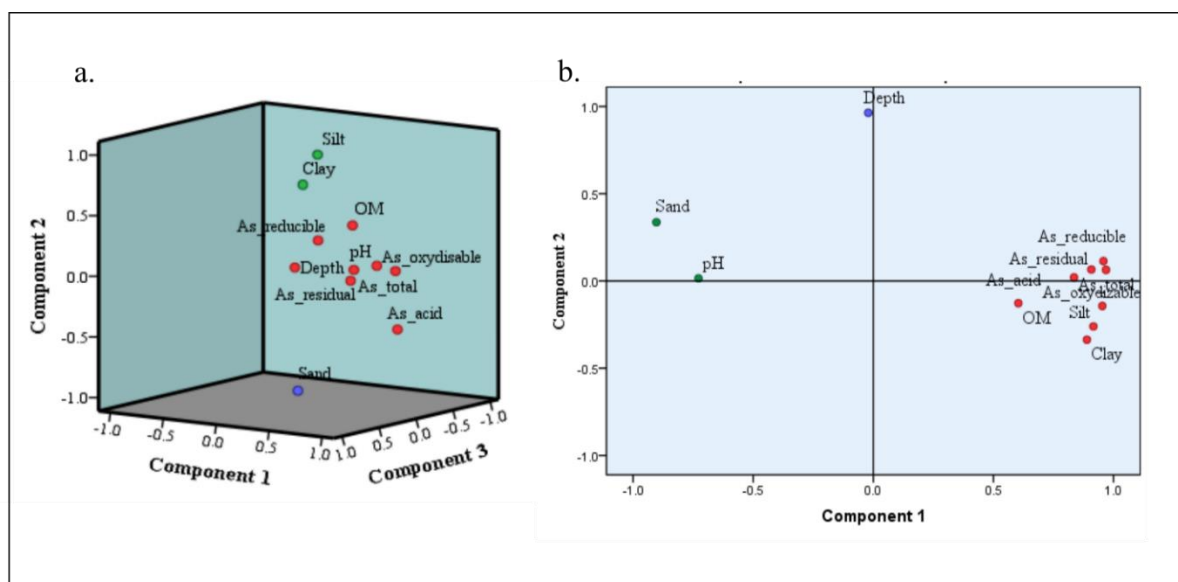


Figure 4.12: 3D Component plot in rotates space, a. Khorabar, b. Farshiya

At Farshiya, PCA was shown only two factors having eigenvalue greater than  $>1$ . Factor 1 and factor 2 both mutually represent 80.95% of the total variance of the data set. Factor 1 is accountable for 69.3% of the total variance with the positive loading of all the As fractionated species, silt, clay, and organic matter; however, negative loading of pH and sand indicates As adsorbed on clay and fine silt sediment. Minerals of clay had attenuation to adsorbed and desorbed the As into the groundwater (Lin & Puls, 2000). Factor 2, accountable for 11.65% of the total variance and has shown a positive loading of depth, an independent variable in this factor.

The principal component analysis (PCA) of core three (at Jagadishpur) was used to identify the linear independent variable in a data set by the dimensional reduction method. A total of two factors had eigenvalue  $>1$  and represented 85.25% of the total variance of the data set. Factor 1 was accountable for 54.7% of the total variance with the positive loading of As total, and fractionated species (Figure 4.13a), pH and silt with the negative loading of depth indicating, the concentration of As (total and fractionated) decreases through the core sediment below the depth. Factor 2 accountable for 30.5% of the total variance with the positive loading of silt, clay, and organic matter and negative loading of sand indicating adsorption of organic matter into the clay were assist to stabilized the carbon into the soil (Sarkar et al., 2018).

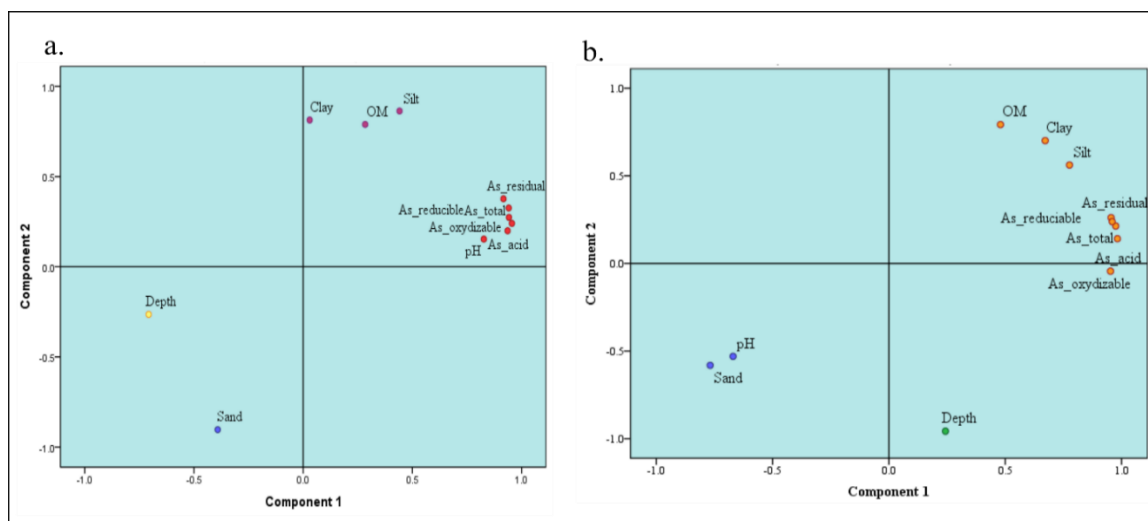


Figure 4.13: 3D Component plot in rotates space, a. Jagadishpur, b. Firozpur

The PCA of core 4 explained around 92.7% of the total variance, with two factors having eigenvalue >1. Factor 1 represented 63.9% of the total variance with the positive loading of As species, clay, silt, and organic matter indicated fine sediments like silt and clay act as a sink for As in the core sediment (Figure 4.10b). The presence of organic matter in fine sediment has assisted the desorption of arsenic from sediment to groundwater (Reza et al., 2010). Factor 2 is accountable for 28.7% of the total variance, with the inverse relationship between depth and organic matter indicated the amount of organic matter decreases below the depth throughout the core sediment.

#### 4.3.3.3. Mineralogy of the subsurface sediment

Mineralogical study of the sediment was an essential aspect of understanding the available minerals in the study area: the mineral composition and their behavior to the solid phases concerning As contaminated in groundwater. The mineralogical analysis revealed that common minerals such as quartz, muscovite, albite, feldspar, and calcite, etc., were reported in the core sediment (Figure 4.11&4.12). The peak of feldspar and chlorite was not constant throughout the entire depth suggested the origin of sand was either sedimentary or metasedimentary (Ahmed et al., 2004; Kumar et al., 2016). The peak of calcite and muscovite was very tiny at the surface sediment. In contrast, at a depth of 12.19 mbgl, a prominent peak was observed a little bigger indicated a close association between them (Figure 4.11b). A hematite peak was reported in yellowish clay sediment (upper section of the core sediment), indicating an oxidizing environment. The goethite (FeOOH) mineral was observed throughout the sediment core. A peak of siderite was observed in the upper surface sediment and at 12.1 mbgl in the sediment core. Many studies of As in Southeast Asia noted the availability of siderite minerals in the sediment (Islam et al., 2004; Anawar et al., 2006; Kumar et al., 2016). Jönsson & Sherman (2008) studied the sorption of As to siderite and reported that As(V) vigorously adsorbed on siderite compare to As(III). As(III) mobility is ten times more to As(V) in a reducing environment that reduces the adsorption of As(III) on siderite. Several published articles have reported that As(III) form is available in deeper sediment of the core (Mumford et al., 2012; Kumar et al., 2016). So, siderite acted as a sink for As. In this study, we did not carry out fractionation, shown to distinguished As(III) and As(V) in the sediment core. Still, it was observed that the total As concentration was decreased in the deeper core section indicate the absence of the peak of siderite and magnetite minerals. The peak appearances of other minerals like goethite, Fe-oxide coated quartz (fine-grained), and clay



minerals such as kaolinite and illite in the upper section also elevated the As concentration in the core sediment Khorabar.

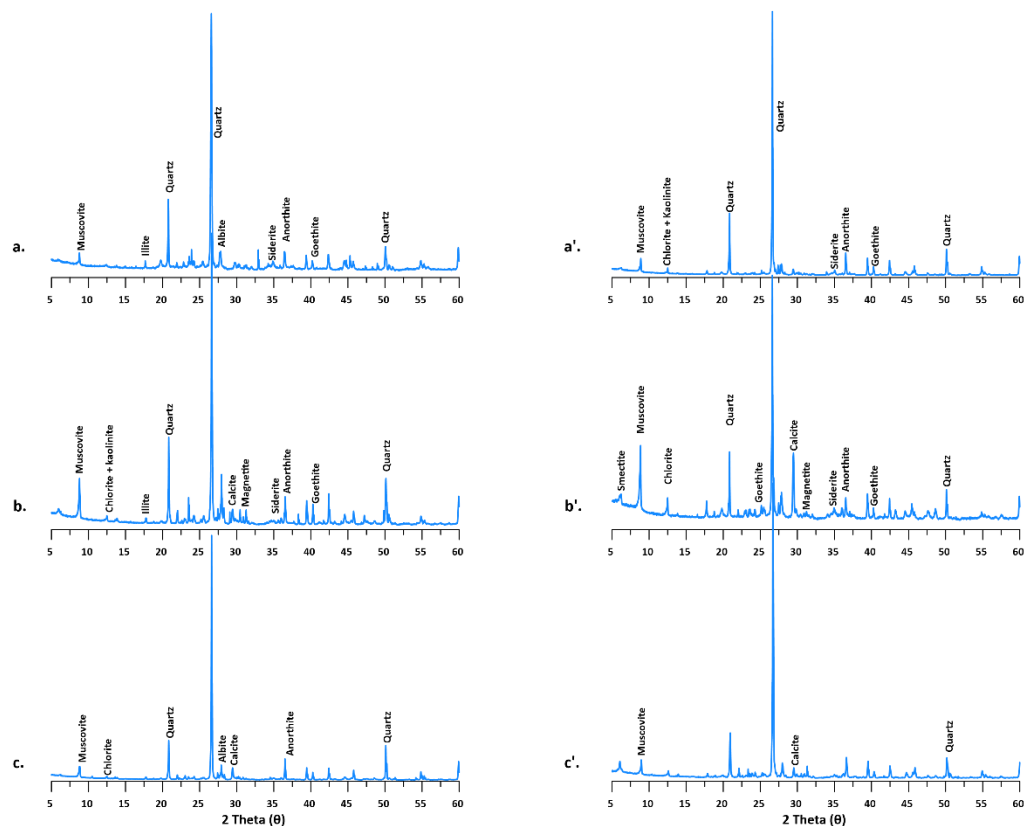


Figure 4.14: The mineralogical composition of the core sediment (XRD analysis results), Khorabar (a. at surface sediment, b. at 12.19 mbgl and c. at 30.48 mbgl) and Farshiya (a'. at surface sediment, b'. at 15.4 mbgl and c'. 21.34 mbgl). (A high-resolution image was attached in the supplementary material)

The mineralogy of Farshiya was almost similar to Khorabar. The high As in core sediment at 15.24 mbgl was associated with siderite. Toward the deeper section, the concentration of arsenic decreased with low concentration at 21.24 mbgl due to the absence of siderite minerals (Figure 4.11c). In the deeper section (33.5mbgl), minerals like goethite and magnetite were observed. These minerals with fine silt and clay have enhanced the As concentration in the deeper section of the sediment core.

The result of the mineralogical study for the sediment cores at Jagadishpur and Firozpur was shown in figure 4.12. The primary minerals such as quartz, muscovite, chlorite, feldspar were

reported in the sediment core of Jagadishpur. Similar to study area 1, muscovite has shown a good association with chlorite. A small peak of calcite was observed in the upper (0.5 mbgl) and middle (15 mbgl) sections of the core sediment (Figure 4.12a&b). In the upper section, the concentration of As was reported higher and is associated with yellow silty clay with organic matter. In this section, minerals of goethite and hematite were reported that it might have enhanced As in the sediment. A small peak of siderite was observed at 15.24 mbgl, indicating the association with high As in the core sediment.

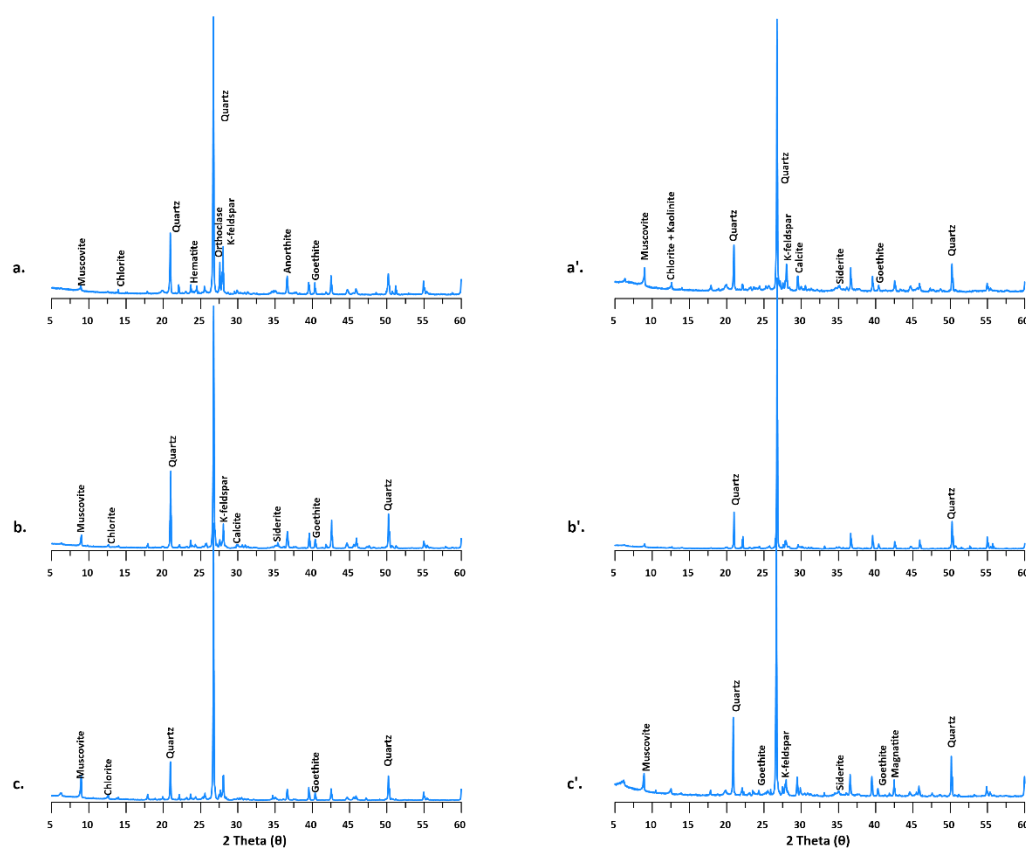


Figure 4.15: The mineralogical composition of the core sediment (XRD analysis results), Jagadishpur (a. at surface sediment, b. at 15.0 mbgl and c. at 33.12 mbgl) and Firozpur (a'. at surface sediment, b'. at 18.29 mbgl and c'. 30.28 mbgl) (A high-resolution image was attached in annexure)

The mineralogy of Firozpur was almost similar to the Jagadishpur. A calcite peak was observed in the surface sediment (Figure 4.12a). The intensity of the carbonates signal was higher in the yellowish silty clay, demonstrating a close link with metal chelation in the oxidation zone (Hasan et al., 2009). Clay minerals like chlorite, kaolinite, and feldspar were reported in the upper

section up to the depth of 9.1 mbgl and at 33.5 mbgl, indicating a high As concentration in these depths. A mineral of siderite and goethite were also reported at the same depth, which might have enhanced As concentration in the sediment core.

#### 4.4. Conclusions

The present study discussed the inorganic As fractionation in groundwater had been carried out using metal soft cartridges. Four sediment cores were collected from the study area based on different geomorphologies (older and younger alluvium). In study area one (Gorakhpur), core one was drilled at Khorabar (Older alluvium), and core two was from Farshiya (younger alluvium). In study area two (Ghazipur), core one was drilled at Jagadishpur (older alluvium) and core two from Firozpur (younger alluvium). The spatial distribution plots indicated that groundwater of YA (younger alluvium) was reported with elevated As(III) concentration, while in the groundwater of OA, either As(III) was less or not detected. In both areas, it was observed that shallow aquifers (20-35 mbgl) were more vulnerable to As contamination compared to the deeper aquifers.

Distribution of As in sediment core was mainly dependent on the aquifers sediment texture and redox potential. In the upper section of all the four cores, the clay and silt percentage are dominated. The sand was available in entire cores with the variable percentage in both the study area. The residual fraction is the dominated fraction followed by reducible, oxidizable, and acid-soluble fractions. The variation of inorganic As in the sediment cores was linked with two factors: first, the aquifer redox conditions represented by the sediment color and second, particle size with darker sediment holds more As.

An elevated As was observed in the upper section of the sediment core at Khorabar. The shallow water table in the study area generates oxidizing conditions, where the metal and As get precipitated. As(V) adsorption is more speedy than As(III) because of their low mobility. The residual fraction of As in the sediment core was tightly incorporated with crystal structure which was quickly not breakable by applying weak acids. So, the other three fractioned species were only involved in As mobilization. The sediment core of Farshiya (younger alluvium) was collected from the agricultural field and close to the river Rapti and flooded every year. Higher the organic matter and agricultural activity initiated high microbial activity and triggered As mobilization from

sediment to aquifer system. An elevated As (15.24 mbgl) was associated with fine dark grey silty clay. The mineralogical evidence suggested that the siderite mineral adsorbed As; therefore, elevated As concentration is reported in the sediment core.

In the sediment core of Jagadishpur (OA), the elevated As concentration was observed in the upper section of the sediment core and is associated with light yellow silty clay with organic matter. Similar to study area one, the upper section of the sediment core was enriched with As due to the shallow water table and the oxidizing environment that reduce its solubility and enhance metal precipitation. Siderite and magnetite were reported in the mineralogy of the sediment core that is associated with the high As concentration. In the sediment core of Firozpur, the upper section of the sediment core was rich in organic matter, and degrades the organic matter and developed a reducing environment, which was favorable for As desorption from sediment. Hence, As concentration was little in the upper section of the Firozpur sediment core. A high As concentration was reported in the deeper sections (27.43 mbgl) that are associated with olive green fine silt texture. In general, minerals like siderite and magnetite act as a sink for As and elevates the As concentration in the sediment cores.

## 4.5. Supplementary material

Table 4.5: PCA loading for the physicochemical parameter, soil texture and arsenic species in sediment cores

	Gorakhpur						Ghazipur			
	Khorabar (OA)				Farshiya (YA)		Jagadishpur (OA)		Firozpur (YA)	
	1	2	3	4	1	2	1	2	1	2
Depth	-.05	.01	-.03	.97	-.02	.96	-.71	-.26	-.71	-.26
pH	.91	.17	.24	-.04	-.73	.02	.83	.15	.83	.15
As(total)	.85	.16	.47	-.13	.97	.06	.94	.33	.94	.33
As(acid)	.87	-.41	-.10	.07	.84	.02	.94	.20	.94	.20
As(reducible)	.61	.40	.61	.04	.96	.11	.94	.27	.94	.27
As(oxydisable)	.89	.08	-.04	.05	.95	-.14	.96	.24	.96	.24
As(residual)	.81	.06	.46	-.27	.91	.07	.92	.38	.92	.38
Sand	-.02	-1.00	-.02	-.03	-.90	.34	-.39	-.90	-.39	-.90
Silt	.12	.95	-.09	-.10	.92	-.26	.44	.86	.44	.86
Clay	.00	.70	-.05	.52	.89	-.34	.03	.81	.03	.81
OM	-.14	.22	-.94	.03	.60	-.13	.28	.79	.28	.79
Total	4.18	2.83	1.76	1.33	7.63	1.28	6.02	3.36	6.02	3.36
% of Variance	38.02	25.75	16.04	12.08	69.33	11.65	54.70	30.56	54.70	30.56
Cumulative %	38.02	63.77	79.82	91.90	69.33	80.99	54.70	85.25	54.70	85.25

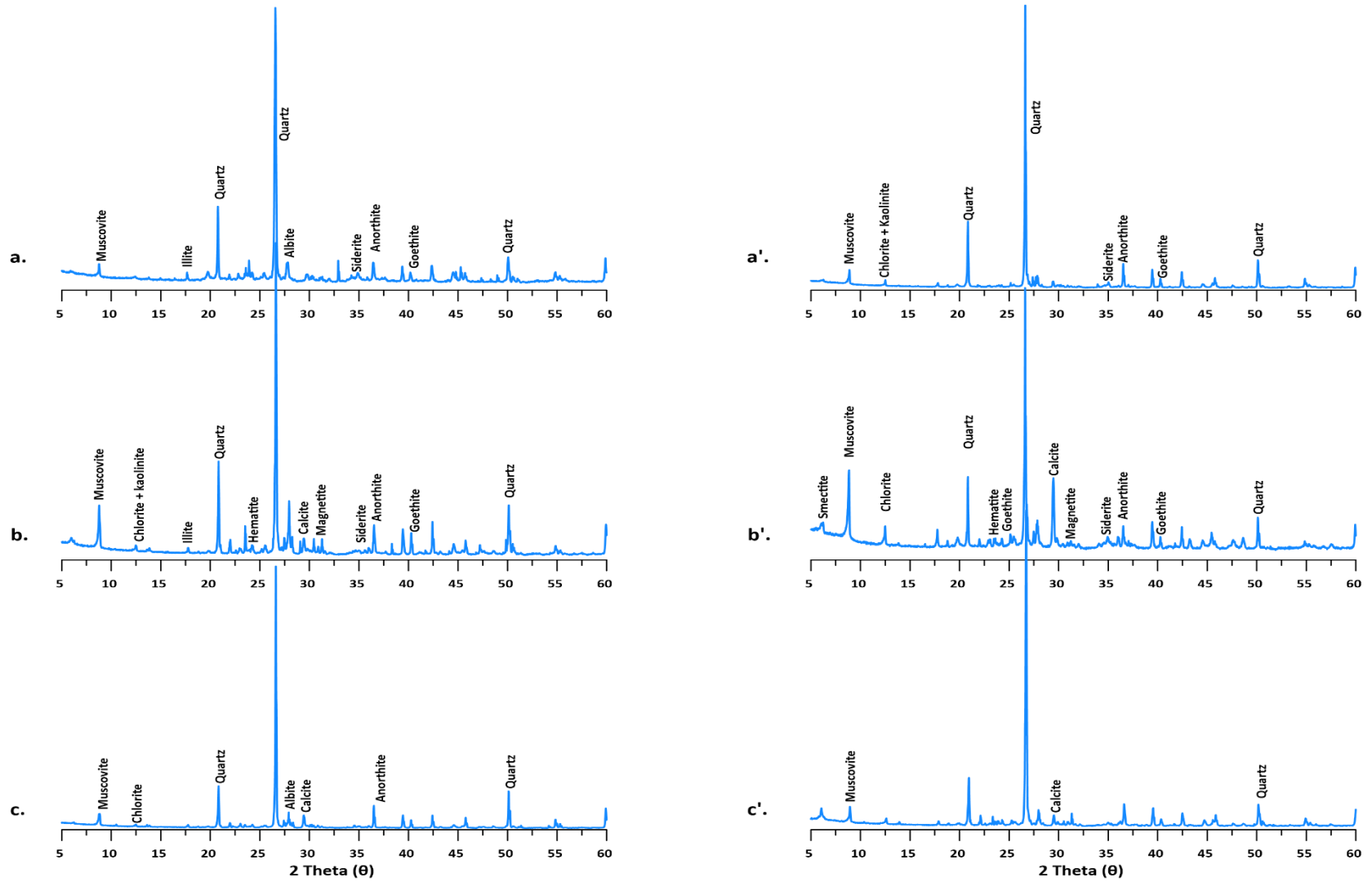


Figure 4.16: The mineralogical composition of the core sediment; a. Khorabar and a'. Farshiya

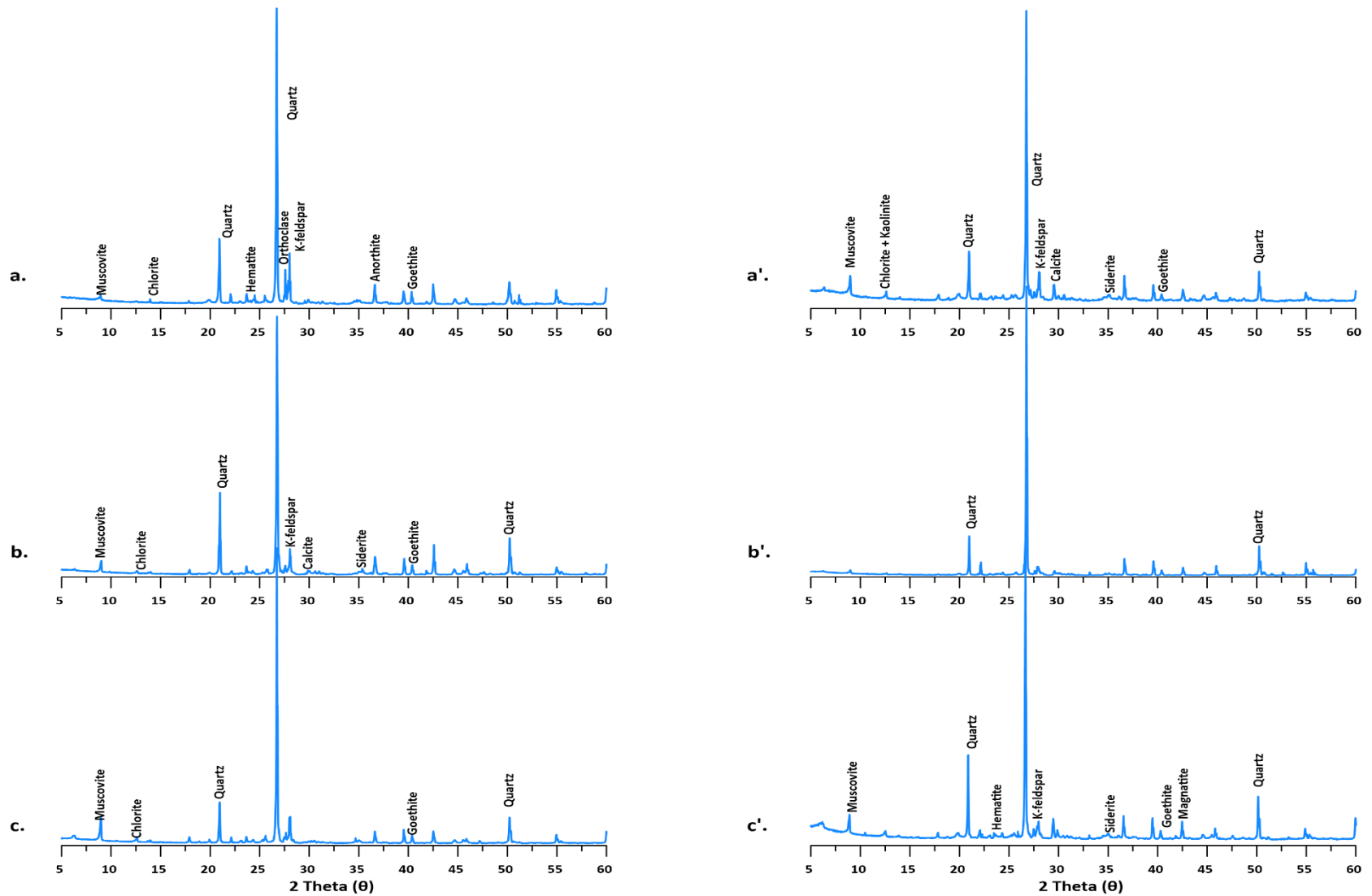


Figure 4.17: The mineralogical composition of the core sediment; a. Jagdishpur and a'. Firozpur

## Chapter 5

# Understand the groundwater dynamics, recharge/discharge and DOC behavior using stable isotopes in relation to arsenic mobilization

- 5 Understand the groundwater dynamics, recharge/discharge and DOC behavior using stable isotopes in relation to arsenic mobilization
  - 5.1 Introduction
  - 5.2 Material and methods
    - 5.2.1. Study area
    - 5.2.2. Sample collection and analysis
    - 5.2.3. Isotopic analysis
  - 5.3. Results and discussion
    - 5.3.1. Solute chemistry and isotope signature
    - 5.3.2. Stable isotope signature of water samples
    - 5.3.3. Sources of groundwater DIC,  $p\text{CO}_2$  and  $\delta^{13}\text{C}$
    - 5.3.4. Interrelationship among stable isotopes and physicochemical parameters
  - 5.4. Conclusions
  - 5.5. Supplementary material



## Abstract

Central Gangetic basin is one of the highly populated basins around the world. Unmanaged groundwater extraction and geogenic arsenic (As) pollution cause severe threats to groundwater sustainability and livelihood. So understanding the source and groundwater recharge is necessary for the long-term management of this aquifer system. In this study, stable isotopes tracer ( $\delta^2\text{H}$  and  $\delta^{18}\text{O}$ ) and  $\delta^{13}\text{C}_{\text{TIC}}$  were used to understand the groundwater recharge, interaction of groundwater and river water, natural carbon sources and dynamics. In study area one (Gorakhpur), stable isotopes ( $\delta^2\text{H}$  and  $\delta^{18}\text{O}$ ) indicate river water recharged from meteoric origin water. While, groundwater of older alluvium (OA) and younger alluvium (YA) was recharged from local meteoric origin water, undergoing little evaporation. River Rapti and its tributaries flowing through the study area contribute little to groundwater recharge, while the pond (known as Ramgarh lake) was not playing any significant role in recharging the adjoining groundwater. In study area two (Ghazipur), River water gets recharged from meteoric origin water, and groundwater of OA and YA were recharged from the meteoric origin water, which undergoes little evaporation. IRMS (Isotopic mass ratio spectrophotometer) results indicate that younger alluviums (YA) were enriched with  $\delta^{13}\text{C}_{\text{TIC}}$  in the study area compared to the older alluvium (OA). A CO2SYS calculator (windows version Xls file) was used to calculate  $p\text{CO}_2$  and DIC in the groundwater. The  $\delta^{13}\text{C}_{\text{TIC}}$  vs.  $p\text{CO}_2$  indicating silicate and carbonate weathering was the major source of DIC in the groundwater of both the study area.

**Keywords:** Stable isotope; Groundwater recharge; Carbon-13; Dissolved organic carbon; Shallow aquifer, Deeper aquifer

## 5.1. Introduction

Aquifer overexploitation can cause long-term groundwater depletion, which is an unexpected outcome of groundwater extraction (Konikow & Kendy, 2005; Kumar et al., 2018). It is well known that socio-economic gain from groundwater uses was dramatically changed in the 20<sup>th</sup> century due to overexploitation of groundwater. Majority of countries facing freshwater depletion includes Middle East Asia, North China, North America, North Africa, Australia and

North Africa, the Middle East, North China, North America and Australia, South and Central Asia, and localized parts of the globe (Konikow & Kendy, 2005; Kumar et al., 2018). India is the world's 2<sup>nd</sup> most populous nation, with only 4% of freshwater supplies from the river. And the unequal distribution of water supplies over the time and space can lead to water shortages (Mancosu et al., 2015; Dhawan, 2017). In India, aquifers providing groundwater are becoming the primary source of domestic and agricultural water use rapidly. It is anticipated that rising water demand and expected climate change would worsen over-reliance on groundwater for domestic and agricultural practices (Howard & Bartram, 2010; Zaveri et al., 2016; Rickards et al., 2020). Misra (2011) reported that climate change could raise temperatures by 2 to 6° C and reduce precipitation by up to 16%, which can turn down groundwater recharge. Hence, to overcome this situation through sustainable management of groundwater resources, it is necessary to know the recharging mechanism and processes responsible for pollution (Shah & Umar, 2015).

Since the early 1960s, naturally available stable isotopes in water samples have been a valuable tool and technique for investigating hydrological systems (Craig, 1961; Datta et al., 1996; Shah & Umar, 2015; Kumar et al., 2018). The stable isotope in groundwater research is commonly utilized to explore the origin, age and form of water. Any changes in isotopic composition along a flow line can indicate the changes in the history of water, such as mixing, mineralization and discharge (Mukherjee et al., 2012; Thilagavathi et al., 2016; Kumar et al., 2018). In aquifers system at low temperatures, stable water isotope ratios are conservative, but they can be isotopically fractionated on the surface at less than 100% humidity (Gat, 1996; Gupta & Deshpande, 2005; Shah & Umar, 2015; Gibson et al., 2016).

$\delta^{18}\text{O}$  and  $\delta^2\text{H}$  are the most widely used isotopes to provide details on the origin of water and the evaporation process (Shah & Umar, 2015). The *d*-excess is a function of the stable isotopes ( $\delta^{18}\text{O}$  and  $\delta^2\text{H}$ ) and is used as complementary tools to classify precipitation sources and vapor transport conditions of an area (Gupta & Deshpande, 2005; Kumar et al., 2018). The degree of isotopic exchange between vapor-water has been shifted as evaporation occurs and magnifies heavier isotope enrichment in residual water and eventually lower *d*-excess value due to comparatively higher  $\delta^{18}\text{O}$  (Gupta & Deshpande, 2005; Gibson et al., 2016). The *d*-excess value can also be helpful to identify the climatic conditions of the zone. The lower *d*-excess value reveals evaporated precipitation, while the higher *d*-excess value suggests high recycled moisture (Bershaw, 2018; Kumar et al., 2018).

In drinking waters, high organic carbon content has the ability to impact their usage as a source of community water (Vartiainen et al., 1987; Kortelainen & Karhu, 2006). In 1960s, the first carbon isotopes ratio was used to distinguish the origins of OM in the coastal area. In the coastal, terrestrial and aquatic environments, carbon isotopes used as tracers provide a better understanding of carbon sources (Emery et al., 1967; Benner et al., 1984; Lamb et al., 2006; Meredith et al., 2020). The primary source of carbon to aquifer TIC loads are carbonate minerals dissolution and microbial mediated decomposition of the soil  $\text{CO}_2$  (Mohammadzadeh & Mahaqi, 2017). Thus, to delineate the carbon source in the groundwater system, stable carbon isotopes ( $\delta^{13}\text{C}$ ) are used.

To estimate the groundwater dynamics, recharge/discharge processes and hydro-geochemical behavior, the lower Gangetic basin has been thoroughly analyzed with the application of stable isotopic composition (Aggarwal, 2000; Harvey et al., 2002; Mukherjee et al., 2007; Mukherjee & Fryar, 2008; Samanta et al., 2015). A few selected studies have been carried out in Bhagalpur and Samastipur, Bihar (Mukherjee et al., 2012; Kumar et al., 2019). This research also helps to explain the role of large rivers and surface water in the recharging aquifers system. Thus the key purpose of the chapter is to analyze groundwater recharge in relation to meteoric circulation/rainfall, to define the shallow aquifer signature and its association with the deep aquifer and the origins and dynamics of carbon and its interaction with recharging water in the selected study area.

## 5.2. Material and methods

### 5.2.1. Study area

The study areas are part of CGB (Central Gangetic Basin) and are occupied around 2610 km<sup>2</sup>. The CGB is one of the world's most complex and active fluvial deposition basins and is deeply impacted by climate-driven sediments, the soil water regime and integumentary tectonics (Sinha et al., 2005; Singh & Pandey, 2014). The study area (Figure 3.1&3.2) was further classified into different geomorphological unit's viz., younger alluvium (YA), older alluvium (OA), active flood plains, channels deposition, river water bodies, paleochannels, and active river channels.

The study area is formed by the deposition of recent unconsolidated sediment, including stream channel and flood channels mentioned as Quaternary Alluvium. It is further classified into older and younger alluviums. The older alluvium consists of sand and clay. It was reported during Late Pleistocene to the Early Holocene. The Younger alluvium is generally argillaceous and consists of silty clay or sandy clay. The younger alluvium is very narrow, mainly covering the area bordering the riversides. The younger alluvial and active flood plains are generally flooded each year uniformly.

The sediment's moisture holding capacity is very high. In the satellite images, they give high spectral resolution. The color of the soil also distinguishes the younger and older alluvium. The older alluvium is yellowish; however, the younger alluvium is grey and represents the reductive subsurface condition due to high microbial activity. On the other hand, older alluvial plains are mainly upland regions with less moisture content (Figures 3.1 and 3.2).

**(The details of the study area with sampling location and geomorphology has been discussed earlier in chapter 3, section 3.2.1)**

### 5.2.2. Sample collection and analysis

Our sampling strategy has been designed to identify the spatial and vertical variations in the isotopic signature of groundwater, river water and lake water samples across both the study areas (Figure 3.1&3.2). Water sampling was carried out for stable isotopes ( $\delta^{18}\text{O}$  and  $\delta^2\text{H}$ ) throughout the study areas during October 2017 and February 2018. We were collected 70

groundwater, 12 river water samples and one lake water sample across the Rapti River in Gorakhpur district. Similarly, 85 groundwater and 13 river water samples were collected across the Ganga River from the Ghazipur district. The groundwater samples were collected from government-installed India mark II or public hand pumps, and before the sampling, wells were purged for 20-30 minutes depending on the depth of the wells. The depth of the tubewell vary from ~15 to 46 mbgl in study area 1 (Gorakhpur district); however, it varies from ~18 to 107 mbgl in study area 2 (Ghazipur).

It should be noted that screening depths for government tube wells and piezometers are recorded only, while depths for public hand pumps and tube wells are based on the local information of the owner. According to the hand pump/tube wells owner, there is typically some displacement during the tubewell installation. Thus, we have assumed the uncertainty of  $\pm 5$  m in the depth of the public wells.

A portable (HORIBA, U-50 series) water quality multiparameter was used to measure the physical parameters such as pH, EC, TDS, and ORP in situ. The accuracy of the multiparameter (HORIBA, U-50) for the measurement of the parameters like pH, EC, TDS and ORP are  $\pm 0.1$ ,  $\pm 1\%$  full scale,  $\pm 5$  mg/L and  $\pm 15$  mV, respectively. Samples location was marked by a portable GPS (Garmin eTrex, accuracy ~3m) meter. Unfiltered water samples were collected from hand pumps/tube wells and rivers in airtight 15 ml glass vials without headspace for the analysis of  $\delta^2\text{H}$  and  $\delta^{18}\text{O}$ . In river water, samples were collected from the main running stream and ~30 cm below the surface. A continuous flow isotope ratio mass spectrometry and dual inlet isotope mass spectrometry with the standard procedure were used for measurements of  $\delta^2\text{H}$  and  $\delta^{18}\text{O}$  (Brenninkmeijer & Morrison, 1987; Joshi et al., 2018) in the groundwater. Estimation of  $\text{Ca}^{2+}$  was done by Inductive Coupled Plasma Optical Emission Spectrometry (ICP-OES 5110, Agilent Technologies, USA). The bicarbonate analysis was performed on Metrohm titrino plus 877 (Switzerland). The dissolved organic carbon (DOC) samples were collected in brown glass vials through the  $0.7\ \mu\text{m}$  glass fiber filter. DOC analysis was done on the analyzer SHIMADZU (VCPH) analyzer. The detection limit was 0.5 mg/l with a precision of  $\pm 10\%$ .

For  $\delta^{13}\text{C}$  analysis, samples were collected from the groundwater in 2 L plastic bottles and added NaOH drop by drop till the pH raised to 10-11 then we added 10 ml saturated  $\text{BaCl}_2$  (Bishop,

1990; Kumar et al., 2019). The samples were sustained to cool until the precipitate appeared. Once the precipitate dried, it was collected in and tightly packed in HDPE bottles. The analysis was supposed not to be affected by particulate contribution, i.e., without visible turbidity. The  $\delta^{13}\text{C}$  analysis was performed on a stable isotopic mass spectrophotometer (Isoprime 100, UK<sup>®</sup>). The precision of the instrument was  $\pm 2$  for the  $\delta^{13}\text{C}$ .

In this study, the DIC concentration,  $p\text{CO}_2$  and Saturation Indices were calculated from the major ions concentration, pH, alkalinity and temperature using the programme PHREEQC interactive 3.6.2 (USGS) software. In the software, Calcite Saturation Indices (CSI) was calculated by using the equation:

$$CSI = \log (IAP/K)$$

Where, IAP is the ion activity product and K is the equilibrium constant for calcite dissolution.

If  $CSI=0$  indicates mineral and aqueous solution are in the equilibrium phase,

$CSI<0$  indicates minerals are undersaturated in the aqueous solution and have a tendency toward more dissolution.

$CSI>0$ , indicate minerals are supersaturated in aqueous solution and have a tendency to precipitate on addition.

All bivariate plots and box-whisker plots were done on Grapher (v. 13.0) software. The study area map was prepared in Arc GIS (v. 10.2). Other plots and calculations were done on Microsoft excel (v. 2016).

### 5.2.3. Isotopic analysis

The stable isotopes ( $\delta^2\text{H}$  and  $\delta^{18}\text{O}$ ) analysis was carried out by using a Dual Inlet Isotope Ratio Mass Spectrometer (IRMS) (GV, Instruments, U.K<sup>®</sup>). The  $\delta^{18}\text{O}$  analysis was done with the  $\text{CO}_2$  equilibrium method (Epstein & Mayeda, 1953), whereas  $\delta^2\text{H}$  was done using hydrogen gas to equate in the presence of platinum catalysis. The analyses were standardized using a triple point

calibration with the international references viz. Vienna-Standard Mean Ocean Water (V-SMOW) and Greenland Ice Sheet Project (GISP). The analytical accuracy of the instrument for  $\delta^2\text{H}$  was within  $\pm 1\text{‰}$  and for  $\delta^{18}\text{O}$  within  $\pm 0.1\text{‰}$ . In the water samples, isotopic ratios are calculated to VSMOW and expressed in parts per mil (‰), shown in the following equation;

$$\delta = \left( \frac{R_{\text{sample}}}{R_{\text{VSMOW}}} - 1 \right) * 1000 \quad \text{‰ VSMOW}$$

Where  $R_{\text{sample}}$  is the ratio of  $^{18}\text{O}/^{16}\text{O}$  or  $^2\text{H}/^1\text{H}$  of groundwater and river water samples, and  $R_{\text{VSMOW}}$  is the corresponding ratio for Vienna Standard Mean Standard Ocean Water. The average precision for the seven times repeated measurement was less than  $\pm 0.1\text{‰}$  for  $\delta^{18}\text{O}$  and  $\pm 1.0\text{‰}$  for  $\delta^2\text{H}$ .

The local meteoric water line (LMWL), Patna (Kumar et al., 2010) and global meteoric water line (GMWL) (Craig, 1961) were used to delineate the source of groundwater recharge in the study area. The equation for both LMWL and GMWL are as follow:

$$\delta^2\text{H} = 7.76 (\pm 0.66) * \delta^{18}\text{O} + 3.02 (\pm 7.43) \quad (r^2 = 0.98) \quad [\text{LMWL, Patna}] \quad (5.1)$$

$$\delta^2\text{H} = 8 * \delta^{18}\text{O} + 10 \quad [\text{GMWL}] \quad (5.2)$$

The slop of the local meteoric water line was close to the GWML.

### 5.3. Results and discussion

#### 5.3.1. Solute chemistry and isotopes signature

The statistics of the physicochemical parameter of the groundwater and river water samples has been shown in table 5.1. Box-whisker plots were plotted (Figure 5.1) to display the overall reaction patterns of the groundwater and river water samples. BOX-whisker plots are useful tools to visualize the range and other functionalities of interactions for a large group of samples. Box-whisker plots (Figure 5.1) offer additional details for each physicochemical parameter from top to bottom, such as; outliers, maximum, whisker upper, quartile upper (75), median (50), quartile lower (25), whisker lower and minimum. The mean concentration of  $\text{HCO}_3^-$  was reported higher in YA groundwater (461.04 mg/L) compare to OA groundwater (421.33 mg/L) and river water (205.02 mg/L) respectively. A similar trend was also reported in calcium concentration. The average concentration of  $\text{Ca}^{2+}$  was reported higher in YA groundwater (90.83 mg/L) compared to the OA groundwater (50.23 mg/L) and river water (50.12 mg/L), respectively, indicated less

geochemical evolution in OA groundwater and river water (Kumar et al., 2019). The DOC concentration in older and younger alluvium groundwater was almost comparable and had a mean of 0.81 mg/L and 0.88 mg/L, respectively. The river water DOC was observed significantly very smaller than groundwater DOC. The average concentration of DOC in river water was 0.13 mg/L. The higher DOC in alluvial groundwater might be due to microbial activities (Akai et al., 2004; Shah, 2008).

Table 5.1: Physiochemical and isotopic composition of groundwater (Gorakhpur)

	Older Alluvium (n=24)	Younger Alluvium (n=42)	River Water (n=13)
<b>Depth (m)</b>			
Mean	30.87	30.49	-
Median	30.49	30.49	-
Range	21.34 to 36.59	15.24 to 45.73	-
<b>HCO<sub>3</sub> (mg/L)</b>			
Mean	421.33	461.04	205.02
Median	364.90	477.45	212.10
Range	98.71 to 1237.91	129.92 to 972.2	118.5 to 278.9
<b>Ca<sup>2+</sup> (mg/L)</b>			
Mean	50.23	82.84	50.12
Median	48.40	90.83	51.57
Range	12.69 to 129	20.94 to 191.78	30.75 to 71.04
<b>DOC (mg/L)</b>			
Mean	0.81	0.88	0.13
Median	0.57	0.51	0.12
Range	0.02 to 3.26	0.01 to 3.19	0.09 to 0.18
<b>δ<sup>18</sup>O (‰)</b>			
Mean	-6.81	-6.61	-4.93
Median	-6.58	-6.51	-5.28
Range	-10.13 to -3.99	-9.42 to -2.54	-7.26 to 2.04
<b>δ<sup>2</sup>H (‰)</b>			
Mean	-50.1875	-47.75	-30.89
Median	-50.50	-48.03	-31.26
Range	-67.45 to -33.5	-61.03 to -25.4	-48.15 to 11.34
<b>δ<sup>13</sup>C (‰)</b>			
Mean	-6.93	-8.43	-
Median	-7.22	-8.85	-
Range	-10.55 to -3.45	-13.18 to -5.67	-



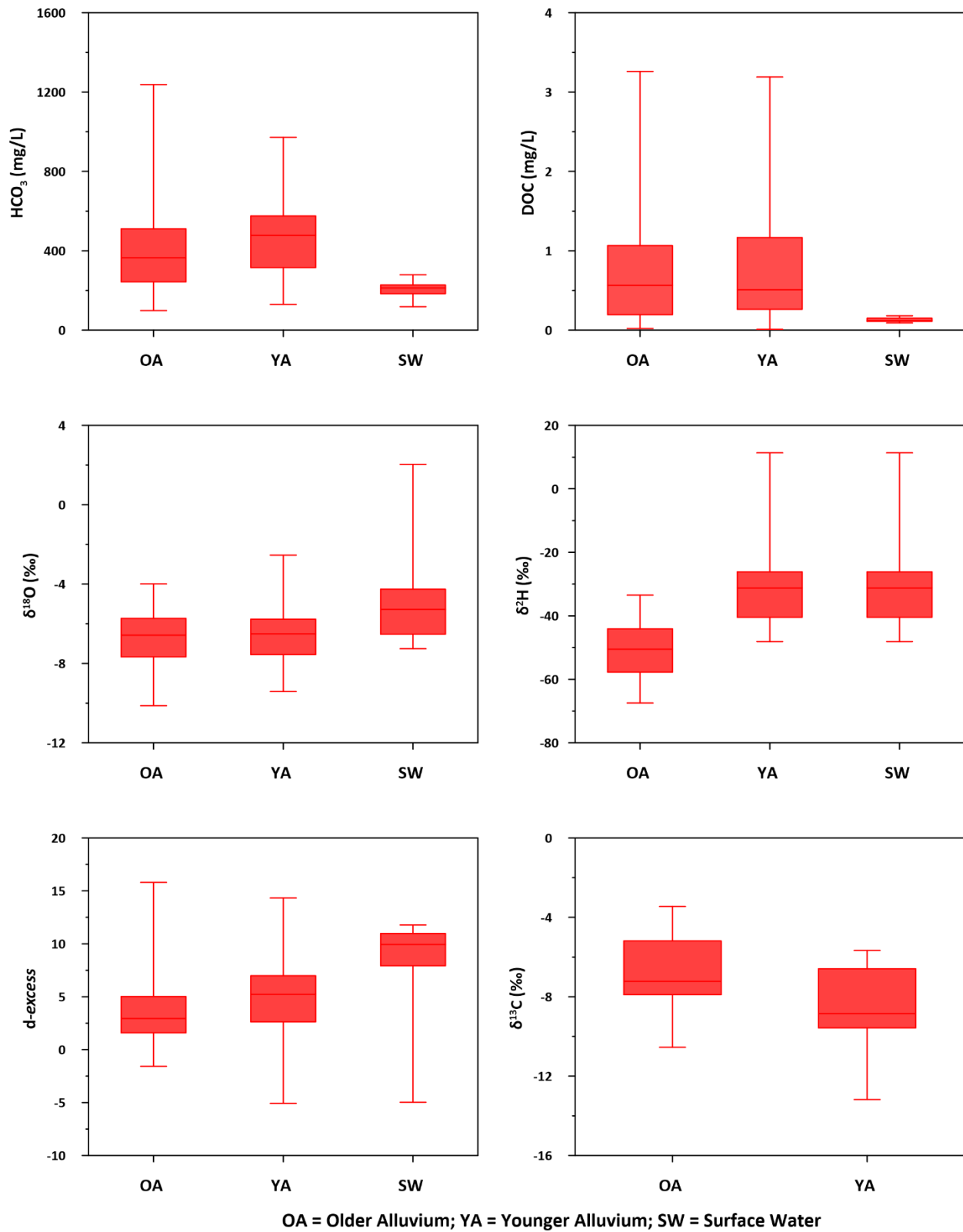


Figure 5.1: Box and Whisker plot of the selected parameters in different geomorphic setups (Gorakhpur)

The isotopic signature for oxygen isotope in groundwater and river water varied between -10.13 to -3.99‰, -9.42 to -2.54‰, and -7.26 to -4.20‰ respectively for OA groundwater, YA groundwater and river water sample. The isotopic value for hydrogen isotope varied from -67.45 to -33.5‰, -61.03 to -25.4‰ and -48.15 to -22.62‰ in OA, YA and River water, respectively. The water sample collected from Ramgarh lake shows the higher value of isotopic signature reported  $\delta^{18}\text{O}$  (2.04‰) and  $\delta^2\text{H}$  (11.34‰). The calculated *d-excess* for groundwater ranged from -1.58 to 15.8 ‰, -5.08 to 14.33‰ and 0.00 to 11.79‰ in OA, YA and river water. The *d-excess* value for Ramgarh Lake was reported -4.98‰ in the study area. A bivariate cross plot of  $\delta^{18}\text{O}$  and  $\delta^2\text{H}$  for groundwater and surface water samples were plotted with the following regression line equations:

$$\text{Older alluvium: } \delta^2\text{H} = 5.77 * \delta^{18}\text{O} - 10.87 \quad (r^2=0.95) \quad (5.3)$$

$$\text{Younger alluvium: } \delta^2\text{H} = 5.35 * \delta^{18}\text{O} - 12.36 \quad (r^2=0.95) \quad (5.4)$$

$$\text{River water: } \delta^2\text{H} = 6.39 * \delta^{18}\text{O} - 0.63 \quad (r^2=0.95) \quad (5.5)$$

The stable carbon isotopes ( $\delta^{13}\text{C}$ ) were ranged from -10.55 to -3.45‰ (mean -6.93‰) in OA groundwater while it ranged from -13.18 to -5.67‰ (mean -8.43‰) in YA groundwater. The narrow range of the carbon isotopes in OA groundwater might be due to low organic matter availability. A study from Samastipur, Bihar, reported a similar result (Kumar et al., 2019).

The statistical summary of the physicochemical parameters in study area 2 (Ghazipur) was given in table 5.2. Box-whisker plots were drawn for all the groundwater and river water samples (Figure 5.2) to display the overall reaction pattern in the study area.

The depth of the tube well in older alluvium ranged from 18.29 to 106.71 mbgl with the median of 36.59 mbgl; however, in younger alluvium, it varied from 24.39 to 54.88 mbgl. The concentration of  $\text{HCO}_3^-$  was ranged from 90.9 to 2173.4 mg/L (mean 774.2 mg/L) in OA groundwater and 98.52 to 2066 mg/L (mean 609.7 mg/L) in YA groundwater, respectively. The concentration of the  $\text{HCO}_3^-$  in river water was varied from 236 to 334 mg/L with a mean of 286.15 mg/L. The average relative concentration of  $\text{HCO}_3^-$  was very low in river water compare to groundwater. A piper diagram was plotted for the major ions to identify the water type in both the study areas. Figure 3.9 (chapter 3) showed that YA groundwater, approx. 90% samples were CaMg- $\text{HCO}_3$  type, 7% CaMg-Cl type and the remaining 3% NaCl type of water in the study area.

Similarly, in OA groundwater, ~95% of groundwater samples shown CaMg-HCO<sub>3</sub> type, and the remaining 5% Ca-Cl type of water was observed. Bicarbonated groundwater might be responsible for elevated As concentration in OA and YA groundwater. At higher pH, bicarbonate can release As from sediment in oxic and anoxic conditions (Anawar et al., 2004). Previous research in the central Gangetic plain has also revealed that elevated bicarbonate ions in groundwater influence hydrogeochemical evolution and enhance As and metal mobilization (Kumar et al., 2010; Verma et al., 2015; Kumar et al., 2018). Around 10% YA groundwater sample shown CaCl or NaCl type of water indicating oxidizing condition in the groundwater might also release As in groundwater.

Table 5.2: Physiochemical and isotopic composition of groundwater (Ghazipur)

	Older Alluvium (n=27)	Younger Alluvium (n=58)	River Water (n=13)
<b>Depth (m)</b>			
Mean	39.65	36.77	-
Median	36.59	36.58	-
Range	18.29 to 106.71	24.39 to 54.88	-
<b>HCO<sub>3</sub> (mg/L)</b>			
Mean	774.22	609.72	286.15
Median	745.40	517.16	285.00
Range	90.9 to 2173.4	98.52 to 2066	236 to 334
<b>Ca<sup>2+</sup> (mg/L)</b>			
Mean	106.93	86.59	48.82
Median	105.84	76.21	48.00
Range	18.87 to 295.33	20.95 to 251.72	35.27 to 58.08
<b>DOC (mg/L)</b>			
Mean	0.80	0.85	0.13
Median	0.55	0.52	0.13
Range	0.03 to 2.95	0.01 to 3.19	0.1 to 0.19
<b>δ<sup>18</sup>O (‰)</b>			
Mean	-6.87	-7.24	-5.31
Median	-6.98	-7.35	-5.25
Range	-10.14 to -2.95	-10.08 to -4.12	-7.56 to -3.29
<b>δ<sup>2</sup>H (‰)</b>			
Mean	-49.29	-51.07	-34.59
Median	-50.04	-51.80	-31.92
Range	-67.83 to -24.5	-68.35 to -33.45	-46.2 to -24.05
<b>δ<sup>13</sup>C (‰)</b>			
Mean	-6.06	-9.49	-
Median	-6.11	-9.85	-
Range	-9.66 to -3.06	-13.96 to -4.59	-

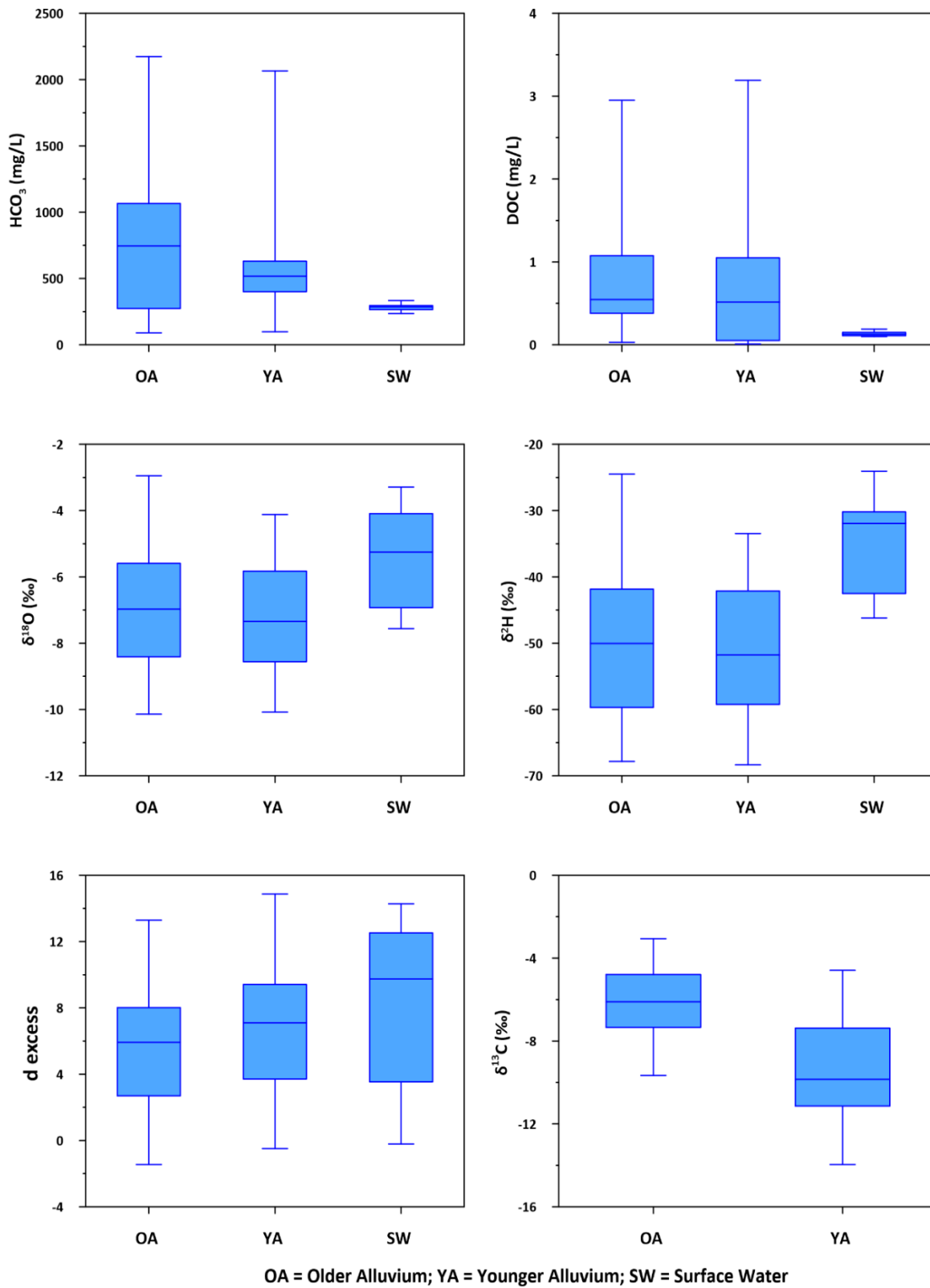


Figure 5.2: Box and Whisker plot of the selected parameters in different geomorphic setups in study area 2 (Ghazipur)

In study area 2 (Ghazipur), all the groundwater and surface water samples were Ca-HCO<sub>3</sub> dominated except one groundwater sample from the younger alluvium region. The individual piper plots for older alluvium, younger alluvium and surface water [figure 3.10](#) (chapter 3).

Ca in the groundwater of OA and YA varied from 18.87 - 295.33 mg/L (mean 106.93 mg/L) and 20.95 - 251.72 mg/L (mean 86.59 mg/L), respectively. The Ca concentration in the surface water was deficient and varied from 35.27 - 58.08 mg/L (mean 48.82 mg/L). The mean low relative concentration of Ca<sup>2+</sup> in YA groundwater and surface water might be due to less geochemical evolution ([Kumar et al., 2010](#); [Kumar et al., 2018](#)). The DOC concentration in OA groundwater was varied from 0.03 - 2.95 mg/L (mean 0.80 mg/L), which was almost comparable to the YA groundwater. The DOC concentration in the groundwater of YA was varied from 0.01 - 3.19 mg/L with a mean of 0.85 mg/L. The higher DOC in YA groundwater might be due to the bacterial metabolism of nutrients. In contrast, the DOC concentration in river water was observed very low, and it ranged from 0.1 - 0.19 mg/L with the mean of 0.13 mg/L. Published research has been revealed that high DOC was concentration found in the younger alluvium region, and microbial degradation of DOC and generate a reducing subsurface environment which enhanced As and metals mobilization in groundwater ([Akai et al., 2004](#); [Shah, 2008](#); [Kumar et al., 2018](#); [Yadav et al., 2020](#)).

The stable  $\delta^{18}\text{O}$  in the OA groundwater was varied from -67.83 to -24.5‰ (mean -6.87‰), and in YA groundwater, it varied from -10.08 to -4.12‰ (mean -7.24‰). The  $\delta^{18}\text{O}$  enrichment was observed in OA groundwater. The  $\delta^{18}\text{O}$  was highly enriched in river water compare to groundwater and varied from -7.56 to -3.29‰ with a mean of -5.31‰. The enrichment of stable isotopes in the river water indicates evaporation processes might be there. The stable  $\delta^2\text{H}$  in OA groundwater was varied from -67.83 to -24.05‰ (mean -49.29‰), and in YA groundwater, it varied from -68.35 to -33.45‰ (mean -51.07‰). The stable  $\delta^2\text{H}$  in river water was varied from -46.2 to -24.05‰ with a mean of -34.59‰. The enrichment of stable isotopes in the river water and OA groundwater suggested the evaporation effect might be high in river water followed by groundwater of OA.

A bivariate cross plot of  $\delta^{18}\text{O}$  and  $\delta^2\text{H}$  for OA and YA groundwater and river water samples were plotted with the following regression line equations:

$$\text{Older alluvium: } \delta^2\text{H} = 6.25 * \delta^{18}\text{O} - 6.3 \quad (r^2=0.98) \quad (5.6)$$

$$\text{Younger alluvium: } \delta^2\text{H} = 5.71 * \delta^{18}\text{O} - 9.71 \quad (r^2=0.97) \quad (5.7)$$

$$\text{River water: } \delta^2\text{H} = 4.83 * \delta^{18}\text{O} - 8.93 \quad (r^2=0.94) \quad (5.8)$$

The stable carbon ( $\delta^{13}\text{C}$ ) isotopes in the OA groundwater varies from -9.66 to -3.06‰ with the mean of -6.06‰ while in the groundwater of younger alluvium, it was ranged from -13.96 to -4.59‰.

### 5.3.2. Stable isotopic signature of water samples

The groundwater recharge in the central Gangetic plain could depend on several sources such as precipitation and surface water infiltration from lakes and rivers (Kumar et al., 2019). A bivariate plot of stable isotopic composition ( $\delta^2\text{H}$  and  $\delta^{18}\text{O}$ ) was constructed (Figure 5.5) to understand the groundwater recharge processes in the study area. Groundwater and river water samples were plotted along with the global meteoric water line (GMWL) and local meteoric water line (LMWL), Patna (Kumar et al., 2010), which was one of the nearest stations from our study area. The river water samples fell close to or below the GWML in the Gorakhpur district (Figure 5.3). In contrast, groundwater samples from both the geomorphic unit (older and younger alluvium) were clustered around the LMWL and below the GWML suggested aquifers get recharged from modern-day precipitation. The regression line equation for older alluvium and younger alluvium (Equation 5.3&5.4) represented negative slope and intercept than their LMWL, and GMWL (Equation 5.1&5.2) indicates the significant role of evaporative enrichment on groundwater sample.

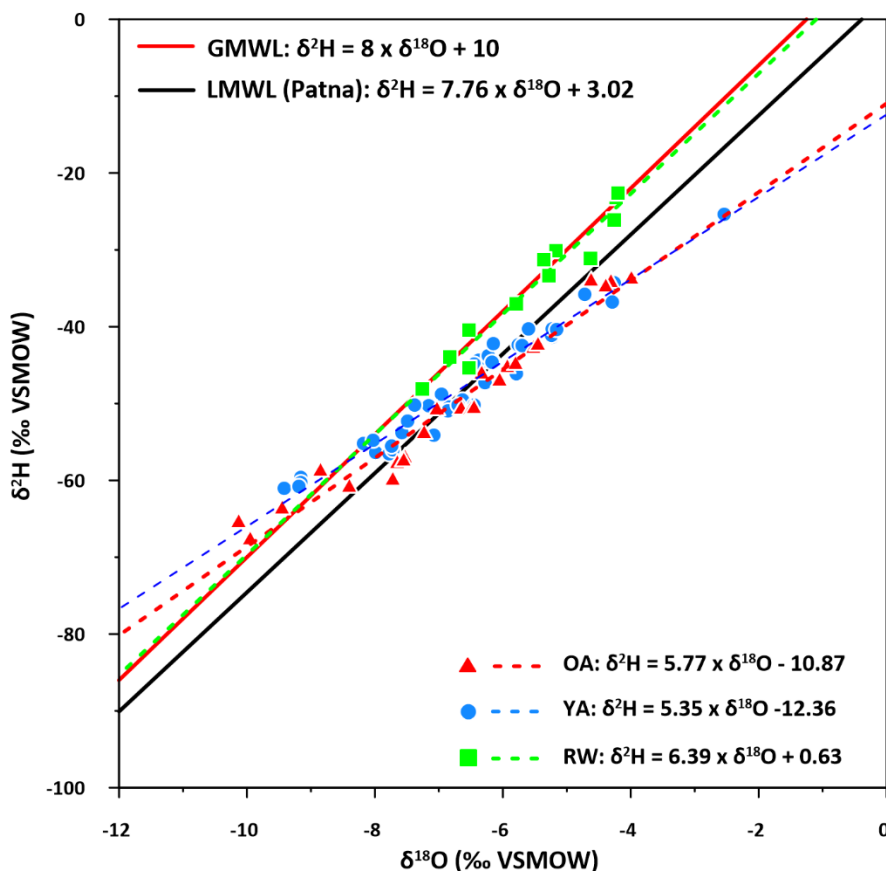


Figure 5.3: Bivariate plot of stable  $\delta^{18}\text{O}$  and  $\delta^2\text{H}$ , the Global Meteoric Waterline (GMWL) of Craig (1961) and Local Meteoric water line (LMWL) Patna (Kumar et al., 2010) in study area 1 (Gorakhpur)

In study area 1, around 55% of OA groundwater samples fall close to the GMWL and LMWL lines, while 45% fall below the GMWL and LMWL lines. Similarly, ~29% YA groundwater samples fall close to the GMWL and LMWL, while 71% of the YA groundwater samples fall below the GMWL and LMWL lines indicating precipitation recharge the groundwater with evaporation effect. The majority of the groundwater samples from OA and YA regions had lighter  $\delta^{18}\text{O}$  isotopes and fall close to the LMWLs, indicating local precipitation plays a significant role in groundwater recharge, followed by the evaporation effect. From figure 5.3, a considerable variation in the isotopic signature was reported in river water samples of Ghaghara and its tributaries, indicating different recharge sources to the river water. The isotopic composition of river water showed variation with the surrounding groundwater, indicating large differences in hydraulic conductivity and much less recharge from the river water except few locations.

Four groundwater samples (A4, A16, A27 and A35, data set attached in the last of this chapter) from the studied area 1 shown virtual isotopic signature with the Rapti river water indicating good hydraulic conductivity and help the aquifer to get recharged from the river. A surface water sample (A78) was collected from a stagnant lake (Ramgarh) and enriched with isotopic composition of  $\delta^{18}\text{O}$  and  $\delta^2\text{H}$  indicates evaporation significantly influences the recharging processes of the lake. Several stable isotopic studies have been documented that ponds do not contribute to the recharge and mixing of organic matter to the groundwater of West Bengal (McArthur et al., 2004; Sengupta et al., 2008; Datta et al., 2011; Richards et al., 2018; Kumar et al., 2019). However, several studies have augmented the above results and reported pond recharging the aquifer system and contributing OC to the arsenic-affected water's shallow water (Harvey et al., 2006; Neumann et al., 2010; Richards et al., 2018; Das & Pal, 2020). The isotopic record shows the rainfall significantly recharges the perennial pond during the highest monsoon season. In study area 1, the connectivity of pond water to groundwater was almost negligible, thus indicating less probability of moving OC from ponds to groundwater. Few groundwater samples from the younger alluvium close to the River Rapti proximities showed similarities in isotopic composition that specify the potential of local groundwater recharge from the river.

The isotopic parameters ( $\delta^{18}\text{O}$  and  $\delta^2\text{H}$  and *d-excess*) were plotted (Figure 5.4) against the depth to understand the role of interconnectivity from the top shallow aquifer to the principal confined aquifer of the study area. From the depth plot (Figure 5.4a), it was clear that shallow aquifers were highly negative in OA and YA. However, increasing the aquifer's depth, groundwater gets enriched with stable isotopes indicating less hydraulic connectivity between the shallow and deeper aquifer of the study area. Few groundwater samples of OA and YA showed almost similar depth and the  $\delta^{18}\text{O}$  values indicating good hydraulic connectivity exist between these samples. The depth vs. *d-excess* plot (Figure 5.4c) showed that some deeper tube wells formed a cluster. The *d-excess* value of the cluster samples was equal to or more than 10, indicating that aquifers get recharged mainly during the monsoon season before evaporation in summer. The closeness to the paths and their intercepts showed tight interlinkages between the shallow aquifer and the middle aquifers of the upper Gangetic basin (Kumar et al., 2019; Kumar et al., 2018). So the above results inferred that the hydraulic connectivity between the shallow aquifer and deeper aquifer is very weak. However, shallow aquifer and upper shallow aquifer in OA and YA indicate



good hydraulic connectivity in the study area. A similar observation has been reported in the central Gangetic basin (Kumar et al., 2019; Saha et al., 2011).

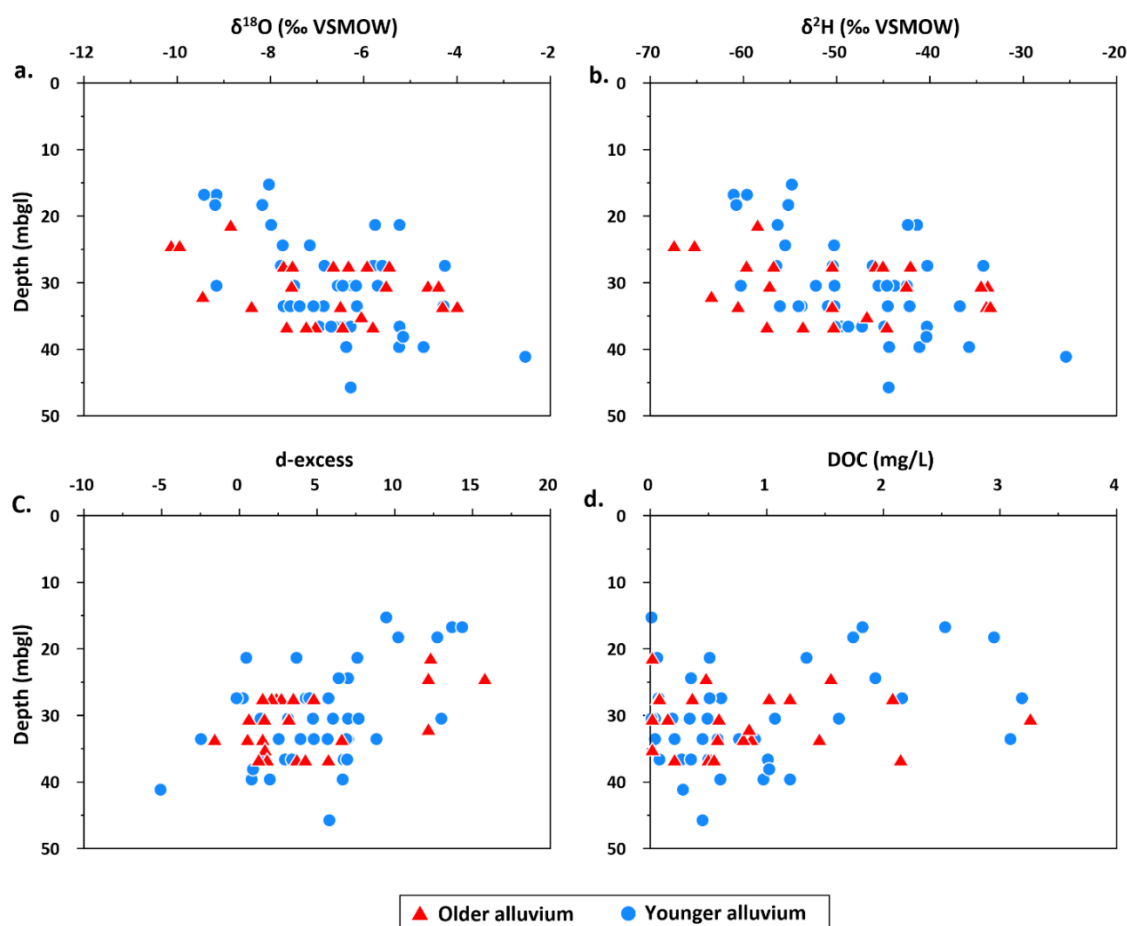


Figure 5.4: Vertical variation (depth-wise) of isotopic species in Gorakhpur district

The bivariate plot of  $d\text{-excess}$  and  $\delta^{18}\text{O}$  was plotted in study area one (Figure 5.5). A reverse correlation was found between the  $d\text{-excess}$  and  $\delta^{18}\text{O}$ . The shallow aquifer in OA and YA showed higher  $d\text{-excess}$  ( $>10$ ), indicating source water has been derived from higher Himalaya and provide additional evidence of groundwater recharge through redistribution of Rapti river and their tributaries (Rai et al., 2014; Joshi et al., 2018; Kumar et al., 2019).

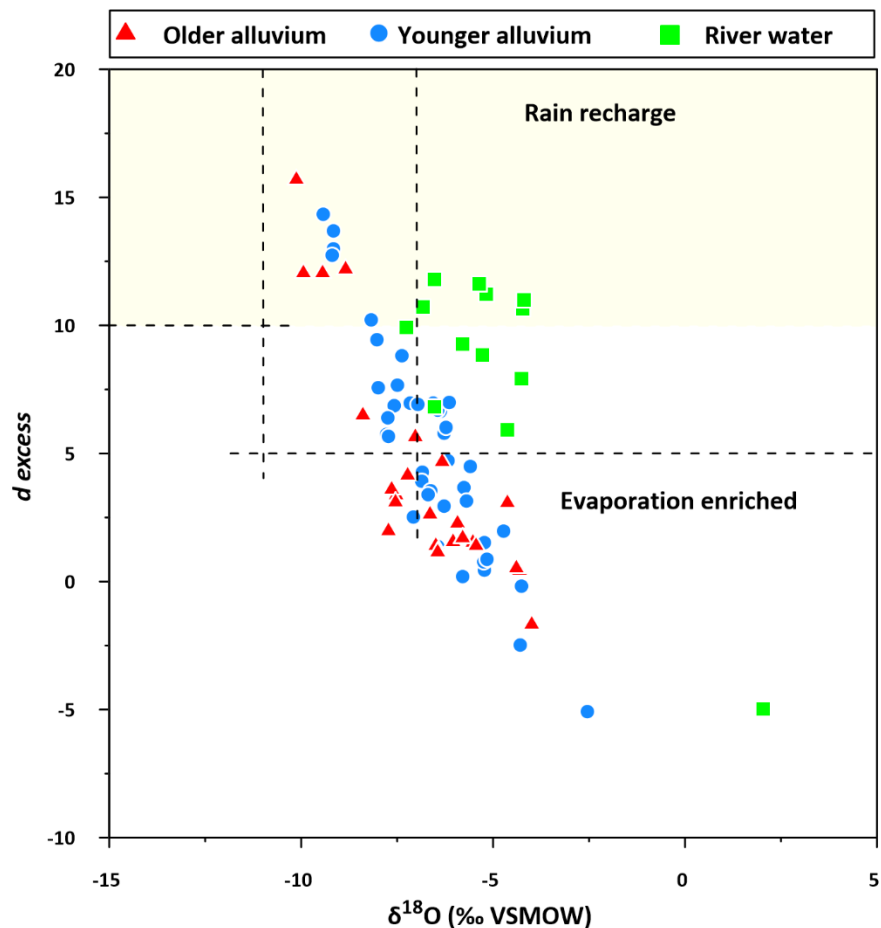


Figure 5.5: The evaporation plot between  $d$ -excess and  $\delta^{18}O$

In study area 2 (Ghazipur), a plot between stable isotopic  $\delta^2H$  and  $\delta^{18}O$  was constructed (Figure 5.6) to identify the major processes behind the groundwater recharge in the study area. All the samples were plotted along the GMWL and LMWL, Patna (Kumar et al., 2010). The plot showed that 62% of river water samples fell close to the GMWL, while the remaining 38% of river water samples fell close to the LMWL line (Figure 5.6). However, all the groundwater samples from the geomorphic setups were clustered around GMWL and LMWL, indicating aquifers get recharged from modern-day precipitation. The regression line equation for OA and YA (Equation 5.3&5.4) represented a negative slope with a smaller intercept indicating the evaporation effect on the groundwater samples.

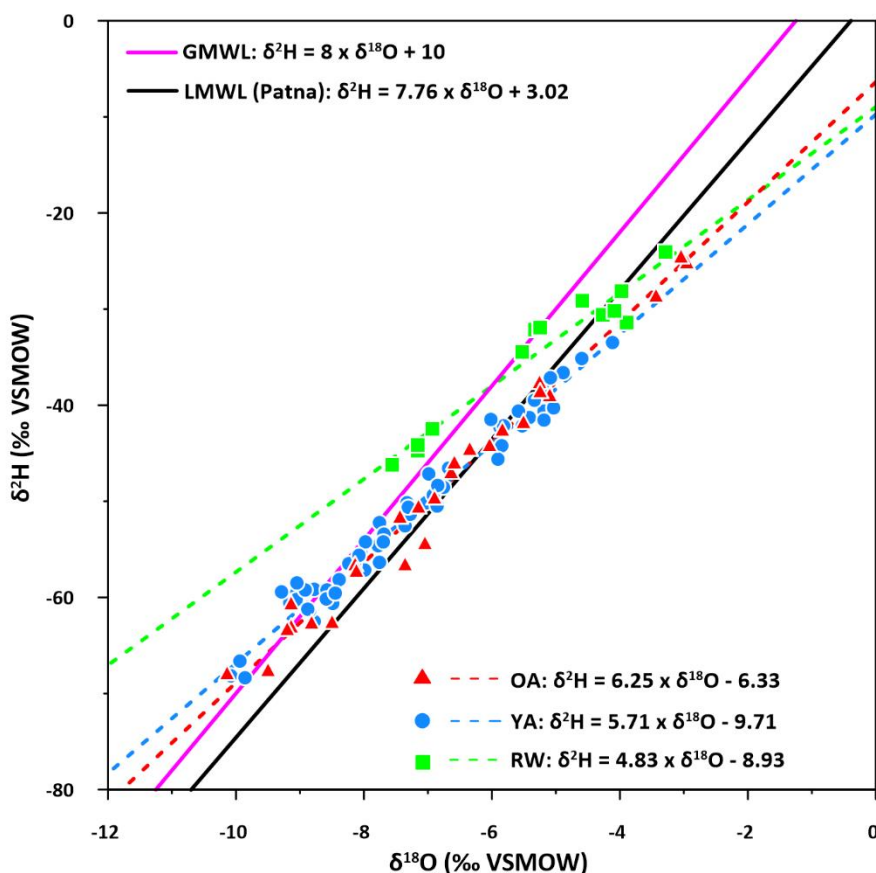


Figure 5.6: Bivariate plot of stable  $\delta^{18}\text{O}$  and  $\delta^2\text{H}$  for Ghazipur, the Global Meteoric Waterline (GMWL) of Craig (1961) and Local Meteoric water line (LMWL) Patna (Kumar et al., 2010)

The groundwater samples contained lighter  $\delta^{18}\text{O}$  isotopes in older and younger alluvium that fall close to the LMWL line, indicating precipitation plays a significant role in groundwater recharge followed by evaporation. A considerable variation was observed between the isotopic values of river water and its surrounding groundwater, indicating the contribution of river water to the groundwater recharge is significantly less in the study area.

Few groundwater samples (B9, B27, B49, B56 and B62) with similar isotopic values of its surrounding river water samples indicate good hydraulic connectivity between river and groundwater and the aquifer might get local recharge from the Ganga river. River water collected from the study area was highly enriched with isotopic signatures ( $\delta^{18}\text{O}$  and  $\delta^2\text{H}$ ), indicating the extensive role of evaporation on groundwater.

The isotopic signatures ( $\delta^{18}\text{O}$  and  $\delta^2\text{H}$ ), *d-excess* and DOC were plotted (Figure 5.7) with depth to understand the role of interconnectivity between the top shallow aquifer and main (deeper) aquifer of the study area (Kumar et al., 2019).

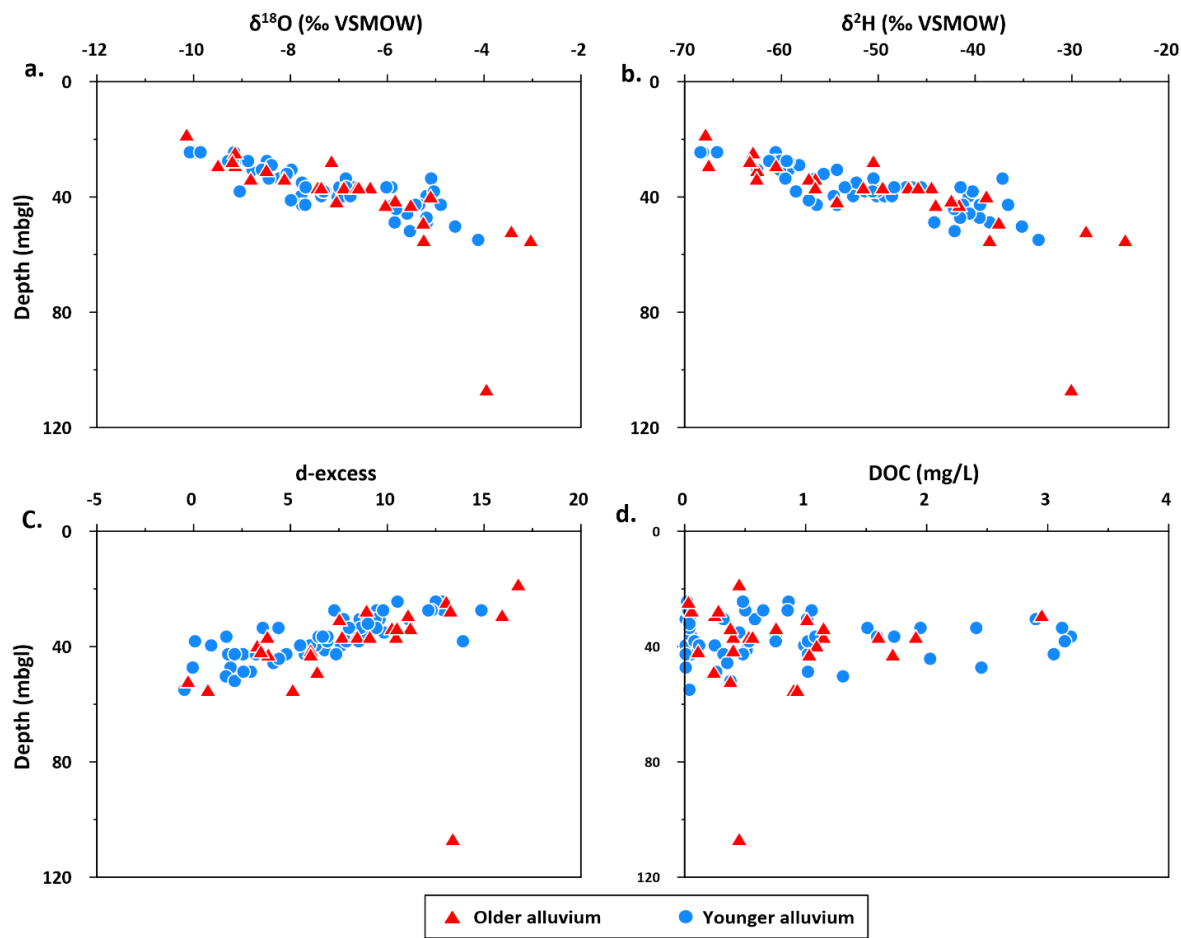


Figure 5.7: Vertical variation of isotopic species in the study area (Ghaziipur)

Scattered depth plot (Figure 5.7) showed that shallow aquifer was highly negative in both the geomorphic setups; however, increasing aquifer's depth, groundwater get enriched with isotopic compositions.

The bivariate plot (Figure 5.7c), depth vs. *d-excess*, showed that shallow aquifers were enriched with *d-excess* in the groundwater, indicating the groundwater getting recharged from local rain; however, evaporation processes significantly involved in the aquifer system. The closeness to the paths and their intercepts showed tight interlinkages between shallow and middle depths aquifers from the upper Gangetic basin (Kumar et al., 2019; Kumar et al., 2018).

Therefore, the above findings suggested that the hydraulic connectivity between the shallow aquifers and deeper aquifers is limited. A similar type of observation was observed in study area 1 (Gorakhpur) and several other studies from the central Gangetic basin (Kumar et al., 2019; Saha et al., 2011). But furthermore, a tritium isotope study is required to understand the groundwater age, recharge, and local evidence of isotopic behavior.

A bivariate plot of  $d$ -excess and  $\delta^{18}\text{O}$  was plotted (Figure 5.8) to identify the source of groundwater recharge in the study area and an opposite correlation was observed between them. Only one sample was collected from a deeper aquifer ( $\sim 106$  mbgl).

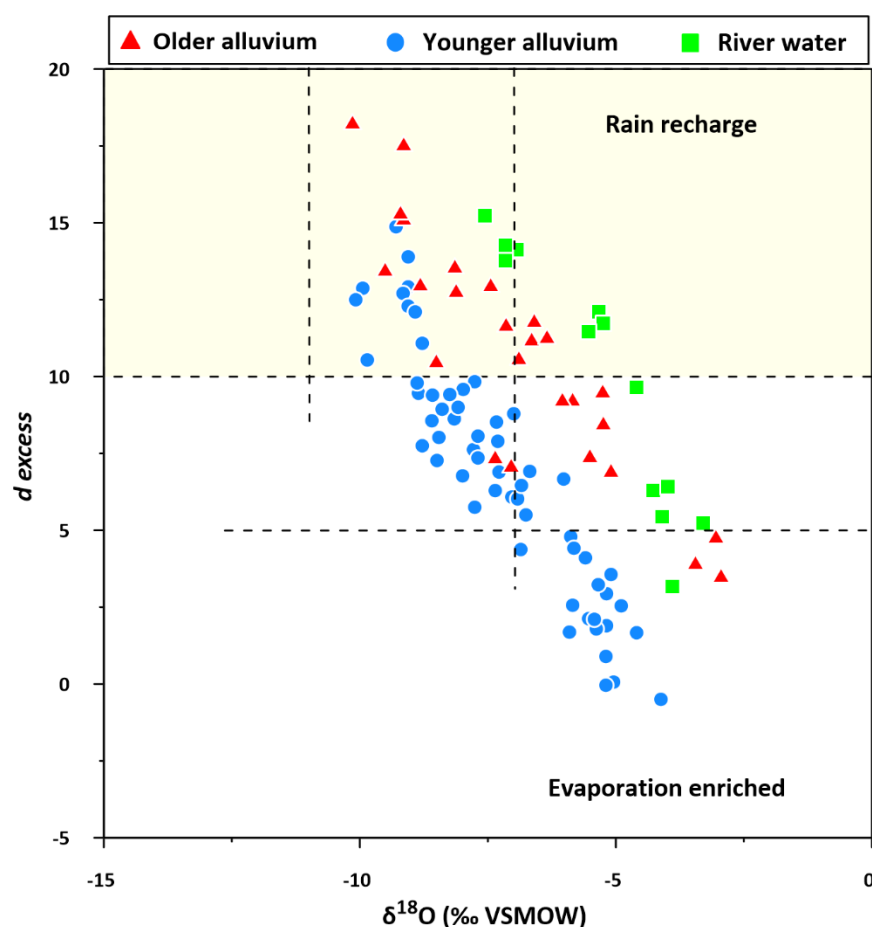


Figure 5.8: The evaporation plot between  $d$ -excess and  $\delta^{18}\text{O}$

The deeper aquifer having higher  $d$ -excess ( $>10$ ) indicates the source of water has been derived from the Himalayan region during the time and provide additional evidence of groundwater recharge through redistribution of the Ganga river in the study area (Rai et al., 2014; Joshi et al., 2018; Kumar et al., 2019). The shallow aquifer with a higher  $d$ -excess value indicates

the groundwater recharge mainly contributed by the local precipitation infiltration. According to an assessment of external water resources, monsoon rainfall accounts for around 80% of annual recharge (Saha & Sahu, 2016).

### 5.3.3. Sources of groundwater DIC, $pCO_2$ and $\delta^{13}C$

The  $pCO_2$  was observed higher than 10000 in the groundwater of OA and YA except for a few. However,  $pCO_2$  in river water was observed between 2000 to 10000 except for two samples from the Ghazipur district.

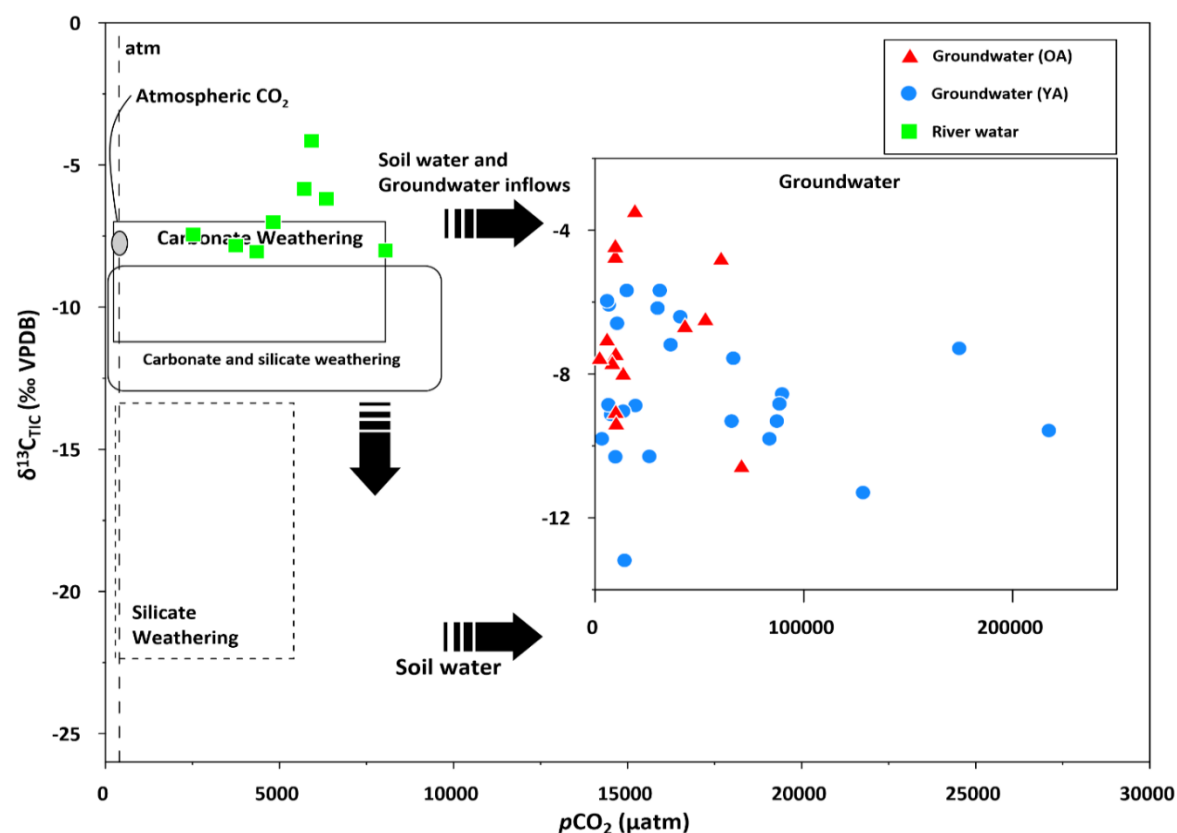


Figure 5.9: Variation between  $\delta^{13}C_{TIC}$  and  $pCO_2$ . Boxes show  $\delta^{13}C_{TIC}$  and  $pCO_2$  for DIC derived from various potentials discussed above. The dotted line (atm.) expressed atmospheric  $CO_2$  around 410 ppm. The Arrow line shows the expected processes and changes in the Gorakhpur district. Figure adapted from (Telmer & Veizer, 1999; Li et al., 2019)

The source of DIC in the groundwater was predominantly by aquifer recharge. Carbonate dissolution in the study area was mainly governed by carbonic acid ( $H_2CO_3$ ), formed by the  $CO_2$  available in the soil rather than the atmosphere. The higher  $pCO_2$  in groundwater was derived from microbial respiration and plant degradation (Doctor et al., 2008; Li et al., 2019). The DIC varied

from 1.81 to 33.59 mM (mean 7.96) in OA groundwater, while it varied from 2.35 to 27.60 mM (mean 11.48) in YA groundwater. The DIC in river water was varied from 2.14 to 5.21 mM with a mean of 3.92 mM. From figure 5.9, it was observed that groundwater of OA and YA were derived from both carbonate and silicate weathering.

The DIC in the river water samples was very low compared to groundwater of OA and YA. In study area 2 (Ghazipur), DIC varied 1.61 to 74.70 mM with a mean of 17.98 mM in OA groundwater while it varied from 1.83 to 58.41 mM with a mean of 10.10 mM in YA groundwater. The DIC concentration in river water was varied from 4.44 to 11.24 mM with a mean of 6.18 mM. A high DIC in YA groundwater was indicating silicate weathering followed by carbonate dissolution (Figure 5.10).

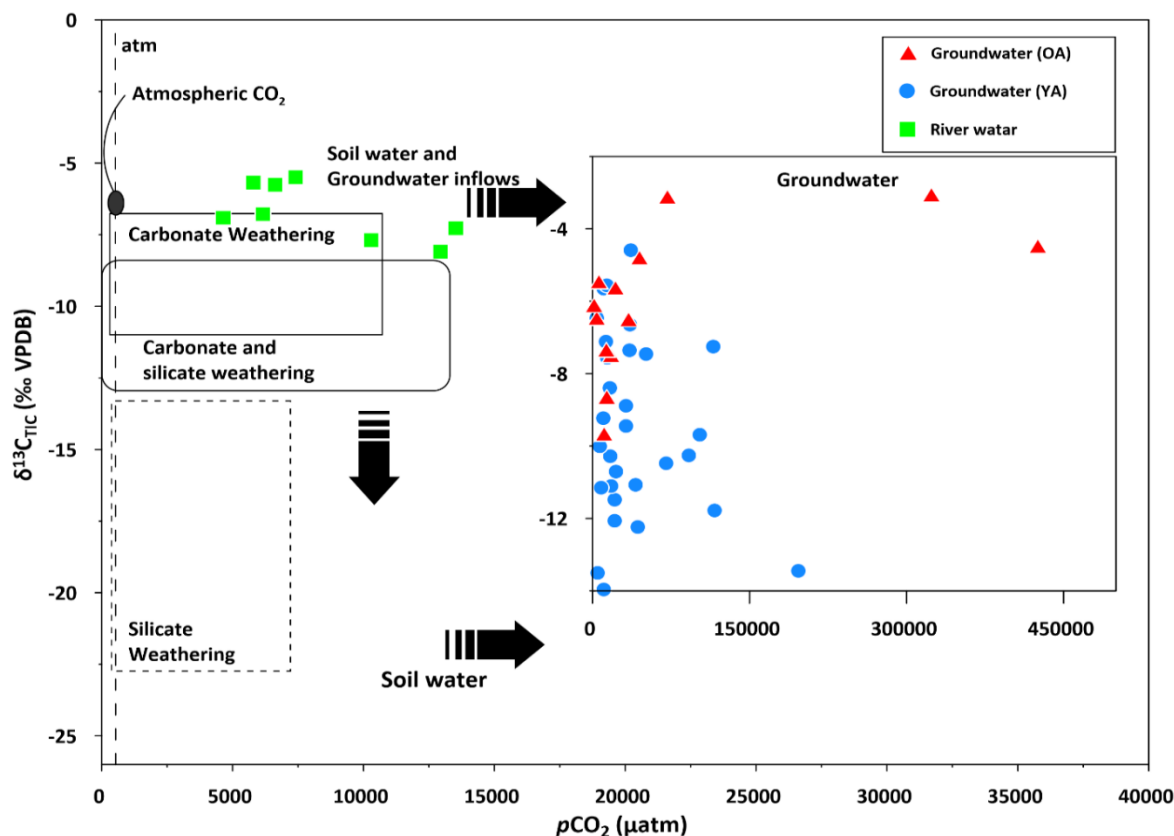


Figure 5.10: Variation between  $\delta^{13}C_{TIC}$  and  $pCO_2$ . Boxes show  $\delta^{13}C_{TIC}$  and  $pCO_2$  for DIC derived from various potentials discussed above. The dotted line (atm.) expressed atmospheric  $CO_2$  around 410 ppm. The Arrow line shows the expected processes and changes in the Ghazipur district. Figure adapted from (Telmer & Veizer, 1999; Li et al., 2019).

### 5.3.4. Interrelationship among stable isotopes and physicochemical parameters

To better understand the significance of various processes regulating DOC and DIC origin and source identification, bivariate plots of stable carbon isotopes ( $\delta^{13}\text{C}_{\text{TIC}}$ ) with other parameters like ORP, DOC, DIC and  $\text{HCO}_3^-$  were plotted (Figure 5.11). The relationship between the isotopic composition and ORP was moderate and  $\delta^{13}\text{C}_{\text{TIC}}$  was negatively correlated with ORP in the groundwater of OA, indicating microbial degradation at moderate temperature in the study area (Hornibrook et al., 2000; Kumar et al., 2019). However, in younger alluvium, two clusters were formed. Cluster one was positively correlated with  $\delta^{13}\text{C}_{\text{TIC}}$ , indicating rock water interaction in the subsurface soil. In contrast, cluster two was negatively correlated with  $\delta^{13}\text{C}_{\text{TIC}}$ , indicating microbial degradation at moderate temperature and generate reducing conditions in the study area 2.

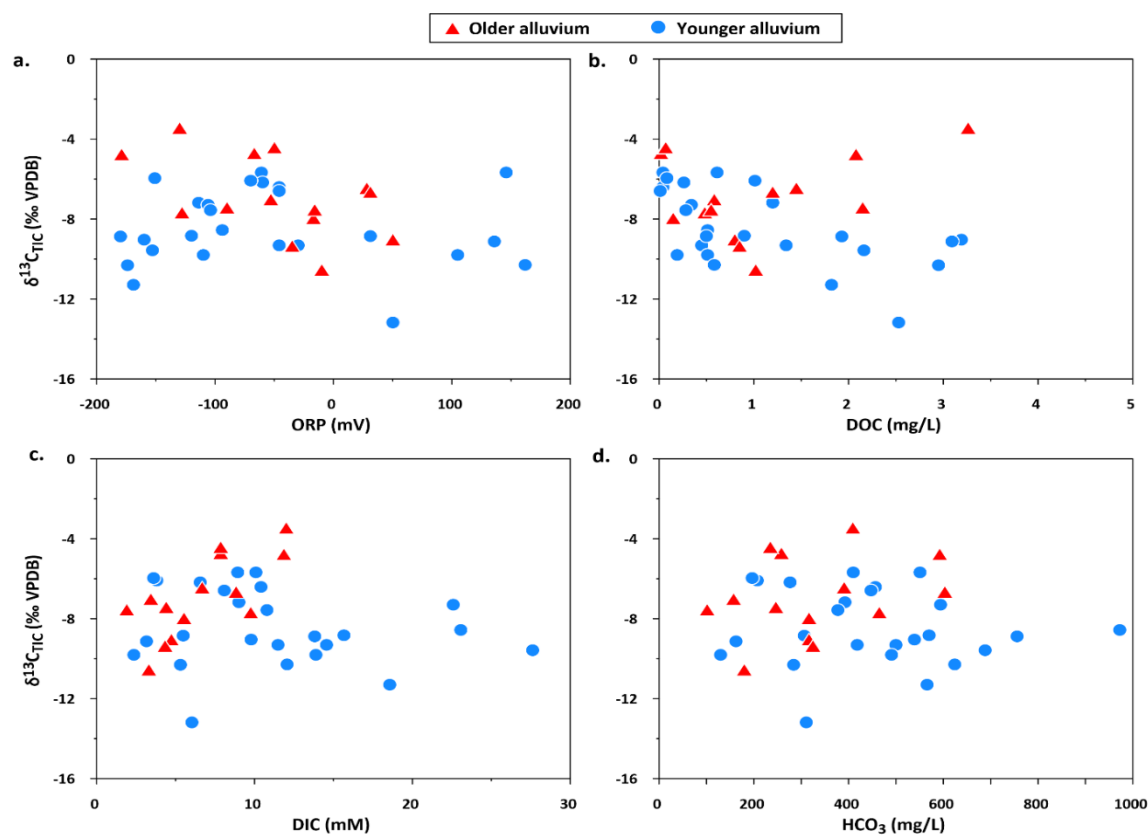


Figure 5.11: Bivariate plots of (a)  $\delta^{13}\text{C}_{\text{TIC}}$  vs. ORP, (b)  $\delta^{13}\text{C}_{\text{TIC}}$  vs. DOC, (c)  $\delta^{13}\text{C}_{\text{TIC}}$  vs. TIC, (d)  $\delta^{13}\text{C}_{\text{TIC}}$  vs.  $\text{HCO}_3^-$  in study area 1 (Gorakhpur).

The DOC concentration in the groundwater of older and younger alluvium was almost similar however, the mean value of the DOC in surface water was very low (0.13 mg/L). The



bivariate plot between  $\delta^{13}\text{C}_{\text{TIC}}$  and DOC was plotted in figure (5.1b). The plot showed that DOC concentration in the YA groundwater decreased with the  $\delta^{13}\text{C}_{\text{TIC}}$ , while in OA groundwater, there was no significant correlation observed. The shallow aquifer in the study area was enriched with carbon isotopes due to kankar ( $\text{CaCO}_3$  nodules) in the central Gangetic basin, coupled with high  $p\text{CO}_2$  (Kumar et al., 2019). A scattered plot (Figure 5.11d) indicates  $\text{HCO}_3^-$  was positively correlated with  $\delta^{13}\text{C}_{\text{TIC}}$  in older alluvium; however, no distinct correlation was observed in the groundwater of younger alluvium. The positive trend in older alluvium indicating biogenic carbon dioxide attribute to depleted  $\delta^{13}\text{C}_{\text{TIC}}$  with increasing  $\text{HCO}_3^-$  in older alluvium. The above trend is also supported by DOC (Figure 5.11b), which was positively correlated with the groundwater of older alluvium; however, in the groundwater of younger alluvium, an insignificant correlation was observed.

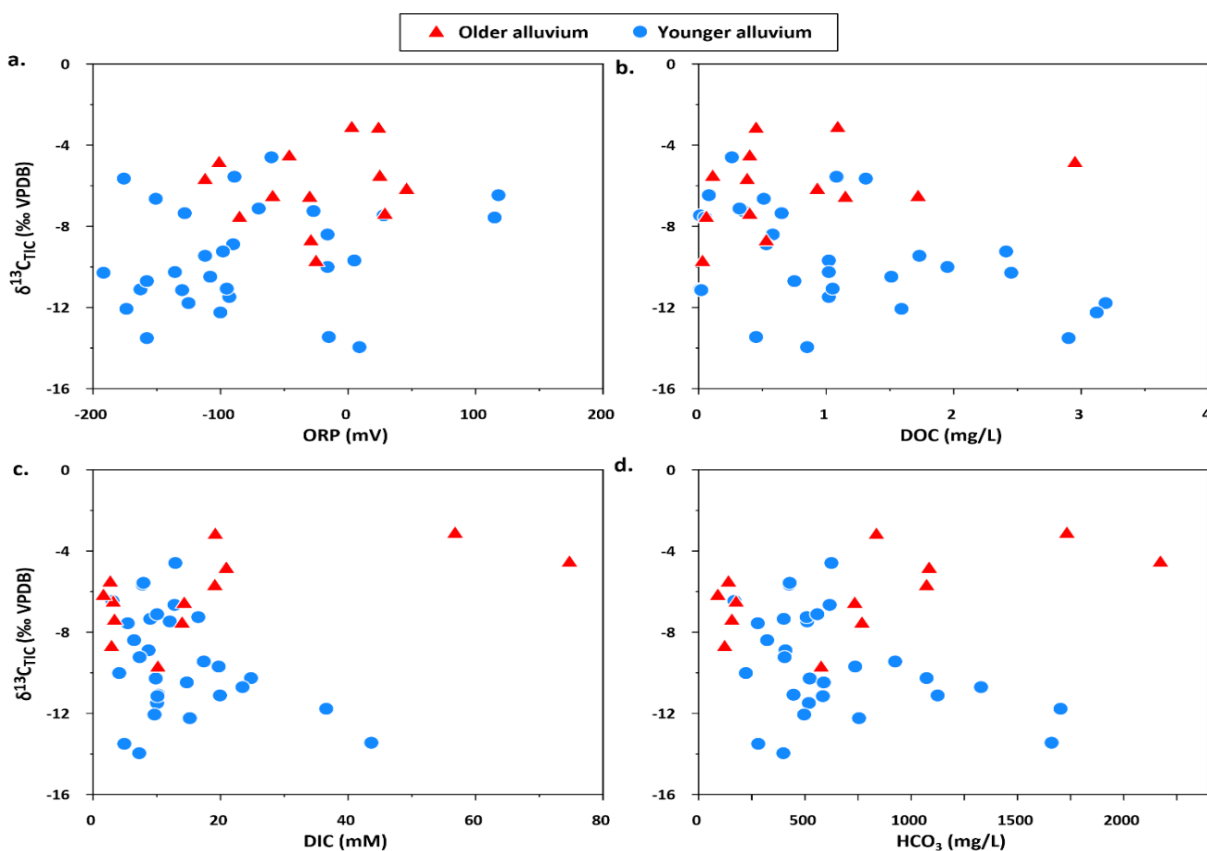


Figure 5.12: Bivariate plots of (a)  $\delta^{13}\text{C}_{\text{TIC}}$  vs. ORP, (b)  $\delta^{13}\text{C}_{\text{TIC}}$  vs. DOC, (c)  $\delta^{13}\text{C}_{\text{TIC}}$  vs. Ca, (d)  $\delta^{13}\text{C}_{\text{TIC}}$  vs.  $\text{HCO}_3^-$ , study area 2 (Ghazipur).

In the study area 2 (Ghazipur), bivariate scattered plots were plotted between  $\delta^{13}\text{C}_{\text{TIC}}$  with other chemical parameters like ORP, DOC, DIC and  $\text{HCO}_3^-$  to identify the various

hydrogeochemical processes regulating the origin and source of DOC and DIC in the study area. In study area 2, a similar trend was observed, like in study area 1.

The plot between  $\delta^{13}\text{C}_{\text{TIC}}$  and ORP (Figure 5.12a) showed an insignificant correlation observed in the groundwater of OA. However, in groundwater of YA, a moderate positive correlation was observed (Figure 5.12a), indicating microbial degradation might be the governing process of carbon in the groundwater (Hornibrook et al., 2000; Kumar et al., 2019). The scatter plot between  $\delta^{13}\text{C}_{\text{TIC}}$  and DOC (Figure 5.12b) showed an inverse relationship indicating DIC derived from the dissolution of the carbonate rocks. The DIC concentration in groundwater is pH-dependent, and at pH 6.4 to 8.3, the DIC in water is mainly derived from bicarbonate (Li et al., 2019). Thus,  $\text{HCO}_3^-$  was the major species of DIC in the groundwater of the study area. A scattered plot between  $\delta^{13}\text{C}_{\text{TIC}}$  and  $\text{HCO}_3^-$  (Figure 5.12d) showed  $\text{HCO}_3^-$  and  $\delta^{13}\text{C}_{\text{TIC}}$  was positively correlated in the groundwater of older alluvium while negatively correlated in the groundwater of younger alluvium. The positive trend in older alluvium indicating biogenic carbon dioxide attributed to depleted  $\delta^{13}\text{C}_{\text{TIC}}$  with increasing  $\text{HCO}_3^-$  in older alluvium.

#### 5.4. Conclusions

The groundwater chemistry was mainly governed by rock-water interaction, ion exchange and reverse ion exchange in both the study areas. Bicarbonate was the dominant anion in the study areas, and it was 2-3 times higher in groundwater than the river water. The piper plot (study area 1) indicated Ca- $\text{HCO}_3$  type of water was dominated in the groundwater; however, alkaline earth metals with strong acid dominated in the river water. The piper plot for study area 2 indicated the Ca- $\text{HCO}_3$  type of water present in groundwater and river water samples. In study area one (Gorakhpur), the stable isotopic composition ( $\delta^2\text{H}$  and  $\delta^{18}\text{O}$ ) represented that river water recharging from meteoric water and groundwater of older and younger alluvium regions. Aquifers recharged from local meteoric water undergo evaporation at few locations. The groundwater connectivity to the pond water in the study area was almost negligible, indicating less probability of organic carbon movement from ponds to groundwater. Thus arsenic mobilization process was restricted between pond and groundwater.

In study area 2 (Ghazipur), river water gets recharged from meteoric water followed by evaporation, while groundwater recharge from local induced meteoric water undergoes evaporation at a few locations. The  $\delta^{13}\text{C}_{\text{TIC}}$  was observed higher in younger alluvium than older and river water of both the study area.  $\delta^{13}\text{C}_{\text{TIC}}$  vs.  $p\text{CO}_2$  indicated carbonate and silicate dissolution was the major source of DIC in the groundwater of both the study area. Higher  $\delta^{13}\text{C}_{\text{TIC}}$  and associated with low TOC indicating microbial activity was enhanced in the Central Gangetic plain. The deeper aquifer of younger and older alluvium zones had lighter isotopes ( $\delta^{13}\text{C}_{\text{TIC}}$ ) because of low microbial activity.

Even though our study area was large, we have to collect samples on a seasonal basis to understand the groundwater sources, particularly in groundwater infiltration aspects. This study has not considered any microbiological experiments; therefore, future studies may incorporate microbial aspects to understand the processes in a better way.

## 5.5. Supplementary material

Table 5.3: Groundwater data collected in Gorakhpur district. (Note: depth expressed in meter,  $HCO_3$ , Ca and DOC in mg/L and isotopic signature expressed in (‰)).

Sp. No.	Geomorphic unit	Latitude	Longitude	Depth	$HCO_3$	Ca	DOC	$\delta^{18}O$	$\delta^2H$	d- excess	$\delta^{13}C$
A1	YA	26.759	83.327	21.34	418.20	101.78	1.34	-5.23	-41.40	0.44	-9.31
A2	YA	26.740	83.351	21.34	972.20	133.80	0.51	-5.76	-42.40	3.68	-8.56
A3	YA	26.717	83.330	45.73	475.30	86.78	0.45	-6.28	-44.45	5.79	-
A4	YA	26.705	83.388	27.44	409.70	41.78	0.61	-6.84	-50.45	4.27	-5.67
A5	YA	26.699	83.389	39.63	418.00	60.83	0.97	-5.24	-41.14	0.78	-
A6	YA	26.691	83.395	39.63	392.60	60.83	1.20	-6.38	-44.40	6.64	-7.18
A7	YA	26.733	83.335	27.44	688.50	95.70	2.16	-5.79	-46.12	0.20	-9.57
A8	YA	26.740	83.330	21.34	543.60	93.68	0.06	-7.99	-56.34	7.58	--
A9	YA	26.740	83.309	16.77	565.80	96.75	1.82	-9.16	-59.60	13.68	-11.30
A10	YA	26.734	83.346	18.29	718.50	114.15	1.74	-8.18	-55.21	10.23	-
A11	YA	26.732	83.352	30.49	594.10	102.83	0.34	-9.16	-60.30	12.98	-7.29
A12	YA	26.717	83.356	27.44	329.60	86.18	0.07	-4.26	-34.26	-0.18	-
A13	YA	26.706	83.359	33.54	549.70	98.96	0.76	-6.16	-44.50	4.78	-
A14	YA	26.706	83.378	30.49	456.50	88.80	0.04	-6.23	-43.82	6.02	-6.41
A15	YA	26.707	83.385	15.24	209.60	30.83	0.01	-8.03	-54.80	9.44	-
A16	YA	26.697	83.417	36.59	276.20	25.64	0.26	-6.45	-44.90	6.70	-6.17
A17	YA	26.695	83.406	41.16	377.70	62.41	0.28	-2.54	-25.40	-5.08	-7.56
A18	YA	26.693	83.393	30.49	491.40	81.84	1.07	-5.70	-42.46	3.14	-
A19	YA	26.703	83.342	33.54	499.70	95.37	0.45	-6.86	-50.96	3.92	-9.31
A20	YA	26.693	83.357	33.54	577.50	106.43	0.20	-6.15	-42.20	7.00	-
A21	YA	26.693	83.366	27.44	490.80	92.86	0.51	-5.60	-40.30	4.50	-9.80
A22	YA	26.684	83.369	33.54	570.10	117.15	0.90	-4.29	-36.80	-2.48	-8.83
A23	YA	26.669	83.375	30.49	479.60	73.81	0.49	-6.56	-45.50	6.98	-
A24	YA	26.758	83.338	36.59	207.02	26.00	1.01	-5.23	-40.31	1.53	-6.08

A25	YA	26.752	83.350	24.39	755.99	191.78	1.93	-7.16	-50.30	6.98	-8.87
A26	YA	26.728	83.331	30.49	218.86	20.94	1.62	-6.17	-44.64	4.72	-
A27	YA	26.705	83.398	27.44	539.39	92.86	3.19	-7.78	-56.50	5.74	-9.03
A28	YA	26.699	83.400	39.63	404.16	50.66	0.60	-4.72	-35.80	1.96	-
A29	YA	26.693	83.406	16.77	310.58	82.37	2.53	-9.42	-61.03	14.33	-13.18
A30	YA	26.735	83.346	36.59	676.26	110.48	0.27	-6.28	-47.30	2.94	-
A31	YA	26.741	83.342	33.54	550.54	64.18	0.04	-7.72	-56.08	5.68	-5.67
A32	YA	26.739	83.328	38.11	651.04	132.20	1.02	-5.16	-40.40	0.88	-
A33	YA	26.736	83.355	33.54	623.74	100.82	0.58	-7.58	-53.78	6.86	-10.29
A34	YA	26.733	83.363	36.59	591.90	98.01	0.35	-6.63	-49.50	3.54	-
A35	YA	26.718	83.367	36.59	196.47	47.03	0.08	-6.96	-48.75	6.93	-5.96
A36	YA	26.705	83.370	33.54	582.05	93.66	0.21	-7.38	-50.23	8.81	-
A37	YA	26.707	83.389	18.29	283.74	96.50	2.95	-9.19	-60.79	12.73	-10.31
A38	YA	26.728	83.384	33.54	162.16	58.07	3.09	-7.08	-54.12	2.52	-9.13
A39	YA	26.698	83.428	30.49	129.92	24.98	0.19	-6.45	-50.23	1.37	-9.80
A40	YA	26.696	83.417	24.39	221.24	55.43	0.35	-7.74	-55.53	6.39	-
A41	YA	26.704	83.394	36.59	306.44	73.04	0.50	-6.70	-50.20	3.40	-8.85
A42	YA	26.712	83.343	30.49	447.44	111.13	0.01	-7.49	-52.25	7.67	-6.59
A43	OA	26.761	83.336	33.54	390.40	44.48	1.45	-4.31	-33.96	0.52	-6.45
A44	OA	26.756	83.339	21.34	1118.50	91.78	0.02	-8.85	-58.50	12.30	-
A45	OA	26.747	83.350	27.44	592.40	79.08	2.08	-6.33	-45.86	4.78	-4.77
A46	OA	26.701	83.471	27.44	393.80	39.28	0.36	-5.93	-45.06	2.38	-
A47	OA	26.700	83.462	30.49	316.70	36.90	0.15	-4.62	-33.80	3.16	-7.97
A48	OA	26.704	83.446	30.49	257.90	52.33	0.02	-4.39	-34.50	0.62	-4.72
A49	OA	26.709	83.454	30.49	502.60	58.95	0.59	-5.52	-42.54	1.62	-
A50	OA	26.704	83.436	27.44	234.50	52.33	0.07	-6.65	-50.49	2.71	-4.42
A51	OA	26.717	83.398	27.44	339.40	55.85	0.08	-7.72	-59.69	2.07	-
A52	OA	26.742	83.383	27.44	602.90	58.98	1.20	-7.53	-56.76	3.48	-6.65
A53	OA	26.714	83.439	33.54	681.10	63.57	0.87	-3.99	-33.50	-1.58	-
A54	OA	26.714	83.435	27.44	179.80	22.10	1.02	-5.45	-42.10	1.50	-10.55

A55	OA	26.762	83.347	33.54	316.63	31.50	0.80	-8.40	-60.60	6.60	-9.03
A56	OA	26.758	83.338	36.59	1237.91	129.00	0.52	-7.65	-57.50	3.70	-
A57	OA	26.769	83.351	30.49	409.17	79.99	3.26	-7.55	-57.20	3.20	-3.45
A58	OA	26.713	83.472	24.39	187.65	18.56	1.55	-10.13	-65.24	15.80	-
A59	OA	26.709	83.462	36.59	246.67	29.46	2.15	-7.03	-50.50	5.74	-7.43
A60	OA	26.703	83.457	33.54	157.34	22.86	0.58	-6.50	-50.50	1.50	-7.02
A61	OA	26.712	83.463	36.59	421.23	43.61	0.50	-7.23	-53.60	4.24	-
A62	OA	26.715	83.437	35.06	98.71	16.41	0.02	-6.05	-46.75	1.65	-
A63	OA	26.724	83.397	32.01	325.08	28.81	0.85	-9.45	-63.45	12.15	-9.36
A64	OA	26.753	83.390	36.59	535.04	71.95	0.21	-5.80	-44.60	1.80	-
A65	OA	26.725	83.438	24.39	465.09	65.10	0.48	-9.95	-67.45	12.15	-7.68
A66	OA	26.693	83.370	36.59	101.48	12.69	0.55	-6.45	-50.35	1.25	-7.54
A67	SW	26.776	83.243	-	196.90	59.04	0.09	-4.26	-26.15	7.93	-8.05
A68	SW	26.770	83.242	-	218.50	51.57	0.15	-4.23	-23.19	10.65	-
A69	SW	26.760	83.246	-	184.10	46.50	0.12	-5.17	-30.15	11.21	-
A70	SW	26.750	83.251	-	269.70	60.63	0.11	-5.36	-31.26	11.62	-5.85
A71	SW	26.749	83.253	-	205.30	53.16	0.11	-4.20	-22.62	10.98	-7.02
A72	SW	26.763	83.288	-	160.90	39.69	0.12	-5.28	-33.39	8.85	-
A73	SW	26.760	83.332	-	146.50	38.22	0.15	-5.79	-37.05	9.27	-7.83
A74	SW	26.758	83.331	-	212.10	30.75	0.18	-4.63	-31.12	5.92	-
A75	SW	26.743	83.341	-	227.70	59.28	0.12	-6.83	-43.92	10.72	-6.19
A76	SW	26.707	83.349	-	233.30	45.81	0.10	-6.53	-45.41	6.83	-
A77	SW	26.699	83.388	-	278.90	38.34	0.09	-6.53	-40.45	11.79	-8.01
A78	SW	26.731	83.396	-	212.90	71.04	0.17	2.04	11.34	-4.98	-4.15
A79	SW	26.734	83.347	-	118.50	57.57	0.15	-7.26	-48.15	9.93	-7.45

Table 5.4: Groundwater data collected in Ghazipur district. (Note: depth expressed in meter, HCO<sub>3</sub>, Ca and DOC in mg/L and isotopic signature expressed in (‰)).

<i>Sp No.</i>	<i>Geomorphic unit</i>	<i>Latitude</i>	<i>Lonitude</i>	<i>Depth</i>	<i>HCO<sub>3</sub></i>	<i>Ca</i>	<i>DOC</i>	<i>δ<sup>18</sup>O</i>	<i>δ<sup>2</sup>H</i>	<i>d- excess</i>	<i>δ<sup>13</sup>C</i>
B1	YA	25.529	83.833	48.78	624.60	79.57	0.26	-5.18	-38.50	2.94	-4.59
B2	YA	25.525	83.862	39.63	512.40	64.33	0.52	-7.03	-50.15	6.09	-
B3	YA	25.538	83.834	47.26	522.40	89.03	2.45	-5.18	-39.55	1.89	-10.28
B4	YA	25.548	83.807	50.30	426.00	90.47	1.31	-4.60	-35.14	1.66	-5.65
B5	YA	25.564	83.799	39.63	549.00	77.13	0.99	-7.78	-54.62	7.62	-
B6	YA	25.589	83.790	42.68	518.50	80.40	1.02	-7.76	-56.34	5.74	-11.48
B7	YA	25.610	83.745	41.16	616.10	81.47	0.51	-7.99	-57.15	6.77	-6.65
B8	YA	25.615	83.716	39.63	439.20	91.57	0.25	-7.36	-52.58	6.30	-
B9	YA	25.625	83.683	51.83	537.00	82.93	0.38	-5.53	-42.12	2.12	-
B10	YA	25.492	83.469	48.78	736.80	101.67	1.02	-5.85	-44.23	2.57	-9.69
B11	YA	25.518	83.479	42.68	707.00	109.43	0.04	-5.38	-41.25	1.79	-
B12	YA	25.611	83.628	30.49	510.00	87.23	0.01	-8.78	-62.50	7.74	-7.46
B13	YA	25.524	83.511	39.63	2066.00	239.73	0.03	-5.19	-40.62	0.90	-
B14	YA	25.546	83.537	35.06	1661.20	195.33	0.45	-7.76	-52.25	9.83	-13.45
B15	YA	25.575	83.627	42.68	590.20	97.13	0.48	-4.89	-36.58	2.54	-
B16	YA	25.579	83.652	33.54	589.00	61.67	1.51	-5.09	-37.15	3.57	-10.48
B17	YA	25.579	83.693	42.68	566.80	79.57	0.32	-5.34	-39.50	3.22	-
B18	YA	25.540	83.717	27.44	445.30	75.17	1.05	-9.05	-59.49	12.91	-11.07
B19	YA	25.526	83.742	42.68	498.00	76.27	0.05	-5.42	-41.25	2.11	-
B20	YA	25.421	83.538	45.73	509.00	91.73	0.35	-5.59	-40.61	4.11	-7.25
B21	YA	25.389	83.546	30.49	582.60	70.47	1.01	-8.78	-59.15	11.09	-
B22	YA	25.465	83.572	24.39	294.50	51.57	0.02	-9.16	-60.58	12.70	-
B23	YA	25.485	83.568	30.49	322.80	75.17	0.58	-7.98	-54.25	9.59	-8.40
B24	YA	25.510	83.563	27.44	399.90	69.53	0.65	-8.85	-61.35	9.45	-7.35
B25	YA	25.542	83.571	27.44	544.10	74.93	0.50	-8.49	-60.65	7.27	-

B26	YA	25.556	83.586	36.59	496.50	65.07	1.59	-5.91	-45.59	1.69	-12.06
B27	YA	25.503	83.804	38.11	1072.10	121.70	1.02	-5.04	-40.25	0.07	-10.26
B28	YA	25.508	83.849	54.88	1008.20	174.61	0.04	-4.12	-33.45	-0.49	-
B29	YA	25.509	83.873	47.26	1125.10	197.53	0.01	-5.19	-41.56	-0.04	-11.11
B30	YA	25.529	83.845	30.49	280.70	38.44	2.90	-8.58	-59.25	9.39	-13.50
B31	YA	25.527	83.863	39.63	351.49	51.46	0.01	-6.92	-49.35	6.01	-
B32	YA	25.538	83.846	30.49	558.21	54.82	0.32	-8.59	-60.15	8.57	-7.12
B33	YA	25.549	83.819	24.39	583.33	79.27	0.02	-9.94	-66.65	12.87	-11.15
B34	YA	25.567	83.799	36.59	503.58	50.95	0.06	-7.69	-53.45	8.07	-
B35	YA	25.603	83.792	38.11	168.11	20.95	0.08	-7.28	-51.34	6.90	-6.46
B36	YA	25.614	83.756	42.68	632.26	68.10	3.05	-7.70	-54.25	7.35	-
B37	YA	25.618	83.727	39.63	384.06	54.40	0.12	-6.76	-48.58	5.50	-
B38	YA	25.638	83.684	38.11	408.52	82.35	0.53	-7.33	-50.12	8.52	-8.89
B39	YA	25.497	83.474	24.39	570.94	74.75	0.86	-10.08	-68.15	12.49	-
B40	YA	25.531	83.479	42.68	681.50	96.05	0.01	-5.88	-42.25	4.79	-
B41	YA	25.625	83.629	36.59	440.26	66.04	0.75	-6.68	-46.53	6.91	-
B42	YA	25.526	83.522	36.59	1703.14	251.72	3.19	-6.99	-47.12	8.80	-11.78
B43	YA	25.547	83.549	33.54	1103.52	139.91	0.04	-8.15	-56.58	8.62	-
B44	YA	25.577	83.638	28.96	278.62	64.70	0.05	-8.39	-58.18	8.94	-7.56
B45	YA	25.579	83.663	24.39	515.81	61.83	0.48	-9.86	-68.35	10.53	-
B46	YA	25.585	83.696	33.54	753.74	89.15	3.12	-8.24	-56.50	9.42	-12.24
B47	YA	25.544	83.725	27.44	371.43	44.59	0.02	-9.06	-60.19	12.29	-
B48	YA	25.527	83.755	27.44	207.35	33.33	0.03	-8.92	-59.25	12.11	-
B49	YA	25.424	83.549	33.54	404.31	60.32	2.41	-6.86	-50.51	4.37	-9.23
B50	YA	25.394	83.556	32.01	364.95	56.05	0.04	-8.08	-55.65	8.99	-
B51	YA	25.475	83.572	33.54	221.39	38.42	1.95	-8.45	-59.58	8.02	-10.01
B52	YA	25.488	83.577	27.44	98.52	27.00	1.05	-8.88	-61.25	9.79	-
B53	YA	25.510	83.574	36.59	429.16	54.43	1.08	-6.85	-48.35	6.45	-5.56
B54	YA	25.551	83.572	27.44	397.56	76.14	0.85	-9.29	-59.45	14.87	-13.96
B55	YA	25.564	83.586	38.11	398.35	63.02	3.14	-7.31	-50.59	7.89	-



B56	YA	25.514	83.807	38.11	1329.50	168.50	0.75	-9.05	-58.50	13.90	-10.70
B57	YA	25.519	83.850	44.21	828.20	95.82	2.03	-5.82	-42.15	4.41	-
B58	YA	25.519	83.874	36.59	925.00	107.10	1.73	-6.02	-41.50	6.66	-9.45
B59	OA	25.610	83.772	27.44	768.30	118.40	0.06	-7.15	-50.50	6.70	-7.49
B60	OA	25.488	83.414	36.59	701.50	99.23	1.15	-6.90	-49.57	5.63	-
B61	OA	25.442	83.482	39.63	1732.00	208.33	1.09	-5.10	-38.85	1.95	-3.06
B62	OA	25.413	83.481	42.68	1144.20	165.47	1.03	-5.51	-41.65	2.43	-
B63	OA	25.577	83.577	106.71	835.60	128.77	0.45	-2.95	-25.05	-1.45	-3.11
B64	OA	25.497	83.710	48.78	704.10	109.53	0.24	-5.26	-37.53	4.55	-
B65	OA	25.423	83.561	36.59	2173.40	295.33	0.40	-6.64	-46.90	6.22	-4.48
B66	OA	25.404	83.561	36.59	422.70	64.17	1.60	-6.35	-44.50	6.30	-
B67	OA	25.490	83.852	36.59	121.20	21.53	0.53	-6.59	-45.89	6.83	-8.65
B68	OA	25.491	83.867	54.88	756.50	121.54	0.90	-3.04	-24.50	-0.18	-
B69	OA	25.432	83.601	51.83	224.20	33.13	0.38	-3.44	-28.56	-1.04	-
B70	OA	25.423	83.671	41.16	156.20	44.33	0.40	-5.84	-42.45	4.27	-7.34
B71	OA	25.454	83.742	36.59	109.20	29.33	0.56	-7.44	-51.53	7.99	-
B72	OA	25.486	83.769	42.68	175.60	30.27	1.72	-6.04	-44.05	4.27	-6.46
B73	OA	25.466	83.839	54.88	90.90	18.87	0.93	-5.25	-38.50	3.50	-6.11
B74	OA	25.613	83.783	28.96	781.34	92.44	0.25	-9.14	-60.54	12.58	-
B75	OA	25.489	83.427	33.54	734.29	102.14	1.15	-8.14	-56.51	8.61	-6.50
B76	OA	25.446	83.492	30.49	1477.06	193.26	1.01	-8.50	-62.49	5.51	-
B77	OA	25.415	83.493	28.96	1084.20	170.67	2.95	-9.50	-67.50	8.50	-4.79
B78	OA	25.579	83.582	33.54	769.34	117.06	0.76	-8.12	-57.15	7.81	-
B79	OA	25.498	83.713	24.39	575.71	67.10	0.03	-9.14	-62.95	10.17	-9.66
B80	OA	25.425	83.573	27.44	1812.72	197.62	0.28	-9.20	-63.25	10.35	-
B81	OA	25.405	83.574	18.29	523.29	63.97	0.45	-10.14	-67.83	13.29	-
B82	OA	25.495	83.863	33.54	1072.00	124.59	0.38	-8.82	-62.54	8.02	-5.63
B83	OA	25.494	83.878	36.59	1045.00	139.33	1.91	-7.36	-56.49	2.39	-
B84	OA	25.435	83.613	41.46	139.10	23.65	0.11	-7.05	-54.28	2.12	-5.46
B85	SW	25.417	83.553	-	254.00	57.70	0.15	-4.59	-29.15	7.57	-6.78

B86	SW	25.529	83.487	-	236.00	48.00	0.10	-6.93	-42.50	12.94	-5.49
B87	SW	25.524	83.498	-	285.00	48.00	0.16	-7.56	-46.20	14.28	-
B88	SW	25.519	83.497	-	255.00	47.10	0.13	-7.16	-44.76	12.52	-
B89	SW	25.491	83.409	-	315.00	58.08	0.11	-4.27	-30.62	3.54	-5.76
B90	SW	25.416	83.484	-	296.00	52.30	0.11	-3.98	-28.15	3.69	-7.69
B91	SW	25.588	83.605	-	334.00	52.00	0.19	-3.29	-24.05	2.27	-
B92	SW	25.585	83.615	-	284.00	56.77	0.12	-5.33	-32.12	10.52	-5.68
B93	SW	25.618	83.690	-	265.00	44.61	0.14	-5.25	-31.92	10.08	
B94	SW	25.613	83.696	-	284.00	51.03	0.16	-3.90	-31.41	-0.21	-6.91
B95	SW	25.585	83.757	-	325.00	37.50	0.13	-5.53	-34.50	9.74	-8.09
B96	SW	25.507	83.806	-	294.00	35.27	0.11	-4.09	-30.20	2.52	-
B97	SW	25.500	83.877	-	293.00	46.36	0.13	-7.16	-44.15	13.13	-7.28

## Chapter 6

# Identification of source and health risk of arsenic and other trace metals to the human population

## 6 Identification of source and health risk of arsenic and other trace metals to the human population

### 6.1 Introduction

### 6.2 Material and methods

- 6.2.1. Study area description, sample collection and preparation
- 6.2.2. Chemical and reagents
- 6.2.3. Sediment digestion procedure
- 6.2.4. Instrumentation
- 6.2.5. Quality control and quality assurance
- 6.2.6. Statistical analysis
- 6.2.7. Pollution evaluation indices and chemical toxicity
  - 6.2.7.1. Degree of contamination
  - 6.2.7.2. Chemical toxicity
    - a. Ingestion pathway
    - b. Dermal contact pathway
- 6.2.8. Assessment of the heavy metals in sediment
  - 6.2.8.1. Geoaccumulation index
  - 6.2.8.2. Enrichment factor
  - 6.2.8.3. Contamination factor

### 6.3. Results and discussion

- 6.3.1. Descriptive analysis of As and trace metals in groundwater
- 6.3.2. Health risk assessment due to As and trace metals exposure
- 6.3.3. Descriptive analysis of As and trace metals in sediment
- 6.3.4. Statistical analysis (Pearson's correlation matrix)
- 6.3.5. Sediment quality assessment
  - 6.3.5.1. Geoaccumulation Index
  - 6.3.5.2. Enrichment factor
  - 6.3.5.3. Contamination factor

### 6.4. Conclusions

## Abstract

As and trace metals (TMs) are considered to be a human carcinogen. Millions of people are continuously exposed to As and TMs contaminants in groundwater and sediment. This objective aims to investigate the source and distribution of As and TMs in groundwater and sediment and analyze contamination levels in both the study area. Around ~30 to 35% of the groundwater in both regions was unfit for human consumption. Degree of contamination was calculated for TMs in groundwater, and it was observed that ~30% from Gorakhpur and 67% from Ghazipur groundwater were fell in category three, indicating metal pollution in groundwater. The calculated cancer index (CI) for adults and children indicated 84.2% groundwater from Gorakhpur, and 78.4% groundwater from Ghazipur was above USEPA ( $10^{-6}$ ) limit, indicating that long-term intake can cause cancer to the human being. Sediment core analysis indicating younger alluvium sediment was more enriched with TMs than the older alluvium. Person correlation plot indicated that As and TMs were positively correlated with silt and clay while negatively with sand, indicating metal adsorption on fine particles. Geoaccumulation index ( $I_{geo}$ ), enrichment factor (EF) and degree of contamination (DC) were used to analyze the contamination of soil. The calculated  $I_{geo}$  indicating that sediments are unpolluted. In study area one (Gorakhpur), calculated EF indicates that the upper section of sediment cores is moderately enriched with metals, while As and Zn are significantly enriched. In study area two (Ghazipur), the upper section of the sediment cores shows deficiency to minimal enrichment for all metals while As is significantly enriched. Calculated DC indicates that all the sediment samples fell in unpolluted to moderately polluted regions.

**Keywords:** As exposure; Trace metal contamination; Geoaccumulation index; Enrichment factor; Sediment core

## 6.1. Introduction

Water is a vital component of life as well as the world's most endangered resources. Out of the total 2.8% freshwater, only 0.60% water is available in the form of groundwater and significantly impacts plant and animal ecosystems in rivers and wetlands. Groundwater quality has deteriorated worldwide due to rock-water interaction, overexploitation, industrialization and intense agricultural practices (Misra, 2011, 2013; Srinivasamoorthy et al., 2014; Rickards et al., 2020; Li et al., 2021). High levels of contaminants in aquatic environments, such as As and trace metals, can make water unfit for drinking, irrigation and recreation (Saha et al., 2017; Vetrimurugan et al., 2017; Belkhiri et al., 2018; Varol, 2019). Trace metals (TMs) are among the most harmful contaminants in aquatic ecosystems because of their bioaccumulation and biomagnification capabilities in the food chain and their negative impacts on organisms and lengthy environmental persistence (Alhashemi et al., 2012; Ali et al., 2019; Bhagat et al., 2021; Kunene et al., 2021). The accumulation of As and TMs in aquatic habitats can cause significant negative consequences for human and biota health (Krishna et al., 2013; S. Hossain et al., 2019; Bhagat et al., 2021). Long-term exposure to the As and TMs causes several consequences in humans, such as cancer, cardiovascular problems, reproductive issues, hematological disorders, liver abscesses, renal failure, nervous system damage etc. (Varol, 2019; Zhang et al., 2019; Rahman et al., 2021).

As and TMs can migrate with seepage and root zone and reach the aquifer zone. Soil works as a trace element immobilizer and prevents them from contaminating the aquifers (Deverel & Fujii, 1990). Soil act as a sink for As and TMs, and this ability is dependent on the soil texture, physicochemical properties and soil water interaction. The source of TMs in the soil is geogenic and anthropogenic. Anthropogenic activities like industrial waste, metal processing, smelting, agricultural inputs, chemical manufacturer and sewage waste (Govil et al., 2001; Kaushik et al., 2009; Yang et al., 2017). So the repository nature of fine-grained sediment gives a record of contamination changes through time. The vertical profile of sediment gives a history of the past depositions feature and major changes. Over the last few decades, the vertical profile is used to identify the core sediment's pollution records (Chatterjee et al., 2007). The TMs concentration and its distribution in the sediment core provide a better understanding of their behavior in the aquifer environment and help figure out the contamination level and its sources. There is currently no

information available on the TMs composition of sediment profiles in the study area. Hence this objective has been instigated with the following aims, i. to identify the As and TMs contamination in groundwater and its effect on human health, ii. identifying the source of the pollutant in the study area, iii. assessment of the geo-accumulation index, degree of contamination, enrichment factor etc.,

## 6.2. Material and Methods

### 6.2.1. Study area description, sample collection and preparation

A total of 70 groundwater samples from Gorakhpur and 84 groundwater samples from Ghazipur district were collected during 2017-18 (Figure 3.1 & 3.2, Chapter 3). Two geomorphological features were considered during the groundwater sampling older alluvium and younger alluvium in both the study area.

**(Details of the study area with sampling location has been discussed in chapter 3)**

### 6.2.2. Chemical and reagents

The analytical grade chemicals and reagents were used in the sediment digestion and analysis and procured from Sigma Aldrich or Merck. All the required utensils and vessels were shocked in 5M HNO<sub>3</sub> overnight and washed properly before being used. For standard preparation and dilution, Milli-Q water was used.

### 6.2.3. Sediment digestion procedure

Sediment samples were digested using a method developed by Shapiro (1975).

**(Detail sample processing and digestion methodology has been explained in chapter 3)**

### 6.2.4. Instrumentation

The groundwater and digested sediment samples were analyzed on inductive coupled plasma optical emission spectrometry (ICP-OES 5110, Agilent Technologies, USA). The instrument was standardized with the reference material (SRM-1643d) available with the instrument. For the trace metal, best fitted linear regression ( $r^2=0.9998$ ) was used to standardized

the instrument against the standards of known concentration. The method detection limit (MLD) for trace metals was given in [table 6.1](#). MLD is the minimum detection concentration of an element that can be reported at 99% confidence level.

*Table 6.1: Elements with their corresponding wavelength and method detection limit*

Element	Wavelength (nm)	MDL ( $\mu\text{g/L}$ )
Aluminum	396.152 nm	1.2
Arsenic	188.980 nm	0.5
Cadmium	228.802 nm	0.4
Calcium	422.673 nm	4
Chromium	267.716 nm	0.7
Copper	327.395 nm	0.4
Iron	238.204 nm	0.4
Lead	220.353 nm	3
Magnesium	285.213 nm	5.1
Manganese	257.610 nm	0.1
Nickel	231.604 nm	3.1
Sodium	589.592 nm	10.1
Zinc	213.857 nm	1.1

#### 6.2.5. Quality control and quality assurance

The National Institute of Standards and Technology (NIST) US-based standard reference material (SRM), 8704 (Buffalo river sediments), was used to verify the result of the trace metal in sediment. The observed value for As, Al, Cd, Co, Cr, Cu, Fe, Mn, Ni, Pb and Zn was compared with the standard certified value (NIST 8704), and recovery achieved for the given metals was 98.3%, 102.1%, 94.4%, 93.6%, 101.1%, 97.7%, 102.3%, 97.3, 92.1%, 99.7% and 98.5%, respectively. The recovery for each metal was under  $\pm 10\%$ .

#### 6.2.6. Statistical analysis

The correlation analysis was carried out to determine the degree of relationship between the two variables. It's a linear association measure that is also known as Pearson's correlation coefficient after its creator. It was measured on a scale of +1 to 0 to -1. A good correlation between

the two variables was expressed by either +1 or -1. A positive correlation was expressed as both the variables increased or decreased parallelly; however, a negative correlation was expressed as one increased with another decreased (inverse relationship). An “R program” was used to plot the Pearson correlation plots.

### 6.2.7. Pollution evaluation indices and chemical toxicity

Degree of contamination and chemical toxicity was calculated in the study area by considering the As and TMs in the groundwater.

#### 6.2.7.1. Degree of contamination:

The degree of contamination is the combined effect of many quality characteristics considered hazardous to the drinking purpose. The degree of contamination ( $C_{deg}$ ) is considered a reference to evaluating the pollution of TMs in water. It is classified into three categories: Low ( $C_{deg} < 1$ ), medium ( $C_{deg} = 1-3$ ) and High ( $C_{deg} > 3$ ) (Backman et al., 1998; Belkhiri et al., 2018; Rahman et al., 2021). The following equations were used to calculate the contamination index:

$$DC = \sum_{i=1}^n C_{fi} \quad (6.1)$$

$$C_{fi} = \frac{C_{Ai}}{C_{Ni}} - 1 \quad (6.2)$$

Where  $C_{fi}$  = contamination factor,  $C_{Ai}$  = analytical value and  $C_{Ni}$  = upper permissible concentration of the  $i^{\text{th}}$  parameter and N = normative value. Here  $C_{Ni}$  was taken from WHO (2008).

#### 6.2.7.2. Chemical Toxicity:

Health risk assessment is a procedure of determining the chances of an event occurring and the likely degree of adverse health impacts to the human being over a particular period of period. The WHO (2004) maximum acceptable limit for As in groundwater is 10 ppb. In the study area, the concentration of As was higher than the WHO acceptable limit at some locations. The European Food Safety Authority's Panel set a benchmark dose lower confidence limit for As was 0.3-8 mg/kg per day. United States Environmental Protection Agency (USEPA-IRIS,1998)



outlines many health risk assessment models for evaluating arsenic's non-carcinogenic and carcinogenic effects.

There are three major pathways or methods through which metals can enter the human body: Direct oral ingestion, inhalation, and dermal absorption through the skin. Out of all three, ingestion and dermal absorption are the most likely routes for water exposure. The following equation was used to calculate the chemical toxicity (USEPA, 2012).

a. **Ingestion pathway:**

The health impact due to intake of As contaminated water was calculated as average daily dosages by the following formula:

$$ADD = \frac{C \times IR}{BW} \times \frac{EF \times ED}{AT} \quad (6.3)$$

ADD is the average daily dosages in mg/L, C is the As concentration in drinking water  $\mu\text{g/L}$ , BW is the body weight (kg), and IR is the average daily intake rate. AT is the averaging time (d), ED represents the exposure duration and ET is referred to as mean exposure duration (yrs.) and EF is the exposure frequency (day/year). The values used in the equation to calculate the average daily dose were given in table 6.2.

This equation was changed to assume that an individual drinks the water over a year (exposure frequency) and a lifetime (exposure length). The exposure frequency and duration will be equal to the average time in that scenario, and the equation will be simplified as follows:

$$ADD = \frac{C \times IR}{BW} \quad (6.4)$$

The following equations were used to calculate Hazard Quotient Index (HQ) (USEPA, 1989):

$$HQ = \frac{ADD}{RfD} \quad (6.5)$$

Where, HQ is the Hazards quotient, ADD is the average daily dose intake for ingestion of the heavy metals in drinking water (mg/kg/day) calculated from equation (6.4). RfD (reference dose) is the maximum amount of heavy metal that a person can be exposed to in a single day without suffering any adverse health effects (mg/ kg/day). Reference doses for various metals were given in Table 6.2.

Table 6.2: Input parameter and abbreviation for risk calculation

Input paramaters for risk analysis	Abbreviation	Unit	Value	Reference
Element Concentration	EC	mg/L	Observed Value	Present Study
Ingestion Rate (Adult)	IR (A)	L/day	3	PC, 2012
Ingestion Rate (Children)	IR (C)	L/day	1.5	Brindha et al.,2016
Exposure Frequency	EF	Day/year	365	USEPA, 1989
Exposure Duration (Adult)	ED (A)	Year	69.4 (India)	World Bank (2018)
Exposure Duration (Children)	ED (C)	Year	6	ICMR, 2009
Body Weight (Adult)	BW (A)	Kg	69.4	ICMR, 2009
Body Weight (Children)	BW (C)	Kg	18.7	USEPA (1991)
Average Time	AT	Day	ED x 365	USEPA (1989)
Exposure Skin Area (Adult)	SA (A)	cm <sup>2</sup>	5700	USEPA (2011)
Exposure Skin Area (Children)	SA (C)	cm <sup>2</sup>	2800	USEPA (2011)
Adherence Factor (Adult)	AF (A)	mg/cm <sup>2</sup>	0.07	USEPA (2011)
Adherence Factor (Children)	AF (C)	mg/cm <sup>2</sup>	0.2	USEPA (2011)
Dermal Absorption Factor	ABSd	NA	0.03	USEPA (2011)
Expopsure Time	ET	hour/event	0.25	USEPA (1997)
Conversion Factor	CF	L/cm <sup>3</sup>	10 <sup>-3</sup>	USEPA (2002)
Dermal permeability coefficient	Kp	cm/hrs	1.1 <sup>-3</sup>	USEPA (2004)
Oral reference dose	RfD(oral)	mg/kg/day	0.0003	USEPA (2005)
Dermal reference dose	RfD(dermal)	mg/kg/day	0.00019	USEPA (2005)
Cancer slope factor (oral)	SF(oral)	mg/kg/day	1.5	USEPA (2005)
Cancer slope factor (dermal)	SF(dermal)	mg/kg/day	3.66	USEPA (2005)

The non-carcinogenic risk to the human being was expressed in the form of hazard index (HI), which is a sum of the hazard quotient (HQ) of all the metal:

$$HI = \sum HQ_i \quad (6.6)$$

Table 6.3: Heavy metal and reference doses for the calculation of non-carcinogenic exposure to human health

Heavy metal	Reference dose (mg/kg/day)	References
Alluminium (Al)	Not Available	
Cadmium (Cd)	$5 \times 10^{-4}$	IRIS from US EPA (2009)
Chromium (Cr)	$3 \times 10^{-3}$	IRIS from US EPA (2009)
Copper (Cu)	$5 \times 10^{-3}$	US EPA from CHMP (2007)
Iron (Fe)	Not Available	
Manganese (Mn)	$1.4 \times 10^{-1}$	IRIS (2011)
Nickel (Ni)	$2 \times 10^{-2}$	Kim et al. (2011)
Lead (Pb)	$3.6 \times 10^{-3}$	Viridor Waste Ltd (2009)
Zinc (Zn)	$3 \times 10^{-1}$	IRIS (2005)
Arsenic (As) <sub>ingestion</sub>	$3 \times 10^{-4}$	IRIS from US EPA (2009)
Arsenic (As) <sub>dermal</sub>	$3 \times 10^{-4}$	IRIS from US EPA (2009)

b. Dermal contact pathway:

The following equation used calculated the non-carcinogenic exposure of As through the dermal pathway:

$$ADD_{dermal} = \frac{EC \times SA \times K_p \times ET \times EF \times ED \times F_{C1} \times F_{C2}}{BW \times AT} \quad (6.7)$$

Where, all the above abbreviations and values were given in table 2.

The carcinogenic risk through oral and dermal was calculated using equations (6.8) and (6.9).

$$CR_{oral} = CDI_{oral} \times SF \quad (6.8)$$

$$CR_{dermal} = CDI_{dermal} \times SF \quad (6.9)$$

$$CI = CR_{oral} + CR_{dermal} \quad (6.10)$$

Where CR is the carcinogenic risk, and it is unitless. It gives the probability of developing cancer in the individual over a lifetime of exposure. CDI is the chronic daily intake, and SF is the carcinogenic slope factor (mg/kg-day).

If carcinogenic risk value surpasses, the  $1 \times 10^{-4}$  is considered to have significant human health effects on individuals. If the CR value is between  $1 \times 10^{-6}$  -  $1 \times 10^{-4}$  considered an acceptable range, and if the CR value is less than  $1 \times 10^{-6}$  is considered insignificant.

### 6.2.8. Assessment of the heavy metals in sediment

Interpretation of geochemical was dependent on the background value. Background value plays a significant role in the assessment of the metals available in the sediment. Several authors used average world shale value or average upper crust value or local calculated background value as a reference (Turekian & Wedepohl, 1961; Singh et al., 2003; Rudnick & Gao, 2014). Singh et al., (2003) were calculated the background value for Gangetic plain.

#### 6.2.8.1. Geoaccumulation Index ( $I_{geo}$ )

Geoaccumulation index ( $I_{geo}$ ) assesses the metal contamination by comparing the currently observed value to the preindustrial concentration in soil or sediment. Initially, it was used for the bottom sediment (Muller, 1969), but nowadays, it is widely used to access soil pollution. The following formula is used to calculate the  $I_{geo}$ :

$$I_{geo} = \log_2 \frac{C_n}{1.5B_n} \quad (6.11)$$

Where  $C_n$  is the observed  $n$  elemental concentration in the analyzed sediment.  $B_n$  is the geochemical average shale background value in the fossil argillaceous sediment. A constant 1.5 use to investigate the essential disparity in the content of a specific material in the natural environment and minor anthropogenic influences. Muller (1969) was classified the  $I_{geo}$  into six classes based on the sediment quality;

$I_{geo}$	Classe
$I_{geo} \leq 0$	Uncontaminated
$I_{geo} = 0-1$	Uncontaminated to moderately contaminated
$I_{geo} = 1-2$	Moderately contaminated
$I_{geo} = 2-3$	Moderately to strong contaminated
$I_{geo} = 3-4$	Strong contaminated
$I_{geo} = 4-5$	Strongly to extremely contaminated
$I_{geo} \geq 5$	Extremely contaminated

The modified calculations were used in the calculations of the geoaccumulation index. The modifications were as follows:  $C_n$  denoted the observed concentration of a particular element on the soil's surface layer, whereas  $B_n$  denoted element concentrations in the Earth's crust (Turekian & Wedepohl, 1961). The average concentration in the earth crust for As, Hg and Sb are substantially higher than the average concentration in the shale used as a reference figure by Muller (1969). In this calculation, we were decided to compare the measured concentration of the element to the concentration in the Earth's crust. Because soil is a component of the surface layer of the Earth's crust, and its chemical and physical components are linked to the Earth's crust. The concentration of the component in the shale was compared to the average concentration of the metals in the Earth's crust given by Rudnick & Gao (2014); the former concentration was found to be much higher. According to Rudnick and Gao (2014), the average concentration of As was 4.8 mg/kg, whereas, Turekian & Wedepohl (1961) considered 13 mg/kg in average shale. In this study, we have taken Turekian & Wedepohl (1961) for As pollution index calculation.

#### 6.2.8.2. Enrichment Factor (EF)

The enrichment factor (EF) was calculated by comparing the analyzed element to a reference element. Reference materials are those materials which are having the lowest occurrence of variability in the Earth's crust. Reference elements such as Sc, Ti, Mn, FE and Al are the most common reference elements and are considered conserved in the Earth's crust (Reimann et al., 2000; Sutherland, 2000; Loska et al., 2004). In this study, we used Al as a conservative (reference) element. Aluminum is the most abundant metallic element in the Earth's crust, and the matrix primarily determines its concentration in soil. Eventually, the following formula is used to calculate the enrichment factor;

$$EF = \frac{C_n / C_{ref}}{B_n / B_{ref}} \quad (6.12)$$

Where,  $C_n$  is the concentration of an analyzed element in the sediment sample.  $C_{ref}$  content of the reference element in the undisturbed or reference environment.  $B_n$  is the concentration of an analyzed element (Al for this calculation), and  $B_{ref}$  is the reference element (Al shale value) to the

reference environment. Sutherland (2000) has been given enrichment factor (EF) class based on the metal enrichment into the sediment;

<b>EF Class</b>	<b>Sediment enrichment</b>
EF < 2	Deficiency to minimal enrichment
2 < EF < 5	Moderate enrichment
EF = 5 - 20	Significant enrichment
EF = 20 - 40	Very high enrichment
EF > 40	Extremely high enrichment

### 6.2.8.3. Contamination Factor (CF)

The contamination factor (CF) was also used to evaluate the sediment or soil pollution in the study area. Hakanson (1980) introduced a soil classification based on soil contamination factors by comparing the metal concentrations in the sediment to the preindustrial level (average shale). The following formula has been used to calculate the contamination factor;

$$CF_{metal} = \frac{C_{metal}}{C_{background}} \quad (6.13)$$

Where  $CF_{metal}$  is the contamination factor for the particular metal or element,  $C_{metal}$  is the elemental concentration measured in the sediment sample, and  $C_{background}$  is the natural elemental concentration in the reference environment. It has been suggested that the lowest concentration of a given element in the soils under investigation may indicate that element's background concentration, which is unlikely to be influenced by human activity. Therefore, the lowest concentration of an element analyzed in the soil sample can be considered as the background value for that element. To estimate the risk of soil contamination, Hakanson (1980) introduce a classification to identify the soil contamination risk to the seven HMs. Depending on the intensity of pollution, the numeric values of this index can range from 1 to over 6 as follows;

<b>Contamination degree</b>	<b>Sediment pollution</b>
CF < 1	No pollution
1 < CF < 3	Moderate plollution
3 < CF < 6	considerable pollution
6 < CF	Very high pollution

### 6.3. Result and discussion

#### 6.3.1. Descriptive analysis of As and trace metals in groundwater

The statistical analysis of the As and trace metals analyzed in the groundwater was described in table 6.4. The pH of the groundwater was neutral to slightly alkaline mentioned in the previous chapter (Chapter 3). The detected concentration of As ranges from BDL to 0.263 mg/L in study area 1. In study area 2, it varied from BDL to 0.62 mg/L (Table 6.4). The WHO (2008) maximum acceptable limit of As in the drinking water can not be beyond 10 ppb. In study area 1, around 36.4% of groundwater samples were above the WHO acceptable limit. However, in study area 2 (Ghazipur), 33.4% of groundwater samples were above the WHO accepted limit and unsafe for drinking.

Table 6.4: Statistical summary of As and trace metal, degree of contamination and hazards index in groundwater study areas.

	Unit	Study area 1 (Gorakhpur)			Study area 2 (Ghazipur)			WHO (2008)
		Mean	Range	SD	Mean	Range	SD	
<b>As</b>	mg/l	0.03	BDL - 0.265	0.05	0.06	BDL - 0.62	0.10	0.01
<b>Cu</b>	"	0.01	BDL - 0.048	0.01	0.02	BDL - 0.08	0.02	2
<b>Cr</b>	"	0.01	BDL - 0.069	0.01	0.01	BDL - 0.078	0.01	0.05
<b>Mn</b>	"	0.41	BDL - 3.90	0.66	2.55	0.034 - 20.62	3.22	0.4
<b>Pb</b>	"	0.02	BDL - 0.079	0.02	0.04	BDL - 0.29	0.06	0.01
<b>Zn</b>	"	2.32	0.02 - 36.78	5.43	1.41	0.02 - 12.23	1.93	3
<b>DC</b>	unitless	13.23	-3.21 - 116.06	17.73	2.75	-3.67 - 34.29	7.17	
HI(adult)	"	25.94	0.14 - 126.69	24.71	14.40	0.03 - 44.98	11.25	
HI(child)	"	48.14	0.25 - 235.09	45.86	26.73	0.05 - 83.48	20.87	

Where DC= degree of contamination, HI= Hazard Index, SD= Standard deviation, BDL=Below detection limit.

The Cu in groundwater was varied from BDL to 0.048 mg/L in study area 1 (Gorakhpur), while it varied from BDL to 0.08 mg/L in study area 2 (Ghazipur). The concentration of Cu was higher in study area two compared to study area one. Similarly, like Cu, other heavy metals such as Cr, Mn, Pb and Zn were measured higher in Ghazipur compared to Gorakhpur.

#### 6.3.2. Health risk assessment due to As and TMs exposure

##### Non-carcinogenic exposure assessment of the metals (As, Cu, Cr, Mn, Pb and Zn)

The degree of contamination was calculated in both the study area. It was varied from -3.67 to 34.29 with a mean of 2.75 in study area 1. Based on the degree of contamination, we observed that ~61% of water samples fell in category 1 ( $C_{deg} < 1$ ), indicating low trace metal pollution. Approx. 9% of water samples fell in category 2 ( $C_{deg} = 1-3$ ), indicating medium trace metals pollution. Approx. 30% of water samples fell in category 3 ( $C_{deg} > 3$ ), indicating metal pollution. In study area 2, the degree of contamination was varied from -3.21 to 116 with a mean of 13.23. Based on the degree of contamination, we have observed that approx. 18.6% of the water samples fell in category 1, which denoted low trace metals contamination. Approx. 14.4% of the groundwater samples fell in category 2, indicating medium metal pollution, and 67% of the water samples were fell in category 3, indicating high metal pollution.

In general, exposure to a substance through the ingestion pathway is more critical than cutaneous absorption. The average daily intake of As for adults and children was varied from 0.0 to  $1.1 \times 10^{-2}$  (mean  $1.5 \times 10^{-3}$  mg/L) and 0.0 to  $2.1 \times 10^{-2}$  (mean  $2.8 \times 10^{-3}$  mg/L), respectively. In addition, the ADD (dermal) of As for adults and children was varied from 0.0 to  $5.9 \times 10^{-6}$  and 0.0 to  $1.09 \times 10^{-5}$ , respectively. The average daily dose through the cutaneous adsorption was only calculated for As because the cancer slope factor is only available for arsenic. In study area 2 (Ghazipur), the ADD of As for adults and children was varied from 0.0 -  $2.7 \times 10^{-2}$  (mean  $2.8 \times 10^{-3}$  mg/L) and 0.0 -  $4.9 \times 10^{-2}$  mg/L (mean  $5.2 \times 10^{-3}$  mg/L), respectively. In contrast, the average daily dose for dermal absorption was varied from 0.0 to  $1.4 \times 10^{-5}$  and 0.0 to  $2.55 \times 10^{-5}$ , respectively.

The  $CR_{(oral)}$  for adults and children varied from 0.0 to  $1.7 \times 10^{-2}$  and 0.0 to  $3.2 \times 10^{-2}$ . In contrast, the  $CR_{(dermal)}$  for adults and children were ranged between 0.0 to  $4.19 \times 10^{-2}$  and 0.0 to  $7.8 \times 10^{-2}$ , respectively. In study area one (Gorakhpur), approx. 15.8% of the water samples were safe for drinking, while 84.2% of water samples were above the US-EPA limit ( $10^{-6}$ ), indicating long-term intake of As contaminated water can cause cancer in human beings.

In study area two (Ghazipur), the  $CR_{(oral)}$  for adults and children varied from 0.0 to  $4.0 \times 10^{-2}$  and 0.0 to  $7.5 \times 10^{-2}$ . In contrast, the  $CR_{(dermal)}$  for adults and children were ranged between 0.0 to  $9.8 \times 10^{-2}$  and 0.0 to  $1.8 \times 10^{-1}$ , respectively. The calculated CI value indicates that 20.6% of the water samples were safe for drinking while 78.4% of the water samples were above the US-EPA limit ( $10^{-6}$ ), indicating long-term intake of As contaminated water can cause cancer in human



beings. The carcinogenic risk was only calculated for As because the cancer slope factor was not available for other trace metals.

The average daily intake of Cr for adults and children was varied from 0.0 to  $2.9 \times 10^{-3}$  and 0.0 to  $5.5 \times 10^{-3}$  mg/L, respectively. The ADD of Cu for adults and children was varied from 0.0 to  $2.1 \times 10^{-3}$  and 0.0 to  $3.8 \times 10^{-3}$  mg/L, respectively. The ADD of As was higher compared to other toxic metals in Gorakhpur.

The mean value of the hazard index for As and TMs was observed 26.73 in Gorakhpur while 48.14 in Ghazipur. It is widely accepted that an HI, less than one, indicates no significant danger of non-carcinogenic consequences and HI value higher than one, significant risk of a carcinogenic effect.

### 6.3.3. Descriptive analysis of As and trace metals in sediment

The pH of study area one was slightly alkaline in nature. It varied from 8.09 to 8.36, with a mean of  $8.23 \pm 0.08$  at Khorabar and 7.92 to 8.37, with a mean of  $8.15 \pm 0.12$  at Farshiya, in Gorakhpur. The pH of both older and younger alluvium was almost comparable. The depth of the sediment core was 0.0 to 33.53 mbgl, with a mean of  $16.64 \pm 10.55$  at Khorabar and 0.0 to 33.53 mbgl, with a mean of  $17.47 \pm 10.4$  (Table 6.5). The mean concentration of As, Al, Cd, Co, Cr, Cu, Fe, Mn, Ni, Pb and Zn were reported  $11.50 \pm 3.88$  mg/kg,  $45217.73 \pm 8941.33$  mg/kg,  $0.26 \pm 0.15$  mg/kg,  $14.09 \pm 5.51$  mg/kg,  $32.93 \pm 15.58$  mg/kg,  $54.07 \pm 16.89$  mg/kg,  $20462.05 \pm 6453.51$  mg/kg,  $514.53 \pm 280.49$  mg/kg,  $21.98 \pm 10.63$  mg/kg and  $100.87 \pm 17.25$  mg/kg, respectively at Khorabar, while at Farshiya it was observed  $11.42 \pm 5.3$  mg/kg,  $45301.29 \pm 12262.48$  mg/kg,  $0.42 \pm 0.17$  mg/kg,  $20.77 \pm 8.88$  mg/kg,  $42.05 \pm 23.91$  mg/kg,  $45.81 \pm 7.78$  mg/kg,  $24269.65 \pm 4499.61$  mg/kg,  $639.24 \pm 100.02$  mg/kg,  $31.55 \pm 4.71$  mg/kg,  $16.22 \pm 4.92$  mg/kg and  $124.37 \pm 22.93$  mg/kg respectively. Maximum deviation was observed in aluminum (Table 6.5). Soil texture results showed that the proportion of sand was highest than silt and clay. Litholog has shown that sand was present in all the sediment cores throughout the entire depth (Figure 4.5&4.6, chapter 4). The mean percent distribution of silt, clay and OM was higher at Farshiya compared to Khorabar due to flooding each year during the flood.

Table 6.5: Statistical summary of the sediment core in the study area 1 (Gorakhpur)

	Unit	Core 1 (Khorabar)			Core 2 (Farshiya)		
		Mean	Range	St. Dev	Mean	Range	St. Dev
<b>Depth</b>	m	16.64	0 - 33.53	10.55	17.47	0.00 - 33.53	10.40
<b>pH</b>		8.23	8.09 - 8.36	0.08	8.15	7.92 - 8.37	0.12
<b>As</b>	mg/kg	11.50	5.028 - 19.19	3.88	11.42	3.65 - 23.96	5.30
<b>Al</b>	"	45217.73	28918.1 - 61621.35	8941.33	45301.29	29000.4 - 69498.25	12262.48
<b>Cd</b>	"	0.26	0.08 - 0.61	0.15	0.42	0.14 - 0.79	0.17
<b>Co</b>	"	14.09	8.60 - 30.90	5.51	20.77	13.20 - 42.60	8.88
<b>Cr</b>	"	32.93	11.20 - 67.50	15.58	42.05	15.80 - 98.50	23.91
<b>Cu</b>	"	54.07	24.30 - 73.20	16.89	45.81	36.10 - 61.30	7.87
<b>Fe</b>	"	20462.05	11793.6 - 33694.5	6453.51	24269.65	17923.5 - 32361.9	4499.61
<b>Mn</b>	"	514.53	163.20 - 1131.00	280.49	639.24	483.60 - 807.70	100.02
<b>Ni</b>	"	21.98	12.30 - 46.80	10.63	31.55	26.50 - 42.50	4.71
<b>Pb</b>	"	25.38	12.20 - 47.20	10.10	16.22	7.60 - 28.10	4.92
<b>Zn</b>	"	100.87	69.50 - 138.70	17.25	124.37	81.50 - 163.20	22.93
<b>Sand</b>	%	50.95	36.84 - 72.67	12.65	40.94	15.56 - 70.19	17.51
<b>Silt</b>	%	43.69	25.37 - 55.45	9.84	51.60	27.26 - 71.62	13.51
<b>Clay</b>	%	6.19	1.58 - 14.03	3.55	6.77	1.45 - 12.82	3.66
<b>OM</b>	%	0.31	0.036 - 0.76	0.22	0.63	0.23 - 1.22	0.35

In study area 2 (Ghazipur), pH ranged from 8.00 - 8.34, with a mean of  $8.16 \pm 0.11$  at Jagadishpur and 7.97 - 8.35, with a mean of  $8.19 \pm 0.11$  at Firozpur. The pH of the study area was slightly alkaline in nature in both older and younger alluvium and almost similar to each other. The sediment cores depth ranged from 0.0 - 33.53 mbgl, with a mean of  $16.76 \pm 11.32$  at Jagadishpur and 0.0 - 33.53 mbgl, with a mean of  $15.73 \pm 10.96$  at Firozpur (Table 6.6). The mean concentration of As, Al, Cd, Co, Cr, Cu, Fe, Mn, Ni, Pb and Zn were reported  $11.08 \pm 7.53$  mg/kg,  $43225.12 \pm 6100.93$  mg/kg,  $0.31 \pm 0.15$  mg/kg,  $8.50 \pm 8.10$  mg/kg,  $94.72 \pm 90.25$  mg/kg,  $25.25 \pm 22.24$  mg/kg,  $26324.85 \pm 8708.28$  mg/kg,  $857.68 \pm 280.59$  mg/kg,  $23.67 \pm 11.06$  mg/kg,  $19.19 \pm 5.86$  mg/kg and  $102.19 \pm 22.39$  mg/kg, respectively at Jagadishpur and  $14.26 \pm 0.11$  mg/kg,  $49153.2 \pm 9960.5$  mg/kg,  $0.37 \pm 0.2$  mg/kg,  $14.88 \pm 9.0$  mg/kg,  $140.67 \pm 103.87$  mg/kg,  $72.88 \pm 21.26$  mg/kg,  $31621.79 \pm 10200.31$  mg/kg,  $965.66 \pm 224.77$  mg/kg,  $32.85 \pm 12.42$  mg/kg,  $15.70 \pm 6.64$  mg/kg and  $110.77 \pm 26.72$  mg/kg, respectively.

Table 6.6: Statistical summary of the sediment core in the study area 2 (Ghazipur)

	Unit	Core 3 (Jagadishpur)			Core 2 (Firozpur)		
		Mean	Range	St. Dev	Mean	Range	St. Dev
<b>Depth</b>	m	16.76	0 - 33.53	11.32	15.73	0.00 - 33.53	10.96
<b>pH</b>		8.16	8.00 - 8.34	0.11	8.19	7.97 - 8.35	0.11
<b>As</b>	mg/kg	11.08	1.40 - 26.31	7.53	14.26	2.59 - 31.52	8.79
<b>Al</b>	"	43225.12	28544.95 - 54936.15	6100.93	49153.20	38858.5 - 68430.21	9960.48
<b>Cd</b>	"	0.31	0.01 - 0.62	0.15	0.37	0.11 - 0.72	0.20
<b>Co</b>	"	8.50	0.00 - 32.1	8.10	14.88	2.10 - 32.50	9.00
<b>Cr</b>	"	94.72	9.80 - 282.50	90.25	140.67	42.87 - 323.75	103.87
<b>Cu</b>	"	25.25	5.02 - 73.16	22.24	72.88	48.91 - 113.23	21.26
<b>Fe</b>	"	26324.85	12774.3 - 43495.2	8708.28	31621.79	18872.7 - 51823.21	10200.31
<b>Mn</b>	"	857.68	378.20 - 1298.70	280.59	965.66	693.90 - 1557.70	224.77
<b>Ni</b>	"	23.67	11.50 - 51.50	11.06	32.85	19.50 - 57.20	12.42
<b>Pb</b>	"	19.19	9.50 - 31.60	5.86	15.70	4.58 - 26.76	6.64
<b>Zn</b>	"	102.19	70.60 - 144.30	22.39	110.77	83.56 - 189.65	26.72
<b>Sand</b>	%	49.72	10.35 - 76.32	18.47	45.40	7.62 - 97.18	30.41
<b>Silt</b>	%	44.90	17.01 - 81.61	17.50	49.87	2.82 - 81.81	27.03
<b>Clay</b>	%	5.18	1.21 - 9.22	2.82	4.73	0.0 - 10.73	3.56
<b>OM</b>	%	0.36	0.054 - 1.95	0.49	0.50	0.1 - 1.23	0.35

Similar to study area one, the sand proportion was highest compared to silt and clay and available in all the sediment core samples from top to bottom. The mean concentration of As was observed higher in Firozpur compared to Jagadishpur (Table 6.6). Jagadishpur fell into older alluvium, while Firozpur fell into younger alluvium and flooded every year during the flood. The elevated As and trace metals in the sediment core of Firozpur were associated with soil texture and color. The concentration of Pb was higher in OA (Jagadishpur) than YA (Firozpur), which might be due to the local anthropogenic source.

#### 6.3.4. Statistical analysis (Pearson's correlation matrix)

A correlation matrix was plotted for the sediment core samples at Khorabar (Figure 6.1). The figure showed that silt and clay are negatively correlated with sand ( $p=0.05$ ), but there was no significant correlation observed between OM and clay. A good correlation was observed between Fe, Mn, Zn, Pb, Ni, Cr, Cd and Co and a negative correlation with OM, indicating a similar origin from a common source or homogeneous geochemical behavior.

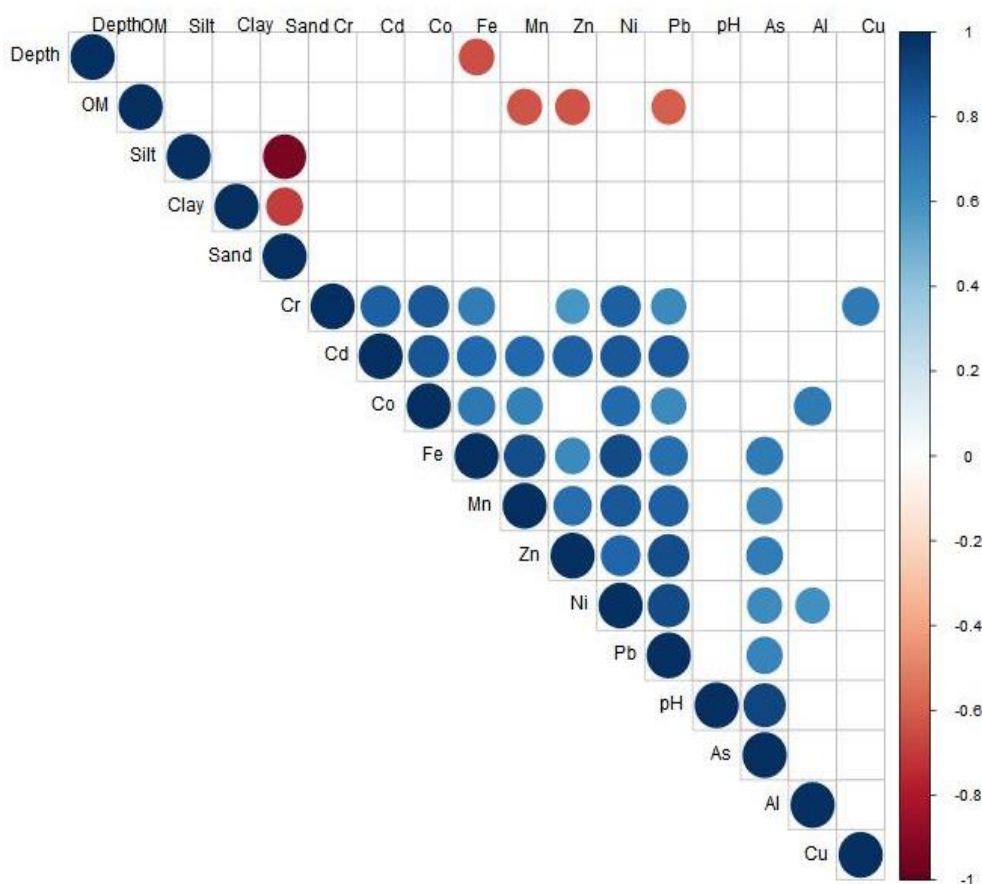


Figure 6.1: Pearson's correlation matrix (at  $p=0.05$ ) for sediment core one at Khorabar, Gorakhpur

As positively correlated with pH, Pb, Ni, Zn, Fe and Mn, indicating metal oxide involved in adsorption or desorption of As at Khorabar. A significant positive correlation was observed between Al with Ni and Co, but with other metals, Al was moderately correlated, indicating a similar source and might be they are coming from metal chelation. A negative correlation was observed between sand and TMs and organic matter in the older alluvium (Khorabar), indicating TMs were release from their minerals.

The Pearson's correlation plot was plotted for the sediment core of younger alluvium (YA) at Farshiya (Figure 6.2). From the plot, pH was negatively correlated with As, TMs clay and silt and positively correlated with sand. The mobility of TMs is the function of pH and depth. Appert from that, mobility of TMs percentage at a given pH is also influenced by the sediment's buffering ability at that pH.

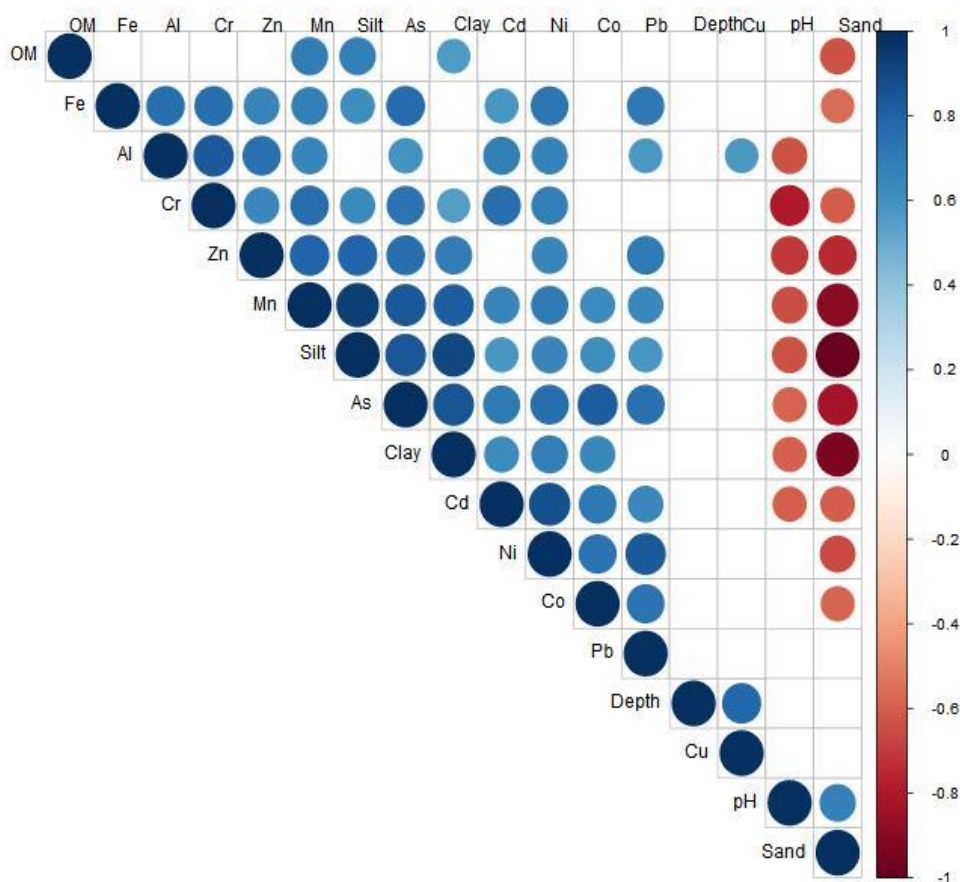


Figure 6.2: Pearson's correlation matrix (at  $p=0.05$ ) for sediment core two at Farshiya, Gorakhpur

The buffering capability of the different layers of the sediment profile differs significantly (Gäbler, 1997). The positive correlation of As and TMs with clay and silt and negative correlation with sand indicating metal adsorbed on fine sediment surfaces of clay and aluminosilicates minerals. A negative correlation of sand with As, TMs and organic matter indicating coarser sediment with the less organic matter was not involved in adsorption or desorption of metals.

The Pearson's correlation plot was plotted for the older alluvium at Jagadishpur (Figure 6.3). Figure 3 shows that depth was negatively correlated with As, Co, Al, Fe, Pb, Cd, Ni, Silt and organic matter, indicating that upper layer sediments were rich in organic matter and had a high affinity to adsorbed As and TMs (Kumar & Ramanathan, 2018).

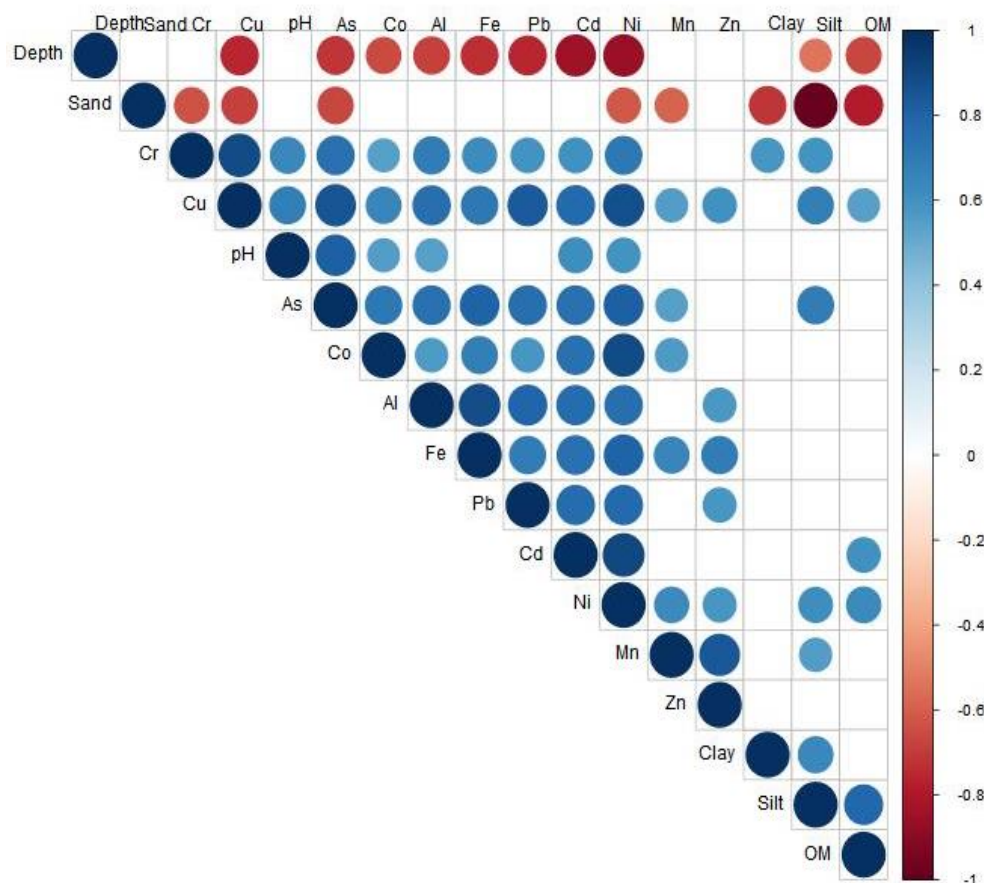


Figure 6.3: Pearson's correlation matrix (at  $p=0.05$ ) for sediment core one at Jagadishpur, Ghazipur

A positive correlation between TMs, indicating a similar source and occurrences, might be responsible for the availability of metal chelation. As positively correlated with Cr, Co, pH, Al, Fe, Pb, Cd, Ni, Mn and silt, indicating As adsorbed on metal oxides, fine particles and aluminosilicate minerals and sorption or desorption of As was pH and redox potential dependent (Hossain et al., 2014). A negative correlation of sand with TMs, clay, silt and OM, indicating coarser sediment with less organic matter, was not efficient in the TMs to their surface because of less available surface area.

The Pearson's correlation plot was plotted for younger alluvium at Firozpur (Figure 6.4). Arsenic negatively correlated with pH and sand while positively correlated with silt, clay, organic matter, Co, Cu, Al, Fe, Ni, Cd and Pb, indicating metal oxide and aluminosilicate in the presence of fine silty clay enhanced the As concentration in soil. A positive correlation of As with organic

matter supports the adsorption of As on fine particles by creating a reducing subsurface environment (Nickson et al., 1998; Smedley & Kinniburgh, 2002; Kumar & Ramanathan, 2018). All the trace metals in the sediment core were positively correlated, indicating similar sources and occurrences in the sediment.

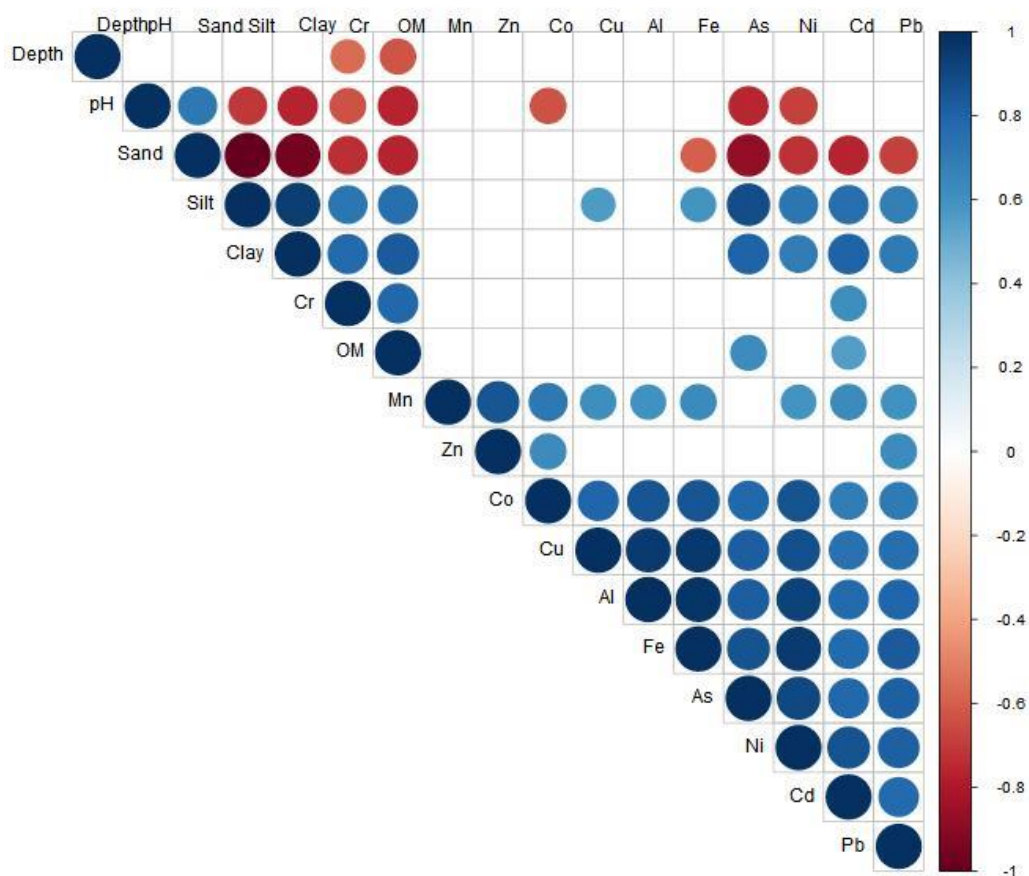


Figure 6.4: Pearson's correlation matrix (at  $p=0.05$ ) for sediment core one at Firozpur, Ghazipur

The positive correlation of organic matter with TMs, indicating probable metal chelation in the presence of reducing conditions, but the positive relationship between metal shows similar sources and geochemical behaviors (Pandey & Singh, 2017).

### 6.3.5. Sediment quality assessment

#### 6.3.5.1. Geoaccumulation Index

The geoaccumulation index was calculated for metals such as As, Al, Cd, Co, Cr, Cu, Fe, Mn, Ni, Pb, and Zn in the sediment cores and plotted with the depth at Khorabar and Farshiya (Figure 6.5a&b). The geoaccumulation index was classified into seven classes based on the unpolluted to extremely polluted sediment quality

The geo-accumulation index is divided into seven grades (0–6), showing varying degrees of enrichment above background values ranging from unpolluted to extremely polluted sediment quality. In study area 1 (Gorakhpur),  $I_{geo}$  values for As and TMs were below 0 (zero), indicating sediment was unpolluted except at a depth of 3.14 mbgl for Pb.

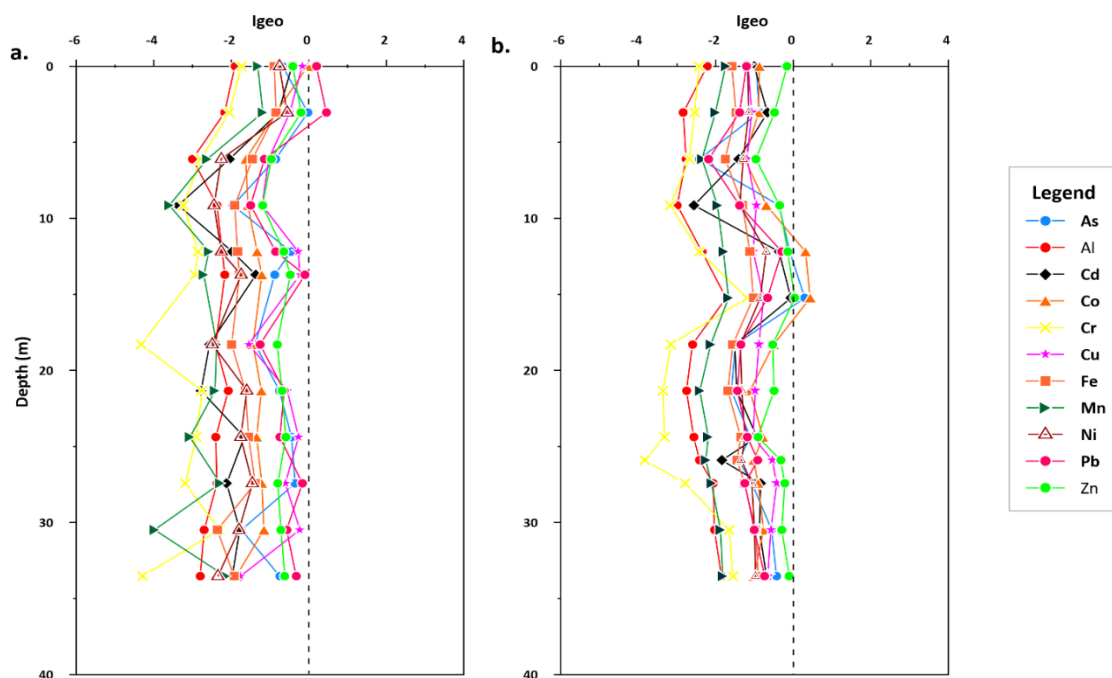


Figure 6.5: Geoaccumulation index ( $I_{geo}$ ) plot for sediment core at, a. Khorabar b. Farshiya

Similar results were also observed in the sediment core of Farshiya (Figure 6.5b). All the metals such as Al, Cd, Cr, Cu, Fe, Mn, Ni and Pb had  $I_{geo}$  values less than 0 (zero) throughout the entire depth indicating sediment core was unpolluted. However,  $I_{geo}$  values for As, Co and Zn were



falling between 0 to 1 at a depth of 12-17 mbgl, indicating uncontaminated to moderately contaminated sediment was reported.

In study area 2 (Ghazipur),  $I_{geo}$  values were less than zero for all the As and trace metals studies. Based on the  $I_{geo}$  classification, TMs and As fell in category 1, representing unpolluted sediment except for some elements (Figure 6.6a). Trace metals such as As, Cu and Cr were shown some anomalies with high concentrations at a depth of 3 mbgl. Based on the  $I_{geo}$  classification, they were falling in unpolluted to moderately polluted class. Co was falling in class 1, unpolluted, but at a depth of 31 mbgl, a sharp peak was reported in  $I_{geo}(0-1)$ , represented unpolluted to moderately polluted sediment class.

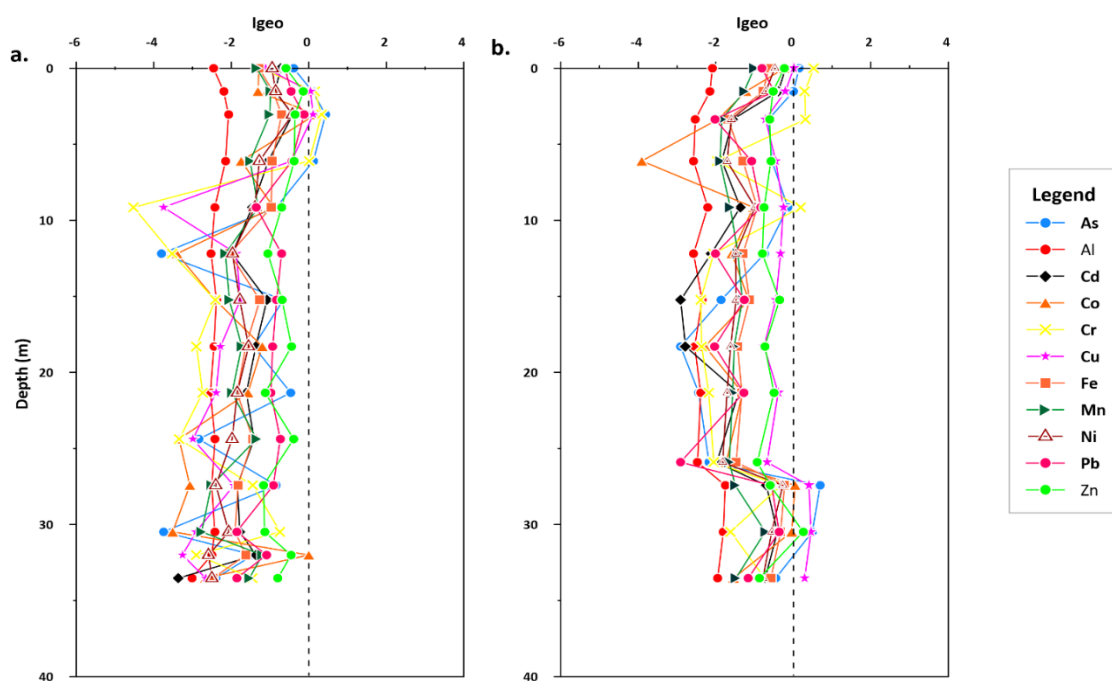


Figure 6.6: Geoaccumulation index ( $I_{geo}$ ) plot for sediment core at, a. Jagadishpur b. Firozpur

The calculated  $I_{geo}$  values for TMs such as Al, Cd, Co, Fe, Mn, Ni and Pb were less than zero in the sediment core of Firozpur (Figure 6.6b), indicating that unpolluted sediment class. Cr showed few sharp peaks of  $I_{geo}$  (0-1) in upper surface sediment and at a depth of 10 mbgl, indicating unpolluted to moderately polluted sediment class at that depth. As, Cu and Zn had  $I_{geo}$  values less than zero in the upper section of the sediment core but at a depth of 27 to 34 mbgl  $I_{geo}$  values between 0-1, indicating unpolluted to moderately polluted sediment class. In both the study

areas, the vertical depth-wise distribution of sediment core shows that most of the studied elements show a similar trend of  $I_{geo}$  below the depth except Cr.

#### 6.3.5.2. Enrichment Factor (EF)

The enrichment factor (EF) is a standardization tool for classifying the metal percentages found in sediments. The EF was calculated in the sediment cores to identify the enrichment of the elements in the study area. [Figure 6.7&6.8](#) shows the vertical distributions of calculated EF for each metal studied in the sediment cores. The mean EF value for the studies metals was found between 2 to 5, indicating moderate enrichment in all four sediment cores.

In study area 1 (Gorakhpur), the enrichment factor for Mn and Cr was found  $< 2$ , indicating deficiency to minimal enrichment of these metals in the sediment core at Khorabar. The mean EF for Fe, Cd and Ni was found less than 2, but in the upper section of the sediment core, the EF was found between 2-5, indicating moderate enrichment of these metals ([Figure 6.7a](#)). The ER for As, Co and Cu was found between 2-5, indicating moderate enrichment. However, at a depth of 24.4 mbgl and 30.48 mbgl, the ER values were higher than 5, indicating significant enrichment of Cu. Similar to Cu, the calculated ER value for Pb and Zn reported that the upper section of the sediment represents deficiency to minimal enrichment. In contrast, the deeper section shows moderate enrichment.

EF was calculated and plotted for the sediment core at Farshiya in [figure 7b](#). The mean EF values for Mn and Cr were below less than 2, indicating deficiency to moderate enrichment. The enrichment mean values for As, Co, Cu, Fe, Ni, Pb and Zn were found in between 2 to 5, indicating moderate enrichment of these elements in the sediment core, while EF for As and Zn at a depth of 9.1 mbgl were observed between 5-10, indicating a significant enrichment of these elements. A higher enrichment of the elements at 9.1 mbgl depth, indicating geochemical processes might be responsible for the elevated elemental concentration.

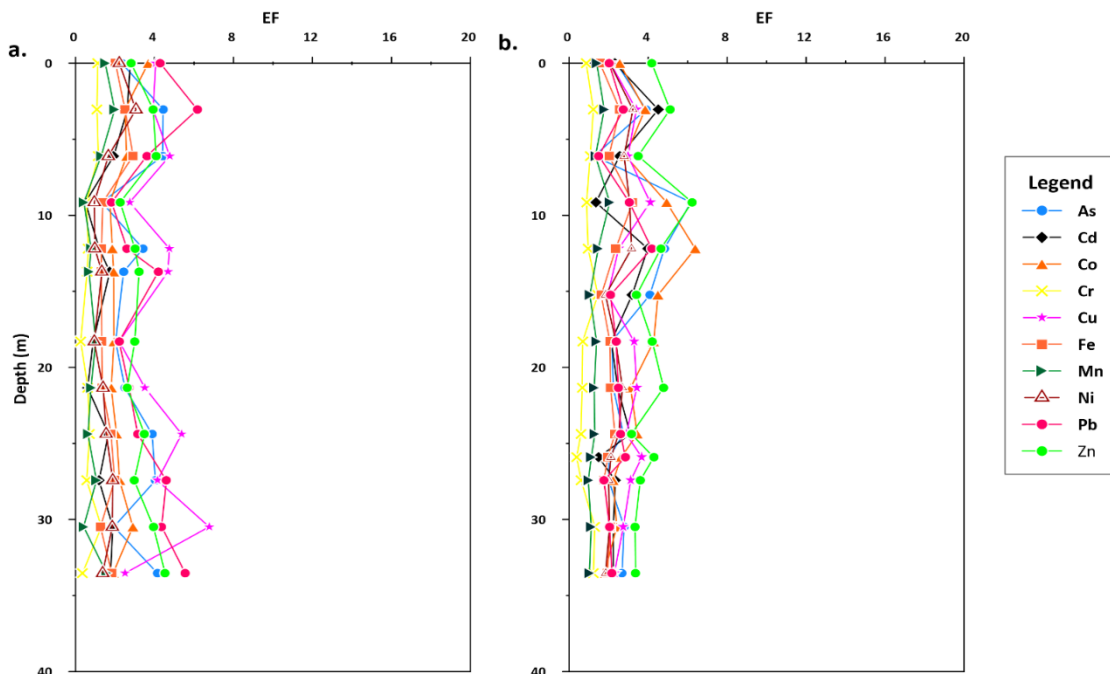


Figure 6.7: Enrichment factor (EF) plot for sediment core at, a. Khorabar b. Farshiya

The EF plots were plotted for the sediment core of Jagadishpur (Figure 6.8a). The mean enrichment values for Cd, Co, Cu and Ni were observed 1.9, 1.3, 1.5 and 1.8, respectively. Based on the EF classification, these elements fell in class 1 ( $EF < 2$ ), representing deficiency to minimal enrichment.

The mean enrichment value for As, Cr, Fe, Mn, Pb and Zn were found 2.8, 2.1, 2.3, 2.02, 2.9 and 3.5, respectively, and these elements represent moderate enrichment of the metal. In the sediment core at a depth of 3.01 and between 24.4 to 27.5, EF was high and representing (ER = 5-10) significant enrichment class.

In the EF plot at Firozpur (Figure 6.8b), we have observed that only two elements Cd and Mn having mean EF values less than 2, representing deficiency to minimal enrichment ( $EF < 2$ ). However, the remaining metals such as As, Co, Cr, Cu, Fe, Ni, Pb and Zn were shown mean value greater than two but less than five, representing moderate enrichment of these elements.

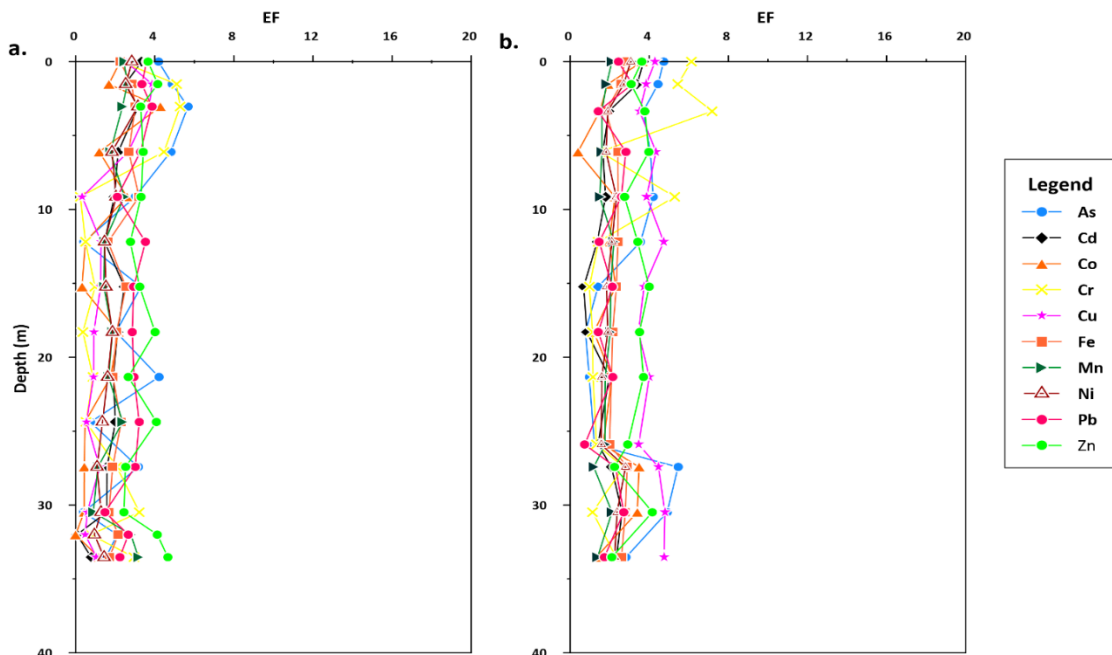


Figure 6.8: Enrichment factor (EF) plot for sediment core at, a. Jagadishpur b. Firozpur

### 6.3.5.3. Contamination Factor

The contamination factor (CF) was calculated for As, Cd, Co, Cr, Cu, Ni, Pb and Zn and plotted in Figures 6.9&6.10.

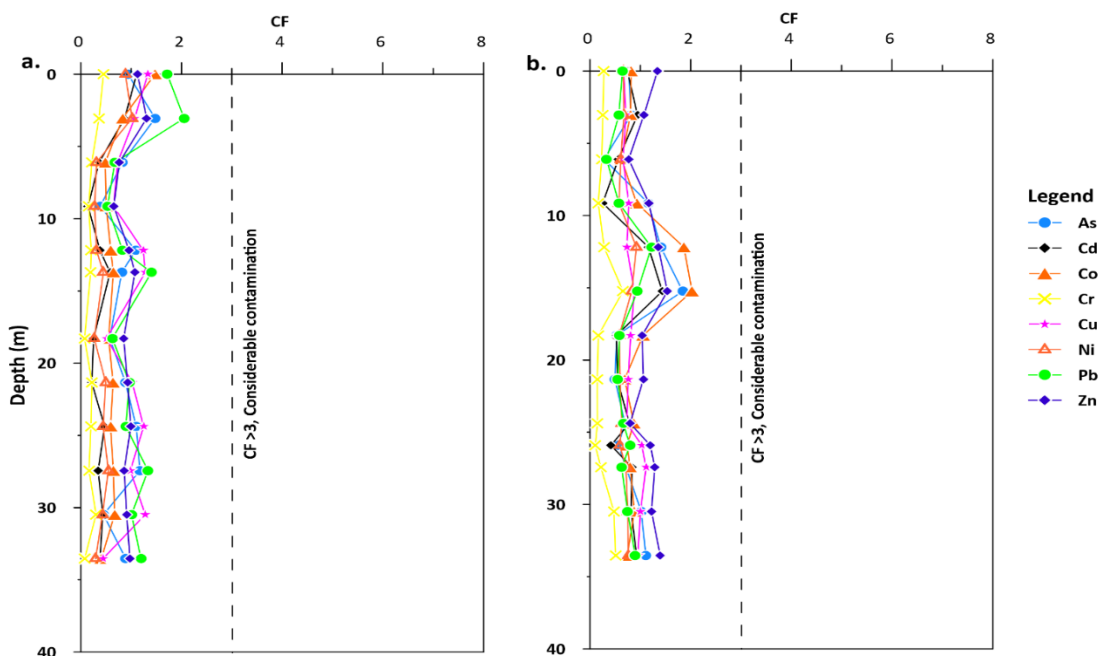


Figure 6.9: Contamination factor (CF) plot for sediment core at, a. Khorabar b. Farshiya

In study area 1 (Gorakhpur), the mean calculated contamination factor values were observed less than one except Pb, indicating no pollution (Figure 6.9a). The mean value of Pb was higher than one but less than three, indicating moderate pollution by Pb at Khorabar. This area comes under the urban region of Gorakhpur so that anthropogenic inputs might be enhanced Pb in sediment cores. The sediment core of Farshiya (Figure 6.9b), showing the calculated CF mean value was less than one except Zn, indicating no pollution in this region. The mean of Zn was greater than one but less than three, representing moderate pollution of Zn in the sediment core of Farshiya. This core was collected from the agricultural field that might be the reason for high Zn in the sediment core.

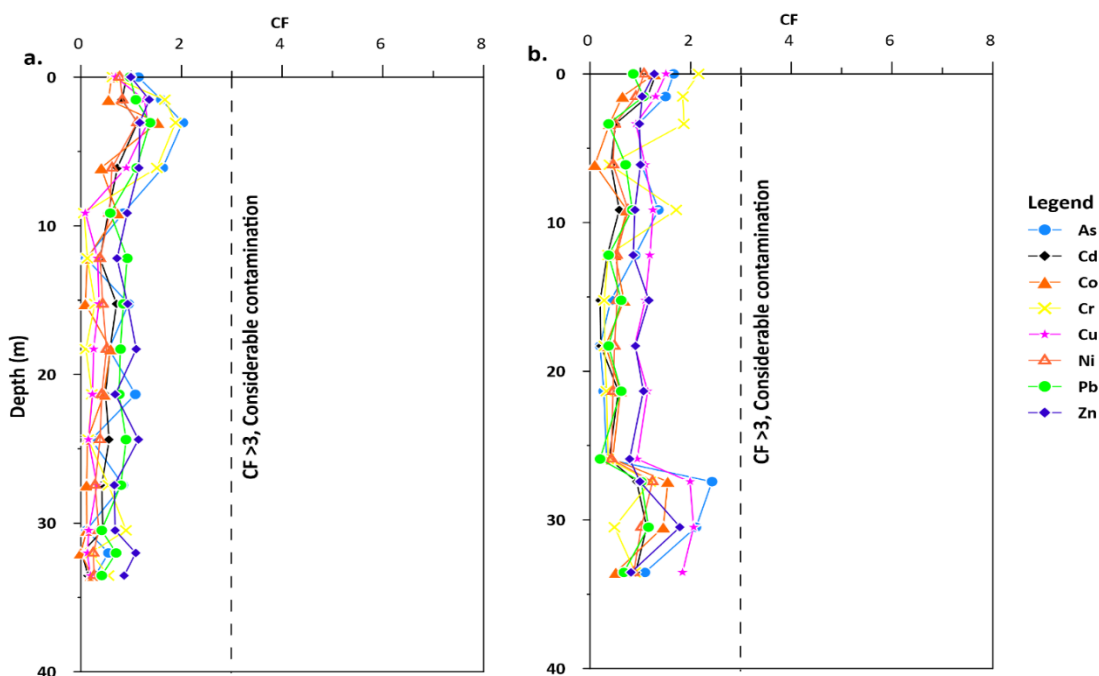


Figure 6.10: Contamination factor (CF) plot for sediment core at, a. Jagadishpur b. Firozpur

In study area 2 (Ghazipur), the mean calculated contamination factor values were observed less than one for As, Cd, Co, Cr, Cu, Ni, Pb and Zn, indicating no pollution in the sediment core at Jagadishpur (Figure 6.10a). However, the mean contamination factor in the sediment core of Firozpur was observed greater than one but less than three for As, Cu and Zn, indicating moderate pollution (Figure 6.10b).

## 6.4. Conclusions

The results have shown that the pH of the water samples was slightly acidic to neutral in nature, while the pH of sediment samples was neutral to slightly alkaline in nature. In Gorakhpur, approx. 36.4% of groundwater samples were above WHO permissible limit while in Ghazipur approx. 33.3% of groundwater samples were above WHO permissible limit. The degree of contamination represented 30% of the water from Gorakhpur, and 67% of the water samples from Ghazipur were highly polluted. The calculated cancer risk (CR) for As showed that 85.2% of water samples were above the US-EPA limit ( $10^{-6}$ ) in Gorakhpur, while in Ghazipur, around 78.4% of water samples were above the US-EPA limit. The correlation plots showed that As and TMs are positively correlated with each other, and their concentration was elevated in the presence of fine silty clay and organic matter. The calculated geoaccumulation indices were indicating that all the sediment cores were fell in the unpolluted region. The enrichment factor for sediment core in study area one, indicating upper section, shows moderate enrichment for all the metals except As and Zn; they were significantly enriched. In study area two, deficiency to minimal enrichment was shown for all the TMs except As. In the upper section and at a depth of 24.4 mbgl As shown a significant enrichment. The contamination factor for As and trace metals was computed, and the findings showed that all metals fell into class 2 represents moderately polluted. At different depths of the sediment cores, the results demonstrated that As, Cd, and Cu had a high range of moderately contaminated to polluted in the research area. Hence, elevated As contamination in agricultural soils and sediment has become a significant problem in the studied area.

## Chapter 7

### Summary and Conclusions

- 7 Conclusions and future research**
  - 7.1. Summary and conclusions
  - 7.2. Outlook for future research

## 7.1. Summary and Conclusions

The present study was conducted on a regional scale to understand the geochemical processes that trigger the As and other solute's mobilization in groundwater and sediment. Geomorphic terrain and groundwater flow significantly influence the As distribution and its mobilization processes in the central Gangetic plain. The study was carried out in two districts (Gorakhpur and Ghazipur) of Uttar Pradesh. Two major geomorphic units (older alluvium and younger alluvium) were recognized and delineated by field observation, remote sensing and available lithologs in the study area. The pH of the groundwater in older alluvium (OA) and younger alluvium (YA) was slightly acidic to neutral. The average As concentration was reported higher in the groundwater of YA (0.05 mg/L) than the OA (0.03 mg/L). However, As concentration in the sediment core of older and younger alluvium was almost comparable. The average concentration of As in YA and OA were observed 11.42 mg/kg and 11.50 mg/kg, respectively, in Gorakhpur. Similarly, in Ghazipur, the average concentration of As in the groundwater of YA (0.06 mg/L) was observed higher than the OA (0.03 mg/L). A similar course of As availability was observed in the sediment cores of Ghazipur district. The average concentration of As in the sediment core of YA (14.26 mg/kg) was observed higher than the OA sediment core (11.08 mg/kg). The results indicate that YA is more susceptible to As contamination compared to the older alluvium.

The piper plot indicates all of the groundwater samples from OA were  $\text{CaHCO}_3$  type. However, a total of 91% of the groundwater samples from YA was of the  $\text{CaHCO}_3$  type, and the remaining 9% of the groundwater from YA and the river water samples were alkaline earth metals with strong acid ( $\text{Cl}$  and  $\text{SO}_4$ ) type, indicating that  $\text{Cl}$  and  $\text{SO}_4$  significantly enhanced As mobilization processes in Gorakhpur district. In contrast, all groundwater and river samples were  $\text{CaHCO}_3$  type, which further stimulates the As mobilization in Ghazipur. The Eh-pH diagram indicates anoxic to post-oxic was existed in the groundwater of both the geomorphic units. In Gorakhpur, ~83% of the groundwater samples from OA and ~88% from YA fell in the  $\text{As}(\text{OH})_3$  field, while the remaining 17% of groundwater samples from OA and 12% from YA fell in the  $\text{HAsO}_4^{2-}$  field. In comparison, ~88% of the groundwater from OA and ~91% from YA were fell in  $\text{As}(\text{OH})_3$  field, and the remaining 12% of the groundwater samples from OA and 9% from YA were fell in the  $\text{HAsO}_4^{2-}$  field.



Hydrogeochemical processes indicate silicate weathering is dominated over carbonate dissolution followed by evaporation and secondary enrichment processes in Gorakhpur districts. Ion exchange and reverse ion exchange are also involved in the groundwater chemistry of OA groundwater. The carbonate weathering is mainly governed by Calcite dissolution in the groundwater of YA, while Dolomite dissolution is the dominant process observed in the groundwater of OA and river water samples. Anthropogenic activities like inputs of fertilizers and sewage discharge contribute nitrate to the groundwater of OA and river water. In Ghazipur, carbonate dissolution is dominated over silicate weathering, followed by ion-exchange processes. Carbonate dissolution was mainly governed by Dolomite dissolution in all the geomorphic units. K and  $\text{NO}_3$  plot indicates sewage discharge and fertilizer inputs enhanced nitrate in OA and YA groundwater, while in river water, nitrate contributed mainly from fertilizers.

The saturation index was used to estimate the degree of equilibrium between water and mineral. The groundwater is in equilibrium with some common minerals such as Albite, Calcite, Dolomite, K-feldspar, Gibbsite, and Hydroxyapatite in the study area indicate changes in the subsurface environment significantly influenced the major ion concentration in the groundwater. The groundwater is supersaturated with Goethite, Hematite, Illite, Kaolinite, and K-mica indicated that clay minerals and metal oxides are precipitated from the groundwater. Siderite, an iron and carbonate mineral, was observed in the study area and existed in equilibrium in groundwater.

According to the thesis findings, reductive dissolution of Fe and Mn oxyhydroxide is the most likely mechanism for As mobilization in the groundwater. Aluminosilicates coated with the Fe and Mn significantly hosting As in the sediment. In study area one (Gorakhpur), arsenic distribution in groundwater and its relationship with major ion chemistry suggested that As releasing mechanism is also linked to anthropogenic inputs (mainly agricultural practices) in the groundwater of OA, while in the groundwater of YA, arsenic mobilization processes are mainly controlled by the reductive dissolution of Fe oxyhydroxide which is supported by microbial degradation of organic matter. In study area two (Ghazipur), dissolution of Fe-Mn oxyhydroxide is the major process for As mobilization in both the geomorphic units; however, the competitive exchange also enhanced As in the groundwater of YA. The interconnectedness of these local circumstances with aquifer sediment and nearby land use in and around the wells often enable As distribution heterogeneity. The local hydrogeological regime (sediment-water interaction) could

also influence As distribution in the water. As release process seems to be more complicated and inconsistent. Additionally to regional geology and hydrogeology may contribute to the diverse As distribution and mobilization patterns.

Geochemical modeling has been carried out to understand the variability of As species in groundwater and sediment cores. An Eh-pH diagram indicated that most groundwater samples fall in the  $\text{As}(\text{OH})_3$  region while river water samples fall in the  $\text{HAsO}_4^{2-}$  region, in both the study area. The oxidation-reduction potential in the groundwater of younger alluvium was more negative than groundwater of older alluvium, which supports As mobilization in the groundwater by desorption of metal (Fe and Mn) oxyhydroxides. Geochemical fractional has been done to identify the As species bound with the different solid minerals phases. A three-step sequential extraction method has been used to separate the As species in aquifer sediment. The result showed that the residual fraction of As was dominant over all the fractions, followed by reducible, oxidizable and acid-soluble fractions. The residual fraction of As in the sediment core was tightly incorporated with crystal structure which was quickly not breakable by applying weak acids. So, the other three fractioned species were only involved in As mobilization. An elevated concentration of As was associated with the upper section of litholog from the older alluvium at Khorabar (Gorakhpur) and Jagadishpur (Ghazipur) is mainly due to the shallow water table, which is responsible for generating an oxidizing subsurface environment and As is getting precipitated over the solid phases of metal oxides. The sediment cores collected from the younger alluvium at Farshiya (Gorakhpur) and Firozpur (Ghazipur) shown an elevated concentration of As associated with the fine dark silty-clay coupled with high organic matter indicates significant holding of As into the solid phases. Results of XRD revealed that secondary minerals like goethite were found in all of the sediment core throughout the profile. The partial solubilization of fibrous goethite indicates As mobilization in the groundwater. The mineralogy study also revealed that a high concentration of As in the sediment core is associated with siderite minerals that act as a sink to the As in subsurface sediment.

It was hypothesized that long-time groundwater abstraction is causing As mobilization and distribution in this aquifer system. Stable isotopic signatures ( $\delta^2\text{H}$ ,  $\delta^{18}\text{O}$  and  $\delta^{13}\text{C}_{\text{TIC}}$ ) were applied to understand the groundwater recharge and discharge processes. Additionally, it also helped to understand the groundwater abstraction impact on hydrogeochemical evolution and subsequent As

release mechanisms. The isotopic result shows that most groundwater samples fall close to the local meteoric water line (LMWL), indicating local precipitation involved in groundwater recharge, which undergoes evaporation at few locations. It indicates that the groundwater used for agricultural practices may have contributed to the drawdown of evaporation. The  $\delta^{13}\text{C}_{\text{TIC}}$  was observed higher in younger alluvium than older alluvium and river water samples in both the study areas. The DIC was calculated from  $\delta^{13}\text{C}_{\text{TIC}}$  and  $p\text{CO}_2$ , indicating silicate weathering and carbonate dissolution were the predominant sources of DIC in the groundwater. An inverse relationship was observed between  $\delta^{13}\text{C}_{\text{TIC}}$  and TOC. The higher  $\delta^{13}\text{C}_{\text{TIC}}$  indicating high microbial activity and vice versa. Deeper aquifers were having limited microbial activity indicating the dominance of lighter isotopes ( $\delta^{13}\text{C}_{\text{TIC}}$ ). DOC positively correlated with Fe and As, indicating enhanced microbial activity that helped to create a reductive environment that supports As mobilization in the study areas.

Arsenic is the most carcinogenic element listed in the drinking water guidelines and may cause health catastrophes even at 10  $\mu\text{g/L}$  levels. Thus, it is absolutely important to measure the concentration of As even at ultra-trace levels in groundwater and in sediments. In the study area, ~34% of groundwater are not safe for drinking purposes. The observed As concentration was higher than the WHO prescribed limit (10  $\mu\text{g/L}$ ). In the sediment core, pH was slightly alkaline in nature. The correlation plot indicating that As and trace metals (TMs) are positively correlated with the fine silty clay and organic matter indicates a similar origin from a common source or homogeneous geochemical behavior and revealed that they might be coming from metals chelation. The negative correlation between trace metals and sand indicated coarse sediment could not be able to adsorb metals on their surfaces. The geoaccumulation indices indicate that all the sediment cores are unpolluted in the OA and YA sediment cores except for As, Co and Zn at a depth of 12-17 mbgl, which indicates dark grey fine silty clay holding these metals in Gorakhpur. A similar result was observed in Ghazipur. All the metals were fell in unpolluted class except for As, Cu and Cr in the upper section of OA, which indicates metals get precipitated under oxidizing subsurface environment. While in YA, a high concentration of As, Cu and Zn was observed and fell in moderately polluted class indicates mineral of these metals associated with metals enrichment. Enrichment factor indicates deficiency to minimal enrichment for all the analyzed TMs except As and Zn. In the upper section of the sediment core and at a depth of 24.4 mbgl, As

and Zn showed significant metal enrichment at this depth. The contamination factor was calculated for As, and trace metals and the results show all metals were fell in class 2 (moderately polluted). These findings are critical in determining soil quality and can assist local governments in taking remediation action. The results revealed that As, Cd and Cu having a high band of moderately polluted to polluted class in the study area at different depths of the sediment cores. As a result, rising arsenic levels in agricultural soils/sediment have become a serious issue.

## 7.2. Outlook of the future research

The present study is carried out on a regional scale to understand the As fate and mobilization in the studied area. Based on the different geomorphological units (older a younger alluvium), a comparative study has been carried out to understand the role of As fate and mobilization in the central Gangetic basin. Although we have collected four sediment cores with a maximum depth of 35 mbgl, it will not be sufficient to understand the behavior of the role of As mobilization in the central Gangetic plain. A deeper sediment core (300 mbgl) will be helpful to recognize the As contaminated aquifer and safe aquifer and their interconnectivity with the groundwater. As speciation in sediment core will be carried out by applying the advanced methodology in a holistic approach to get better results. Since our observations show that As adsorbed /desorbed by reductive dissolution of metal oxyhydroxide, which is triggered by micro-bacterial degradation of organic matter. Hence, future studies will also be focusing on identifying the micro-bacterial genera that reduced Fe-bearing minerals in the central Gangetic plain and liberated As into the groundwater.

Although we have calculated the As and trace metals exposure through groundwater, we were not considered the food and raw vegetable in dietary intake in this study. The daily intake of As and other toxic elements from different exposure pathways such as cooked food and raw vegetables need to be adequately estimated to compute the actual As and trace metal exposure for the local population resided in the study area. So, future studies should also focus on groundwater and other food components (grains and vegetables) on a large sample basis to get an appropriate result.

---

## References

- Acharyya, S. K., & Shah, B. A. (2004). Risk of arsenic contamination in groundwater affecting the Ganga Alluvial Plain, India. *Environmental Health Perspectives*, 112(1). <https://doi.org/10.1289/ehp.112-a19>
- Acharyya, S. K., & Shah, B. A. (2007). Groundwater arsenic contamination affecting different geologic domains in India—a review: Influence of geological setting, fluvial geomorphology and Quaternary stratigraphy. *Journal of Environmental Science and Health, Part A*, 42(12), 1795–1805. <https://doi.org/10.1080/10934520701566744>
- Acharyya, S. K., Chakraborty, P., Lahiri, S., Raymahashay, B. C., Guha, S., & Bhowmik, A. (1999). Arsenic poisoning in the Ganges delta. *Nature*, 401(6753), 545; discussion 546–547. <https://doi.org/10.1038/44052>
- Aggarwal, P. K. (2000). Isotope Hydrology of Groundwater in Bangladesh: Implications for Characterization and Mitigation of Arsenic in Groundwater: a Report on. IAEA.
- Ahamed, S., Kumar Sengupta, M., Mukherjee, A., Amir Hossain, M., Das, B., Nayak, B., Pal, A., Chandra Mukherjee, S., Pati, S., Nath Dutta, R., Chatterjee, G., Mukherjee, A., Srivastava, R., & Chakraborti, D. (2006). Arsenic groundwater contamination and its health effects in the state of Uttar Pradesh (UP) in upper and middle Ganga plain, India: A severe danger. *Science of The Total Environment*, 370(2–3), 310–322. <https://doi.org/10.1016/j.scitotenv.2006.06.015>
- Ahmed, K. M., Bhattacharya, P., Hasan, M. A., Akhter, S. H., Alam, S. M., Bhuyian, M. H., Imam, M. B., Khan, A. A., & Sracek, O. (2004). Arsenic enrichment in groundwater of the alluvial aquifers in Bangladesh: An overview. *Applied Geochemistry*, 19(2), 181–200.
- Ahsan, D. A., DelValls, T. A., & Blasco, J. (2009). Distribution of arsenic and trace metals in the floodplain agricultural soil of Bangladesh. *Bulletin of Environmental Contamination and Toxicology*, 82(1), 11–15.
- Akai, J., Izumi, K., Fukuhara, H., Masuda, H., Nakano, S., Yoshimura, T., Ohfuji, H., Md Anawar, H., & Akai, K. (2004). Mineralogical and geomicrobiological investigations on groundwater arsenic enrichment in Bangladesh. *Applied Geochemistry*, 19(2), 215–230. <https://doi.org/10.1016/j.apgeochem.2003.09.008>
- Alam, M. B., & Sattar, M. A. (2000). Assessment of arsenic contamination in soils and waters in some areas of Bangladesh. *Water Science and Technology*, 42(7–8), 185–192.
- Alhashemi, A. H., Sekhavatjou, M. S., Kiabi, B. H., & Karbassi, A. R. (2012). Bioaccumulation of trace elements in water, sediment, and six fish species from a freshwater wetland, Iran. *Microchemical Journal*, 104, 1–6.
- Ali, H., Khan, E., & Ilahi, I. (2019). Environmental Chemistry and Ecotoxicology of Hazardous Heavy Metals: Environmental Persistence, Toxicity, and Bioaccumulation. *Journal of Chemistry*, 2019, e6730305. <https://doi.org/10.1155/2019/6730305>

- 
- Ali, I., Rahman, A., Khan, T. A., Alam, S. D., & Khan, J. (2012). *Recent Trends of Arsenic Contamination in Groundwater of Ballia District, Uttar Pradesh, India*. *Gazi University Journal of Science*, 25(4), 853-861.
- Anawar, H. M., Akai, J., & Sakugawa, H. (2004). Mobilization of arsenic from subsurface sediments by effect of bicarbonate ions in groundwater. *Chemosphere*, 54(6), 753-762.
- Anawar, H. M., Akai, J., Komaki, K., Terao, H., Yoshioka, T., Ishizuka, T., Safiullah, S., & Kato, K. (2003). Geochemical occurrence of arsenic in groundwater of Bangladesh: Sources and mobilization processes. *Journal of Geochemical Exploration*, 77(2-3), 109-131. [https://doi.org/10.1016/S0375-6742\(02\)00273-X](https://doi.org/10.1016/S0375-6742(02)00273-X)
- Anawar, H. M., Akai, J., Yoshioka, T., Konohira, E., Lee, J. Y., Fukuhara, H., Alam, M. T. K., & Garcia-Sanchez, A. (2006). Mobilization of arsenic in groundwater of Bangladesh: Evidence from an incubation study. *Environmental Geochemistry and Health*, 28(6), 553-565.
- Appleyard, S. J., Angeloni, J., & Watkins, R. (2006). Arsenic-rich groundwater in an urban area experiencing drought and increasing population density, Perth, Australia. *Applied Geochemistry*, 21(1), 83-97.
- Backman, B., Bodiš, D., Lahermo, P., Rapant, S., & Tarvainen, T. (1998). Application of a groundwater contamination index in Finland and Slovakia. *Environmental Geology*, 36(1), 55-64.
- Bagchi, S. (2007). *Arsenic threat reaching global dimensions*. Can Med Assoc.
- Baig, J. A., Kazi, T. G., Arain, M. B., Shah, A. Q., Sarfraz, R. A., Afridi, H. I., Kandhro, G. A., Jamali, M. K., & Khan, S. (2009). Arsenic fractionation in sediments of different origins using BCR sequential and single extraction methods. *Journal of Hazardous Materials*, 167(1-3), 745-751. <https://doi.org/10.1016/j.jhazmat.2009.01.040>
- Ball, J. W., & Nordstrom, D. K. (1991). *WATEQ4F-User's manual with revised thermodynamic data base and test cases for calculating speciation of major, trace and redox elements in natural waters*.
- Barringer, J. L., & Reilly, P. A. (2013). Arsenic in groundwater: A summary of sources and the biogeochemical and hydrogeologic factors affecting arsenic occurrence and mobility. *Current perspectives in contaminant hydrology and water resources sustainability*. InTech, 83-116.
- Belkhiri, L., Tiri, A., & Mouni, L. (2018). Assessment of Heavy Metals Contamination in Groundwater: A Case Study of the South of Setif Area, East Algeria. In D. Komatina (Ed.), *Achievements and Challenges of Integrated River Basin Management*. InTech. <https://doi.org/10.5772/intechopen.75734>
- Benner, R., Newell, S. Y., Maccubbin, A. E., & Hodson, R. E. (1984). Relative contributions of bacteria and fungi to rates of degradation of lignocellulosic detritus in salt-marsh sediments. *Applied and Environmental Microbiology*, 48(1), 36-40.
- Bershaw, J. (2018). Controls on Deuterium Excess across Asia. *Geosciences*, 8(7), 257. <https://doi.org/10.3390/geosciences8070257>
-

- Bhagat, S. K., Tung, T. M., & Yaseen, Z. M. (2021). Heavy metal contamination prediction using ensemble model: Case study of Bay sedimentation, Australia. *Journal of Hazardous Materials*, 403, 123492. <https://doi.org/10.1016/j.jhazmat.2020.123492>
- Bhanja, S. N., Mukherjee, A., Rodell, M., Wada, Y., Chattopadhyay, S., Velicogna, I., Velicogna, I., Pangaluru, K., & Famiglietti, J. S. (2017). Groundwater rejuvenation in parts of India influenced by water-policy change implementation. *Scientific reports*, 7(1), 1-7.
- Bhardwaj, V., & Singh, D. S. (2011). Surface and groundwater quality characterization of Deoria District, Ganga Plain, India. *Environmental Earth Sciences*, 63(2), 383–395. <https://doi.org/10.1007/s12665-010-0709-x>
- Bhardwaj, V., Singh, D. S., & Singh, A. K. (2010). Water quality of the Chhoti Gandak River using principal component analysis, Ganga Plain, India. *Journal of Earth System Science*, 119(1), 117–127. <https://doi.org/10.1007/s12040-010-0007-8>
- Bhattacharya, P., Chatterjee, D., & Jacks, G. (1997). Occurrence of arsenic-contaminated Groundwater in alluvial aquifers from Delta plains, eastern India: Options for safe drinking water supply. *International Journal of Water Resources Development*, 13(1), 79–92.
- Bhattacharya, P., Mukherjee, A., & Mukherjee, A. B. (2011). *Arsenic in Groundwater of India* (pp. 150–164). Elsevier Inc. <http://urn.kb.se/resolve?urn=urn:nbn:se:kth:diva-261514>
- BIS (Bureau of Indian Standard, 2012) IS 10500 (2012): Drinking water (cgwb.gov.in) (Accessed on 29/07/21)
- Bishop, P. K. (1990). Precipitation of dissolved carbonate species from natural waters for  $\delta^{13}\text{C}$  analysis—A critical appraisal. *Chemical Geology: Isotope Geoscience Section*, 80(3), 251–259.
- Bissen, M., & Frimmel, F. H. (2003). Arsenic—a review. Part I: Occurrence, toxicity, speciation, mobility. *Acta Hydrochimica et Hydrobiologica*, 31(1), 9–18.
- Biswas, A., Nath, B., Bhattacharya, P., Halder, D., Kundu, A. K., Mandal, U., Mukherjee, A., Chatterjee, D., Mörth, C. M., & Jacks, G. (2012a). Hydrogeochemical contrast between brown and grey sand aquifers in shallow depth of Bengal Basin: Consequences for sustainable drinking water supply. *Science of the Total Environment*, 431, 402–412. <https://doi.org/10.1016/j.scitotenv.2012.05.031>
- Bjorn, P., & Roychoudhury, A. N. (2015). Application, chemical interaction and fate of iron minerals in polluted sediment and soils. *Current Pollution Reports*, 1(4), 265–279.
- Blowes, D. W., Ptacek, C. J., Jambor, J. L., Weisener, C. G., Paktunc, D., Gould, W. D., & Johnson, D. B. (2014). 11.5—The Geochemistry of Acid Mine Drainage. In H. D. Holland & K. K. Turekian (Eds.), *Treatise on Geochemistry (Second Edition)* (pp. 131–190). Elsevier. <https://doi.org/10.1016/B978-0-08-095975-7.00905-0>
- Bonsor, H. C., MacDonald, A. M., Ahmed, K. M., Burgess, W. G., Basharat, M., Calow, R. C., Dixit, A., Foster, S. S. D., Gopal, K., Lapworth, D. J., Moench, M., Mukherjee, A., Rao, M. S., Shamsudduha, M., Smith, L., Taylor, R. G., Tucker, J., van Steenbergen, F., Yadav, S. K., & Zahid, A. (2017). Hydrogeological typologies of the Indo-Gangetic basin alluvial aquifer, South Asia. *Hydrogeology Journal*, 25(5), 1377–1406. <https://doi.org/10.1007/s10040-017-1550-z>

- Boretti, A., & Rosa, L. (2019). Reassessing the projections of the world water development report. *NPJ Clean Water*, 2(1), 1-6.
- Brammer, H., & Ravenscroft, P. (2009). Arsenic in groundwater: A threat to sustainable agriculture in South and South-east Asia. *Environment International*, 35(3), 647–654.
- Brenninkmeijer, C. A. M., & Morrison, P. D. (1987). An automated system for isotopic equilibration of CO<sub>2</sub> and H<sub>2</sub>O for 18O analysis of water. *Chemical Geology: Isotope Geoscience Section*, 66(1–2), 21–26.
- Brevik, E. C., Slaughter, L., Singh, B. R., Steffan, J. J., Collier, D., Barnhart, P., & Pereira, P. (2020). Soil and human health: Current status and future needs. *Air, Soil and Water Research*, 13, 1178622120934441.
- Bundschuh, J., & Maity, J. P. (2015). Geothermal arsenic: Occurrence, mobility and environmental implications. *Renewable and Sustainable Energy Reviews*, 42, 1214–1222. <https://doi.org/10.1016/j.rser.2014.10.092>
- Burgess, W. G., Hoque, M. A., Michael, H. A., Voss, C. I., Breit, G. N., & Ahmed, K. M. (2010). Vulnerability of deep groundwater in the Bengal Aquifer System to contamination by arsenic. *Nature Geoscience*, 3(2), 83–87. <https://doi.org/10.1038/ngeo750>
- Carrard, N., Foster, T., & Willetts, J. (2019). Groundwater as a source of drinking water in southeast Asia and the Pacific: A multi-country review of current reliance and resource concerns. *Water*, 11(8), 1605.
- Central Ground Water Board Gorakhpur .pdf (cgwb.gov.in) (Accessed on 26.05.2021).
- Central Ground Water Board.<http://cgwb.gov.in> (Accessed on 23/02/2021), Year Book 17-18 .pdf
- Chakraborti, D., Mukherjee, S. C., Pati, S., Sengupta, M. K., Rahman, M. M., Chowdhury, U. K., Lodh, D., Chanda, C. R., Chakraborti, A. K., & Basu, G. K. (2003). Arsenic groundwater contamination in Middle Ganga Plain, Bihar, India: A future danger? *Environmental Health Perspectives*, 111(9), 1194–1201. <https://doi.org/10.1289/ehp.5966>
- Chakraborti, D., Rahman, M. M., Das, B., Chatterjee, A., Das, D., Nayak, B., Pal, A., Chowdhury, U. K., Ahmed, S., Biswas, B. K., Sengupta, M. K., Hossain, Md. A., Samanta, G., Roy, M. M., Dutta, R. N., Saha, K. C., Mukherjee, S. C., Pati, S., Kar, P. B., Kumar, M. (2017). Groundwater arsenic contamination and its health effects in India. *Hydrogeology Journal*, 25(4), 1165–1181. <https://doi.org/10.1007/s10040-017-1556-6>
- Chakraborti, D., Sengupta, M. K., Rahman, M. M., Ahamed, S., Chowdhury, U. K., Hossain, M. A., Mukherjee, S. C., Pati, S., Saha, K. C., Dutta, R. N., & Quamruzzaman, Q. (2004). Groundwater arsenic contamination and its health effects in the Ganga-Meghna-Brahmaputra plain. *Journal of Environmental Monitoring: JEM*, 6(6), 74N-83N.
- Chakraborti, D., Singh, S. K., Rahman, M. M., Dutta, R. N., Mukherjee, S. C., Pati, S., & Kar, P. B. (2018). Groundwater Arsenic Contamination in the Ganga River Basin: A Future Health Danger. *International Journal of Environmental Research and Public Health*, 15(2), 180. <https://doi.org/10.3390/ijerph15020180>
- Chakraborty, M., Mukherjee, A., & Ahmed, K. M. (2015). A Review of Groundwater Arsenic in the Bengal Basin, Bangladesh and India: From Source to Sink. *Current Pollution Reports*, 1(4), 220–247. <https://doi.org/10.1007/s40726-015-0022-0>



- Chakraborty, S., Weindorf, D. C., Deb, S., Li, B., Paul, S., Choudhury, A., & Ray, D. P. (2017). Rapid assessment of regional soil arsenic pollution risk via diffuse reflectance spectroscopy. *Geoderma*, 289, 72–81. <https://doi.org/10.1016/j.geoderma.2016.11.024>
- Chandrasekharam, D., Joshi, A., & Chandrasekhar, V. (2007). *Arsenic content in groundwater and soils of Ballia, Uttar Pradesh*. Taylor & Francis Ltd.
- Charlet, L., Chakraborty, S., Appelo, C. A. J., Roman-Ross, G., Nath, B., Ansari, A. A., Lanson, M., Chatterjee, D., & Mallik, S. B. (2007). Chemodynamics of an arsenic “hotspot” in a West Bengal aquifer: A field and reactive transport modeling study. *Applied Geochemistry*, 22(7), 1273–1292.
- Chatterjee, M., Silva Filho, E. V., Sarkar, S. K., Sella, S. M., Bhattacharya, A., Satpathy, K. K., Prasad, M. V. R., Chakraborty, S., & Bhattacharya, B. D. (2007). Distribution and possible source of trace elements in the sediment cores of a tropical macrotidal estuary and their ecotoxicological significance. *Environment International*, 33(3), 346–356. <https://doi.org/10.1016/j.envint.2006.11.013>
- Chatterjee, S., Moogoui, R., & Gupta, D. K. (2017). Arsenic: Source, occurrence, cycle, and detection. In *Arsenic Contamination in the Environment* (pp. 13–35). Springer.
- Chattopadhyay, A., Singh, A. P., Singh, S. K., Barman, A., Patra, A., Mondal, B. P., & Banerjee, K. (2020). Spatial variability of arsenic in Indo-Gangetic basin of Varanasi and its cancer risk assessment. *Chemosphere*, 238, 124623. <https://doi.org/10.1016/j.chemosphere.2019.124623>
- Chauhan, V. S., Nickson, R. T., Chauhan, D., Iyengar, L., & Sankararamakrishnan, N. (2009). Ground water geochemistry of Ballia district, Uttar Pradesh, India and mechanism of arsenic release. *Chemosphere*, 75(1), 83–91. <https://doi.org/10.1016/j.chemosphere.2008.11.065>
- Chen, M., & Ma, L. Q. (2001). Comparison of Three Aqua Regia Digestion Methods for Twenty Florida Soils. *Soil Science Society of America Journal*, 65(2), 491–499. <https://doi.org/10.2136/sssaj2001.652491x>
- Chen, Y.-W., Yu, X., & Belzile, N. (2019). Arsenic speciation in surface waters and lake sediments in an abandoned mine site and field observations of arsenic eco-toxicity. *Journal of Geochemical Exploration*, 205, 106349. <https://doi.org/10.1016/j.gexplo.2019.106349>
- Chidambaram, S., Karmegam, U., Sasidhar, P., Prasanna, M. V., Manivannan, R., Arunachalam, S., Manikandan, S., & Anandhan, P. (2011). Significance of saturation index of certain clay minerals in shallow coastal groundwater, in and around Kalpakkam, Tamil Nadu, India. *Journal of Earth System Science*, 120(5), 897–909.
- Connon, S. A., Koski, A. K., Neal, A. L., Wood, S. A., & Magnuson, T. S. (2008). Ecophysiology and geochemistry of microbial arsenic oxidation within a high arsenic, circumneutral hot spring system of the Alvord Desert: Ecophysiology and geochemistry of microbial arsenic oxidation. *FEMS Microbiology Ecology*, 64(1), 117–128. <https://doi.org/10.1111/j.1574-6941.2008.00456.x>
- Cooper, K. J., Whitaker, F. F., Anesio, A. M., Naish, M., Reynolds, D. M., & Evans, E. L. (2016). Dissolved organic carbon transformations and microbial community response to variations

- in recharge waters in a shallow carbonate aquifer. *Biogeochemistry*, 129(1), 215–234. <https://doi.org/10.1007/s10533-016-0226-4>
- Cornell, R. M., & Schwertmann, U. (2003). *The iron oxides: Structure, properties, reactions, occurrences and uses*. John Wiley & Sons.
- Craig, H. (1961). Isotopic Variations in Meteoric Waters. *Science*, 133(3465), 1702–1703. <https://doi.org/10.1126/science.133.3465.1702>
- Das, B., & Pal, S. C. (2020). Assessment of groundwater recharge and its potential zone identification in groundwater-stressed Goghat-I block of Hugli District, West Bengal, India. *Environment, Development and Sustainability*, 22(6), 5905–5923. <https://doi.org/10.1007/s10668-019-00457-7>
- Das, B., & Pal, S. C. (2020). Assessment of groundwater recharge and its potential zone identification in groundwater-stressed Goghat-I block of Hugli District, West Bengal, India. *Environment, Development and Sustainability*, 22(6), 5905–5923.
- Datta, D. V., & Kaul, M. K. (1976). Arsenic content of drinking water in villages in northern India. A concept of arsenicosis. *The Journal of the Association of Physicians of India*, 24(9), 599–604.
- Datta, P. S., Deb, D. L., & Tyagi, S. K. (1996). Stable isotope ( $^{18}\text{O}$ ) investigations on the processes controlling fluoride contamination of groundwater. *Journal of Contaminant Hydrology*, 12.
- Datta, S., Neal, A. W., Mohajerin, T. J., Ocheltree, T., Rosenheim, B. E., White, C. D., & Johannesson, K. H. (2011). Perennial ponds are not an important source of water or dissolved organic matter to groundwaters with high arsenic concentrations in West Bengal, India: HIGH ARSENIC GROUNDWATERS OF WEST BENGAL. *Geophysical Research Letters*, 38(20), n/a-n/a. <https://doi.org/10.1029/2011GL049301>
- Deverel, S. J., & Fujii, R. (1990). Chemistry of trace elements in soils and groundwater. *Agricultural Salinity Assessment and Management. American Society of Civil Engineers, New York*, 64–90.
- DeVore, C. L., Rodriguez-Freire, L., Mehdi-Ali, A., Ducheneaux, C., Artyushkova, K., Zhou, Z., Latta, D. E., Lueth, V. W., Gonzales, M., & Lewis, J. (2019). Effect of bicarbonate and phosphate on arsenic release from mining-impacted sediments in the Cheyenne river watershed, South Dakota, USA. *Environmental Science: Processes & Impacts*, 21(3), 456–468.
- Dhawan, V. (2017, January). Water and agriculture in India. In *Background paper for the South Asia expert panel during the Global Forum for Food and Agriculture (GFFA)* (p. 15).
- Dixit, S., & Hering, J. G. (2003). Comparison of arsenic (V) and arsenic (III) sorption onto iron oxide minerals: Implications for arsenic mobility. *Environmental Science & Technology*, 37(18), 4182–4189.
- Doctor, D. H., Kendall, C., Sebestyen, S. D., Shanley, J. B., Ohte, N., & Boyer, E. W. (2008). Carbon isotope fractionation of dissolved inorganic carbon (DIC) due to outgassing of carbon dioxide from a headwater stream. *Hydrological Processes*, 22(14), 2410–2423. <https://doi.org/10.1002/hyp.6833>

- 
- Doušová, B., Grygar, T., Martaus, A., Fuitová, L., Koloušek, D., & Machovič, V. (2006). Sorption of AsV on aluminosilicates treated with FeII nanoparticles. *Journal of Colloid and Interface Science*, 302(2), 424–431.
- Emery, K. O., Wigley, R. L., Bartlett, A. S., Rubin, M., & Barghoorn, E. S. (1967). Freshwater peat on the continental shelf. *Science*, 158(3806), 1301–1307.
- Epstein, S., & Mayeda, T. (1953). Variation of O18 content of waters from natural sources. *Geochimica et Cosmochimica Acta*, 4(5), 213–224.
- Federation, W. E., & Association, A. P. H. (2005). Standard methods for the examination of water and wastewater. *American Public Health Association (APHA): Washington, DC, USA*.
- Gäbler, H.-E. (1997). Mobility of heavy metals as a function of pH of samples from an overbank sediment profile contaminated by mining activities. *Journal of Geochemical Exploration*, 58(2), 185–194. [https://doi.org/10.1016/S0375-6742\(96\)00061-1](https://doi.org/10.1016/S0375-6742(96)00061-1)
- Garat, R., Chakraborty, A. K., Dey, S. B., & Saha, K. C. (1984). Chronic arsenic poisoning from tube-well water. *Journal of the Indian Medical Association*, 82(1), 34–35.
- Garg, N. K., & Hassan, Q. (2007). Alarming scarcity of water in India. *Current Science*, 93(7), 932–941.
- Gat, J. R. (1996). Oxygen and hydrogen isotopes in the hydrologic cycle. *Annual Review of Earth and Planetary Sciences*, 24(1), 225–262.
- Gates-Rector, S., & Blanton, T. (2019). The powder diffraction file: A quality materials characterization database. *Powder Diffraction*, 34(4), 352–360.
- Gault, A. G., Polya, D. A., Lythgoe, P. R., Farquhar, M. L., Charnock, J. M., & Wogelius, R. A. (2003). Arsenic speciation in surface waters and sediments in a contaminated waterway: An IC–ICP–MS and XAS based study. *Applied Geochemistry*, 18(9), 1387–1397. [https://doi.org/10.1016/S0883-2927\(03\)00058-1](https://doi.org/10.1016/S0883-2927(03)00058-1)
- Ghosh, A., Singh, S. K., Bose, N., & Chowdhary, S. (2007). Arsenic contaminated aquifers: A study of the Ganga levee zone in Bihar, India. *Symposium on Arsenic: The Geography of a Global Problem, Royal Geographical Society, London, 29th August*.
- Ghosh, D., Deb, A., Patra, K. K., Sengupta, R., & Bera, S. (2007). Double Health Risk in Arsenic Contaminated Drinking Water – Evidence of Enhanced Alpha Radioactivity. *Water, Air, and Soil Pollution*, 187(1–4), 81–87. <https://doi.org/10.1007/s11270-007-9499-5>
- Ghosh, N. C., Saha, D., Sinharay, S. P., & Srivastava, D. S. (2010). Mitigation and remedy of ground water arsenic menace in India: A vision document. *New Delhi: National Institute of Hydrology, Roorkee and Central Ground Water Board*, 143.
- Ghosh, N. C., Saha, D., Sinharay, S. P., & Srivastava, D. S. (2010). Mitigation and remedy of ground water arsenic menace in India: a vision document. *New Delhi: National Institute of Hydrology, Roorkee and Central Ground Water Board*, 143.
- Gibson, J. J., Birks, S. J., & Yi, Y. (2016). Stable isotope mass balance of lakes: A contemporary perspective. *Quaternary Science Reviews*, 131, 316–328. <https://doi.org/10.1016/j.quascirev.2015.04.013>
-

- 
- Govil, P., Reddy, G., & Krishna, A. (2001). Contamination of soil due to heavy metals in the Patancheru industrial development area, Andhra Pradesh, India. *Environmental Geology*, 41(3–4), 461–469. <https://doi.org/10.1007/s002540100415>
- Guo, H., Zhang, D., Wen, D., Wu, Y., Ni, P., Jiang, Y., Guo, Q., Li, F., Zheng, H., & Zhou, Y. (2014). Arsenic mobilization in aquifers of the southwest Songnen basin, P.R. China: Evidences from chemical and isotopic characteristics. *Science of The Total Environment*, 490, 590–602. <https://doi.org/10.1016/j.scitotenv.2014.05.050>
- Guo, M., Li, J., Sheng, C., Xu, J., & Wu, L. (2017). A Review of Wetland Remote Sensing. *Sensors (Basel, Switzerland)*, 17(4), 777. <https://doi.org/10.3390/s17040777>
- Guo, Z., Li, Y., & Wu, W. (2009). Sorption of U(VI) on goethite: Effects of pH, ionic strength, phosphate, carbonate and fulvic acid. *Applied Radiation and Isotopes*, 67(6), 996–1000. <https://doi.org/10.1016/j.apradiso.2009.02.001>
- Gupta, S. K., & Deshpande, R. D. (2003). Synoptic hydrology of India from the data of isotopes in precipitation. *Current Science*, 1591–1595.
- Gupta, S. K., & Deshpande, R. D. (2005). The need and potential applications of a network for monitoring of isotopes in waters of India. *CURRENT SCIENCE*, 88(1), 12.
- Hakanson, L. (1980). An ecological risk index for aquatic pollution control. a sedimentological approach. *Water Research*, 14(8), 975–1001. [https://doi.org/10.1016/0043-1354\(80\)90143-8](https://doi.org/10.1016/0043-1354(80)90143-8)
- Hamid, A., Bhat, S. U., & Jehangir, A. (2020). Local determinants influencing stream water quality. *Applied Water Science*, 10(1), 24. <https://doi.org/10.1007/s13201-019-1043-4>
- Hao, L., Liu, M., Wang, N., & Li, G. (2018). A critical review on arsenic removal from water using iron-based adsorbents. *RSC Advances*, 8(69), 39545–39560.
- Haque, T. A., Tabassum, M., Jamilur Rahman, M., Siddique, M. N. E. A., Mostafa, M. G., Abdul Khalaque, M., Abedine, Z., & Hamidi, H. (2020). Environmental Analysis of Arsenic in Water, Soil and Food Materials from Highly Contaminated Area of Alampur Village, Amjhupi Union, Meherpur. *Advanced Journal of Chemistry-Section A*, 3(2), 181–191.
- Harvey, C. F., Ashfaque, K. N., Yu, W., Badruzzaman, A. B. M., Ali, M. A., Oates, P. M., Michael, H. A., Neumann, R. B., Beckie, R., Islam, S., & Ahmed, M. F. (2006). Groundwater dynamics and arsenic contamination in Bangladesh. *Chemical Geology*, 228(1–3), 112–136. <https://doi.org/10.1016/j.chemgeo.2005.11.025>
- Harvey, C. F., Swartz, C. H., Badruzzaman, A. B. M., Keon-Blute, N., Yu, W., Ali, M. A., Jay, J., Beckie, R., Niedan, V., & Brabander, D. (2005). Groundwater arsenic contamination on the Ganges Delta: Biogeochemistry, hydrology, human perturbations, and human suffering on a large scale. *Comptes Rendus Geoscience*, 337(1–2), 285–296.
- Harvey, C. F., Swartz, C. H., Badruzzaman, A. B. M., Keon-Blute, N., Yu, W., Ali, M. A., Jay, J., Beckie, R., Niedan, V., & Brabander, D. (2002). Arsenic mobility and groundwater extraction in Bangladesh. *Science*, 298(5598), 1602–1606.
- Hasan, M. A., Sikder, A. M., Jacks, G., & Sracek, O. (2009). Geochemistry and mineralogy of shallow alluvial aquifers in Daudkandi upazila in the Meghna flood plain, Bangladesh. *Environ Geol*, 13.
-

- 
- Hem, J. D. (1959). *Study and interpretation of the chemical characteristics of natural water*. (Vol. 2254). Department of the Interior, *US Geological Survey*.
- Herath, I., Vithanage, M., Bundschuh, J., Maity, J. P., & Bhattacharya, P. (2016). *Natural Arsenic in Global Groundwaters: Distribution and Geochemical Triggers for Mobilization*. 22.
- Herath, I., Vithanage, M., Bundschuh, J., Maity, J. P., & Bhattacharya, P. (2016). Natural arsenic in global groundwaters: distribution and geochemical triggers for mobilization. *Current pollution reports*, 2(1), 68-89.
- Heroy, D. C., Kuehl, S. A., & Goodbred, S. L. (2003). Mineralogy of the Ganges and Brahmaputra Rivers: Implications for river switching and Late Quaternary climate change. *Sedimentary Geology*, 155(3–4), 343–359. [https://doi.org/10.1016/S0037-0738\(02\)00186-0](https://doi.org/10.1016/S0037-0738(02)00186-0)
- Ho, H. H., Swennen, R., Cappuyns, V., Vassilieva, E., & Van Tran, T. (2012). Necessity of normalization to aluminum to assess the contamination by heavy metals and arsenic in sediments near Haiphong Harbor, Vietnam. *Journal of Asian Earth Sciences*, 56, 229–239.
- Hornibrook, E. R. C., Longstaffe, F. J., & Fyfe, W. S. (2000). Evolution of stable carbon isotope compositions for methane and carbon dioxide in freshwater wetlands and other anaerobic environments. *Geochimica et Cosmochimica Acta*, 64(6), 1013–1027. [https://doi.org/10.1016/S0016-7037\(99\)00321-X](https://doi.org/10.1016/S0016-7037(99)00321-X)
- Hossain, M., Bhattacharya, P., Frappe, S. K., Jacks, G., Islam, M. M., Rahman, M. M., von Brömssen, M., Hasan, M. A., & Ahmed, K. M. (2014). Sediment color tool for targeting arsenic-safe aquifers for the installation of shallow drinking water tubewells. *Science of The Total Environment*, 493, 615–625. <https://doi.org/10.1016/j.scitotenv.2014.05.064>
- Hossain, S., Ishiyama, T., Hachinohe, S., & Oguchi, C. T. (2019). Leaching Behavior of As, Pb, Ni, Fe, and Mn from Subsurface Marine and Nonmarine Depositional Environment in Central Kanto Plain, Japan. *Geosciences*, 9(10), 435. <https://doi.org/10.3390/geosciences9100435>
- Howard, G., & Bartram, J. (2010). The resilience of water supply and sanitation in the face of climate change Technical report. *WHO vision, 2030*.
- ICMR-NIN Expert Group on Nutrient Requirement for Indians, Recommended Dietary Allowance (RDA) and Estimated Average Requirements (EAR)-2020 [National Institute of Nutrition, India (nin.res.in) accessed on 03/07/2021]
- India at a glance | FAO in India | Food and Agriculture Organization of the United Nations (Accessed on 01/06/2021)
- Intarasunanont, P., Navasumrit, P., Waraprasit, S., Chaisatra, K., Suk, W. A., Mahidol, C., & Ruchirawat, M. (2012). Effects of arsenic exposure on DNA methylation in cord blood samples from newborn babies and in a human lymphoblast cell line. *Environmental Health*, 11(1), 31. <https://doi.org/10.1186/1476-069X-11-31>
- Islam, F. S., Gault, A. G., Boothman, C., Polya, D. A., Charnock, J. M., Chatterjee, D., & Lloyd, J. R. (2004). Role of metal-reducing bacteria in arsenic release from Bengal delta sediments. *Nature*, 430(6995), 68–71.
-

- Islam, M. A., Romić, D., Akber, M. A., & Romić, M. (2018). Trace metals accumulation in soil irrigated with polluted water and assessment of human health risk from vegetable consumption in Bangladesh. *Environmental Geochemistry and Health*, 40(1), 59–85.
- Islam, Md. E., Reza, A. H. M. S., Sattar, G. S., Ahsan, Md. A., Akbor, Md. A., & Siddique, Md. A. B. (2019). Distribution of arsenic in core sediments and groundwater in the Chapai Nawabganj district, Bangladesh. *Arabian Journal of Geosciences*, 12(3), 99. <https://doi.org/10.1007/s12517-019-4272-9>
- Islam, S. N. (2016). Deltaic floodplains development and wetland ecosystems management in the Ganges–Brahmaputra–Meghna Rivers Delta in Bangladesh. *Sustainable Water Resources Management*, 2(3), 237–256. <https://doi.org/10.1007/s40899-016-0047-6>
- Jadhav, R. (2017). 19% of Indians drink water with lethal levels of arsenic | India News - Times of India (indiatimes.com) <https://timesofindia.indiatimes.com/india/19-of-indians-drink-water-with-lethal-levels-of-arsenic/articleshow/62226542.cms> Accessed on 09/07/2021
- Jain, C. K., & Ram, D. (1997). Adsorption of metal ions on bed sediments. *Hydrological Sciences Journal*, 42:5, 713–723. <https://doi.org/10.1080/02626669709492068>
- [Jal Jeevan Mission - Uttar Pradesh \( JJM - UP \) \(jjmup.org\) \(Accessed on 27.05.2021\)](http://www.jeevanmission.org)
- Jamil, N. B., & Feng, H. (2017). Arsenic contamination in groundwater, sediment and soil in Araihasar, Bangladesh. In *Trace Metals: Evolution, Environmental and Ecological Significance* (pp. 37–55). Nova Science Publishers, Inc.
- Janardhana Raju, N. (2012). Arsenic exposure through groundwater in the middle Ganga plain in the Varanasi environs, India: A future threat. *Journal of the Geological Society of India*, 79(3), 302–314. <https://doi.org/10.1007/s12594-012-0044-9>
- Jang, Y. C., Somanna, Y., & Kim, H. (2016). Source, distribution, toxicity and remediation of arsenic in the environment—a review. *Int J Appl Environ Sci*, 11(2), 559–581.
- Javed, M. B., Kachanoski, G., & Siddique, T. (2013). A modified sequential extraction method for arsenic fractionation in sediments. *Analytica Chimica Acta*, 787, 102–110. <https://doi.org/10.1016/j.aca.2013.05.050>
- Jeong, Y., Fan, M., Singh, S., Chuang, C.-L., Saha, B., & Hans van Leeuwen, J. (2007). Evaluation of iron oxide and aluminum oxide as potential arsenic(V) adsorbents. *Chemical Engineering and Processing - Process Intensification*, 46(10), 1030–1039. <https://doi.org/10.1016/j.cep.2007.05.004>
- Jönsson, J., & Sherman, D. M. (2008). Sorption of As (III) and As (V) to siderite, green rust (fougerite) and magnetite: Implications for arsenic release in anoxic groundwaters. *Chemical Geology*, 255(1–2), 173–181.
- Joshi, S. K., Rai, S. P., Sinha, R., Gupta, S., Densmore, A. L., Rawat, Y. S., & Shekhar, S. (2018). Tracing groundwater recharge sources in the northwestern Indian alluvial aquifer using water isotopes ( $\delta^{18}\text{O}$ ,  $\delta^2\text{H}$  and  $3\text{H}$ ). *Journal of Hydrology*, 559, 835–847.
- Kaur, L., Rishi, M. S., Sharma, S., Sharma, B., Lata, R., & Singh, G. (2019). Hydrogeochemical characterization of groundwater in alluvial plains of river Yamuna in northern India: An insight of controlling processes. *Journal of King Saud University - Science*, 31(4), 1245–1253. <https://doi.org/10.1016/j.jksus.2019.01.005>

- Kaushik, A., Kansal, A., Santosh, Meena, Kumari, S., & Kaushik, C. P. (2009). Heavy metal contamination of river Yamuna, Haryana, India: Assessment by Metal Enrichment Factor of the Sediments. *Journal of Hazardous Materials*, 164(1), 265–270. <https://doi.org/10.1016/j.jhazmat.2008.08.031>
- Keon, N. E., Swartz, C. H., Brabander, D. J., Harvey, C., & Hemond, H. F. (2001). Validation of an Arsenic Sequential Extraction Method for Evaluating Mobility in Sediments. *Environmental Science & Technology*, 35(13), 2778–2784. <https://doi.org/10.1021/es001511o>
- Khairul, I., Wang, Q. Q., Jiang, Y. H., Wang, C., & Naranmandura, H. (2017). Metabolism, toxicity and anticancer activities of arsenic compounds. *Oncotarget*, 8(14), 23905.
- Khan, A., Umar, R., & Khan, H. H. (2015). Significance of silica in identifying the processes affecting groundwater chemistry in parts of Kali watershed, Central Ganga Plain, India. *Applied Water Science*, 5(1), 65–72.
- Kim, H. S., Kim, Y. J., & Seo, Y. R. (2015). An overview of carcinogenic heavy metal: Molecular toxicity mechanism and prevention. *Journal of Cancer Prevention*, 20(4), 232.
- Kim, K., Kim, S.-H., Jeong, G. Y., & Kim, R.-H. (2012). Relations of As concentrations among groundwater, soil, and bedrock in Chungnam, Korea: Implications for As mobilization in groundwater according to the As-hosting mineral change. *Journal of Hazardous Materials*, 199–200, 25–35. <https://doi.org/10.1016/j.jhazmat.2011.10.037>
- Konikow, L. F., & Kendy, E. (2005). Groundwater depletion: A global problem. *Hydrogeology Journal*, 13(1), 317–320.
- Kortelainen, N. M., & Karhu, J. A. (2006). Tracing the decomposition of dissolved organic carbon in artificial groundwater recharge using carbon isotope ratios. *Applied Geochemistry*, 21(4), 547–562. <https://doi.org/10.1016/j.apgeochem.2006.01.004>
- Krishna, A. K., Mohan, K. R., Murthy, N. N., Periasamy, V., Bipinkumar, G., Manohar, K., & Rao, S. S. (2013). Assessment of heavy metal contamination in soils around chromite mining areas, Nuggihalli, Karnataka, India. *Environmental Earth Sciences*, 70(2), 699–708. <https://doi.org/10.1007/s12665-012-2153-6>
- Kumar, A., Tiwari, S. K., Verma, A., & Gupta, A. K. (2018). Tracing isotopic signatures ( $\delta D$  and  $\delta^{18}O$ ) in precipitation and glacier melt over Chorabari Glacier–Hydroclimatic inferences for the Upper Ganga Basin (UGB), Garhwal Himalaya. *Journal of Hydrology: Regional Studies*, 15, 68–89.
- Kumar, B., Rai, S. P., Kumar, U. S., Verma, S. K., Garg, P., Kumar, S. V. V., Jaiswal, R., Purendra, B. K., Kumar, S. R., & Pande, N. G. (2010). Isotopic characteristics of Indian precipitation: ISOTOPIC CHARACTERISTICS OF INDIAN PRECIPITATION. *Water Resources Research*, 46(12). <https://doi.org/10.1029/2009WR008532>
- Kumar, B., Rai, S. P., Kumar, U. S., Verma, S. K., Garg, P., Kumar, S. V., Jaiswal, R., Purendra, B. K., Kumar, S. R., & Pande, N. G. (2010). Isotopic characteristics of Indian precipitation. *Water Resources Research*, 46(12).
- Kumar, G., Khanna, P. C., Prasad, S., & KHAN, E. (1996). SEQUENCE STRATIGRAPHY OF THE FOREDEEP AND EVOLUTION OF THE INDO-GANGETIC PLAIN, UTTAR

---

PRADESH. DISCUSSION. *Vivesa Prakasana-Bharatiya Bhuvaijñanika Sarveksana*, 21, 173–207.

- Kumar, M., & Ramanathan, Al. (2018). Vertical Geochemical Variations and Speciation Studies of As, Fe, Mn, Zn, and Cu in the Sediments of the Central Gangetic Basin: Sequential Extraction and Statistical Approach. *International Journal of Environmental Research and Public Health*, 15(2), 183. <https://doi.org/10.3390/ijerph15020183>
- Kumar, M., Kumar, P., Ramanathan, A. L., Bhattacharya, P., Thunvik, R., Singh, U. K., Tsujimura, M., & Sracek, O. (2010). Arsenic enrichment in groundwater in the middle Gangetic Plain of Ghazipur District in Uttar Pradesh, India. *Journal of Geochemical Exploration*, 105(3), 83–94. <https://doi.org/10.1016/j.gexplo.2010.04.008>
- Kumar, M., Kumari, K., Ramanathan, A. L., & Saxena, R. (2007). A comparative evaluation of groundwater suitability for irrigation and drinking purposes in two intensively cultivated districts of Punjab, India. *Environmental Geology*, 53(3), 553–574.
- Kumar, M., Patel, A. K., Das, A., Kumar, P., Goswami, R., Deka, P., & Das, N. (2017). Hydrogeochemical controls on mobilization of arsenic and associated health risk in Nagaon district of the central Brahmaputra Plain, India. *Environmental Geochemistry and Health*, 39(1), 161–178. <https://doi.org/10.1007/s10653-016-9816-2>
- Kumar, M., Rahman, M. M., Ramanathan, Al., & Naidu, R. (2016a). Arsenic and other elements in drinking water and dietary components from the middle Gangetic plain of Bihar, India: Health risk index. *Science of The Total Environment*, 539, 125–134. <https://doi.org/10.1016/j.scitotenv.2015.08.039>
- Kumar, M., Ramanathan, A. L., Kumar, A., & Yadav, S. K. (2016b). Evolution of Arsenic Contamination Process and Mobilization in Central Gangetic Plain Aquifer System and Its Remedial Measures. In *Groundwater Assessment, Modeling, and Management* (pp. 327–337). CRC Press.
- Kumar, M., Ramanathan, A. L., Mahmudur, M., & Naidu, R. (2016c). Science of the Total Environment Concentrations of inorganic arsenic in groundwater, agricultural soils and subsurface sediments from the middle Gangetic plain of Bihar, India. *Science of the Total Environment*, 573, 1103–1114. <https://doi.org/10.1016/j.scitotenv.2016.08.109>
- Kumar, M., Ramanathan, A. L., Rao, M. S., & Kumar, B. (2006). Identification and evaluation of hydrogeochemical processes in the groundwater environment of Delhi, India. *Environmental Geology*, 50(7), 1025–1039.
- Kumar, M., Ramanathan, Al., Mukherjee, A., Sawlani, R., & Ranjan, S. (2019). Delineating sources of groundwater recharge and carbon in Holocene aquifers of the central Gangetic basin using stable isotopic signatures. *Isotopes in Environmental and Health Studies*, 55(3), 254–271. <https://doi.org/10.1080/10256016.2019.1600515>
- Kumar, M., Ramanathan, Al., Mukherjee, A., Verma, S., Rahman, M. M., & Naidu, R. (2018). Hydrogeo-morphological influences for arsenic release and fate in the central Gangetic Basin, India. *Environmental Technology & Innovation*, 12, 243–260. <https://doi.org/10.1016/j.eti.2018.09.004>
- Kumar, M., Ramanathan, Al., Rahman, M. M., & Naidu, R. (2016). Concentrations of inorganic arsenic in groundwater, agricultural soils and subsurface sediments from the middle



- Gangetic plain of Bihar, India. *Science of The Total Environment*, 573, 1103–1114. <https://doi.org/10.1016/j.scitotenv.2016.08.109>
- Kumar, M., Ramanathan, A., Ranjan, S., Singh, V. B., Kumar, N., Yadav, S. K., Rao, M. S., Ritch, S., & Bhattacharya, P. (2018). Groundwater evolution and its utility in upper Ganges-Yamuna Alluvial plain of Northern India, India: Evidence from solute chemistry and stable isotopes. *Groundwater for Sustainable Development*, 7, 400–409. <https://doi.org/10.1016/j.gsd.2018.07.001>
- Kumar, P., Avtar, R., Kumar, A., Singh, C. K., Tripathi, P., Senthil Kumar, G., & Ramanathan, A. L. (2014). Geophysical approach to delineate arsenic hot spots in the alluvial aquifers of Bhagalpur district, Bihar (India) in the central Gangetic plains. *Applied Water Science*, 4(2), 89–97. <https://doi.org/10.1007/s13201-013-0133-y>
- Kumar, P., Kumar, M., Ramanathan, A. L., & Tsujimura, M. (2010). Tracing the factors responsible for arsenic enrichment in groundwater of the middle Gangetic Plain, India: A source identification perspective. *Environmental Geochemistry and Health*, 32(2), 129–146. <https://doi.org/10.1007/s10653-009-9270-5>
- Kunene, S. C., Lin, K.-S., Mdlovu, N. V., & Shih, W.-C. (2021). Bioaccumulation of trace metals and speciation of copper and zinc in Pacific oysters (*Crassostrea gigas*) using XANES/EXAFS spectroscopies. *Chemosphere*, 265, 129067. <https://doi.org/10.1016/j.chemosphere.2020.129067>
- Lakshmanan, E., Kannan, R., & Senthil Kumar, M. (2003). Major ion chemistry and identification of hydrogeochemical processes of ground water in a part of Kancheepuram district, Tamil Nadu, India. *Environmental Geosciences*, 10(4), 157–166. <https://doi.org/10.1306/eg100403011>
- Lamb, A. L., Wilson, G. P., & Leng, M. J. (2006). A review of coastal palaeoclimate and relative sea-level reconstructions using  $\delta^{13}\text{C}$  and C/N ratios in organic material. *Earth-Science Reviews*, 75(1–4), 29–57.
- Li, P., Karunanidhi, D., Subramani, T., & Srinivasamoorthy, K. (2021). Sources and Consequences of Groundwater Contamination. *Archives of Environmental Contamination and Toxicology*, 80(1), 1–10. <https://doi.org/10.1007/s00244-020-00805-z>
- Li, X., Han, G., Liu, M., Song, C., Zhang, Q., Yang, K., & Liu, J. (2019). Hydrochemistry and Dissolved Inorganic Carbon (DIC) Cycling in a Tropical Agricultural River, Mun River Basin, Northeast Thailand. *Int. J. Environ. Res. Public Health*, 13.
- Lin, Z., & Puls, R. W. (2000). Adsorption, desorption and oxidation of arsenic affected by clay minerals and aging process. *Environmental Geology*, 39(7), 753–759.
- Lombi, E., Sletten, R. S., & Wenzel, W. W. (n.d.). *Sequentially Extracted Arsenic from Different Size Fractions of Contaminated Soils*. 14.
- Loska, K., Wiechuła, D., & Korus, I. (2004). Metal contamination of farming soils affected by industry. *Environment International*, 30(2), 159–165. [https://doi.org/10.1016/S0160-4120\(03\)00157-0](https://doi.org/10.1016/S0160-4120(03)00157-0)
- Lourma, S. (2010). *Geologic research in Maner block, Bihar, India*.

- 
- Luo, T., Sun, J., Liu, Y., Cui, L., & Fu, Q. (2019). Adsorption and transport behavior of arsenate on saline-alkali soils of tidal flat of Yellow Sea, Eastern China. *Environmental Pollutants and Bioavailability*, 31(1), 166–173. <https://doi.org/10.1080/26395940.2019.1604162>
- Lupker, M., France-Lanord, C., Galy, V., Lavé, J., Gaillardet, J., Gajurel, A. P., Guilmette, C., Rahman, M., Singh, S. K., & Sinha, R. (2012). Predominant floodplain over mountain weathering of Himalayan sediments (Ganga basin). *Geochimica et Cosmochimica Acta*, 84, 410–432. <https://doi.org/10.1016/j.gca.2012.02.001>
- Mackenzie, F. T., & Garrels, R. M. (1971). *Evolution of sedimentary rocks*. Norton New York.
- Mahanta, C., Enmark, G., Nordborg, D., Sracek, O., Nath, B., Nickson, R. T., Herbert, R., Jacks, G., Mukherjee, A., Ramanathan, A. L., Choudhury, R., & Bhattacharya, P. (2015). Hydrogeochemical controls on mobilization of arsenic in groundwater of a part of Brahmaputra river floodplain, India. *Journal of Hydrology: Regional Studies*, 4, 154–171. <https://doi.org/10.1016/j.ejrh.2015.03.002>
- Maier, M. V., Wolter, Y., Zentler, D., Scholz, C., Stirn, C. N., & Isenbeck-Schröter, M. (2019). Phosphate Induced Arsenic Mobilization as a Potentially Effective In-Situ Remediation Technique—Preliminary Column Tests. *Water*, 11(11), 2364.
- Mamindy-Pajany, Y., Hurel, C., Marmier, N., & Roméo, M. (2011). Arsenic (V) adsorption from aqueous solution onto goethite, hematite, magnetite and zero-valent iron: Effects of pH, concentration and reversibility. *Desalination*, 281, 93–99. <https://doi.org/10.1016/j.desal.2011.07.046>
- Mancosu, N., Snyder, R. L., Kyriakakis, G., & Spano, D. (2015). Water scarcity and future challenges for food production. *Water*, 7(3), 975-992.
- Mandal, B. (2002). Arsenic round the world: A review. *Talanta*, 58(1), 201–235. [https://doi.org/10.1016/S0039-9140\(02\)00268-0](https://doi.org/10.1016/S0039-9140(02)00268-0)
- Manning, B. A., & Goldberg, S. (1997). Adsorption and stability of arsenic (III) at the clay mineral- water interface. *Environmental Science & Technology*, 31(7), 2005–2011.
- Marchand, G. (2001). *Surface-water and ground water interaction and source of nitrate in municipal water supply aquifer, San Jose, Costa Rica*. Graduate Studies.
- Martinez, V. D., Vucic, E. A., Becker-Santos, D. D., Gil, L., & Lam, W. L. (2011). Arsenic exposure and the induction of human cancers. *Journal of toxicology*, 2011.
- Maurya, J., Pradhan, S. N., Seema, & Ghosh, A. K. (2021). Evaluation of ground water quality and health risk assessment due to nitrate and fluoride in the Middle Indo-Gangetic plains of India. *Human and Ecological Risk Assessment: An International Journal*, 27(5), 1349–1365. <https://doi.org/10.1080/10807039.2020.1844559>
- Mayer, J. E., & Goldman, R. H. (2016). Arsenic and skin cancer in the USA: The current evidence regarding arsenic-contaminated drinking water. *International Journal of Dermatology*, 55(11), e585–e591.
- Mazumder, D. N. G. (2008). Chronic arsenic toxicity & human health. *INDIAN J MED RES*, 12.
- McArthur, J. M., Banerjee, D. M., Hudson-Edwards, K. A., Mishra, R., Purohit, R., Ravenscroft, P., Cronin, A., Howarth, R. J., Chatterjee, A., Talukder, T., Lowry, D., Houghton, S., &
-

- 
- Chadha, D. K. (2004). Natural organic matter in sedimentary basins and its relation to arsenic in anoxic ground water: The example of West Bengal and its worldwide implications. *Applied Geochemistry*, 19(8), 1255–1293. <https://doi.org/10.1016/j.apgeochem.2004.02.001>
- McArthur, J. M., Banerjee, D. M., Sengupta, S., Ravenscroft, P., Klump, S., Sarkar, A., Disch, B., & Kipfer, R. (2010). Migration of As, and  $3\text{H}/3\text{He}$  ages, in groundwater from West Bengal: Implications for monitoring. *Water Research*, 44(14), 4171–4185.
- McLean, J. E. (1992). *Behavior of metals in soils*. Technology Innovation Office, Office of Solid Waste and Emergency Response.
- Meredith, K. T., Baker, A., Andersen, M. S., O'Carroll, D. M., Rutledge, H., McDonough, L. K., Oudone, P., Bryan, E., & Zainuddin, N. S. (2020). Isotopic and chromatographic fingerprinting of the sources of dissolved organic carbon in a shallow coastal aquifer. *Hydrology and Earth System Sciences*, 24(4), 2167–2178. <https://doi.org/10.5194/hess-24-2167-2020>
- Meybeck, M. (1987). Global chemical weathering of surficial rocks estimated from river dissolved loads. *American Journal of Science*, 287(5), 401–428.
- Mihajlov, I., Mozumder, M. R. H., Bostick, B. C., Stute, M., Mailloux, B. J., Knappett, P. S., Choudhury, I., Ahmed, K. M., Schlosser, P., & van Geen, A. (2020). Arsenic contamination of Bangladesh aquifers exacerbated by clay layers. *Nature Communications*, 11(1), 1–9.
- Mihaljevič, M., Poňavič, M., Ettler, V., & Šebek, O. (2003). A comparison of sequential extraction techniques for determining arsenic fractionation in synthetic mineral mixtures. *Analytical and Bioanalytical Chemistry*, 377(4), 723–729.
- Misra, A. K. (2011). Impact of Urbanization on the Hydrology of Ganga Basin (India). *Water Resources Management*, 25(2), 705–719. <https://doi.org/10.1007/s11269-010-9722-9>
- Misra, A. K. (2013). Influence of stone quarries on groundwater quality and health in Fatehpur Sikri, India. *International Journal of Sustainable Built Environment*, 2(1), 73–88. <https://doi.org/10.1016/j.ijsbe.2013.11.002>
- Mohammadzadeh, H., & Mahaqi, A. (2017). Stable isotopes ( $\delta\text{D}$ ,  $\delta^{18}\text{O}$  and  $\delta^{13}\text{C}_{\text{DIC}}$ ) characteristics of karstic groundwater in Qori Meydan plain, NE of Iran. Proc. 12th Int. Symp. Appl. Isot. Geochemistry. Colorado, USA, 1–5.
- Mukherjee, A. (2018). Groundwater Chemistry and Arsenic Enrichment of the Ganges River Basin Aquifer Systems. In A. Mukherjee (Ed.), *Groundwater of South Asia* (pp. 275–289). Springer Singapore. [https://doi.org/10.1007/978-981-10-3889-1\\_17](https://doi.org/10.1007/978-981-10-3889-1_17)
- Mukherjee, A., & Fryar, A. E. (2008a). Deeper groundwater chemistry and geochemical modeling of the arsenic affected western Bengal basin, West Bengal, India. *Applied Geochemistry*, 23(4), 863–894. <https://doi.org/10.1016/j.apgeochem.2007.07.011>
- Mukherjee, A., Bhattacharya, P., Savage, K., Foster, A., & Bundschuh, J. (2008b). Distribution of geogenic arsenic in hydrologic systems: Controls and challenges. *Journal of Contaminant Hydrology*, 99(1–4), 1–7. <https://doi.org/10.1016/j.jconhyd.2008.04.002>
-

- 
- Mukherjee, A., Fryar, A. E., & Rowe, H. D. (2007). Regional-scale stable isotopic signatures of recharge and deep groundwater in the arsenic affected areas of West Bengal, India. *Journal of Hydrology*, 334(1–2), 151–161.
- Mukherjee, A., Fryar, A. E., & Thomas, W. A. (2009). Geologic, geomorphic and hydrologic framework and evolution of the Bengal basin, India and Bangladesh. *Journal of Asian Earth Sciences*, 34(3), 227–244. <https://doi.org/10.1016/j.jseaes.2008.05.011>
- Mukherjee, A., Saha, D., Harvey, C. F., Taylor, R. G., Ahmed, K. M., & Bhanja, S. N. (2015). Groundwater systems of the Indian Sub-Continent. *Journal of Hydrology: Regional Studies*, 4, 1–14. <https://doi.org/10.1016/j.ejrh.2015.03.005>
- Mukherjee, A., Sarkar, S., Chakraborty, M., Duttagupta, S., Bhattacharya, A., Saha, D., Bhattacharya, P., Mitra, A., & Gupta, S. (2021). Occurrence, predictors and hazards of elevated groundwater arsenic across India through field observations and regional-scale AI-based modeling. *Science of The Total Environment*, 759, 143511. <https://doi.org/10.1016/j.scitotenv.2020.143511>
- Mukherjee, A., Scanlon, B. R., Fryar, A. E., Saha, D., Ghosh, A., Chowdhuri, S., & Mishra, R. (2012). Solute chemistry and arsenic fate in aquifers between the Himalayan foothills and Indian craton (including central Gangetic plain): Influence of geology and geomorphology. *Geochimica et Cosmochimica Acta*, 90, 283–302. <https://doi.org/10.1016/j.gca.2012.05.015>
- Mukherjee, A., Scanlon, B. R., Fryar, A. E., Saha, D., Ghosh, A., Chowdhuri, S., & Mishra, R. (2012). Solute chemistry and arsenic fate in aquifers between the Himalayan foothills and Indian craton (including central Gangetic plain): Influence of geology and geomorphology. *Geochimica et Cosmochimica Acta*, 90, 283–302. <https://doi.org/10.1016/j.gca.2012.05.015>
- Mukherjee, A., Sengupta, M. K., Hossain, M. A., Ahamed, S., Das, B., Nayak, B., Lodh, D., Rahman, M. M., & Chakraborti, D. (2006). Arsenic contamination in groundwater: A global perspective with emphasis on the Asian scenario. *Journal of Health, Population and Nutrition*, 142–163.
- Muller, G. (1969). Index of geoaccumulation in sediments of the Rhine River. *Geojournal*, 2, 108–118.
- Mumford, A. C., Barringer, J. L., Benzel, W. M., Reilly, P. A., & Young, L. Y. (2012). Microbial transformations of arsenic: Mobilization from glauconitic sediments to water. *Water Research*, 46(9), 2859–2868.
- Murcott, S. (2012). *Arsenic contamination in the world*. IWA publishing.
- Nath, A., Samanta, S., Banerjee, S., Danda, A. A., & Hazra, S. (2021). Threat of arsenic contamination, salinity and water pollution in agricultural practices of Sundarban Delta, India, and mitigation strategies. *SN Applied Sciences*, 3(5), 1-15.
- National Rural Drinking Water Programme (Ministry of Jal Shakti) [201707111554.pdf \(jalshakti-ddws.gov.in\)](https://www.jalshakti-ddws.gov.in) (Accesses on 28/07/2021)
-

- Naudet, V., Revil, A., Rizzo, E., Bottero, J.-Y., & Bégassat, P. (2004). Groundwater redox conditions and conductivity in a contaminant plume from geoelectrical investigations. *Hydrology and Earth System Sciences*, 8(1), 8–22.
- Neumann, R. B., Ashfaq, K. N., Badruzzaman, A. B. M., Ashraf Ali, M., Shoemaker, J. K., & Harvey, C. F. (2010). Anthropogenic influences on groundwater arsenic concentrations in Bangladesh. *Nature Geoscience*, 3(1), 46–52. <https://doi.org/10.1038/ngeo685>
- Nickson, R., McArthur, J., Burgess, W., Ahmed, K. M., Ravenscroft, P., & Rahman, M. (1998). Arsenic poisoning of Bangladesh groundwater. *Nature*, 395(6700), 338–338.
- Nikova, I., Tsoleva, V., Hristov, B., Zdravkov, A., & Ruskov, K. (2016). Geochemical pattern of soils in Bobovdol valley, Bulgaria. Assessment of Cd and Co contents. *Eurasian Journal of Soil Science*, 5(3), 172–181. <https://doi.org/10.18393/ejss.2016.3.172-181>
- Nriagu, J. O., Bhattacharya, P., Mukherjee, A. B., Bundschuh, J., Zevenhoven, R., & Loeppert, R. H. (2007). *Arsenic in soil and groundwater: An overview* (pp. 3–60). Elsevier. <http://urn.kb.se/resolve?urn=urn:nbn:se:kth:diva-86384>
- Page, G. William. (1981). Comparison of groundwater and surface water for patterns and levels of contamination by toxic substances. *Environmental Science & Technology*, 15(12), 1475–1481. <https://doi.org/10.1021/es00094a008>
- Pandey, J., & Singh, R. (2017). Heavy metals in sediments of Ganga River: Up- and downstream urban influences. *Applied Water Science*, 7(4), 1669–1678. <https://doi.org/10.1007/s13201-015-0334-7>
- Parkhurst, D. L. (1995). *User's guide to PHREEQC: A computer program for speciation, reaction-path, advective-transport, and inverse geochemical calculations* (Vol. 95). US Department of the Interior, US Geological Survey.
- Piper, A. M. (1944). A graphic procedure in the geochemical interpretation of water-analyses. *Transactions, American Geophysical Union*, 25(6), 914. <https://doi.org/10.1029/TR025i006p00914>
- Planning Commission (2011) Report of the working group on rural domestic water and sanitation, Twelfth five year plan-2012–2017, Ministry of Drinking Water and Sanitation, Government of India, p 220
- Popkin, B. M., D'Anci, K. E., & Rosenberg, I. H. (2010). Water, hydration, and health. *Nutrition Reviews*, 68(8), 439–458.
- Prada, S., Cruz, J. V., & Figueira, C. (2016). Using stable isotopes to characterize groundwater recharge sources in the volcanic island of Madeira, Portugal. *Journal of Hydrology*, 536, 409–425.
- Rahaman, S., Sinha, A. C., Pati, R., & Mukhopadhyay, D. (2013). Arsenic contamination: A potential hazard to the affected areas of West Bengal, India. *Environmental Geochemistry and Health*, 35(1), 119–132. <https://doi.org/10.1007/s10653-012-9460-4>
- Rahman, A., Mondal, N. C., & Fauzia, F. (2021). Arsenic enrichment and its natural background in groundwater at the proximity of active floodplains of Ganga River, northern India. *Chemosphere*, 265, 129096. <https://doi.org/10.1016/j.chemosphere.2020.129096>

- Rai, S. P., Purushothaman, P., Kumar, B., Jacob, N., & Rawat, Y. S. (2014). Stable isotopic composition of precipitation in the River Bhagirathi Basin and identification of source vapour. *Environmental Earth Sciences*, 71(11), 4835–4847. <https://doi.org/10.1007/s12665-013-2875-0>
- Ramanathan, A. L., Johnston, S., Mukherjee, A., & Nath, B. (2015). *Safe and sustainable use of arsenic-contaminated aquifers in the Gangetic Plain*. Springer.
- Ranjan, R. K., Ramanathan, A. L., Parthasarathy, P., & Kumar, A. (2013). Hydrochemical characteristics of groundwater in the plains of Phalgu River in Gaya, Bihar, India. *Arabian Journal of Geosciences*, 6(9), 3257–3267. <https://doi.org/10.1007/s12517-012-0599-1>
- Rauret, G., López-Sánchez, J. F., Sahuquillo, A., Rubio, R., Davidson, C., Ure, A., & Quevauviller, Ph. (1999). Improvement of the BCR three step sequential extraction procedure prior to the certification of new sediment and soil reference materials. *Journal of Environmental Monitoring*, 1(1), 57–61. <https://doi.org/10.1039/a807854h>
- Ravenscroft, P. 175913, Richards, K. 175915, & 175914 Brammer, H. (2009). *Arsenic pollution: A global synthesis*. <https://agris.fao.org/agris-search/search.do?recordID=XF2015044429>
- Ravenscroft, P., Burgess, W. G., Ahmed, K. M., Burren, M., & Perrin, J. (2005). Arsenic in groundwater of the Bengal Basin, Bangladesh: Distribution, field relations, and hydrogeological setting. *Hydrogeology Journal*, 13(5–6), 727–751. <https://doi.org/10.1007/s10040-003-0314-0>
- Reimann, C., Siewers, U., Tarvainen, T., Bitjukova, L., Eriksson, J., Gilucis, A., Gregorauskiene, V., Lukashov, V., Matinian, N. N., & Pasioczna, A. (2000). Baltic soil survey: Total concentrations of major and selected trace elements in arable soils from 10 countries around the Baltic Sea. *Science of the Total Environment*, 257(2–3), 155–170.
- Ren, C., Dong, Y., Xue, P., & Xu, W. (2019). Analysis of Water Supply and Demand based on Logistic Model. *IOP Conference Series: Earth and Environmental Science*, 300, 022013. <https://doi.org/10.1088/1755-1315/300/2/022013>
- Reza, A. S., Jean, J.-S., Lee, M.-K., Liu, C.-C., Bundschuh, J., Yang, H.-J., Lee, J.-F., & Lee, Y.-C. (2010). Implications of organic matter on arsenic mobilization into groundwater: Evidence from northwestern (Chapai-Nawabganj), central (Manikganj) and southeastern (Chandpur) Bangladesh. *Water Research*, 44(19), 5556–5574.
- Richards, L. A., Magnone, D., Boyce, A. J., Casanueva-Marenco, M. J., van Dongen, B. E., Ballentine, C. J., & Polya, D. A. (2018). Delineating sources of groundwater recharge in an arsenic-affected Holocene aquifer in Cambodia using stable isotope-based mixing models. *Journal of Hydrology*, 557, 321–334. <https://doi.org/10.1016/j.jhydrol.2017.12.012>
- Rickards, N., Thomas, T., Kaelin, A., Houghton-Carr, H., Jain, S. K., Mishra, P. K., Nema, M. K., Dixon, H., Rahman, M. M., Horan, R., Jenkins, A., & Rees, G. (2020). Understanding Future Water Challenges in a Highly Regulated Indian River Basin—Modelling the Impact of Climate Change on the Hydrology of the Upper Narmada. *Water*, 12(6), 1762. <https://doi.org/10.3390/w12061762>
- Rijsberman, F. R. (2006). Water scarcity: Fact or fiction? *Agricultural Water Management*, 80(1), 5–22. <https://doi.org/10.1016/j.agwat.2005.07.001>

- Robinson, G., Caldwell, G. S., Wade, M. J., Free, A., Jones, C. L., & Stead, S. M. (2016). Profiling bacterial communities associated with sediment-based aquaculture bioremediation systems under contrasting redox regimes. *Scientific reports*, 6(1), 1-13.
- Rodriguez, R. R., Basta, N. T., Casteel, S. W., Armstrong, F. P., & Ward, D. C. (2003). Chemical extraction methods to assess bioavailable arsenic in soil and solid media. *Journal of Environmental Quality*, 32(3), 876-884.
- Roman-Ross, G., Cuello, G. J., Turrillas, X., Fernandez-Martinez, A., & Charlet, L. (2006). Arsenite sorption and co-precipitation with calcite. *Chemical Geology*, 233(3-4), 328-336.
- Roychowdhury, T. (2010). Groundwater arsenic contamination in one of the 107 arsenic-affected blocks in West Bengal, India: Status, distribution, health effects and factors responsible for arsenic poisoning. *International journal of hygiene and environmental health*, 213(6), 414-427.
- Rudnick, R., & Gao, S. (2014). *Composition of the Continental Crust*. <https://doi.org/10.1016/B978-0-08-095975-7.00301-6>
- Sadiq, M. (1997). Arsenic chemistry in soils: An overview of thermodynamic predictions and field observations. *Water, Air, and Soil Pollution*, 93(1), 117-136.
- Saha, D. (2009). Arsenic groundwater contamination in parts of middle Ganga plain, Bihar. *CURRENT SCIENCE*, 97(6), 3.
- Saha, D., & Sahu, S. (2016). A decade of investigations on groundwater arsenic contamination in Middle Ganga Plain, India. *Environmental Geochemistry and Health*, 38(2), 315-337. <https://doi.org/10.1007/s10653-015-9730-z>
- Saha, D., & Sahu, S. (2016). A decade of investigations on groundwater arsenic contamination in Middle Ganga Plain, India. *Environmental geochemistry and health*, 38(2), 315-337.
- Saha, D., & Shukla, R. R. (2013). Genesis of Arsenic-Rich Groundwater and the Search for Alternative Safe Aquifers in the Gangetic Plain, India. *Water Environment Research*, 85(12), 2254-2264.
- Saha, D., Dhar, Y. R., & Vittala, S. S. (2010). Delineation of groundwater development potential zones in parts of marginal Ganga Alluvial Plain in South Bihar, Eastern India. *Environmental Monitoring and Assessment*, 165(1-4), 179-191. <https://doi.org/10.1007/s10661-009-0937-2>
- Saha, D., Sahu, S., & Chandra, P. C. (2011). Arsenic-safe alternate aquifers and their hydraulic characteristics in contaminated areas of Middle Ganga Plain, Eastern India. *Environmental Monitoring and Assessment*, 175(1-4), 331-348. <https://doi.org/10.1007/s10661-010-1535-z>
- Saha, D., Sarangam, S. S., Dwivedi, S. N., & Bhartariya, K. G. (2010). Evaluation of hydrogeochemical processes in arsenic-contaminated alluvial aquifers in parts of Mid-Ganga Basin, Bihar, Eastern India. *Environmental Earth Sciences*, 61(4), 799-811. <https://doi.org/10.1007/s12665-009-0392-y>

- Saha, J. C., Dikshit, A. K., Bandyopadhyay, M., & Saha, K. C. (1999). A Review of Arsenic Poisoning and its Effects on Human Health. *Critical Reviews in Environmental Science and Technology*, 29(3), 281–313. <https://doi.org/10.1080/10643389991259227>
- Saha, N., Rahman, M. S., Ahmed, M. B., Zhou, J. L., Ngo, H. H., & Guo, W. (2017). Industrial metal pollution in water and probabilistic assessment of human health risk. *Journal of Environmental Management*, 185, 70–78. <https://doi.org/10.1016/j.jenvman.2016.10.023>
- Sakizadeh, M., Mirzaei, R., & Ghorbani, H. (2016). Geochemical influences on the quality of groundwater in eastern part of Semnan Province, Iran. *Environmental Earth Sciences*, 75(10), 917. <https://doi.org/10.1007/s12665-016-5722-2>
- Samanta, S., Dalai, T. K., Pattanaik, J. K., Rai, S. K., & Mazumdar, A. (2015). Dissolved inorganic carbon (DIC) and its  $\delta^{13}\text{C}$  in the Ganga (Hooghly) River estuary, India: Evidence of DIC generation via organic carbon degradation and carbonate dissolution. *Geochimica et Cosmochimica Acta*, 165, 226–248. <https://doi.org/10.1016/j.gca.2015.05.040>
- Sankhla, M. S., Kumari, M., Sharma, K., Kushwah, R. S., & Kumar, R. (2018). *Heavy Metal Pollution of Holy River Ganga: A Review*. 05(01), 14.
- Sanyal, S. K., & Nasar, S. K. T. (2002). Arsenic contamination of groundwater in West Bengal (India): Build-up in soil-crop systems. *International Conference on Water Related Disasters. Kolkata. 5th-6th December*.
- Sappa, G., Ergul, S., & Ferranti, F. (2014). Geochemical modeling and multivariate statistical evaluation of trace elements in arsenic contaminated groundwater systems of Viterbo Area, (Central Italy). *SpringerPlus*, 3(1), 237. <https://doi.org/10.1186/2193-1801-3-237>
- Sarin, M. M., & Krishnaswami, S. (1984). Major ion chemistry of the Ganga–Brahmaputra river systems, India. *Nature*, 312(5994), 538–541.
- Sarin, M. M., Krishnaswami, S., Dilli, K., Somayajulu, B. L. K., & Moore, W. S. (1989). Major ion chemistry of the Ganga–Brahmaputra river system: Weathering processes and fluxes to the Bay of Bengal. *Geochimica et Cosmochimica Acta*, 53(5), 997–1009. [https://doi.org/10.1016/0016-7037\(89\)90205-6](https://doi.org/10.1016/0016-7037(89)90205-6)
- Sarkar, B., Singh, M., Mandal, S., Churchman, G. J., & Bolan, N. S. (2018). Clay minerals—Organic matter interactions in relation to carbon stabilization in soils. In *The future of soil carbon* (pp. 71–86). Elsevier.
- Sasakova, N., Gregova, G., Takacova, D., Mojziso, J., Papajova, I., Venglovsky, J., Szaboova, T., & Kovacova, S. (2018). Pollution of Surface and Ground Water by Sources Related to Agricultural Activities. *Frontiers in Sustainable Food Systems*, 2. <https://doi.org/10.3389/fsufs.2018.00042>
- Schramel, P., Michalke, B., Emons, H., Göen, T., Hartwig, A., & MAK Commission. (2002). Arsenic and arsenic compounds—Determination of arsenic species (As (III), As (V), monomethylarsonic acid, dimethylarsinic acid and arsenobetaine) in urine by HPLC-ICP-MS [Biomonitoring Methods, 2018]. *The MAK-Collection for Occupational Health and Safety: Annual Thresholds and Classifications for the Workplace*, 3(4), 2149–2169.



- 
- Schreiber, M. E., Simo, J. A., & Freiberg, P. G. (2000). Stratigraphic and geochemical controls on naturally occurring arsenic in groundwater, eastern Wisconsin, USA. *Hydrogeology Journal*, 8(2), 161–176.
- Selim Reza, A. H. M., Jean, J.-S., Yang, H.-J., Lee, M.-K., Woodall, B., Liu, C.-C., Lee, J.-F., & Luo, S.-D. (2010). Occurrence of arsenic in core sediments and groundwater in the Chapai-Nawabganj District, northwestern Bangladesh. *Water Research*, 44(6), 2021–2037. <https://doi.org/10.1016/j.watres.2009.12.006>
- Sengupta, S., McArthur, J. M., Sarkar, A., Leng, M. J., Ravenscroft, P., Howarth, R. J., & Banerjee, D. M. (2008). Do Ponds Cause Arsenic-Pollution of Groundwater in the Bengal Basin? An Answer from West Bengal. *Environmental Science & Technology*, 42(14), 5156–5164. <https://doi.org/10.1021/es702988m>
- Shah, B. A. (2008). Role of Quaternary stratigraphy on arsenic-contaminated groundwater from parts of Middle Ganga Plain, UP–Bihar, India. *Environmental Geology*, 53(7), 1553–1561. <https://doi.org/10.1007/s00254-007-0766-y>
- Shah, B. A. (2014). Arsenic in groundwater, Quaternary sediments, and suspended river sediments from the Middle Gangetic Plain, India: Distribution, field relations, and geomorphological setting. *Arabian Journal of Geosciences*, 7(9), 3525–3536. <https://doi.org/10.1007/s12517-013-1012-4>
- Shah, B. A. (2015). Arsenic Contamination in Groundwater in the Middle Gangetic Plain, India: Its Relations to Fluvial Geomorphology and Quaternary Stratigraphy. In A. Ramanathan, S. Johnston, A. Mukherjee, & B. Nath (Eds.), *Safe and Sustainable Use of Arsenic-Contaminated Aquifers in the Gangetic Plain* (pp. 33–53). Springer International Publishing. [https://doi.org/10.1007/978-3-319-16124-2\\_3](https://doi.org/10.1007/978-3-319-16124-2_3)
- Shah, Z. A., & Umar, R. (2015). Stable isotopic and hydrochemical studies in a part of central Ganga basin. *Journal of the Geological Society of India*, 85(6), 706–716. <https://doi.org/10.1007/s12594-015-0267-7>
- Shaji, E., Santosh, M., Sarath, K. V., Prakash, P., Deepchand, V., & Divya, B. V. (2021). Arsenic contamination of groundwater: A global synopsis with focus on the Indian Peninsula. *Geoscience Frontiers*, 12(3), 101079. <https://doi.org/10.1016/j.gsf.2020.08.015>
- Shankar, S., Shanker, U., & Shikha. (2014). Arsenic Contamination of Groundwater: A Review of Sources, Prevalence, Health Risks, and Strategies for Mitigation. *The Scientific World Journal*, 2014, 1–18. <https://doi.org/10.1155/2014/304524>
- Shapiro, L. (1975). *Rapid analysis of silicate, carbonate, and phosphate rocks: Revised edition*.
- Sharma, D. A., Keesari, T., Rishi, M. S., & Pant, D. (2018). A study on the role of hydrogeology on the distribution of uranium in alluvial aquifers of northwest India. *Environmental Monitoring and Assessment*, 190(12), 746.
- Sharma, P. K., Mayank, M., Ojha, C. S. P., & Shukla, S. K. (2020). A review on groundwater contaminant transport and remediation. *ISH Journal of Hydraulic Engineering*, 26(1), 112–121. <https://doi.org/10.1080/09715010.2018.1438213>
-

- 
- Sherman, D. M., & Randall, S. R. (2003). Surface complexation of arsenic (V) to iron (III)(hydr) oxides: Structural mechanism from ab initio molecular geometries and EXAFS spectroscopy. *Geochimica et Cosmochimica Acta*, 67(22), 4223–4230.
- Sidhu, P. S., & Gilkes, R. J. (1977). Mineralogy of Soils Developed on Alluvium in the Indo-Gangetic Plain (India). *Soil Science Society of America Journal*, 41(6), 1194–1201. <https://doi.org/10.2136/sssaj1977.03615995004100060037x>
- Singh, A. K. (2006). Chemistry of arsenic in groundwater of Ganges–Brahmaputra river basin. *Current Science*, 91(5), 599–606.
- Singh, A., & Choudhary, S. K. (2010). ARSENIC IN GROUND WATER IN FIVE VILLAGES UNDER NATHNAGAR BLOCK OF BHAGALPUR DISTRICT, BIHAR. *Ecoscan*, 4(2-3), 213-216.
- Singh, A., Patel, A. K., Deka, J. P., & Kumar, M. (2020). Natural recharge transcends anthropogenic forcing that influences arsenic vulnerability of the quaternary alluviums of the Mid-Gangetic Plain. *Npj Clean Water*, 3(1), 27. <https://doi.org/10.1038/s41545-020-0075-5>
- Singh, D. S., Awasthi, A., & Bhardwaj, V. (2009). Control of tectonics and climate on Chhoti Gandak river basin, East Ganga Plain, India. *Himalyan Geology*, 30(2), 147–154.
- Singh, D. S., Prajapati, S. K., Singh, P., Singh, K., & Kumar, D. (2015). Climatically induced levee break and flood risk management of the Gorakhpur region, Rapti River Basin, Ganga Plain, India. *Journal of the Geological Society of India*, 85(1), 79–86.
- Singh, I. B. (2004). Late quaternary history of the Ganga plain. *JOURNAL-GEOLOGICAL SOCIETY OF INDIA*, 64(4), 431–454.
- Singh, M., Kumar, S., Kumar, B., Singh, S., & Singh, I. B. (2013). Investigation on the hydrodynamics of Ganga Alluvial Plain using environmental isotopes: A case study of the Gomati River Basin, northern India. *Hydrogeology Journal*, 21(3), 687–700. <https://doi.org/10.1007/s10040-013-0958-3>
- Singh, M., Müller, G., & Singh, I. B. (2003). Geogenic distribution and baseline concentration of heavy metals in sediments of the Ganges River, India. *Journal of Geochemical Exploration*, 80(1), 1–17. [https://doi.org/10.1016/S0375-6742\(03\)00016-5](https://doi.org/10.1016/S0375-6742(03)00016-5)
- Singh, M., Singh, A. K., Swati, Srivastava, N., Singh, S., & Chowdhary, A. K. (2010). Arsenic mobility in fluvial environment of the Ganga Plain, northern India. *Environmental Earth Sciences*, 59(8), 1703–1715. <https://doi.org/10.1007/s12665-009-0152-z>
- Singh, S. K., & Pandey, A. C. (2014). Geomorphology and the controls of geohydrology on waterlogging in Gangetic Plains, North Bihar, India. *Environmental Earth Sciences*, 71(4), 1561–1579. <https://doi.org/10.1007/s12665-013-2562-1>
- Sinha, R., Jain, V., Babu, G. P., & Ghosh, S. (2005). Geomorphic characterization and diversity of the fluvial systems of the Gangetic Plains. *Geomorphology*, 70(3–4), 207–225. <https://doi.org/10.1016/j.geomorph.2005.02.006>
- Sinha, R., Tandon, S. K., Gibling, M. R., Bhattacharjee, P. S., & Dasgupta, A. S. (2005). *Late Quaternary geology and alluvial stratigraphy of the ganga basin*. *Himalayan Geology*, 26(1), 223-240.
-

- 
- Smedley, P. L., & Kinniburgh, D. G. (2002). A review of the source, behaviour and distribution of arsenic in natural waters. *Applied Geochemistry*, 17(5), 517–568. [https://doi.org/10.1016/S0883-2927\(02\)00018-5](https://doi.org/10.1016/S0883-2927(02)00018-5)
- Smith, A. H., Lingas, E. O., & Rahman, M. (2000). Contamination of drinking-water by arsenic in Bangladesh: a public health emergency. *Bulletin of the World Health Organization*, 78, 1093–1103.
- Smith, E. R. G., Naidu, R., & Alston, A. M. (1998). *Arsenic in the soil environment*.
- Smith, E., Smith, J., Smith, L., Biswas, T., Correll, R., & Naidu, R. (2003). Arsenic in Australian environment: An overview. *Journal of Environmental Science and Health, Part A*, 38(1), 223–239.
- Srinivasamoorthy, K., Gopinath, M., Chidambaram, S., Vasanthavigar, M., & Sarma, V. S. (2014). Hydrochemical characterization and quality appraisal of groundwater from Pungar sub basin, Tamilnadu, India. *Journal of King Saud University - Science*, 26(1), 37–52. <https://doi.org/10.1016/j.jksus.2013.08.001>
- Srivastava, S. (Ed.). (2020). *Arsenic in Drinking Water and Food*. Springer Singapore. <https://doi.org/10.1007/978-981-13-8587-2>
- Srivastava, S., & Sharma, Y. K. (2013). Arsenic occurrence and accumulation in soil and water of eastern districts of Uttar Pradesh, India. *Environmental Monitoring and Assessment*, 185(6), 4995–5002. <https://doi.org/10.1007/s10661-012-2920-6>
- Stefanakis, A., Zouzias, D., & Marsellos, A. (2015). *Groundwater Pollution: Human and Natural Sources and Risks* (pp. 82–102).
- Stollenwerk, K. G. (2003). Geochemical Processes Controlling Transport of Arsenic in Groundwater: A Review of Adsorption. In A. H. Welch & K. G. Stollenwerk (Eds.), *Arsenic in Ground Water* (pp. 67–100). Kluwer Academic Publishers. [https://doi.org/10.1007/0-306-47956-7\\_3](https://doi.org/10.1007/0-306-47956-7_3)
- Stüben, D., Berner, Z., Chandrasekharam, D., & Karmakar, J. (2003). Arsenic enrichment in groundwater of West Bengal, India: Geochemical evidence for mobilization of As under reducing conditions. *Applied Geochemistry*, 18(9), 1417–1434.
- Sun, Y., Liang, X., Xiao, C., Wang, G., & Meng, F. (2019). Hydrogeochemical Characteristics of Fluoride in the Groundwater of Shuangliao City, China. *E3S Web of Conferences*, 98, 09028.
- Sutherland, R. A. (2000). Bed sediment-associated trace metals in an urban stream, Oahu, Hawaii. *Environmental Geology*, 39(6), 611–627.
- Tandon, S. K., Sinha, R., Gibling, M. R., Dasgupta, A. S., & Ghazanfari, P. (2008). Late Quaternary evolution of the Ganga Plains: Myths and misconceptions, recent developments and future directions. *Golden Jubilee Memoir of the Geological Society of India*, 66, 259–299.
- Telmer, K., & Veizer, J. (1999). Carbon fluxes, pCO<sub>2</sub> and substrate weathering in a large northern river basin, Canada: Carbon isotope perspectives. *Chemical Geology*, 159(1–4), 61–86. [https://doi.org/10.1016/S0009-2541\(99\)00034-0](https://doi.org/10.1016/S0009-2541(99)00034-0)
-

- 
- Thilagavathi, R., Chidambaram, S., Pethaperumal, S., Thivya, C., Rao, M. S., Tirumalesh, K., & Prasanna, M. V. (2016). An attempt to understand the behavior of dissolved organic carbon in coastal aquifers of Pondicherry region, South India. *Environmental Earth Sciences*, 75(3), 235. <https://doi.org/10.1007/s12665-015-4833-5>
- Tlustoš, P., Száková, J., Stárková, A., & Pavlíková, D. (2005). A comparison of sequential extraction procedures for fractionation of arsenic, cadmium, lead, and zinc in soil. *Open Chemistry*, 3(4), 830–851. <https://doi.org/10.2478/BF02475207>
- Turekian, K. K., & Wedepohl, K. H. (1961). Distribution of the Elements in Some Major Units of the Earth's Crust. *Geological Society of America Bulletin*, 72(2), 175. [https://doi.org/10.1130/0016-7606\(1961\)72\[175:DOTEIS\]2.0.CO;2](https://doi.org/10.1130/0016-7606(1961)72[175:DOTEIS]2.0.CO;2)
- Udmale, P., Ichikawa, Y., Nakamura, T., Shaowei, N., Ishidaira, H., & Kazama, F. (2016). Rural drinking water issues in India's drought-prone area: A case of Maharashtra state. *Environmental Research Letters*, 11(7), 074013.
- Varol, M. (2019). Arsenic and trace metals in a large reservoir: Seasonal and spatial variations, source identification and risk assessment for both residential and recreational users. *Chemosphere*, 228, 1–8. <https://doi.org/10.1016/j.chemosphere.2019.04.126>
- Vartiainen, T., Liimatainen, A., & Kauranen, P. (1987). The use of TSK size exclusion columns in determination of the quality and quantity of humus in raw waters and drinking waters. *Science of the Total Environment*, 62, 75–84.
- Venkatesan, G., & Subramani, T. (2018). Environmental degradation due to the Industrial Wastewater discharge in Vellore District, Tamil Nadu, India. *IJMS Vol.47(11) [November 2018]*. <http://nopr.niscair.res.in/handle/123456789/45298>
- Verma, S., Mukherjee, A., Choudhury, R., & Mahanta, C. (2015). Brahmaputra river basin groundwater: Solute distribution, chemical evolution and arsenic occurrences in different geomorphic settings. *Journal of Hydrology: Regional Studies*, 4, 131–153. <https://doi.org/10.1016/j.ejrh.2015.03.001>
- Vetrimurugan, E., Brindha, K., Elango, L., & Ndwandwe, O. M. (2017). Human exposure risk to heavy metals through groundwater used for drinking in an intensively irrigated river delta. *Applied Water Science*, 7(6), 3267–3280. <https://doi.org/10.1007/s13201-016-0472-6>
- Villa-lojo, M. C., Beceiro-González, E., Alonso-Rodríguez, E., & Prada-Rodríguez, D. (1997). Arsenic Speciation in Marine Sediments: Effects of Redox Potential and Reducing conditions. *International Journal of Environmental Analytical Chemistry*, 68(3), 377–389. <https://doi.org/10.1080/03067319708030502>
- Wang, X., Xu, G., Chen, P., Liu, X., Fang, Y., Yang, S., & Wang, G. (2016). Arsenic speciation analysis in environmental water, sediment and soil samples by magnetic ionic liquid-based air-assisted liquid–liquid microextraction. *RSC Advances*, 6(111), 110247–110254. <https://doi.org/10.1039/C6RA21199B>
- Wei, T., & Simko, V. (2017). R package “corrplot”: Visualization of a Correlation Matrix. <https://github.com/taiyun/corrplot>
-

- 
- Wenzel, W. W., Kirchbaumer, N., Prohaska, T., Stingeder, G., Lombi, E., & Adriano, D. C. (2001). Arsenic fractionation in soils using an improved sequential extraction procedure. *Analytica Chimica Acta*, 436(2), 309–323.
- WHO (World Health Organization, 2011) [Guidelines for Drinking-water Quality, Fourth Edition \(who.int\)](#) (Accessed on 29/07/21)
- Wilkie, J. A., & Hering, J. G. (1998). Rapid oxidation of geothermal arsenic (III) in streamwaters of the eastern Sierra Nevada. *Environmental Science & Technology*, 32(5), 657–662.
- Winkel, L. H., Trang, P. T. K., Lan, V. M., Stengel, C., Amini, M., Ha, N. T., Viet, P.H. & Berg, M. (2011). Arsenic pollution of groundwater in Vietnam exacerbated by deep aquifer exploitation for more than a century. *Proceedings of the National Academy of Sciences*, 108(4), 1246-1251.
- Wu, C., Huang, L., Xue, S.-G., Pan, W.-S., Zou, Q., Hartley, W., & Wong, M.-H. (2017). Oxidic and anoxic conditions affect arsenic (As) accumulation and arsenite transporter expression in rice. *Chemosphere*, 168, 969–975.
- Wu, Y., Wang, Y., & Xie, X. (2014). Occurrence, behavior and distribution of high levels of uranium in shallow groundwater at Datong basin, northern China. *Science of The Total Environment*, 472, 809–817. <https://doi.org/10.1016/j.scitotenv.2013.11.109>
- Wuana, R. A., & Okieimen, F. E. (2011). Heavy metals in contaminated soils: A review of sources, chemistry, risks and best available strategies for remediation. *International Scholarly Research Notices*, 2011.
- Xiao, Z., Xie, X., Pi, K., Yan, Y., Li, J., Chi, Z., Qian, K., & Wang, Y. (2018). Effects of irrigation-induced water table fluctuation on arsenic mobilization in the unsaturated zone of the Datong Basin, northern China. *Journal of Hydrology*, 564, 256–265.
- Yadav, S. K., Ramanathan, A. L., Kumar, M., Chidambaram, S., Gautam, Y. P., & Tiwari, C. (2020). Assessment of arsenic and uranium co-occurrences in groundwater of central Gangetic Plain, Uttar Pradesh, India. *Environmental Earth Sciences*, 79(6), 1–14.
- Yang, X., Xia, L., Li, J., Dai, M., Yang, G., & Song, S. (2017). Adsorption of As(III) on porous hematite synthesized from goethite concentrate. *Chemosphere*, 169, 188–193. <https://doi.org/10.1016/j.chemosphere.2016.11.061>
- Zavala, Y. J., Gerads, R., Gürleyük, H., & Duxbury, J. M. (2008). Arsenic in rice: II. Arsenic speciation in USA grain and implications for human health. *Environmental Science & Technology*, 42(10), 3861–3866.
- Zaveri, E., Grogan, D. S., Fisher-Vanden, K., Frolking, S., Lammers, R. B., Wrenn, D. H., Prusevich, A., & Nicholas, R. E. (2016). Invisible water, visible impact: Groundwater use and Indian agriculture under climate change. *Environmental Research Letters*, 11(8), 084005. <https://doi.org/10.1088/1748-9326/11/8/084005>
- Zhang, Y., Xu, B., Guo, Z., Han, J., Li, H., Jin, L., Chen, F., & Xiong, Y. (2019). Human health risk assessment of groundwater arsenic contamination in Jinghui irrigation district, China. *Journal of Environmental Management*, 237, 163–169. <https://doi.org/10.1016/j.jenvman.2019.02.067>
-

- 
- Zheng, J., Hintelmann, H., Dimock, B., & Dzurko, M. S. (2003). Speciation of arsenic in water, sediment, and plants of the Moira watershed, Canada, using HPLC coupled to high resolution ICP-MS. *Analytical and Bioanalytical Chemistry*, 377(1), 14–24. <https://doi.org/10.1007/s00216-003-1920-3>
- Zhou, Q., Blean, W., & Soldat, D. (2020). *The Impact of Water Loss by Evaporation and Calcite Precipitation on the Sodium Adsorption Ratio (SAR) and an Alternative Method of Estimating the SAR of Irrigation Drainage Water*. <https://doi.org/10.20944/preprints202010.0187.v1>
- Zimmerman, A. J., & Weindorf, D. C. (2010). Heavy Metal and Trace Metal Analysis in Soil by Sequential Extraction: A Review of Procedures. *International Journal of Analytical Chemistry*, 2010, 1–7. <https://doi.org/10.1155/2010/387803>



## SHAILESH KUMAR YADAV

PhD. student

Jawaharlal Nehru University

Lab No- 209/214, School of Environmental Sciences

Jawaharlal Nehru University, New Delhi, India, Post code-110067

**Mobile:** +91-9868065634

**E-Mail:** shaileshyadav.jnu@gmail.com

## Education

- July 2015- till now **Jawaharlal Nehru University, New Delhi**  
**PhD (pursuing)** in Environmental Sciences  
Title: **“Solute Geochemistry, Arsenic Mobilization and their effect on Human Health in Ghazipur and Gorakhpur districts, Uttar Pradesh, India”**  
Supervisor: Prof. AL. Ramanathan
- July 2013- July 2015 **Jawaharlal Nehru University, New Delhi**  
**M.Phil. Awarded** (February 2016) in Environmental Sciences  
Title: **“Distribution of As and U in groundwater of Gorakhpur and Ballia districts, Uttar Pradesh”**  
Supervisor: Prof. AL. Ramanathan
- Jul 2011- May 2013 **Jawaharlal Nehru University, New Delhi**  
**Master of Science, Environmental Sciences**  
Title of dissertation: Assessment of hydrogeochemical characteristics of groundwater in parts of Rapti-Ghaghara interfluvial region, Gorakhpur district, Uttar Pradesh, India 2012-2013  
Supervisor: Prof. AL. Ramanathan
- Jun 2007- Jun 2010 **DAV PG College, Gorakhpur University, Gorakhpur**  
**Bachelor of Science, Botany, Chemistry and Zoology**

## Awards

Qualified Joint **CSIR-UGC test for Junior Research Fellowship** and Eligibility for Lectureship (**NET**) of **June 2013** (AIR-26)

## Personal skills & competence

Technical expertise	Hydrochemistry, dealing with instruments like XRD, XRF, Laser Particle Analyzer (LPA), ICP-OES (Inductively Coupled Plasma-Atomic Emission Spectroscopy), IC (Ion Chromatography), AAS(Atomic Absorption Spectroscopy), Flame Photometer, Spectrophotometer, LED Fluorimeter etc.
Com. Programming	MATLAB (basic), R Programming (basics)
Computer Software	Arc GIS, ERDAS, Surfer, SPSS, Grapher, Origin, etc.
Languages	English, Hindi

## Hydrogeology training/ course/ meeting/ achievements

2016	Participated in “ <i>Palaeochannels - Evolution and Ground Water Prospect</i> ” Organized by Central Ground Water Board (CGWB) on 16 <sup>th</sup> June 2016, at CSMRS, New Delhi, India.
2015	Attended and was part of organizing team of <b>GLACINDIA WORKSHOP</b> (training program on climate modeling and climate change research, innovation and services) from April 9th to April 10th, 2015, at Jawaharlal Nehru University, New Delhi, India.
2014	Attended the Indian-African training program on “ <b>Natural Resources and water management</b> ” 2 <sup>nd</sup> - 22 <sup>nd</sup> December 2014, at Jawaharlal Nehru University, New Delhi, India.
2014	Participated in “ <b>16<sup>th</sup> International Association for Mathematical Geosciences</b> ” 17 <sup>th</sup> - 20 <sup>th</sup> October 2014, at Jawaharlal Nehru University, New Delhi, India.
2013	Participated in ‘ <b>1<sup>st</sup> International Forum on Asian Water Environmental Technology (IFAWET)</b> ’ 18 <sup>th</sup> -20 <sup>th</sup> December, 2013 at Jawaharlal Nehru University, New Delhi, India.
2013	TF-DTU-NTU Training programme on “ <b>Water Sector Training and Capacity Building Programme for the National Capital Territory of Delhi, India</b> ”, 11 <sup>th</sup> -15 <sup>th</sup> March, 2013, Organized by- Delhi technological University Delhi, India in collaboration with Nanyang Technological University, Singapore.
2013	Participated in “ <b>International Humboldt Kolleg-2013 on Management of Water, Energy and Bio-resources in Changing Climate Regime: Emerging Issues and Environmental Challenges</b> ” 8-9 February, 2013, Jawaharlal Nehru University, New Delhi, India.



2012 Participated in “**Indo-Australian workshop on Arsenic**, October 3<sup>rd</sup>-4<sup>th</sup>, 2012, Jawaharlal Nehru University New Delhi, India.

### **Oral/poster Presentation**

- 2021 Shailesh Kumar Yadav, Manoj Kumar and AL Ramanathan “**Groundwater arsenic contamination from quaternary alluvium in the central Gangetic plain, U.P., India**” online oral presentation in Fourth Indian National Groundwater Conference (INGWC-2021) on Groundwater Management in Arid and Semi-Arid Regions of Hard Rock Terrains, Jawaharlal Nehru Technological University Hyderabad, Kukatpally, Hyderabad, 22<sup>nd</sup> – 24<sup>th</sup> March 2021, Hyderabad, India
- 2020 Shailesh Kumar Yadav and AL Ramanathan “**Health Risk Assessments of Arsenic and Toxic Heavy Metals Exposure in Drinking Water in Central Gangetic Plain, Uttar Pradesh**” online oral presentation in European Geosciences Union (EGU), 3<sup>rd</sup> – 8<sup>th</sup> May 2020, Vienna, Austria.
- 2015 Shailesh Kumar Yadav, Manoj Kumar and AL Ramanathan “**Hydrogeochemical Characterization and Arsenic Distribution in Groundwater of Gorakhpur District, Uttar Pradesh, India**” oral presentation in National Seminar on Past and Present Geochemical Processes -Impacts on Climate Change & Annual General Body Meeting –2015 Indian Society of Applied Geochemists, Hyderabad, 22<sup>nd</sup> 23<sup>rd</sup> Dec 2015 at Jawaharlal Nehru University New Delhi, India.
- 2012 Shailesh Kumar Yadav and AL Ramanathan “**Assessment of Hydrogeochemical characteristics of Groundwater in parts of Rapti-Ghaghara interfluvial region of Gorakhpur district, Uttar Pradesh, India**”, Poster Presented in Tropical Ecological Congress, 10<sup>th</sup>- 12<sup>th</sup> December 2014, at Jawaharlal Nehru University New Delhi, India.

### **Publication**

- **Shailesh Kumar Yadav**, AL Ramanathan, Manoj Kumar, S. Chidambaram, Y. P. Gautam & C. Tiwari (2020). “**Assessment of arsenic and uranium co-occurrences in groundwater of central Gangetic Plain, Uttar Pradesh, India**”. Environmental Earth Sciences, 79(6), 1-14.
- Manoj Kumar, AL ramanathan, Shayam Ranjan, Virendra Bahadur Singh, Naveen Kumar, **Shailesh Kumar Yadav** & Bhattacharya, P. (2018). “**Groundwater evolution and its utility in upper Ganges-Yamuna Alluvial plain of Northern India, India: Evidence from solute chemistry and stable isotopes**”. Groundwater for Sustainable Development, 7, 400-409.
- Virendra Bahadur Singh, AL Ramanathan, A. K. Keshari, Shayam Ranjan, Naveen Kumar & **Shailesh Kumar Yadav** (2018). “**Climatic Influence on Hydrogeochemistry of Meltwater Draining from Chhota Shigri Glacier, Himachal Pradesh, India**”. Journal of Climate Change, 4(1), 23-31.

- Rajesh Kumar Dash, AL. Ramanathan, **Shailesh Kumar Yadav**, Manoj Kumar, T. Kuriakose, Y.P. Gautam (2016), “**Uranium in Ground Water in India: A Review.**” ISAG-Journal of Applied Geosciences Jag/MS/VII/16/75a.

## Book Chapter

- Manoj Kumar, AL Ramanathan, Alok Kumar & **Shailesh Kumar Yadav** (2016). “**Evolution of Arsenic Contamination Process and Mobilization in Central Gangetic Plain Aquifer System and Its Remedial Measures**”. In *Groundwater Assessment, Modeling, and Management* (pp. 327-337). CRC Press.
- Hariom Kumar, Rajesh Kumar Ranjan, **Shailesh Yadav**, Alok Kumar, AL. Ramanathan, (2014), Hydrogeochemistry and Arsenic Distribution in the Gorakhpur District in the Middle Gangetic Plain, India. **Safe and Sustainable Use of Arsenic-Contaminated Aquifers in the Middle Gangetic Plains: A Multidisciplinary Approach**, Capital Publishers (India), pp. 107-117. ISBN: 978-93-81891-08-7

I pledge and pronounce that all the above information is true of my knowledge and belief.

---

### Reference

**Prof. AL. Ramanathan**, Professor, School of Environmental Sciences, Jawaharlal Nehru University, New Delhi, India.

Web page: <http://www.jnu.ac.in/Faculty/alramanathan/index.html>

Email: [alrjnu@gmail.com](mailto:alrjnu@gmail.com), [alr0400@mail.jnu.ac.in](mailto:alr0400@mail.jnu.ac.in)

Phone: 91-011-26704314

**Dr. Gurmeet Singh**, Scientist C Futuristic Research Division, National Centre for Sustainable Coastal Management, Ministry of Environment and Forests, Koodal Building, Anna University Campus, Chennai 600 025, India.

Email: [gurmeet@ncscm.res.in](mailto:gurmeet@ncscm.res.in), [gurmeet@hotmail.com](mailto:gurmeet@hotmail.com) Phone: [+91]-44-2230-0108 (Ext. -226)

---



# Assessment of arsenic and uranium co-occurrences in groundwater of central Gangetic Plain, Uttar Pradesh, India

Shailesh Kumar Yadav<sup>1</sup> · A. L. Ramanathan<sup>1</sup> · Manoj Kumar<sup>2</sup> · S. Chidambaram<sup>3</sup> · Y. P. Gautam<sup>4</sup> · C. Tiwari<sup>5</sup>

Received: 5 November 2018 / Accepted: 1 March 2020  
© Springer-Verlag GmbH Germany, part of Springer Nature 2020

## Abstract

Arsenic and uranium in the aquatic environment are recognized as a major catastrophic problem worldwide and have natural as well as human-made sources such as mining, industry and agriculture. The severity of this problem is further accelerated by in-situ physio-chemical factors in the fluvial environment which enhances the concentration of arsenic and uranium in groundwater that feeds millions of people in Central Gangetic Plain in India. This study aims to establish a better understanding of the processes responsible for the co-occurrence of arsenic and uranium along with the factors controlling their solubility and mobility in the groundwater of central Gangetic plain. This study is an attempt to bring out the (a) the spatial distribution pattern of arsenic and uranium, (b) insight into the hydrogeochemical characteristics of aquifers that are controlling their co-occurrence and provides (c) information of their source which are validated by statistical tools. Silicate weathering controls U mobilization and distribution whereas carbonate dissolution and ion exchange process controls As in groundwater. The land use and land cover pattern of the North-eastern (NE) part of the study area is agriculture dominated and is composed of Holocene older alluvium. However, the South and South-western areas which are closer to the river are formed by the deposition of river born newer alluvial. Newer alluvium in the SW part has unoxidized organic-rich clay that enhances arsenic mobilization by reductive dissolution of Fe-oxyhydroxide. In the NE region, the abundance of fertilizers in the subsurface oxidizing environment augments the solubility and mobility of uranium.

**Keywords** Arsenic · Central Gangetic plain · Uranium · Ghaghara · Rapti

## Introduction

Since last few decades, high concentrations of arsenic and uranium in groundwater have been a significant environmental problem and have been identified as a major public health concern in several parts of the world (Gas'kova et al. 2000; Mukherjee et al. 2006). It can cause chronic human health

disorders such as skin pigmentation, dermal hyperkeratosis and cancers (Mazumder 2008; Martinez et al. 2011). Intake of U contaminated drinking water can lead to chronic lung diseases and nephrotoxic damage (Zamora et al. 1998; Kurtio et al. 2002; Guo et al. 2016). Therefore, the World Health Organization (WHO 2011) elucidated a provisional health-based As (10 µg/L) and U (30 µg/L) guideline concentration in drinking water (Ravenscroft et al. 2009).

Although groundwater As is entirely geogenic (Brown et al. 2007; Cinti et al. 2015; Guo et al. 2016) and derived from physical weathering and erosion of lithified sediments and crystalline rocks, it gets deposited on floodplains and deltaic regions where it is subjected to intense chemical weathering (Stollenwerk et al. 2007). The redistribution processes of arsenic in lower deltaic floodplains are mainly dependent on factors viz. pH, variable redox conditions and mineral precipitation/dissolution in oxic and anoxic aquifer conditions (Acharyya et al. 2000; Stollenwerk et al. 2007). Dissimilatory reduction of Fe/Mn oxyhydroxide in anoxic aquifers conditions is

✉ A. L. Ramanathan  
alrjnu@gmail.com

<sup>1</sup> School of Environmental Sciences, Jawaharlal Nehru University, New Delhi 110067, India

<sup>2</sup> Central University of Haryana, Mahendergarh, Pali, Haryana 123031, India

<sup>3</sup> Water Research Center, Kuwait Institute for Scientific Research, 13109, Safat, Kuwait

<sup>4</sup> Nuclear Atomic Power Station (NAPS), Narora, Uttar Pradesh 203389, India

<sup>5</sup> Central University of South Bihar, Patna, Bihar 800014, India